UNIVERSITÉ DE STRASBOURG

ÉCOLE DOCTORALE DES SCIENCES CHIMIQUES

INSTITUT DE CHIMIE, UMR 7177 CNRS

THÈSE

PRESENTEE PAR

Nallusamy NATARAJAN

SOUTENUE LE : **14 SEPTEMBRE 2018**

POUR OBTENIR LE GRADE DE : **DOCTEUR DE L'UNIVERSITE DE STRASBOURG**

DISCIPLINE/ SPECIALITE : CHIMIE

> ## Ligands construits sur des plates-formes macrocycliques : la cavité macrocyclique peut-elle influencer le résultat catalytique ?

Thèse dirigée par :

Dr. SEMERIL David   Chargé de Recherche CNRS, Université de Strasbourg/ Directeur de Thèse.

Dr. MATT Dominique   Directeur de Recherche CNRS, Université de Strasbourg/ Co-Directeur de Thèse.

Rapporteurs

Pr. KNORR Michael   Professeur, Université de France-Comté, Besançon.

Dr. FISCHMEISTER Cédric Ingénieur de Recherche CNRS, Université de Rennes.

Examinateur

Pr. RAMESH Rengan   Professeur, Université Bharathidasan, India.

Table of contents

Chapter I

The use of resorcinarene-cavitands in metal-based catalysis

Chapter II

Chiral calixarene and resorcinarene derivatives. Conical cavities substituted at their upper rim by two phosphito units and their use as ligands in Rh-catalysed hydroformylation

Chapter III

Cavitand chemistry: nickel half-sandwich complexes with imidazolylidene ligands bearing one or two resorcinarenyl substituents

Chapter IV

Resorcin[4]arene-functionalised triazolium salts as a ligand source for Suzuki-Miyaura cross-coupling catalysts

List of abbreviations

δ	chemical shift
1D	one-dimensional
Å	Ångström
Anal. Calcd.	analysis calculated
acac	acetylacetone
AcOEt	ethyl acetate
Ar	aryl
arom.	aromatic
n BuLi	*n*-butyl lithium
br	broad
CCDC	Cambridge Crystallographic Data Centre
CIF	crystallographic information file
cod	1,5-cyclooctadiene
Cp	cyclopentadienyl
d	doublet
dd	doublet of doublets
eq.	equivalent
ESI-TOF	electron spray ionisation - time-of-flight mass analyzer
Fig.	figure
GC	gas chromatography
h	hour
Hz	hertz
IR	infrared
J	coupling constant
m	multiplet
Mes	2,4,6-trimethylphenyl
MS	mass spectrometry
m/z	mass to charge ratio
NHC	*N*-heterocyclic carbene
NMR	nuclear magnetic resonance
PEPPSI	pyridine rnhanced precatalyst preparation, stabilisation, initiation

Ph	phenyl
ppm	parts per million
R_f	retardation factor
ROESY	rotating frame nuclear overhauser effect spectroscopy
r.t	room temperature
s	singulet
t	triplet
Tf	triflate
THF	tetrahydrofuran
TOF	turnover frequency

ACKNOWLEDGEMENTS

Chapter I

The use of resorcinarene-cavitands in metal-based catalysis

Abstract

The utility of resorcinarene cavitands in catalysis arises from: i) their ability to create metal confinement and thus to make reactions either shape selective or to enhance their rates through supramolecular assistance by the receptor subunit; ii) their ability to enforce steric interactions with a coordinated metal centre and thereby favour carbon-carbon bond forming reactions. This review gives an overview on the promise that exists in this area.
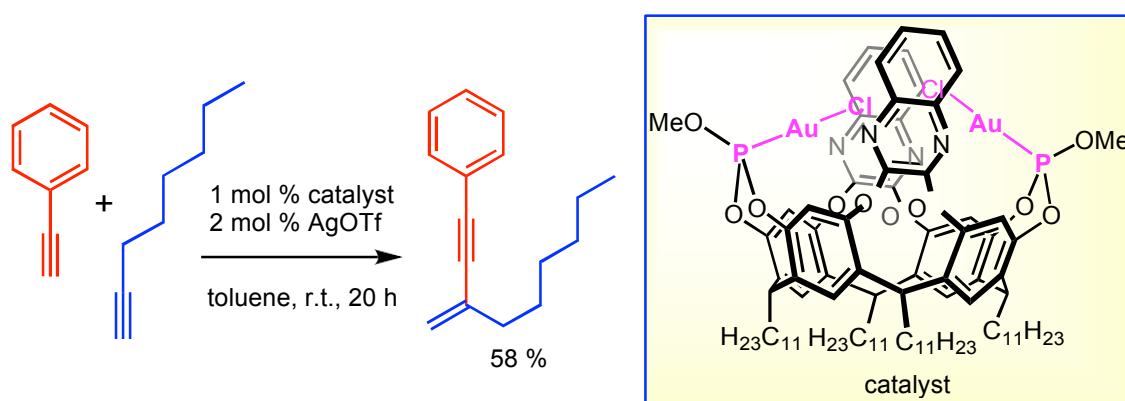
1. Introduction. Synthesis and properties of generic resorcinarenes and resorcinarene-cavitands

Resorcinarenes are a class of macrocycles first correctly identified in 1940,[1] although their chemistry can be traced back to work of Baeyer in the nineteenth century.[2] Typically, these compounds can be obtained in high yields by condensation of resorcinol or its derivatives and an aldehyde in EtOH/H_2O under acidic conditions, the thermodynamically strongly favoured end product from an initially complex mixture of linear species being the macrocycle resulting from condensation of four units each of resorcinol and aldehyde (Scheme 1),[3] although under certain conditions a less stable macrocycle incoprporating six units can be isolated.[4] In fact, the use of a solvent for their preparation is not mandatory,[5] although solvent-free synthesis may result in inseparable mixtures of isomers.[6] Methods for their functionalisation have been widely explored so that numerous very sophisticated derivatives have become accessible.[7] The first crystallographic characterisation of a resorcinarene was reported in 1968 (Fig. 1).[8]
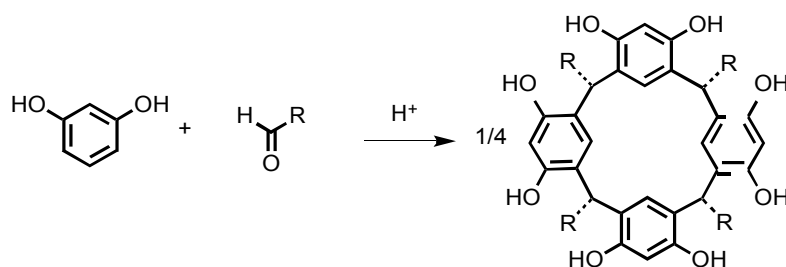
Scheme 1. Synthesis of resorcinarenes

The stereochemistry of the resorcinarenes is complicated both by the facts that the substituents on the bridging units may adopt different relative orientations (usually defined with respect to the mean plane of the macrocycle) and that facile rotation about the C-C bonds linking the aromatic rings to the bridging atoms leads to several conformational minima. Hydrogen bonding is also an important stereochemical influence in parent resorcinarenes where hydroxyl groups are retained . The rapid equilibration between different isomers in acidic media coupled to differences in solubility can, however, mean that a single species can be crystallised in good yield from a given reaction mixture.[3, 9] Importantly, this is usually the *cis,cis,cis* isomer, the formal precursor to all bowl-shaped cavitands. The conformational flexibility of generic resorcinarenes is revealed in numerous solid state structure determinations (321 currently in the CSD, plus

2
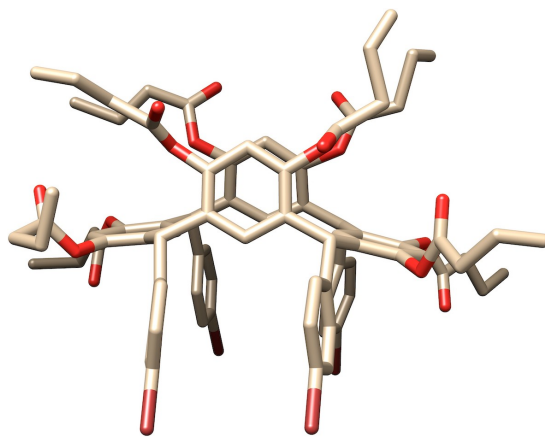
Figure 1. Molecular structure within the crystal of the product of reaction of resorcinol with 4-bromobenzaldehyde (after butanoylation of all hydroxyl groups).

several thousand for derivatives) by X-ray diffraction where the conformation varies considerably depending on associated molecules present in the lattice as well as the nature of the bridge substituent. Thus, for example, for the simplest resorcinarene, generated from acetaldehyde and resorcinol, as the *cis,cis,cis* isomer, it has been found in several instances[10] to adopt a *crown* or *cone* conformation close to C_{4v} symmetry, in others[11] C_{2v}-symmetric conformations varying between a "flattened" *cone* (when the distortion is slight) and a *boat* or *pseudo-saddle* forms (as seen also in Figure 1) where greater distortion occurs, as well as to adopt a *chair* form of at most C_s symmetry.[12] With bridge substituents other than methyl, as well as for isomers other than the *cis,cis,cis*, a similar range of conformations is known[13] the chair form of the *cis,trans,cis* isomer with 4-hydroxyphenyl substituents, for example, being established in early work.[14] Some examples of conformations established by X-ray crystallography for the *cis,cis,cis* isomer of the tetramethyl resorcinarene are given in Figure 2.

Modification of the *cis,cis,cis* resorcinarene core was first achieved by introduction of methylene bridges between oxygen atoms of adjacent resorcinolic rings.[9a] The term "cavitand" was coined to describe these materials which, locked into a symmetrical cone conformation, were considered to define a rigid molecular cavity.[15] Heteroatoms,[9a, 15a, 15b, 16] hydrocarbon chains,[17] phenylene[18] or quinoxaline-diyl[19] units can also be used for linking the resorcinol rings and thus create a cavitand (Fig. 3). While inhibiting conformational changes of the resorcinarene core,
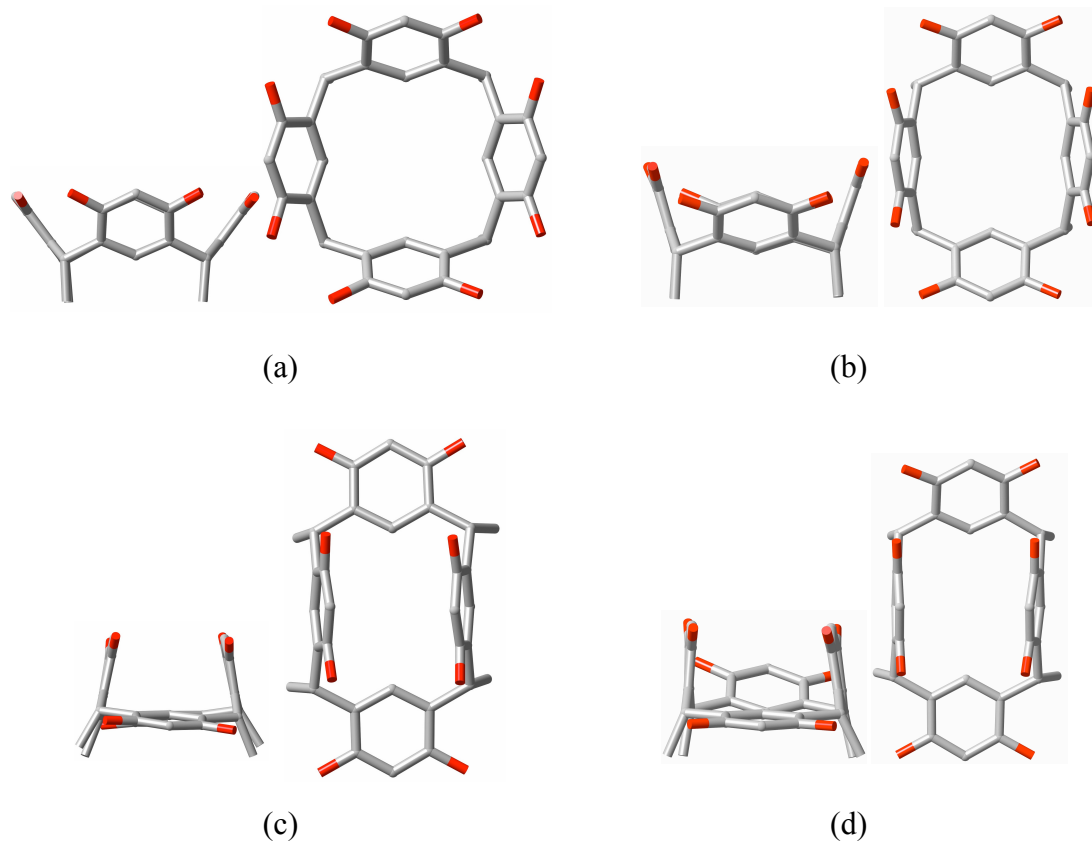
Figure 2. Orthogonal views of the conformations of the *cis,cis,cis* isomer of tetramethylresorcinarene found in different solid state adducts. For clarity, H-atoms are omitted. *(a)* A conformer of near C_{4v} symmetry;[10a] *(b), (c)* increasingly distorted conformers of near C_{2v} symmetry;[11b, 11c] *(d)* a chairlike conformer of C_s symmetry.[12]

these links can be associated with their own conformational equilibria giving rise to control of the cavitand's behaviour as a receptor, as seen with the "vase" and "kite" forms of the quinoxaline-bridged species.[20] Combined with the rigidity of cavitands, the many possible variations in the bridging groups has been the basis of the continual development of cavitand chemistry over the past 4 decades. Major advances have concerned : a) the ability of many resorcinarene-cavitands to function as receptors towards small molecules and ions;[21] b) the ease of extension of the core for the construction of larger container molecules for the encapsulation of neutral and ionic compounds,[22] including metal complexes;[23] c) the ease with which they can be selectively functionalised at inequivalent sites, facilitating the synthesis of sophisticated multitopic ligands.[7, 24] The ease of linking resorcinarene units one to another has of course been the basis of the development of the major field of carcerand chemistry.[22a, 22d, 25] Finally, it must be emphasised here that, from a practical point of view, the synthesis of cavitand platforms is relatively simple, and notably less intricate than that of calix[4]arenes.

The following pages provide a survey on the catalytic applications of ligands based on the resorcinarene cavitand platform. While extensive studies have been made of equilibrium binding, catalysis based on metal ion complexes of cavitands has, in contrast to the situation for ligands based on the similar calix[4]arene core,[17] been given quite limited attention.[7, 27] Catalysis employing non-rigidified resorcinarenes has been reported but examples are few.[28] The initial interest of resorcinarene-derived cavitands in catalysis was essentially related to their ability to create metal confinement and thus, potentially, to make catalytic reactions shape and/or substrate selective. Much research on cavitand ligands was also undertaken with the aim of exploiting the receptor properties of the cavitand subunit so as to provide an entry into supramolecular catalysis.
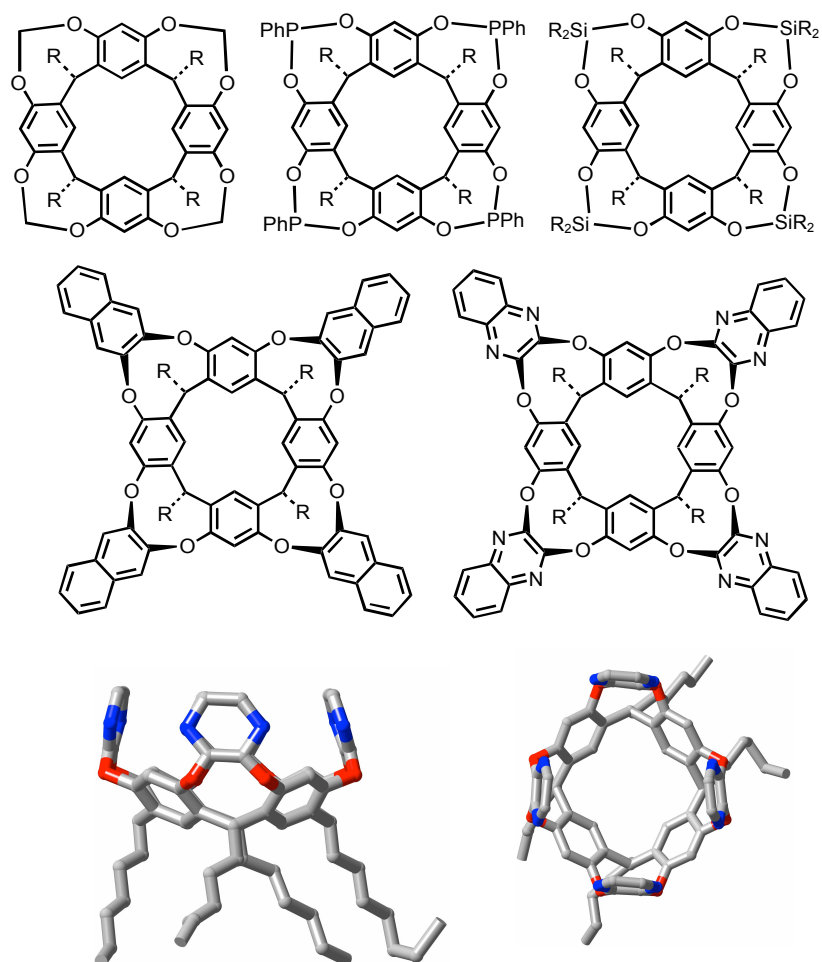
Figure 3. (Upper) Examples of resorcinarene-based cavitands; (Lower) Orthogonal views of the molecular species with the lattice of a vase-form pyrazine-bridged cavitand,[26] showing the well-formed, symmetrical cavity.

2. Catalytic chemistry with cavitands substituted with P donors

The first use in transition metal catalysis of a ligand built upon a resorcinarene-cavitand was reported in 2002 by Gibson and Rebek.[29] The authors used the phosphite-oxazoline chelator **1** (Fig. 4) to perform allylic alkylations. Here, the ligand core was an expanded cavitand unit known to bind size- and shape-complementary molecules such as adamantanes.
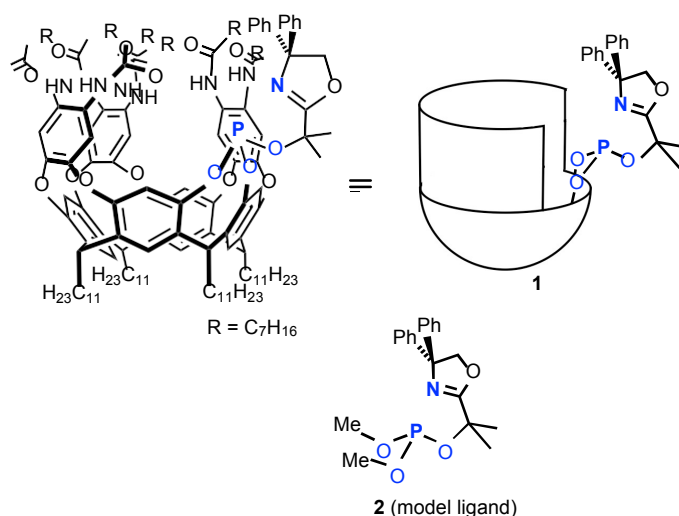
Figure 4. Cavitand phosphite **1** and reference ligand **2**

In the presence of palladium(II) and allyl acetate, the ligand produced an allyl palladium η^3-complex, in which the allyl fragment appeared to be oriented towards the cavity axis and within the cavity (Scheme 2). Two ways of coordinating the allylic fragment $(H_2C^1–C^2H=C^3HR')^-$ are possible, depending on whether the carbon trans to phosphorus is the terminal carbon atom C^1 or carbon atom C^3 of the allyl ligand. The left pathway in Scheme 2 was expected to dominate as this minimises steric repulsions.

Nucleophilic attack by, for example, malonate, was found to occur selectively on carbon C(1), consistent with the supposed steric effect and electronic factors. The electronic factor influencing the selectivity was considered to be that the C atom trans to the P atom, which has a stronger trans influence than N, is more electrophilic. Note that the reference ligand **2**[29] displayed the same selectivity for a linear product.

The reaction rate was found to depend on the substrate (substrates tested: **S$_a$-S$_e$**, Table 1). For example, the conversion of substrates **S$_b$** and **S$_c$** was complete after 2 days, while that of the
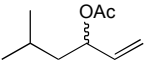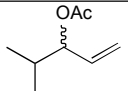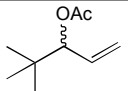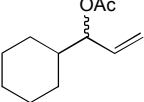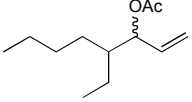
bulkier substrates S_d and S_e was approximately four times lower (Table 1). Remarkably, the smallest substrate S_a exhibited the lowest reaction rate. Careful examination of competitive
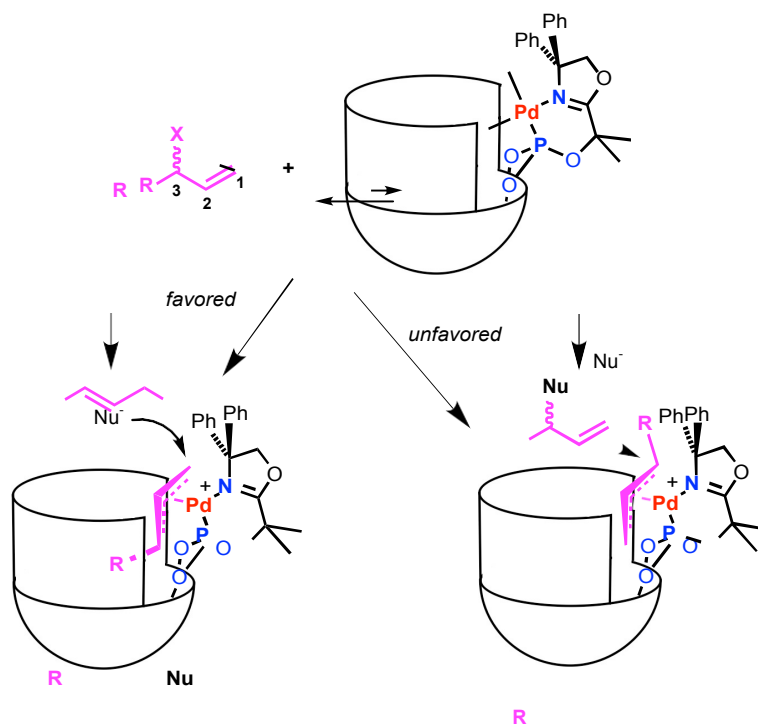
Scheme 2. Nucleophilic attack on the two possible η^3-allyl complexes $[Pd(RC_3H_4)\cdot\mathbf{1}]$. The steric hindrance created by the geminal phenyl groups of the oxazoline moiety favors the left pathway, which results in the linear alkylation product.

experiments (conducted by mixing pairs of substrates) relying on MS analyses revealed that the allylic complexes formed by oxidative addition were more rapidly formed with substrate S_a (bearing a secondary homoallylic C atom) than with S_b (tertiary homoallylic atom), the latter more rapidly than S_c (quaternary homoallylic atom). The rate of the oxidative addition (*i.e.* formation of the allyl-Pd complex) varied in the order R' = $^tBu > ^iPr >> ^iBu$. However, as mentioned before, the reactivity of the complexes in the presence of malonate followed a different order. Once the S_a-complex formed, for example, the reaction was inhibited.

Table 1. Allylic alkylation of substrates S$_{a-e}$ using ligands **1** and **2**.
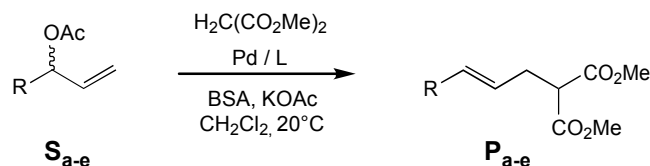
Substrate		Ligand **1**		Ligand **2**	
		Reaction time	Yield (%)	Reaction time	Yield (%)
	S$_a$	6 d[b]	38	2 h	85
	S$_b$	2 d	76	2 h	91
	S$_c$	2 d	96	2 h	81
	S$_d$	6 d[b]	74	2 h	78
	S$_e$	6 d[b]	60	2 h	82

General conditions: [Pd(C$_3$H$_5$)Cl]$_2$ (1.4 mol %), L (3.2 mol %), CH$_2$(CO$_2$Me)$_2$ (3 equiv) and *N,O*-bis(trimethylsilyl)acetamide (BSA). [b] Substrate was not completely converted.

For the substrates **S$_b$**, **S$_d$**, and **S$_e$**, all of which have a tertiary carbon atom in the homoallylic position, pairwise comparison of these substrates using Pd(II) and reference ligand **2** showed no significant difference in reaction rates for either the oxidative addition or the overall reaction. The ability of the palladium catalyst formed with **1** to stabilise the transition state of the oxidative addition decreased in the order cyclohexyl > iso-propyl > 1-ethylpentyl. This substrate specificity strongly correlated with the selectivity in product formation (**P$_b$**, **P$_d$**, **P$_e$**). Thus, the observed selectivities appear to be a direct consequence of the molecular recognition properties of the cavity and underscore the potential of cavitand-containing catalysts in organic synthesis.

The catalytic efficiency of cavitand-based phosphines is not necessarily related to the receptor or confining properties of the cavity. Thus, it was found that cavitand phosphine **3** having

its P atom separated from the cavity by a methylene group resulted, in the presence of Pd(II), in a fast Suzuki-Miyaura (SM) cross-coupling catalyst.[30] The reaction rates were found to be 5-7 times faster than that those observed with PPh$_3$. A possible explanation is that during the catalytic process intermediates are formed in which one of the O atoms close to the P forms with this atom a chelate ring. This could stabilise monophosphine complexes in the same manner as do Buchwald phosphines, and incidently favour the oxidative addition step. An argument for this interpretation, which thus would exclude a supramolecular effect, is that the cavity-free anisole phosphine **4** showed activities comparable to those of the cavitand phosphine. When repeating the experiments with benzyldiphenylphosphine, the activity dropped by ca. 50%.
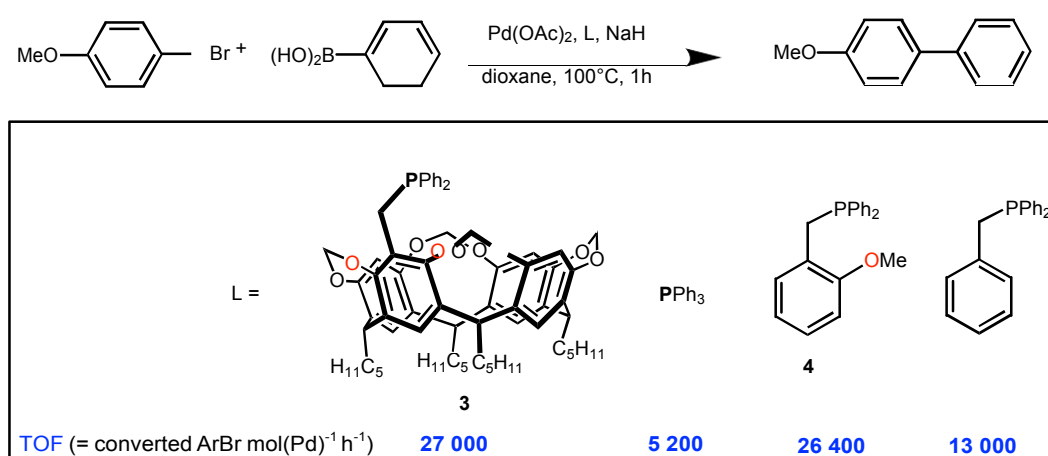
Scheme 3. Suzuki-Miyaura cross-coupling catalysis by cavitand-phosphine **3** and three cavity-free phosphines

Diphosphines **5** and **6** (Fig. 5) were tested in the coupling of 4-bromotoluene with PhB(OH)$_2$ and were shown to be more effective than monophosphine **3**. Their higher performance was attributed to the formation of complexes with PMP angles larger than 90°, these resulting either from steric repulsions occuring in cyclic oligomeric intermediates (which may form with ligand **5**) or arising from the formation of strained chelate complexes (which may form with ligand **6**). Larger PMP angles are known to favour the final reductive elimination step of the catalytic process.[30]

9
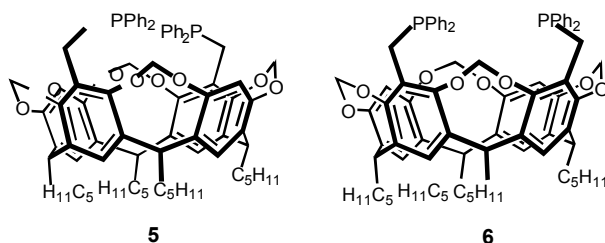
Figure 5. Cavitand diphosphines **5** (distally difunctionalised) and **6** (proximally difunctionalised)

The first tetraphosphine built upon a cavitand (**7**) was reported in 2009 (Scheme 4).[31] Complexation studies coupled with MS measurements revealed that each pair of adjacent phosphine arms of this ligand may function as a chelating unit. The authors showed that in the presence of [Pd(OAc)₂] and a base, ligand **7** is active in Heck coupling reactions (Scheme 4). The catalytic results indicated that the rate of the reaction had a maximal value when only one equivalent of cavitand was added to the palladium, any excess of **7** drastically decreasing the yield. This finding together with ^{31}P NMR investigations indicated that the presence of free phosphane units is required for stabilisation and/or generation of the catalytically active species. The activities themselves were not unusual when compared with that of PPh₃. Disappointingly, the presence, after complexation, of four phosphine ligands near the metal centre did not markedly accelerate the reaction, unlike the observations made by Santelli for similar reactions with another tetraphosphine, *cis,cis,cis*-1,2,3,4-tetrakis(diphenylphos phinomethyl)cyctopentane (TEDICYP), in which motions of the P atoms are more restricted.[32]
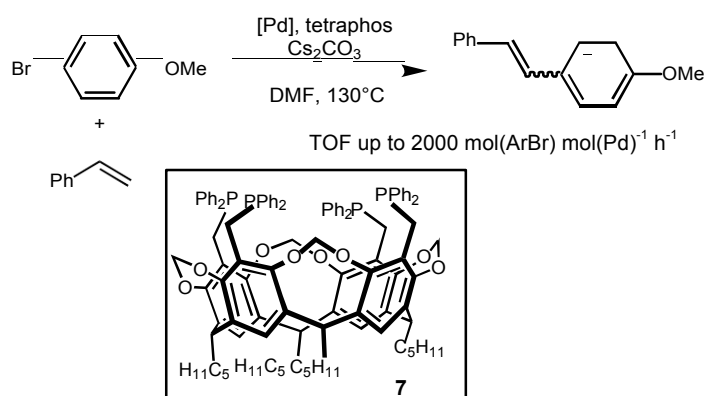
Scheme 4. Heck reaction with tetraphosphine **7**

A structural study combined with molecular modelling revealed that monophosphine **8** (Fig. 6), a cavitand with a P atom directly attached to the upper rim of the bowl, behaves as a

ligand with variable bulk, its encumbrance depending on the orientation of the P lone pair.[33] Thus, when the P atom points towards the cavitand axis, its cone angle is by ca. 45° greater than if it points towards the exterior of the cavity. Consistent with its strong crowding, ligand **8**, when
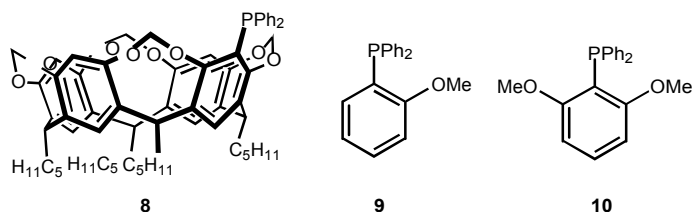
Figure 6. Cavitand-phosphine **8** and cavity-devoid ligands **9** and **10**

Table **2**. Suzuki-Miyaura cross-coupling of aryl bromides catalyzed by [Pd(OAc)$_2$]/triarylphosphines.

Entry	ArBr	Triarylphosphine, % conversion			
		PPh$_3$	**9**	**10**	**8**
1	(ArBr structure, MeO-)	8.1	18.3	22.6	25.1
2	(ArBr structure, Br)	2.5	5.4	7.1	16.1
3	(ArBr structure, Er)	6.5	13.2	17.3	26.6
4	(ArBr structure, MeO, Br)	7.0	14.8	16.1	24.1

General conditions: [Pd(OAc)$_2$] (5 x 10^{-7} mmol, 1 x 10^{-4} mol %), phosphine (1 x 10^{-6} mmol, 2 x 10^{-4} mol %), ArBr (0.5 mmol), PhB(OH)$_2$ (1 mmol), NaH (60 % dispersion in mineral oil; 1 mmol), 1,4-dioxane (1.5 mL), decane (0.050 mL), 100°C, 1 h. The conversions were determined by GC, the calibrations being based on decane.

combined with [Pd(OAc)$_2$], provided an efficient catalyst for the coupling of a variety of aryl boronic acids with aryl chlorides. Depending on the substrates used, the catalytic system was found to be 3-7 times more active than PPh$_3$ (study carried out with aryl bromides, see Table 2). Comparison with bulkier triarylphosphines as well as phosphines **9** and **10**, bearing respectively

one and two *o*-MeO groups on one of their aryl substituents – all leading to higher activities –, suggested that the high catalytic activity of **8** arose from a combination of two features, namely (i) its ability to form *P,O* chelate complexes, this making the metal environment sterically more crowded and the metal more electron-rich, and (ii) its increased bulkiness when the P lone pair points towards the cavitand axis, this favouring the formation of monoligated intermediates. However, care must be taken with the interpretation that *P,O* chelation increases the activity, as it was recently found that when the metal centre bears a positive charge (which is not the case here), *P,O* chelation may result in cavitand cleavage with formation of a phosphino-enolato metal complex,[34] this being inactive in cross coupling. Note that nickel complexes of this type were found active in ethylene oligomerisation.

The design of coordination complexes (excluding complexes resulting from a reversible, supramolecular self-assembly process) that allow metal-catalysed reactions to take place inside a restricted space (bowl, clip, capsule) with the aim of controlling activity and selectivity are currently attracting the attention of several research groups.[29, 35] In the particular field of resorcinarene chemistry, Iwasawa et al. have used the digold complexes **11** and **12** (Figure 7), both based on a cavity flanked by aromatic rings, in the catalytic cross-dimerisation of terminal alkynes.[19] For example, the reaction of ethynylbenzene with 1-octyne in the presence of a mixture of **11** (1 mol %) and 2 equiv. of AgOTf gave after 20 h (rt) cross adduct **14** (58 %) and homoadduct **15** with a **14**/**15** ratio of 3.0:1 (Scheme 5, top). With the less expanded cavity **12** the yield of **14** dropped to 6% with a **14**/**15** ratio of 4.3:1, while model compound **13** did not catalyse the reaction at all. The authors also investigated the homodimerisation of 1-octyne, leading to **16** and its isomer *iso*-**16** (Scheme 5, bottom) The bis-quinoxaline-bridged complex **11** gave **16** selectively in 63 % yield. In contrast, with bis-pyrazine **12,** the yield of **16** droped to 18 %, and the formation of small amounts of *iso*-**16** was observed (**16**:*iso*-**16** = 97:3). With the non-walled cavitand **13**, only trace amounts of coupling adducts were observed. Overall, these studies illustrate the superiority of quinoxaline-expanded cavitand **11** over that of **12** and **13** in the catalytic dimerisation of terminal alkynes. The authors proposed that the catalysis with **11** occurred in a supramolecular
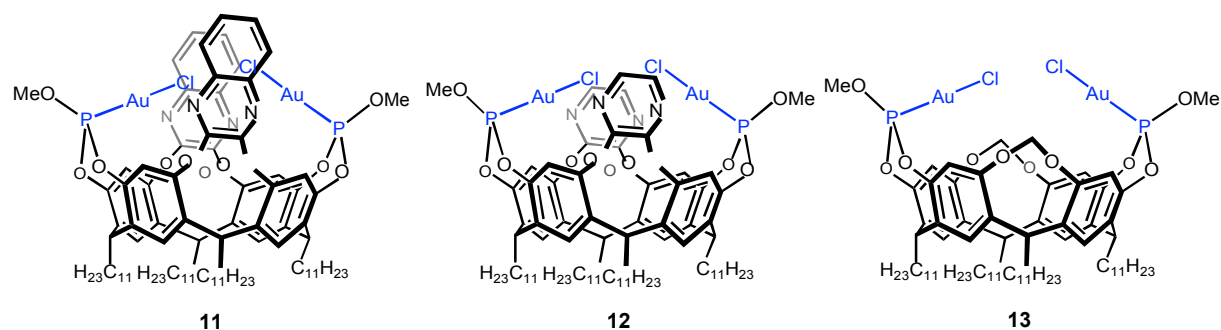
Figure 7. Digold complexes based on resorcinarene cavitands

manner, the quinoxaline parts providing a stronger π-cloud than that found in the interior of **11** and **12**, thereby strongly enhancing the interaction of the two alkyne partners. The confinement created by **11** further limits the number of transition-state geometries, this possibly being at the origin of the slightly higher selectivity found with **11** *vs*. **12**. The authors also showed that the presence of *two* introverted Au atoms is quintessential for catalysis.[36] Similar results were obtained with analogues of **11** having NMe$_2$ instead of OMe substituents on phosphorus.[37]

catalyst	yield of **14**	ratio **14/15**
cat. **11**	58 %	3.0:1
cat. **12**	6 %	4.3:1
cat. **13**	0 %	-

catalyst	yield of **16**	ratio **16**/*iso*-**16**
cat. **11**	63 %	100:0
cat. **12**	18 %	97:3
cat. **13**	trace	> 99:1
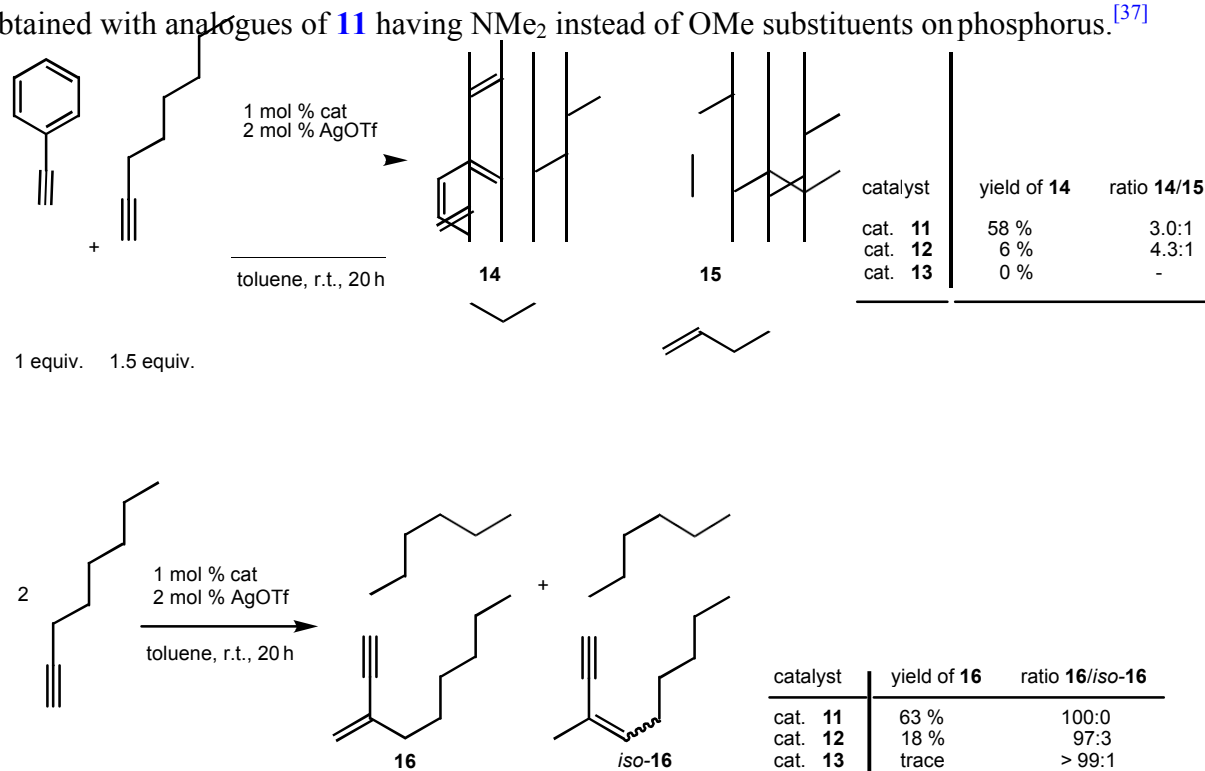
Scheme 5. Catalytic reactions involving terminal alkynes with digold catalysts **11-13**

The same research team also synthesised cavitands **17-19**, all equipped with three quinoxaline walls and bearing a single, inwardly directed P-Au unit (Scheme 6).[38] Complex **17** turned out to be efficient in the catalytic hydration of 9-ethynylanthracene (Scheme 6). All three complexes also catalysed a Conia-ene reaction of the β-keto ester alkyne **20** (Scheme 6). The

main conclusion of these investigations was that the top of the catalytic site of these complexes remains open so that guests can sample the space, enter and leave, and thus these complexes may efficiently operate as catalysts.
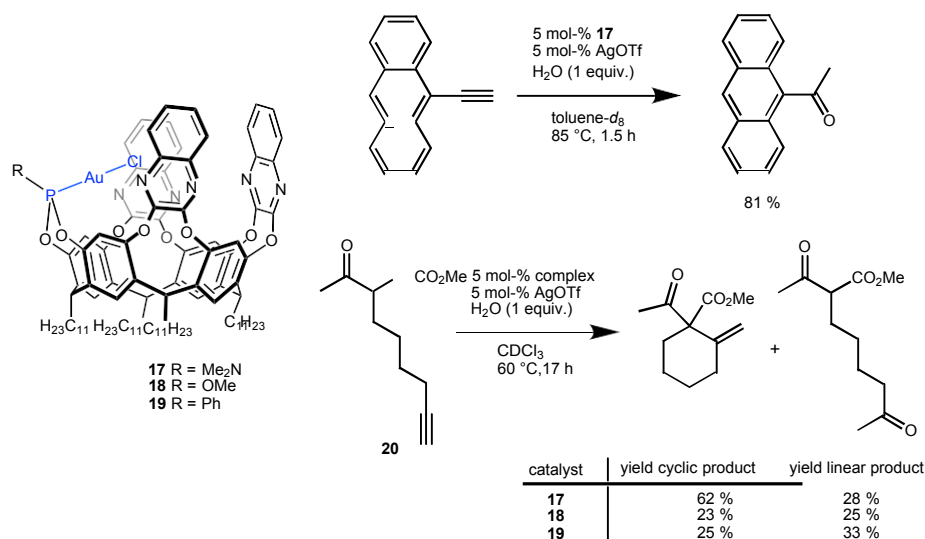
Scheme 6. Catalytic reactions carried out with the bowl-shaped monogold complexes **17-19**

The first Buchwald-type biarylphosphine based on a cavitand, **21**, was reported by Elaieb et al. (Fig. 8).[39] This ligand displayed activities in SM coupling of bulky aryl chlorides with sterically hindered arylboronic acids that were ca. 40 % higher than those of the Buchwald analogue S-Phos (**22**), which is devoid of a cavity. Its better performance has been attributed to the permanent *exo*-positioning of the metal during catalysis, which enables steric interactions of two pentyl substituents with the second coordination sphere of the metal, this influencing the reductive elimination step (a similar effect was invoked with catalysts derived from **36-38**, *vide infra*).
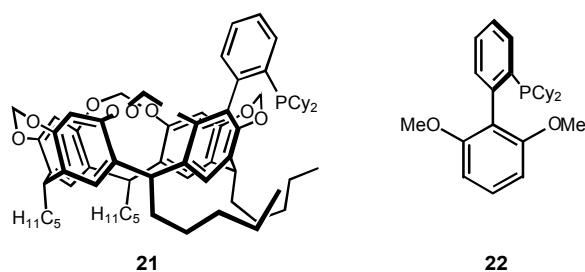
Figure 8. Biarylphosphines **21** and **22**

Several recent publications have illustrated the manner in which cavitands can be used for the generation of molecular capsules.[40] Capsule synthesis may be realised by covalent construction,[22d] a procedure extensively developed as the basis of carcerand chemistry but, more conveniently, such molecules can also be generated by self-assembly processes, these involving either metal complexation,[22c, 41] hydrogen bonding[42] or van der Waals interactions.[43] Many of the reported cages have been shown suitable for hosting large guests. An example of capsule formation through metal chelation and which does not involve a self-assembly process, is provided in the use of a diphosphine built on a backbone consisting of two covalently linked cavitands (23).[44] Reaction of 23 with [PtCl₂(PhCN)₂] under high dilution afforded the metallo-capsules *cis*-24 and *trans*-24 (Scheme 7). The former was used succesfully in combination with
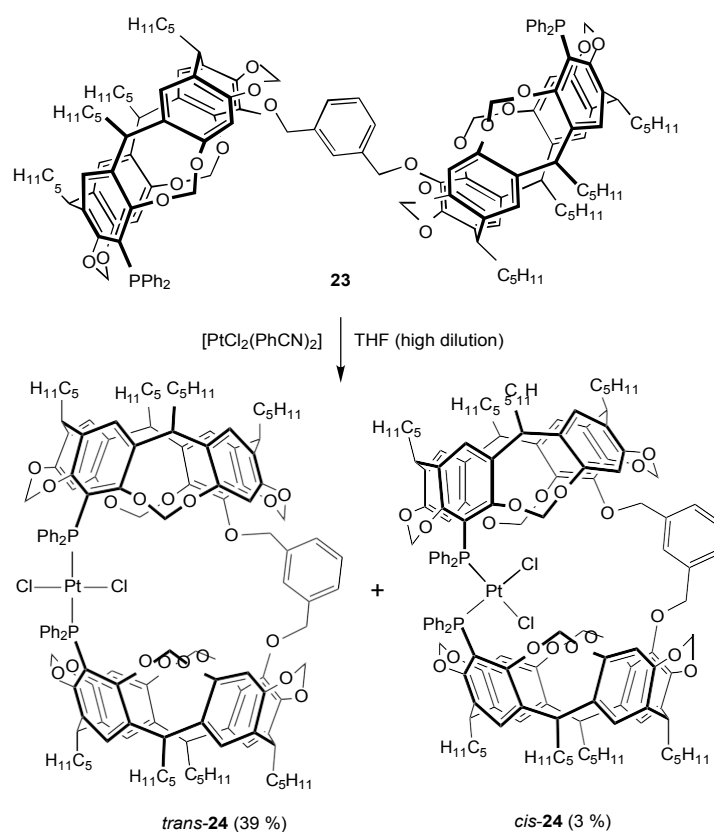
Scheme 7. Formation of metallocapsules from diphosphine 23

SnCl₂ for the hydroformylation of styrene. The activity and selectivity (Table 3) of the system towards the branched aldehyde were both significantly superior to those observed for the reference complex *trans*-PtCl₂L₂, in which L is the monophosphane-monocavitand 8, as well as PPh₃. The increased activity of the capsular complex may reflect the initial formation of a hydrido intermediate with a somewhat *distorted* trigonal-bipyramidal structure that facilitates the intracapsular olefin/PtH insertion step. The observed aldehyde selectivity can be understood as a

15

consequence of the shape of the capsule, which is sterically better suited for hosting a branched Pt–alkyl unit than a linear one (Scheme 8). The catalytic outcome with *trans*-**24** was similar to that obtained with *trans*-[PtCl(SnCl$_3$)(**23**)] (run performed without additional SnCl$_2$).

Table 3. Hydroformylation of styrene with *trans*-**24**/SnCl$_2$

Entry	Platinum complex	Time (h)	Conversion (%)	Aldehydes distribution	
				Linear (%)	Branched (%)
1	*trans*-**24**	24	55	36	64
2	*trans*-[PtCl$_2$(**8**)$_2$]	24	15	46	54
3	*trans*-[PtCl$_2$(PPh$_3$)$_2$]	24	40	53	47
4	*trans*-[PtCl(SnCl$_3$)(**23**)]	16	60	38	62

General conditions: [Pt] (1 mol %), SnCl$_2$ (2 mol %; except for entry 4: 0%), styrene (1 mmol), P(CO/H$_2$) = 45 bar, T = 100°C, toluene (5 mL). The conversions were determined by ^{1}H NMR spectroscopy.
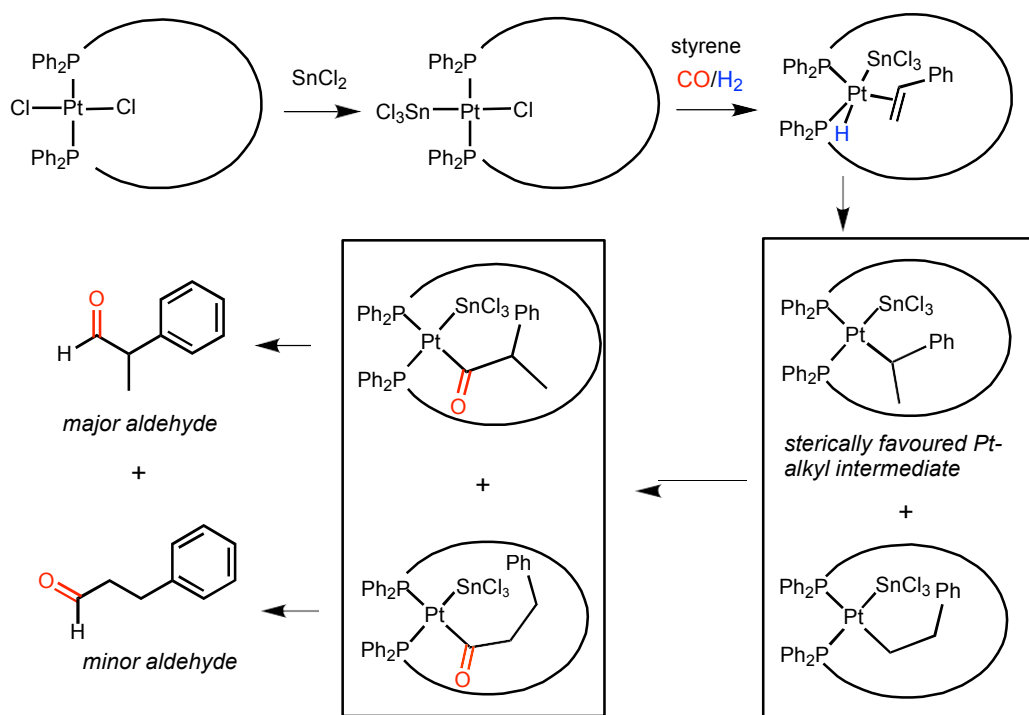
Scheme 8. Styrene hydroformylation with *trans*-**24**/SnCl$_2$

3. Catalytic chemistry with cavitands bearing *N*-heterocyclic carbene (NHC) units

El Moll et al. have described the synthesis of the imidazolium salts **25**-**35** (Fig. 9).[45] These are procarbenes which were assessed in Suzuki–Miyaura cross-coupling between phenyl boronic acid and several aryl bromides. Note that before this study imidazolium salts built on a resorcinarene skeleton had already been reported, but their use was restricted to molecular recognition studies.[46] In combination with [Pd(OAc)$_2$] and a base, **25**-**35** provided efficient Suzuki–Miyaura catalysts for the cross-coupling of aryl bromides with phenylboronic acid. The highest activity (TOF = 41,600 mol(ArBr) mol(Pd)$^{-1}$ h^{-1}) was observed in the arylation of 1-bromonaphthalene in the presence of the proximally-disubstituted cavitand **30**. In fact, only relatively small differences in activity were observed within the three series of imidazolium salts, indicating that they all behave as single-site NHC sources.

25 R = Ph
26 R = Mes
27 R = *i*Pr$_2$C$_6$H$_3$

28 R = *n*Bu
29 R = Ph
30 R = Mes
31 R = *i*Pr$_2$C$_6$H$_3$

32 R = *n*Bu
33 R = Ph
34 R = Mes
35 R = *i*Pr$_2$C$_6$H$_3$
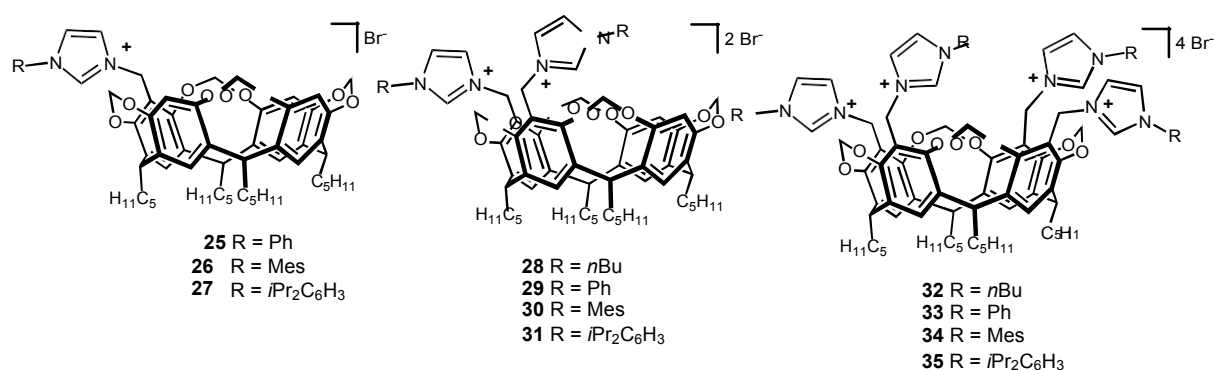
Figure 9. Procarbenes **25**-**35**

Cavitands having an imidazolium ring directly attached through an N atom to the upper rim of a cavitand (Fig. 10) have also been assessed in coupling reactions. For example, the three imidazolium salts **36**-**38** were used as catalyst precursors in Suzuki–Miyaura (SM) cross-coupling.[47] In these pro-carbenes, the second N atom was substituted by an alkyl group (R = n-propyl, iso-propyl, benzyl), and the bridging atoms of the resorcinarene unit had pentyl substituents. Optimal catalytic performances were obtained by using an imidazolium/Pd ratio of 1:1. The catalytic systems displayed high activities, which increased in the order R = *n*-propyl (**36**) < *i*-propyl (**37**) < benzyl (**38**). With **38**, activities up to 30,100 mol(converted ArX) mol(Pd)$^{-1}$ h^{-1} were reached in the arylation of bromotoluene at 100°C in dioxane. Comparative studies showed that the performance of **38** was up to 10 times superior to that of related salts devoid of a

cavity-shaped unit (**39-41**). These experiments illustrate the active role of the cavity core of the ex-**38** carbene ligand, the steric encumbrance of which facilitates the reductive elimination step (Figure 11, left part). Modification of the cavitand structure by replacement of the pentyl substituents of **38** with phenyl groups (leading to **42**) resulted in considerably lower activities, this being consistent with steric interactions between the metal centre and two pentyl groups of the ex-**38** carbene during catalysis (Figure 11, right part). The fact that the catalytic outcome may be influenced by the nature of the bridge substituents is further evidence that the Pd catalysts obtained from **36**–**38** have their metal centre preferentially located outside the cavity.

36 R = *n*Pr
37 R = *i*Pr
38 R = Bn
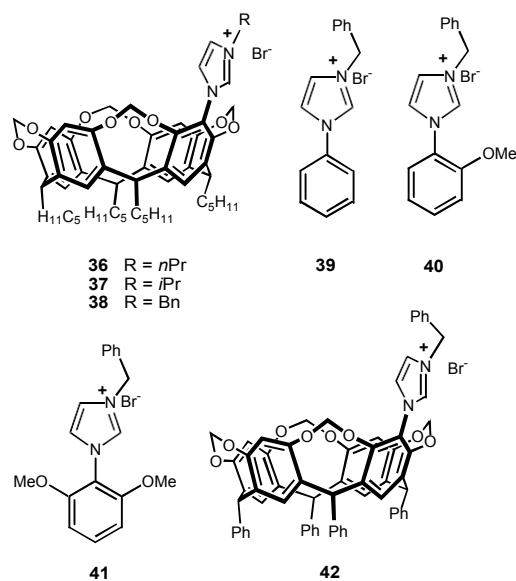
Figure 10. Procarbenes **36**-**42**
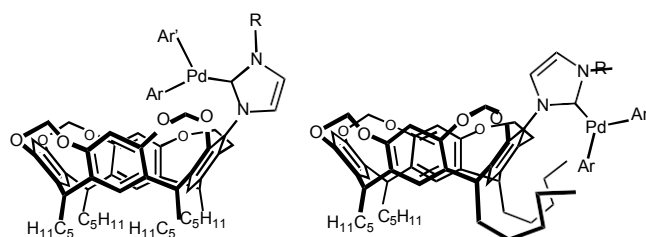
Figure 11. Sites of steric interactions in catalytic intermediates derived from **36**-**38**.

It is worth mentioning here that SM tests were also performed starting from the isolated PEPPSI-Pd complex **43**[48] (Fig. 12) (PEPPSI[49] = pyridine-enhanced precatalyst preparation stabilization and initiation) as well as related bulky ones,[50] which led to similar conclusions regarding the role played by the flexible pentyl groups at the lower rim. The investigations carried out with **43** further revealed that this catalyst is very effective in the coupling of aryl chlorides

18

with *sterically hindered* boronic acids. However, there was no clear indication that the cavity subunit operated as a receptor.
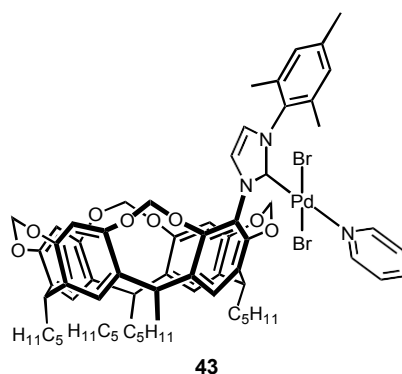
Figure 12. N-heterocyclic carbene complex **43** (PEPPSI-type)

Imidazolium salts **34-36** have been further assessed in Ni-catalysed Kumada–Tamao–Corriu cross-coupling of aryl halides with arylmagnesium halides (Scheme 9).[51] Such reactions are generally performed with palladium, but it is highly desirable to conduct these reactions with more cost-efficient catalysts, notably those based on nickel. Actually, the 1:1 combination of **34-36** with [Ni(cod)$_2$] (cod = 1,5-cyclooctadiene) resulted in very efficient systems, the activities of which varied in the same order as above for the SM coupling reactions: R = *n*-propyl (**34**) isopropyl (**35**) ≈ benzyl (**36**). A remarkable turnover frequency of 60,400 mol(ArX) mol(Ni)$^{-1}$ h^{-1} was obtained in the coupling of 2-bromo-6-methoxynaphthalene with PhMgBr (100 °C in dioxane, with precursor **36**) (Scheme 10). The high activities of these cavitands were attributed to steric effects that facilitated the reductive-elimination/product decoordination step. Comparative experiments carried out with the benzyl-bridged resorcinarene **40**, as well as cavity-free imidazolium salts bearing 2-methoxyaryl substituents, indicated that the efficiency of the above catalytic systems again was mainly due to steric interactions between the metal and the flexible pentyl substituents attached to the two methine carbon atoms closest to the heterocycle. As usual with nickel, homocoupling products were observed in the above runs, although their proportion did not exceed 13%.
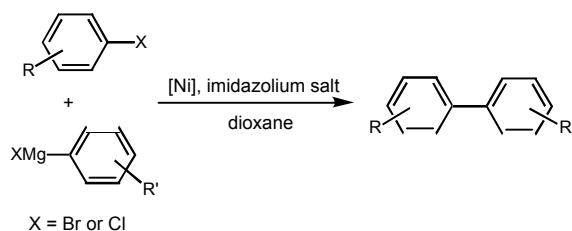
Scheme 9. Kumada-Tamao-Corriu cross-coupling with nickel
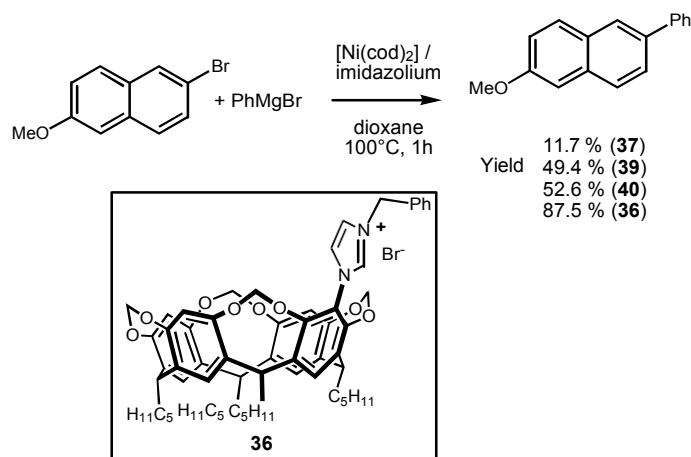
Scheme 10. Ni-catalysed coupling of 2-bromo-6-methoxynaphthalene with PhMgBr using procarbenes **36**, **37**, **39**, and **40**

Allylic substitution with organo-copper compounds has recently emerged as a method which usefully complements the palladium-catalysed version of this reaction. The main advantage of copper over palladium, besides its lower price, is that it generally allows the reaction to occur with S_N2' selectivity, *i.e.* to favour the γ-product over the α one (Scheme 11). This in turn is
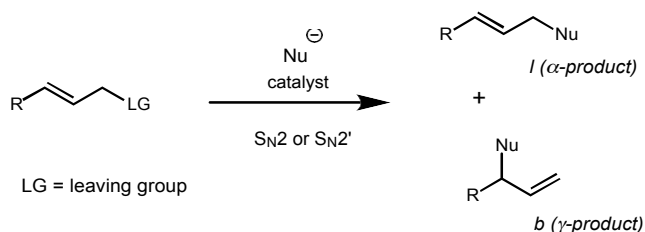
Scheme 11. Allylic substitution

relevant to the synthesis of chiral compounds. The procarbene salts **36** and **42**-**46**, all having one of their nitrogen atoms substituted by a 2,8,14,20-tetrapentylresorcinarenyl (TPR) group, were tested in situ in the copper-catalysed arylation of cinnamyl bromide with arylmagnesium halides.[52] The catalytic systems produced mixtures of linear (l) and branched (b) arylation compounds in variable proportions, the highest b/l ratio (78:22) being observed for the crowded imidazolium salt **44** (in which the second nitrogen atom bears a bulky mesityl group). Although bulky substituents are expected to favour the reductive elimination step leading to the γ-product,[52] the bulky TPR group had only a small influence on the selectivity (Figure 13). The authors proposed that it would make sense to modify the catalyst structure so as to force the

20
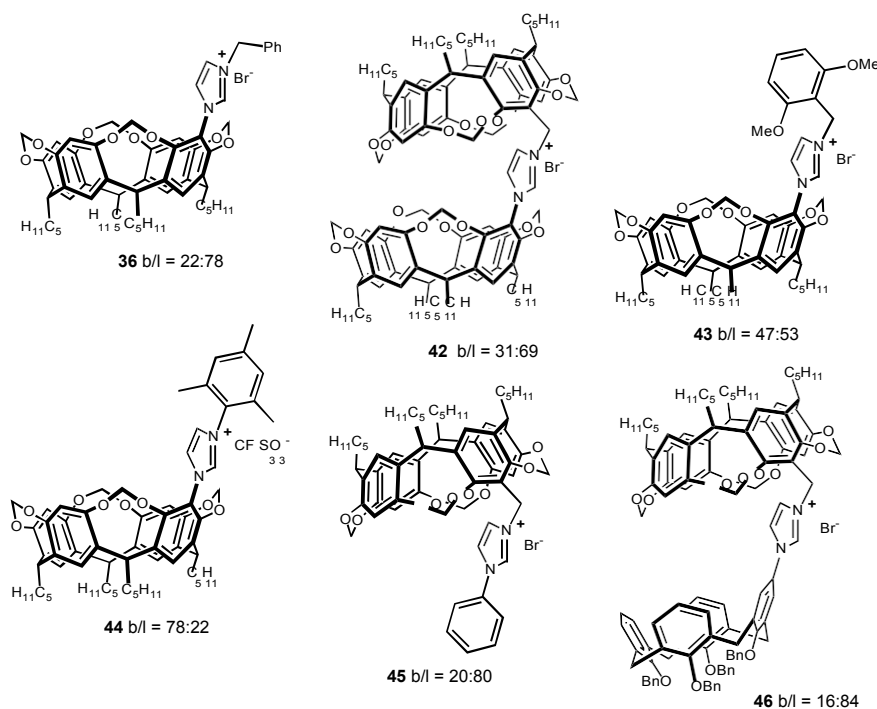
Figure 13. Branched/linear aldehyde ratios obtained in the copper-catalysed allylic alkylation of cinnamyl bromide and phenyl magnesium bromide with salts **36** and **42**-**46** (Reaction conditions: [Cu(OTf)$_2$] (1 mol-%), imidazolium salt (1 mol-%), PhCH=CHCH$_2$Br (0.32 mmol), PhMgX (0.39 mmol), Et$_2$O (3 mL), –78 °C, 1 h)
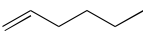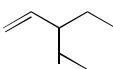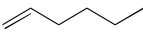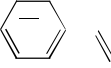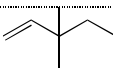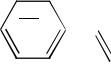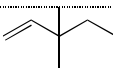
metal centre to remain located permanently above the cavitand entrance (rather than being pushed towards its exterior), markedly augmenting the ligand bulk. Finally, it should be mentioned that starting from an isolated [CuBr(NHC)] complex instead of using an imidazolium/Cu(OTf)$_2$ mixture for the catalytic runs did not significantly modify the catalytic outcome.[52]

4. Catalysis using cavitands substituted with nitrogen donors

Cavitands substituted with groups that contain a nitrogen donor atom have been little used in catalysis. Chavagnan et al. have prepared the iminophosphoranes **49**-**52**.[53] Molecular modeling revealed that because of the large N...N separation, **47** cannot act as a chelating ligand. A 1:1 mixture of **49** and [Rh(COD)$_2$]BF$_4$ was used as a catalytic system for the competitive hydrogenation of 1:1 mixtures of terminal olefins (Table 4). A remarkable substrate-selectivity factor of 39.2 in favour of the linear olefin was observed after 1 h in the reduction of a hex-1-

21

ene/3-ethyl-pent-1-ene mixture. After 8 h, the selectivity was still as high as 4.1. Carrying out the test with hex-1-ene and dec-1-ene gave selectivity factors of 5.4 and 1.6 respectively after 1 h and 8 h. The substrate selectivity was considerably lower with a mixture of olefins of similar size, such as styrene and 3-ethyl-pent-1-ene (Table 4).

Table 4. Competitive hydrogenation of α-olefins catalysed by the $[Rh(cod)_2]BF_4$/**49** system.

Entry	$R^1CH=CH_2$	$R^2CH=CH_2$	Time (h)	Hydrogenated products (%) $R^1CH_2CH_3/R^2CH_2CH_3$
1			1	19.6 / 0.5 = 39.2
2			5	62.6 / 8.4 = 7.4
3			8	84.6 / 20.4 = 4.1
4			1	13.5 / 2.5 = 5.4
5			5	48.1 / 10.2 = 4.7
6			8	77.4 / 47.8 = 1.6
7			5	36.2 / 15.0 = 2.4
8			8	58.2 / 29.0 = 2.0

General conditions: $[Rh(cod)_2]BF_4$ (1 mol %), **49** (1 mol %), olefins (1.0 mmol of each), $P(H_2)$ = 5 bar, THF (5 mL), r.t. The conversions were determined by GC.

Olefin discrimination also occurred with the glucosidic substrate **53** (Scheme 12) which contains two C=C double bonds in different steric environments. When the reaction with **53** was conducted with a H_2 pressure of 5 bar and with 2 mol-% of the catalyst, product **54**, in which only the allylic double bond had been hydrogenated, was formed exclusively in 84 % yield after 14 h.
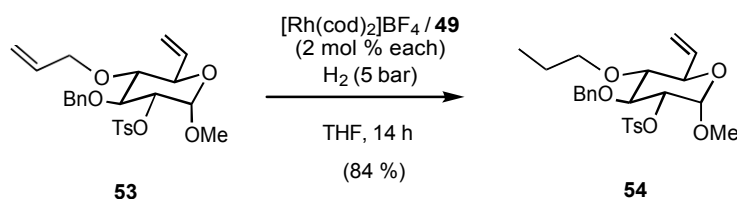
Scheme 12. Selective hydrogenation leading to **54**

By carrying out comparative studies with the iminophosphoranes **50-52** (Table 5) the authors came to the conclusion that substrate discrimination is only observed if: a) two iminophosphorane units are available per Rh centre; b) the nitrogen atoms are substituted with an aryl ring that bears a methoxy group; and c) the two iminophosphorane units are tethered to the same resorcinarene platform. Consistent with these observations, they concluded that both iminophosphorane moieties of **49** are involved in the catalytic process. Owing to the large N···N separation, this cannot occur via catalytic intermediates containing an *N,N*-chelated rhodium centre. Instead, one of the two nitrogen atoms and a methoxy group of the other anisyl-

Table 5. Competitive hydrogenation of α-olefins, influence of the ligand.[a]

| | 49 | 50 | 51 | 52 |
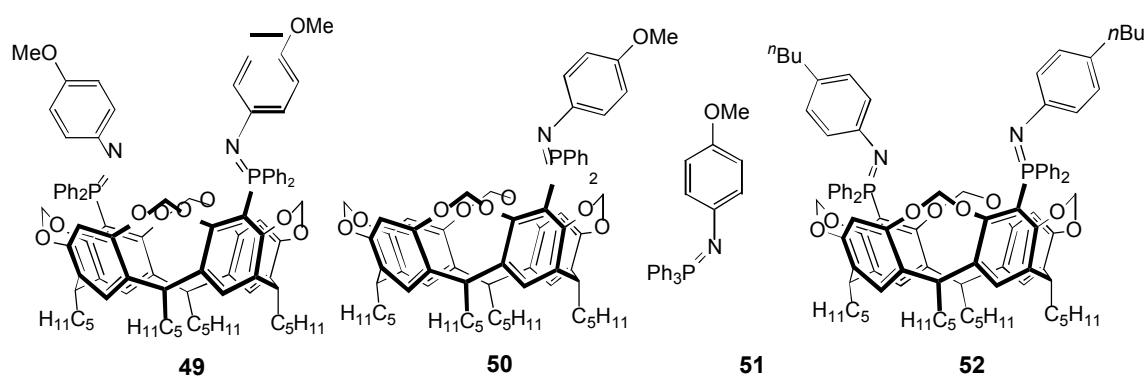
Entry	$R^1CH=CH_2$	$R^2CH=CH_2$	Ligand (L/Rh)	Hydrogenated products (%) $R^1CH_2CH_3/R^2CH_2CH_3$
1			**49** (1:1)	13.5 / 2.5 = 5.4
2			**49** (1:2)	100 / 100 = 1.0
3			**49** (2:1)	33.6 / 22.0 = 1.5
4			**50** (2:1)	35.3 / 19.5 = 1.8
5[b]			**51** (2:1)	26.2 / 20.3 = 1.3
6[c]			**52** (1:1)	36.4 / 22.6 = 1.3
7			no ligand	94.8 / 83.6 = 1.1

General conditions: [a] [Rh(cod)$_2$]BF$_4$ (1 mol %), ligand, olefins (1.0 mmol of each), P(H$_2$) = 5 bar, THF (5 mL), r.t., 1 h. The conversions were determined by GC; [b] [Rh(cod)$_2$]BF$_4$ (0.1 mol %), **51** (0.2 mol %), olefins (each 10.0 mmol), 0.1 h; [c] [Rh(cod)$_2$]BF$_4$ (0.1 mol %), **52** (0.1 mol %), olefins (each 10.0 mmol), 0.25 h.

iminophosphorane moiety must form a chelating *N,O* unit that spans the wider face of the cavitand. This would locate the rhodium centre above the main entry to the cavity and orientate two free coordination sites towards the cavity interior (Figure 14). The observed substrate selectivity can then be seen as due to a shape selective process controlled by the cavity size.
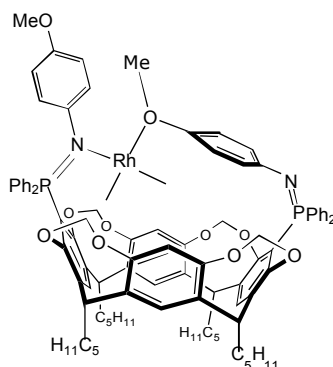
Figure 14. Proposed catalytic intermediate formed with **49**

5. Conclusions

As shown in the present review, the potential of resorcinarene-derived cavitands in catalysis arises mainly from two features: i) their ability to function as ligands suitable for metal confinement and thus for making catalytic reactions either substrate selective or by increasing efficiently reaction rates through supramolecular assistance by the cavity walls; ii) their ability to create controlled steric interactions with a coordinated metal centre and/or its first coordination sphere, thereby increasing the efficiency of carbon-carbon bond forming reactions. Interestingly, their use as platforms for the attachment of different ligating sites for the generation of multifunctional ligands that may give rise to anchimeric assistance has as yet been little exploited. As generic cavitands can be easily expanded so as to provide large, bowl-shaped structures as well as capsular containers, it may be anticipated that future research in this field will focus on sophisticated microreactors (including water-soluble versions) that will enable highly selective transformations. Such chemistry has been explored with carcerand systems but the novel aspects of what is presently proposed are the ready accessibility of the cavities and the fact that the appended species are sites of catalytic activity.

References

[1]   J. B. Niederl and H. J. Vogel, *J. Am. Chem. Soc.* **1940**, 2512-2540.

[2]   a) A. Baeyer, *Ber. Dtsch. Chem. Ges.* **1872**, *5*, 25-26; b) A. Baeyer, *Ber. Dtsch. Chem. Ges.* **1872**, *5*, 280-282.

[3]   a) A. G. S. Högberg, *J. Org. Chem.* **1980**, *45*, 4498-4500; b) A. G. S. Högberg, *J. Am. Chem. Soc.* **1980**, *102*, 6046-6050.

[4]   H. Konishi, K. Ohata, O. Morikawa and K. Kobayashi, *Chem. Comm.* **1995**, 309-310.

[5]   J. Antesberger, G. W. V. Cave, M. C. Ferrarelli, M. W. Heaven, C. L. Raston and J. L. Atwood, *Chem. Commun.* **2005**, 892-894.

[6]   B. A. Roberts, G. W. V. Cave, C. L. Raston and J. L. Scott, *Green Chemistry* **2001**, *3*, 280-284.

[7]   V. K. Jain and P. H. Kanaiya, *Russ. Chem. Rev.* **2011**, *80*, 75-102.

[8]   a) H. Erdtman, S. Högberg, S. A. Abrahamson and B. Nilsson, *Tetrahedron Lett.* **1968**, *14*, 1679-1682; b) B. Nilsson, *Acta Chem. Scand.* **1968**, *22*, 732-747.

[9]   a) J. R. Moran, S. Karbach and D. J. Cram, *J. Am. Chem. Soc.* **1982**, *104*, 5826-5828; b) F. Weinelt and H. J. Schneider, *J. Org. Chem.* **1991**, *56*, 5527-5535; c) D. J. Cram and J. M. Cram; d) I. Thondorf, A. Shivanyuk and V. Böhmer, in *Calixarenes 2001,* V. Böhmer, J. Harrowfield and J. Vicens Eds., Kluwer, The Netherlands, 2001, pp 26-53; e) I. Thondorf, in *Calixarenes 2001,* V. Böhmer, J. Harrowfield and J. Vicens Eds., Kluwer, The Netherlands, 2001, pp 280-295.

[10]   a) C. L. Raston and G. W. V. Cave, *Chem. Eur. J.* **2004**, *10*, 279-282; b) O. Ugono and K. T. Holman, *Chem. Comm.* **2006**, 2144-2146; c) R. S. Patil, A. M. Drachnik, H. Kumari, C. L. Barnes, C. A. Deakyne and J. L. Atwood, *Cryst. Growth Des.* **2015**, *15*, 2781-2786.

[11]   a) B. Q. Ma, Y. G. Zhang and P. Coppens, *Cryst. Growth Des.* **2002**, *2*, 7-13; b) A. Nakamura, T. Sato and R. Kuroda, *CrystEngComm* **2003**, *5*, 318-325; c) B. Q. Ma, L. F. V. Ferreira and P. Coppens, *Org. Lett.* **2004**, *6*, 1087-1090.

[12]   R. Puttreddy, N. K. Beyeh and K. Rissanen, *CrystEngComm* **2016**, *18*, 4971-4976.

[13]   R. S. Patil, C. Zhang and J. L. Atwood, *Chem. Eur. J.* **2016**, *22*, 15202-15207.

[14]   A. Shivanyuk, E. F. Paulus, V. Böhmer and W. Vogt, *Angew. Chem. Int. Ed.* **1997**, *36*, 1301-1303.

[15]   a) J. R. Moran, J. L. Ericson, E. Dalcanale, J. A. Bryant, C. B. Knobler and D. J. Cram, *J. Am. Chem. Soc.* **1991**, *113*, 5707-5714; b) V. A. Azov, A. Beeby, M. Cacciarini, A. G. Cheetham, F. Diederich, M. Frei, J. K. Gimzewski, V. Gramlich, B. Hecht, B. Jaun, T. Latychevskaia, A. Lieb, Y. Lill, F. Marotti, A. Schlegel, R. R. Schlittler, P. J. Skinner, P.

Seiler and Y. Yamakoshi, *Adv. Funct. Mater.* **2006**, *16*, 147-156; c) D. J. Cram, *Science* **1983**, *219*, 1177-1183; d) W. Verboom, in *Calixarenes 2001,* V. Böhmer, J. Harrowfield and J. Vicens Eds., Kluwer, The Netherlands, 2001, pp 181-198.

[16] a) W. Xu, J. P. Rourke, J. J. Vittal and R. J. Puddephatt, *Inorg. Chem.* **1995**, *34*, 323-329; b) P. Sakhaii, I. Neda, M. Freytag, H. Thönnessen, P. G. Jones and R. Schmutzler, *Z. Anorg. Allg. Chem.* **2000**, *626*, 1246-1254; c) R. Pinalli, M. Suman and E. Dalcanale, *Eur. J. Org. Chem.* **2004**, 451-462; d) R. J. Puddephatt, *Can. J. Chem.* **2006**, *84*, 1505-1514; e) J. Vachon, S. Harthong, B. Dubessy, J. P. Dutasta, N. Vanthuyne, C. Roussel and J. V. Naubron, *Tet. Asymmetry* **2010**, *21*, 1534-1541.

[17] S. N. Parulekar, K. Muppalla, F. R. Fronczek and K. S. Bisht, *Chem. Comm.* **2007**, 4901-4903.

[18] D. Masseroni, S. Mosca, M. P. Mower, D. G. Blackmond and J. Rebek, *Angew. Chem. Int. Edit.* **2016**, *55*, 8290-8293.

[19] M. Kanaura, N. Endo, M. P. Schramm and T. Iwasawa, *Eur. J. Org. Chem.* **2016**, 4970-4975.

[20] D. J. Cram and J. M. Cram, *Container Molecules and their Guests,* monographs in Supramolecular Chemistry, No.4, J. F Stoddart, Series Editor, Royal Society of Chemistry, Cambridge, 1994, Ch. 6, pp.107-130.

[21] a) S. M. Butterfield and J. Rebek, *Chem. Commun.* **2007**, 1605-1607; b) E. Biavardi, G. Battistini, M. Montalti, R. M. Yebeutchou, L. Prodi and E. Dalcanale, *Chem. Commun.* **2008**, 1638-1640; c) T. V. Nguyen, D. J. Sinclair, A. C. Willis and M. S. Sherburn, *Chem. Eur. J.* **2009**, *15*, 5892-5895; d) S. Javor and J. Rebek, *J. Am. Chem. Soc.* **2011**, *133*, 17473-17478.

[22] a) D. J. Cram, S. Karbach, Y. H. Kim, L. Baczynskyj and G. W. Kalleymeyn, *J. Am. Chem. Soc.* **1985**, *107*, 2575-2576; b) P. Timmerman, M. G. A. van Mook, W. Verboom, G. J. Vanhummel, S. Harkema and D. N. Reinhoudt, *Tet. Lett.* **1992**, *33*, 3377-3380; c) P. Jacopozzi and E. Dalcanale, *Angew. Chem. Int. Edit.* **1997**, *36*, 613-615; d) R. Warmuth, *J. Incl. Phenom. Macrocyclic Chem.* **2000**, *37*, 1-38; e) J. Sherman, *Chem. Comm.* **2003**, 1617-1623; f) R. J. Hooley and J. Rebek, *Chem Biol.* **2009**, *16*, 255-264.

[23] S. Mendoza, P. D. Davidov and A. E. Kaifer, *Chem. Eur. J.* **1998**, *4*, 864-870.

[24] a) J. Gout, A. Visˇnjevac, S. Rat, O. Bistri, N. Le Poul, Y. Le Mest and O. Reinaud, *Eur. J. Inorg. Chem.* **2013**, *2013*, 5171-5180; b) D. Sémeril and D. Matt, *Coord. Chem. Rev.* **2014**, *279*, 58-95; c) J. Gout, S. Rat, O. Bistri and O. Reinaud, *Eur. J. Inorg. Chem.* **2014**, *2014*, 2819-2828.

[25] a) J. C. Sherman, *Tetrahedron* **1995**, *51*, 3395-3422; b) C. Naumann and J. C. Sherman, in *Calixarenes 2001,* V. Böhmer, J. Harrowfield and J. Vicens Eds., Kluwer, The Netherlands, 2001, pp 199-218.

[26] P. Roncucci, L. Pirondini, G. Paderni, C. Massera, E. Dalcanale, V. A. Azov and F. Diederich, *Chem. Eur. J.* **2006**, *12*, 4775-4784.

[27] R. Gramage-Doria, D. Armspach and D. Matt, *Coord. Chem. Rev.* **2013**, *257*, 776-816.

[28] a) G. Arnott, H. Heaney, R. Hunter and P. C. B. Page, *Eur. J. Org. Chem.* **2004**, 5126-5134; b) L. Ngodwana, S. Bose, V. Smith, W. A. L. van Otterlo and G. E. Arnott, *Eur. J. Inorg. Chem.* **2017**, 1923-1929.

[29] C. Gibson and J. Rebek Jr., *Org. Lett.* **2002**, *4*, 1887-1890.

[30] H. El Moll, D. Sémeril, D. Matt and L. Toupet, *Adv. Synth. Catal.* **2010**, *352*, 901-908.

[31] H. El Moll, D. Sémeril, D. Matt, M. T. Youinou and L. Toupet, *Org. Biomol. Chem.* **2009**, *7*, 495-501.

[32] M. Feuerstein, H. Doucet and M. Santelli, *J. Org. Chem.* **2001**, *66*, 5923-5925.

[33] L. Monnereau, H. El Moll, D. Sémeril, D. Matt and L. Toupet, *Eur. J. Inorg. Chem.* **2014**, *2014*, 1364-1372.

[34] a) T. Chavagnan, D. Sémeril, D. Matt, J. Harrowfield and L. Toupet, *Chem. Eur. J.* **2015**, *21*, 6678-6681; b) T. Chavagnan, D. Sémeril, D. Matt, L. Toupet, J. Harrowfield and R. Welter, *Eur. J. Inorg. Chem.* **2016**, 497-502.

[35] a) P. Thordarson, E. J. A. Bijsterveld, A. E. Rowan and R. J. M. Nolte, *Nature* **2003**, *424*, 915-918; b) D. Sémeril, C. Jeunesse, D. Matt and L. Toupet, *Angew. Chem. Int. Ed.* **2006**, *45*, 5810-5814; c) M. Jouffroy, R. Gramage-Doria, D. Sémeril, D. Armspach, D. Matt, W. Oberhauser and L. Toupet, *Beilstein J. Org. Chem.* **2014**, *10*, 2388-2405; d) M. Teci, E. Brenner, D. Matt, C. Gourlaouen and L. Toupet, *Dalton Trans.* **2015**, *44*, 9260-9268; e) M. Teci, N. Lentz, E. Brenner, D. Matt and L. Toupet, *Dalton Trans.* **2015**, *44*, 13991-13998; f) M. Jouffroy, D. Armspach, D. Matt, K. Osakada and D. Takeuchi, *Angew. Chem. Int. Edit.* **2016**, *55*, 8367-8370.

[36] N. Endo, M. Kanaura, M. P. Schramm and T. Iwasawa, *Tet. Lett.* **2016**, *57*, 4754-4757.

[37] N. Endo, M. Kanaura, M. P. Schramm and T. Iwasawa, *Eur. J. Org. Chem.* **2016**, 2514-2521.

[38] M. P. Schramm, M. Kanaura, K. Ito, M. Ide and T. Iwasawa, *Eur. J. Org. Chem.* **2016**, 813-820.

[39] F. Elaieb, D. Sémeril and D. Matt, *Eur. J. Inorg. Chem.* **2017**, 685-693.

[40] W. Śliwa, *Arkivoc* **2006**, 137-159.

[41]   a) Y. Cohen, L. Avram and L. Frish, *Angew. Chem. Int. Ed.* **2005**, *44*, 520-554; b) D. Zuccaccia, L. Pirondini, R. Pinalli, E. Dalcanale and A. Macchioni, *J. Am. Chem. Soc.* **2005**, *127*, 7025-7032.

[42]   A. Lledó, S. Kamioka, A. C. Sather and J. Rebek, *Angew. Chem. Int. Ed.* **2011**, *50*, 1299-1301.

[43]   F. Corbellini, F. W. B. van Leeuwen, H. Beijleveld, H. Kooijman, A. L. Spek, W. Verboom, M. Crego-Calama and D. N. Reinhoudt, *New J. Chem.* **2005**, *29*, 243-248.

[44]   T. Chavagnan, D. Sémeril, D. Matt and L. Toupet, *Eur. J. Org. Chem.* **2017**, 313-323.

[45]   H. El Moll, D. Sémeril, D. Matt, L. Toupet and J. J. Harrowfield, *Org. Biomol. Chem.* **2012**, *10*, 372-382.

[46]   a) S. K. Kim, B. G. Kang, H. S. Koh, Y. J. Yoon, S. J. Jung, B. Jeong, K. D. Lee and J. Yoon, *Org. Lett.* **2004**, *6*, 4655-4658; b) S. K. Kim, B. S. Moon, J. H. Park, Y. Seo, H. S. Koh, Y. J. Yoon, K. D. Lee and J. Yoon, *Tetrahedron Lett.* **2005**, *46*, 6617-6620; c) W. W. H. Wong, M. S. Vickers, A. R. Cowley, R. L. Paul and P. D. Beer, *Org. Biomol. Chem.* **2005**, *3*, 4201-4208.

[47]   N. Şahin, D. Sémeril, E. Brenner, D. Matt, I. Özdemir, C. Kaya and L. Toupet, *ChemCatChem* **2013**, *5*, 1116-1125.

[48]   M. Kaloğlu, D. Sémeril, E. Brenner, D. Matt, I. Özdemir and L. Toupet, *Eur. J. Inorg. Chem.* **2016**, 1115-1120.

[49]   M. G. Organ, M. Abdel-Hadi, S. Avola, N. Hadei, J. Nasielski, C. J. O'Brien and C. Valente, *Chem. Eur. J.* **2007**, *13*, 150-157.

[50]   N. Şahin, D. Sémeril, E. Brenner, D. Matt, C. Kaya and L. Toupet, *Turk. J. Chem.* **2015**, *39*, 1171-1179.

[51]   N. Şahin, D. Sémeril, E. Brenner, D. Matt, I. Özdemir, C. Kaya and L. Toupet, *Eur. J. Org. Chem.* **2013**, *2013*, 4443-4449.

[52]   M. Kaloğlu, N. Şahin, D. Sémeril, E. Brenner, D. Matt, I. Özdemir, C. Kaya and L. Toupet, *Eur. J. Org. Chem.* **2015**, 7310-7316.

[53]   T. Chavagnan, C. Bauder, D. Sémeril, D. Matt and L. Toupet, *Eur. J. Inorg. Chem.* **2017**, 70-76.

Objectives of the thesis

The preorganising properties of cavity-shaped calix[4]arene and resorcin[4]arene platforms have been exploited for the synthesis of difunctional ligands able to control the first and second coordination spheres of coordinated transition metals, this being achieved through grafting of coordinating units on the cavity walls. In our approach, the upper rim of conical building blocks have been functionalised with phosphite, imidazole or triazole coordinating units.

Chapter II

Chiral calixarene and resorcinarene derivatives. Conical cavities substituted at their upper rim by two phosphito units and their use as ligands in Rh-catalysed hydroformylation

Abstract

Two chiral diphosphites, (*S*,*S*)-5,17-bis(1,1'-binaphthyl-2,2'-dioxyphosphanyloxy)-25,26,27,28-tetrapropyloxycalix[4]arene (**1**) and (*S*,*S*)-5,11-bis(1,1'-binaphthyl-2,2'-dioxyphosphanyloxy)-4(24),6(10),12(16),18(22)-tetramethylenedioxy-2,8,14,20-tetrapentylre sorcin[4]arene (**2**), each based on a conical cavity, were synthesised and assessed in the rhodium-catalysed hydroformylation of vinyl arenes. Under optimised conditions, both ligands led to ca. 89 % branched aldehyde in the hydroformylation of styrene. The observed enantioselectivity was significantly higher for **1** than for **2** (cf. 89 % vs. 50 % ee), this being probably related to the formation of a chelate complex only with the former ligand, which enables a more efficient chirality transfer to the catalytic centre.

Introduction

The hydroformylation reaction (or oxo process) is the synthesis of aldehydes from alkenes by the addition of carbon monoxide and hydrogen in the presence of a metal catalyst. This process, the discovery of which stretches back to 1938,[1] currently constitutes the main route for the industrial production of linear C_3-C_{19} aldehydes (Scheme 1). These can be subsequently converted into plasticisers and detergent alcohols, as well as acids and other derivatives. The annual world production of oxo products reaches almost 10 million tons.[2]
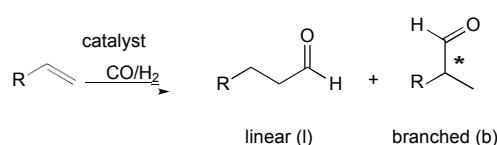
Scheme 1: Hydroformylation of α-olefins.

Until the early 1970s, most hydroformylation catalysts were based on cobalt, but their low reactivities needed to be compensated for by high temperatures and pressures. In 1965, Wilkinson, Osborn and Young demonstrated that rhodium associated with triphenylphosphine led to efficient systems able to catalyse the hydroformylation of α-olefins under milder conditions.[3] Since then, cobalt catalysts have gradually been replaced by rhodium, this metal being most often associated with P(III) ligands (typically phosphines or phosphites).[4]

On the other hand, asymmetric hydroformylation, which can be achieved with chiral ligands, represents a valuable synthetic route for the formation of optically pure (branched) aldehydes.[5] Thus for example, the biological active molecules ibuprofen, ketoprofen and naproxen (Figure 1) can be synthesised readily from appropriate styrene derivatives via an asymmetric hydroformylation step.[6] Note that in the case of styrene the branched aldehyde is generally predominantly formed owing to the facile formation of a stable η^3-allyl intermediate involving the α-C atom of the nearby phenyl ring.[7]
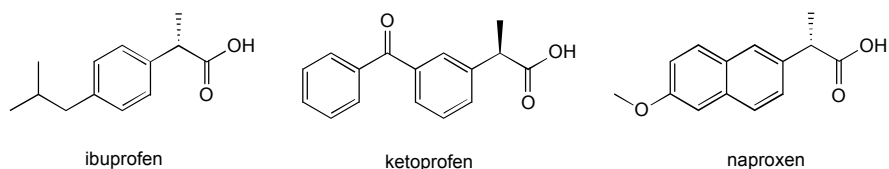
Figure 1: Molecules of biological interest obtained via asymmetric hydroformylation.

As an extension to our studies on large diphosphites built upon cavity-shaped building blocks, we now describe the synthesis of two cone-shaped cavities (calixarene **1** and resorcinarene **2**) having both their wider rim substituted by two chiral "O-P(bino)" units (binoH = 1,1'-bi-2-naphthol) (Figure 2). Both ligands were assessed in the asymmetric hydroformylation of vinyl arenes. Diphosphite **1** constitutes the first example of a calixarene having phosphito groups directly attached to its upper rim. Conical calixarenes bearing two phosphito groups attached to their smaller rim have already been reported, but these were found not suitable for the selective synthesis of branched aldehydes.[8]
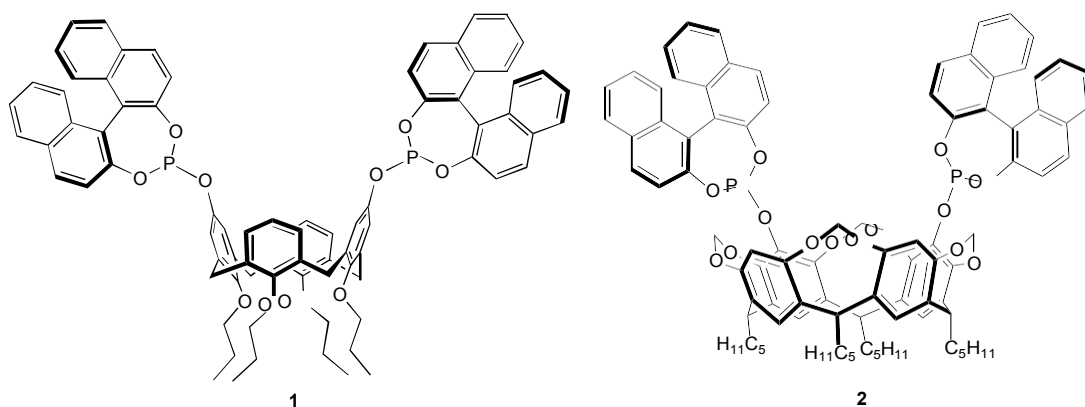
Figure 2: Macrocyclic diphosphites **1** and **2** synthetized and assessed in asymmetric hydroformylation.

Results and discussion

Diphosphite **1** was synthesised by double deprotonation with NaH of the dihydroxy-calix[4]arene **3** followed by reaction with (*S*)-(1,1'-binaphthalene-2,2'-diyl)chlorophosphite (Scheme 2). After purification, diphosphite **1** was obtained in 37 % yield. Its ^{31}P NMR spectrum displays a singlet at 143.4 ppm. In keeping with a C_2-symmetrical structure, the ^{1}H NMR spectrum of **1** displays two

distinct AB patterns for the diastereotopic ArCH$_2$Ar protons. The conical conformation of the calix[4]arene skeleton was inferred from the corresponding ^{13}C NMR spectrum, which shows ArCH_2Ar signals at 31.44 and 31.33 ppm. These two values lie in a range typical for this conformation.[9]
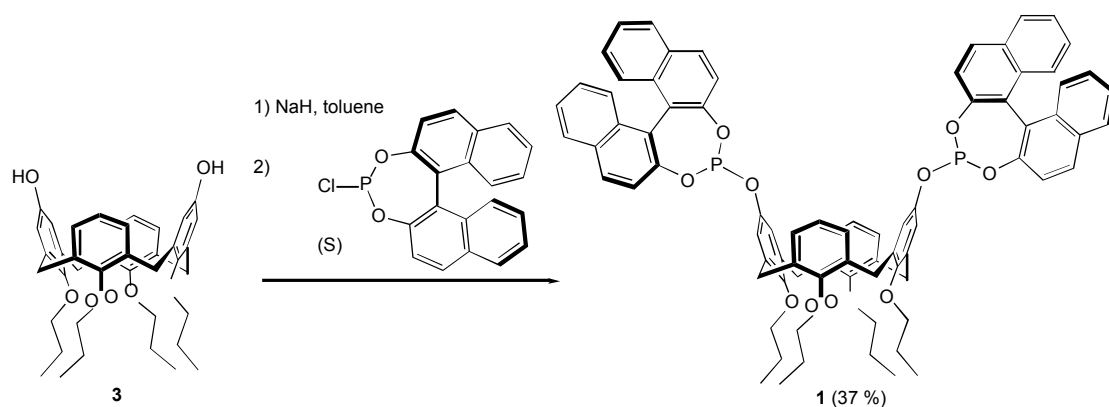
Scheme 2: Synthesis of the calixarenyl-diphosphite **1**.

The resorcinarene-diphosphite **2** was prepared in two steps from bromo-cavitand **4**, as shown in Scheme 3. Its synthesis began with a halogen/lithium exchange followed by reaction with B(OMe)$_3$. Subsequent oxidation with H$_2$O$_2$/NaOH led to the expected dihydroxy-cavitand **5**, isolated in 73 % yield. The phosphorus atoms were then introduced by double deprotonation with NaH of **5** followed by reaction with (*S*)-(1,1'-binaphthalene-2,2'-diyl)chlorophosphite in toluene. After workup, compound **2** was obtained in 23 % yield. In keeping with a *C$_1$*-symmetrical molecule diphosphite **2** shows two singlets in its ^{31}P NMR spectrum (δ = 149.7 and 149.2 ppm) and the corresponding ^{1}H NMR spectrum reveals the presence of four AB patterns for the four OCH$_2$O groups and four triplets for the methine groups.
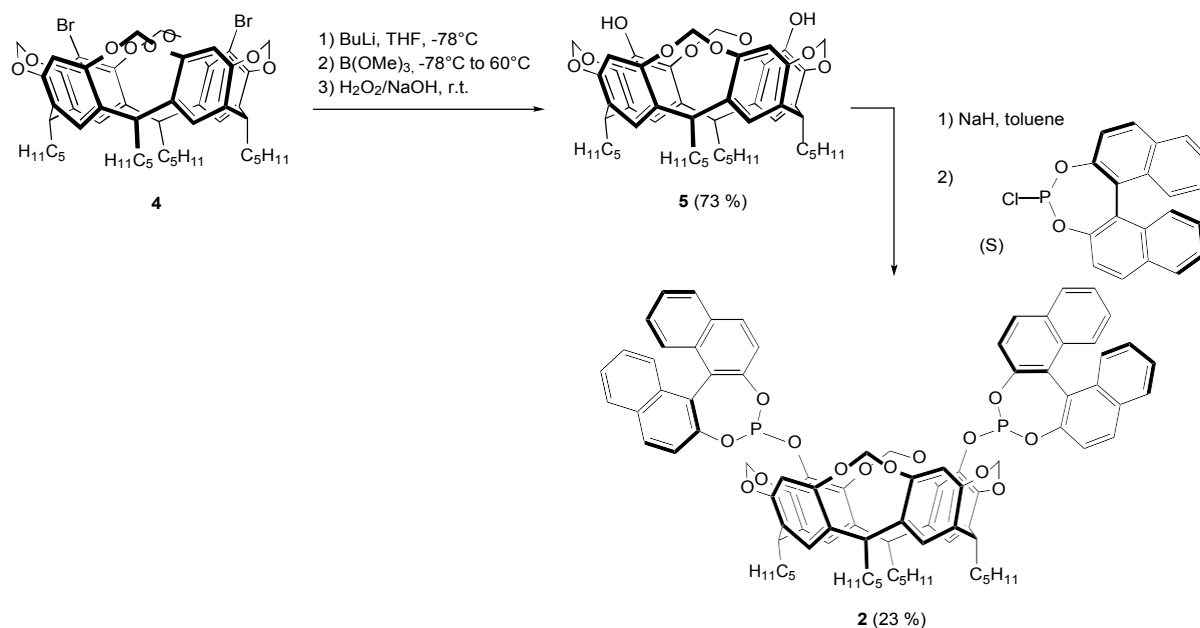
Scheme 3: Synthesis of resorcinarene-diphosphite **2**.

Catalytic asymmetric hydroformylation of vinyl arenes with diphosphites **1** and **2**

Both diphosphites were assessed in the rhodium-catalysed asymmetric hydroformylation of vinyl arenes. The catalysts were generated *in situ* by mixing [Rh(acac)(CO)$_2$] with an appropriate amount of ligand in toluene. Catalyst activation was then carried out with a CO/H$_2$ mixture (1:1, v/v; 15 bar) at 80°C and during 16 h.

To determine the optimal catalytic conditions, a series of styrene hydroformylation tests were performed. The runs were conducted not only at various CO/H$_2$ and **1**/Rh ratios, but also at several temperatures and pressures (Table 1). We started the study by using one equivalent of ligand per rhodium atom and applying a styrene/Rh ratio of 5000. In this case, the conversion observed after 24 h for a reaction carried out at 80°C under 20 bar was 89 % with a branched aldehyde regioselectivity of 75 % and an enantiomeric excess (ee) of 46 % (Table 1, entry 1). Reaction monitoring by gas chromatography revealed that the aldehyde distribution varied during the experiment, the proportion of branched aldehyde decreasing from 92 % (after 4 h) to 75 % (after 24 h; see SI). These results clearly show an evolution of the active species, which is probably related to ligand dissociation during catalysis with formation of phosphite-free rhodium complexes. In order to favor the formation of phosphite-stabilised complexes, we carried out a second run using a **1**/Rh ratio of 10 : 1. This maintained the regioselectivity constant (b/l = 91:9) over the whole test, although the conversion was then weaker (28 % vs. 89 % using a **1**/Rh ratio

of 1 : 1) (Table 1, entry 2). The conversion could be increased by applying a **1**/Rh ratio of 5 : 1, this occurring without loss of branched aldehyde selectivity. In this experiment 2-phenylpropanal was formed with an enantiomeric excess (ee) of 74 % (Table 1, entry 3). The variation of the partial pressures of hydrogen and carbon monoxide did not significantly affect the regioselectivities nor the ees of the branched aldehydes (Table 1, entries 4 and 5). As expected, lower temperatures slowed down the reaction rate and increased the proportion of branched aldehyde as well as the enantioselectivity (Table 1, entries 6-8). At an optimal temperature of 50°C, 2-phenylpropanal was produced with a regioselectivity of 97 % and an ee of 88 % (Table 1, entry 6). Further, the olefin conversion could be increased with a higher catalyst loading. Thus, operating with a styrene/Rh ratio of 1000, a conversion of 82 % with a b/l ratio of 88:12 and an ee of 89 % were measured after 24 h (Table 1, entry 9).
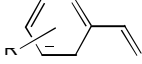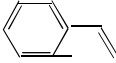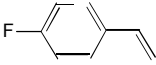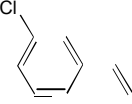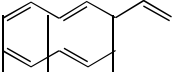
Table 1: Rhodium-catalysed hydroformylation of styrene using diphosphite **1** – search of the optimal catalytic conditions.[a]

Entry	Rh/**1**	T (°C)	P(CO)/P(H$_2$) (bar)	(v/v)	Conversion (%)[b]	Aldehyde distribution		
						l (%)[c]	b (%)[c]	ee (%)[d]
1	1/1	80	20	1:1	89	25	75	46
2	1/10	80	20	1:1	29	9	91	74
3	1/5	80	20	1:1	67	6	94	74
4	1/5	80	20	1:2	72	11	89	73
5	1/5	80	20	2:1	48	8	92	74
6	1/5	50	20	1:1	45	3	97	88
7	1/5	40	20	1:1	12	traces	> 99	83
8	1/5	40	40	1:1	20	traces	> 99	82
9[b]	1/5	50	20	1:1	82	12	88	89

Reagents and conditions: [a] [Rh(acac)(CO)$_2$] (2 µmol), **1**, styrene (10 mmol), toluene/*n*-decane (15 mL/0.5 mL), 24 h, incubation over night at 80°C under P(CO/H$_2$) = 15 bar; [b] styrene (2 mmol); [c] determined by GC using decane as internal standard; [d] determined by chiral-phase GC after reduction with LiAlH$_4$.

Applying these optimised conditions ([Rh(acac)(CO)$_2$], diphosphite/Rh = 5, vinyl arene/Rh = 1000, P(CO/H$_2$) = 20 bar (1:1, v/v), 24 h at 50°C), six vinyl arenes, namely styrene, 4-

Table 2: Rhodium-catalysed hydroformylation of vinyl arenes using diphosphites **1** and **2**.[a]

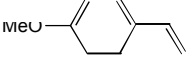| Entry		Ligand	Conversion (%)[b]	Aldehyde distribution		
				l (%)[b]	b (%)[b]	ee (%)[c]
1		**1**	82	12	88	89
2		**2**	100	13	87	50
3[d]		Rh complex **6**	59	12	88	12
4[e]		Rh complex **6** + **1**	39	15	85	6
5[f]		**7**	82	9	91	6
6[f]		**8**	88	17	83	14
7		**1**	100	26	74	62
8		**2**	100	17	83	60
9		**1**	15	24	76	41
10		**2**	28	16	84	48
11		**1**	38	9	91	62
12		**2**	57	25	75	57
13		**1**	64	16	84	9
14		**2**	48	49	51	34
15		**1**	80	17	83	76
16		**2**	94	19	81	86

Reagents and conditions: [a] [Rh(acac)(CO)$_2$] (2 μmol), diphosphite (10 μmol), vinyl arene (2 mmol), toluene/*n*-decane (15 mL/0.5 mL), P(CO/H$_2$) = 20 bar, 24 h, 50°C, incubation over night at 80°C under P(CO/H$_2$) = 15 bar; [b] determined by GC using decane as internal standard; [c] determined by chiral-phase GC after reduction with LiAlH$_4$; [d] complex **6** (2 μmol); [e] complex **6** (2 μmol), diphosphite **1** (6 μmol); [f] monophosphite (20 μmol).

fluorostyrene, 4-methoxystyrene, 4-*tert*-butylstyrene, 3-chlorostyrene and 2-vinylnaphthalene, were used for hydroformylation runs with **1** and **2** (Table 2). In the hydroformylation of styrene, diphosphite **2** resulted in a more active system than **1** (100 % conversion for **2** vs. 89 % for **1**), but led to a lower ee (Table 2, entries 1 and 2). In the case of 4-fluorostyrene, full conversions and almost identical ees were obtained with both ligands, but the branched aldehyde selectivity was higher for **2** (b/l = 83:17; Table 2, entries 7 and 8). For 4-methoxystyrene and 2-vinylnaphthalene, higher activities were obtained with cavitand **2**, which led to ees of 48 and 86 %, respectively (Table 2, entries 9, 10, 15 and 16). In the hydroformylation of 4-*tert*-butylstyrene and 3-chlorostyrene using calixarene diphosphite **1**, only moderate conversions were measured, although the proportions of branched aldehydes (respectively 91 and 84 %) remained relatively high (Table 2, entries 11-12). For the former substrate, the highest ee (62 %) was obtained with diphosphite **1**, while for the latter resorcinarene **2** gave the better ee (34 %, vs. 9% with **1**) (Table 2, entries 11, 12, 15, 16).

In order to get some insight into the active species, additional hydroformylation tests were carried out with the calixarenyl- and resorcinarenyl-monophosphites **7** and **8** (Figure 3). These tests were performed using styrene as substrate in the presence of 10 equiv. of phosphite per rhodium atom. In both cases, high conversions and good regioselectivities towards the formation of the branched aldehyde were obtained. However, the ees remained very low, respectively 6 % (**7**) and 14 % (**8**) (Table 2, entries 5 and 6). Similarly, repeating the runs with complex **6** (see experimental part), which features two η^1-bound diphosphites (Figure 3), very low ees were measured (Table 2, entries 3 and 4).
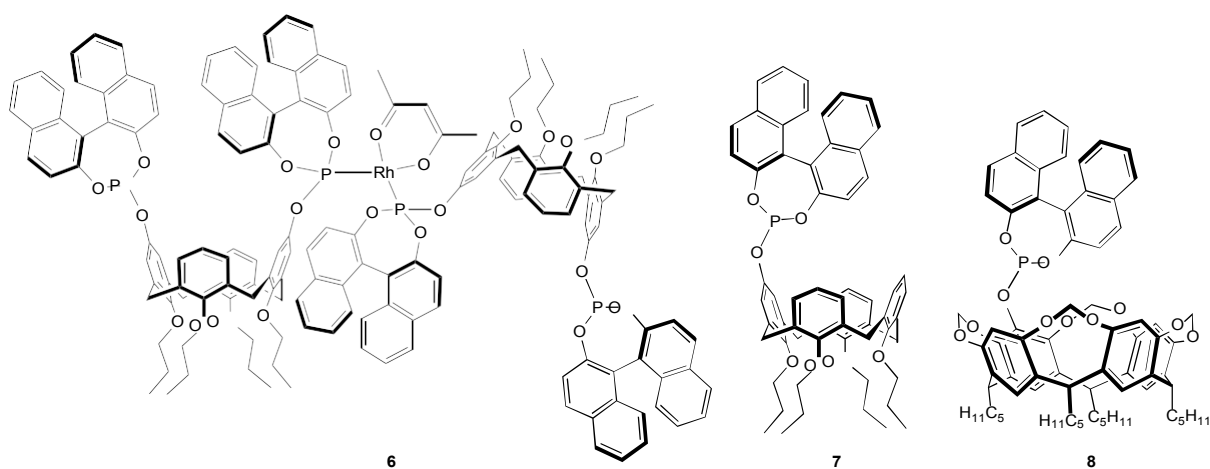

Figure 3: Rhodium complex **6** and phosphites **7** and **8** used to rank the macrocyclic derivatives **1** and **2** in asymmetric hydroformylation.

The above results show that only calixarene-diphosphite **1** allows for good chirality transfer. Interestingly, when [Rh(cod)$_2$]BF$_4$ (cod = 1,5-cyclooctodiene) was reacted with 1 equiv. of diphosphite **1** in CH$_2$Cl$_2$, the chelate complex [Rh(cod)(**1**)]BF$_4$ formed nearly quantitatively. Its ESI-TOF spectrum shows an intense peak at *m/z* = 1463.45, which corresponds to the [Rh(cod)(**1**)]$^+$ cation. In the corresponding ^{1}H NMR spectrum, the ArCH$_2$Ar protons appear as two distinct AB patterns, in keeping with a complex displaying C_2 symmetry in solution. Molecular mechanics calculations using Spartan[10] further indicate that the least-strained and sterically most favourable conformation of the hypothetical trigonal bipyramidal complex [RhH(CO)$_2$(**1**)], a likely catalytic intermediate in the reactions with **1**,[8e, 11] has the metal atom located outside the cavity (Figure 4). The calculated ligand bite angle is 118°. The simulation further indicates that the apical hydride and the equatorial carbon monoxide ligands lie in a sterically hindered environment created by the two "P-bino" units. This constrained asymmetric environment may be responsible for the good chiral induction observed with **1** in the hydroformylation of vinyl arenes.
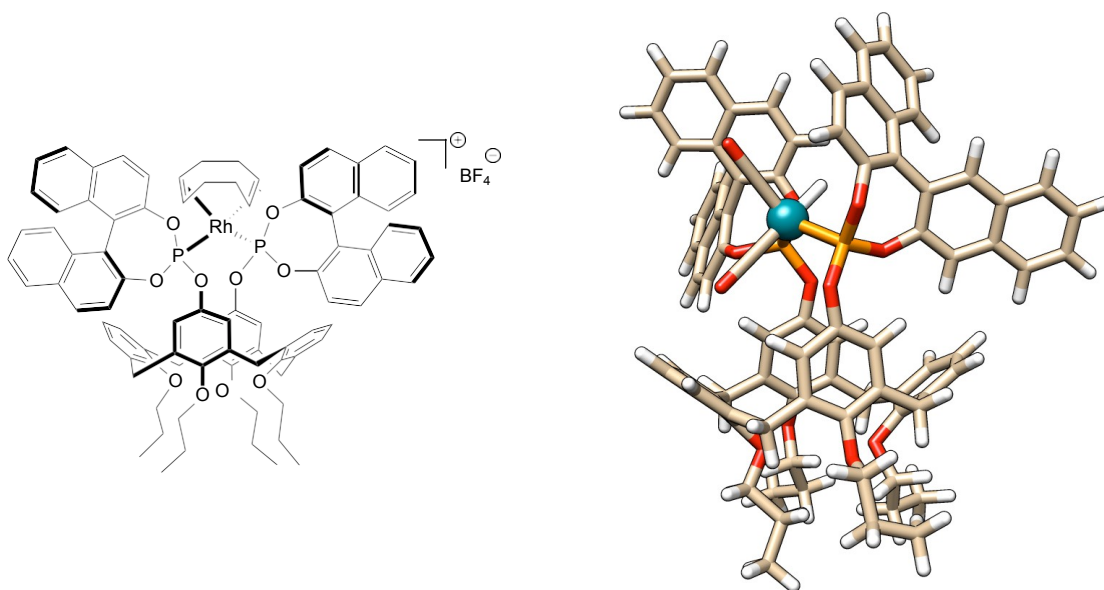
Figure 4: [Rh(cod)(**1**)]BF$_4$ (left) and calculated structure of [RhH(CO)$_2$(**1**)] (right).

Comparaison of resorcinarenes **2** and **8** showed that the ees were considerably better with **2**, although the enantioselectivity remained moderate. Owing to the large separation between the P atoms in resorcinarene **2**, the formation of a chelate complex is totally prevented with this ligand, unlike the observations made for **1** (see above). We found that reaction of diphosphite **2** with a stoichiometric amount of [Rh(cod)$_2$]BF$_4$ in CH$_2$Cl$_2$ led to a mixture of complexes as well as another P-containing compound, which could not be separated. Careful analysis of the ESI-TOF mass spectrum of this mixture revealed the presence of a cationic species of formula

[Rh$_2$(cod)$_2$(**2**)$_2$]$^{2+}$ (Figure 5) (peak at *m/z* = 1687.55 (z = 2) with expected isotopic profile). The corresponding ^{31}P NMR spectrum showed the presence of a major compound in the mixture). The latter is charactersied by a well-resolved ABX spin system (δ_A = 124.7 ppm, $^1J_{PRh}$ = 255 Hz, $^2J_{PP}$ = 50 Hz; δ_B =121.3 ppm, $^1J_{PRh}$ = 267 Hz, $^2J_{PP}$ = 50 Hz) (Figure 6), consistent with the formation of a species in which the P atoms bound to the same metal centre are non equivalent. These findings provide a good indication for the ease of forming dimeric complexes (possibly also higher oligomers) with **2** rather than chelated species. In such dimers, the metal is considerably less strained than in chelate complexes obtained with calixarene-diphosphite **1**, this making the latter more effecient for chirality transfer.

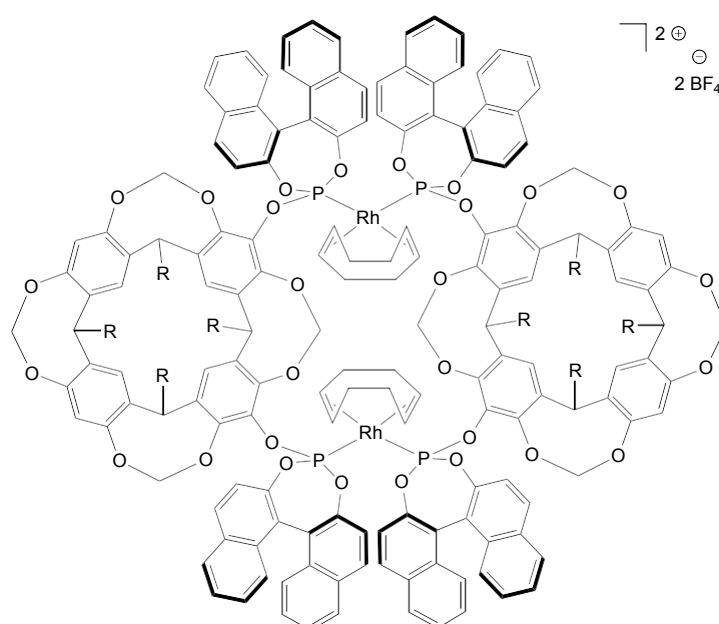Figure 5: Dimeric complex formed during the reaction between [Rh(cod)$_2$]BF$_4$ and diphosphite **2**.

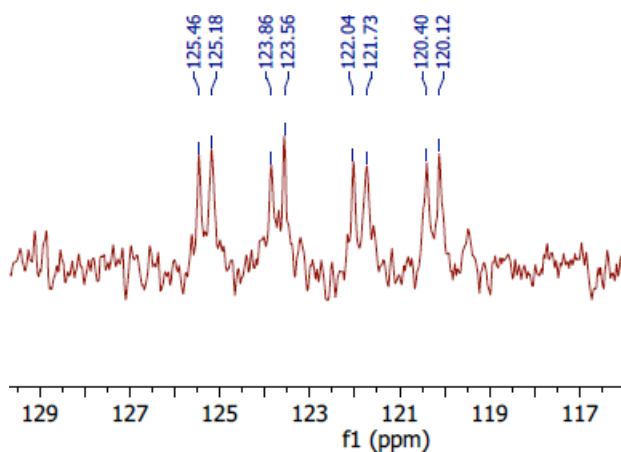Figure 6: ^{31}P{^{1}H} NMR spectrum of [Rh$_2$(cod)$_2$(**2**)$_2$]2BF$_4$ complex.

Conclusion

In summary, we have prepared the first conical calixarene featuring two chiral phosphito units tethered at its upper rim (**1**). High branched aldehyde selectivity and good enantioselectivities could be obtained with this ligand in the hydroformylation of vinyl arenes, thereby contrasting with previously reported analogues having the phosphito groups attached to the lower rim, which gave very low amounts of branched aldehyde. The good chirality transfer observed with this ligand can reasonably be attributed to the formation of chelated species during catalysis in which the binaphthyl moieties efficiently embrace the metal centre. The findings made for the resorcinarene-diphosphite **2** are consistent with the formation of oligomers when this phosphite is opposed to rhodium.

References

[1]   O. Roelen, *Ger. Patent* 849 548, **1938**.

[2]   a) *Rhodium Catalysed Hydroformylation* (Eds.: P. W. N. M. van Leeuwen, C. Claver), Kluwer, Dordrecht, **2002**; b) R. Franke, D. Selent, A. Börner, *Chem. Rev.* **2012**, *112*, 5675-5732; c) *Hydroformylation for Organic Synthesis* (Eds. M. Taddei and A. Mann), Springer Verlag Berlin, Heidelberg, **2013**.

[3]   J. A. Osborn, G. Wilkinson, J. F. Young, *Chem. Commun.* **1965**, 17-17.

[4]   a) D. N. Gorbunov, A. V. Volkov, Y. S. Kardasheva, A. L. Maksimov, E. A. Karakhanov, *Pet. Chem.* **2015**, *55*, 587-603; b) P. W. N. M. van Leeuwen, P. C. J. Kamer, *Catal. Sci. Technol.* **2018**, *8*, 26-113; c) S. S. Nurttila, P. R. Linnebank, T. Krachko, J. N. H. Reek, *ACS Catal.* **2018**, *8*, 3469-3488.

[5]   a) N. Sakai, S. Mano, K. Nozaki, H. Takaya, *J. Am. Chem. Soc.* **1993**, *115*, 7033-7034; b) F. Agbossou, J.-F. Carpentier, A. Mortreux, *Chem. Rev.* **1995**, *95*, 2485-2506; c) G. J. H. Buisman, M. E. Martin, E. J. Vos, A. Klootwijk, P. C. J. Kamer, P. W. N. M. van Leeuwen, *Tetrahedron Asym.* **1995**, *6*, 719-738; d) M. R. Axet, J. Benet-Buchholz, C. Claver, S. Castillón, *Adv. Synth. Catal.* **2007**, *349*, 1983-1998; e) A. L. Watkins, B. G. Hashiguchi, C. R. Landis, *Org. Lett.* **2008**, *10*, 4553-4556; f) A. T. Axtell, J. Klosin, G. T. Whiteker, *Organometallics* **2009**, *28*, 2993-2999; g) A. Gual, C. Godard, C. Claver, S. Castillón, *Eur.*

J. Org. Chem. **2009**, 1191-1201; h) T. Robert, Z. Abiri, J. Wassenaar, A. J. Sandee, S. Romanski, J.-M. Neudörfl, H.-G. Schmalz, J. N. H. Reek, *Organometallics* **2010**, *29*, 478-483; i) A. Gual, C. Godard, S. Castillón, C. Claver, *Adv. Synth. Catal.* **2010**, *352*, 463-477; j) A. Gual, C. Godard, S. Castillón, C. Claver, *Tetrahedron: Asym.* **2010**, *21*, 1135-1146; k) R. Bellini, J. N. H. Reek, *Chem. Eur. J.* **2012**, *18*, 13510-13519; l) I. A. Tonks, R. D. Froese, C. R. Landis, *ACS Catal.* **2013**, *3*, 2905-2909; m) T. T. Adint, G. W. Wong, C. R. Landis, *J. Org. Chem.* **2013**, *78*, 4231-4238; n) K. Xu, X. Zheng, Z. Wang, X. Zhang, *Chem. Eur. J.* **2014**, *20*, 4357-4362; o) S. H. Chikkali, J. I. van der Vlugt, J. N. H. Reek, *Coord. Chem. Rev.* **2014**, *262*, 1-15; p) M. Jouffroy, R. Gramage-Doria, D. Armspach, D. Sémeril, W. Oberhauser, D. Matt, L. Toupet, *Angew. Chem. Int. Ed.* **2014**, *53*, 3937-3940; q) M. Jouffroy, R. Gramage-Doria, D. Sémeril, D. Armspach, D. Matt, W. Oberhauser, L. Toupet, *Beilstein J. Org. Chem.* **2014**, *10*, 2388-2405; r) C. F. Czauderna, D. B. Cordes, A. M. Z. Slawin, C. Müller, J. I. van der Vlugt, D. Vogt, P. C. J. Kamer, *Eur. J. Inorg. Chem.* **2014**, 1797-1810; s) G. M. Noonan, C. J. Cobley, T. Mahoney, M. L. Clarke, *Chem. Commun.* **2014**, *50*, 1475-1477; t) J. R. Lao, J. Benet-Buchholz, A. Vidal-Ferran, *Organometallics* **2014**, *33*, 2960-2963; u) S. Allmendinger, H. Kinuta, B. Breit, *Adv. Synth. Catal.* **2015**, *357*, 41-45; v) A. Vidal-Ferran, I. Mon, A. Bauzá, A. Frontera, L. Rovira, *Chem. Eur. J.* **2015**, *21*, 11417-11426; w) L. Rovira, M. Vaquero, A. Vidal-Ferran, *J. Org. Chem.* **2015**, *80*, 10397-10403; x) M. J. Bravo, R. M. Ceder, A. Grabulosa, G. Muller, M. Rocamora, J. C. Bayón, D. Peral, *Organometallics* **2015**, *34*, 3799-3808; y) C. Schmitz, K. Holthusen, W. Leitner, G. Franciò, *ACS Catal.* **2016**, *6*, 1584-1589.

[6]   R. V. Chaudhari, *Top. Catal.* **2012**, *55*, 439-445.

[7]   E. R. Nelsen, A. C. Brezny, C. R. Landis, *J. Am. Chem. Soc.* **2015**, *137*, 14208-14219.

[8]   a) D. Sémeril, C. Jeunesse, D. Matt, L. Toupet, *Angew. Chem. Int. Ed.* **2006**, *45*, 5810-5814; b) D. Sémeril, D. Matt, L. Toupet, *Chem. Eur. J.* **2008**, *14*, 7144-7155; c) L. Monnereau, D. Sémeril, D. Matt, L. Toupet, *Adv. Synth. Catal.* **2009**, *351*, 1629-1636; d) L. Monnereau, D. Sémeril, D. Matt, *Eur. J. Org. Chem.* **2010**, 3068-3073; e) D. Sémeril, D. Matt, W. Oberhauser, C. Bianchini, *Chem. Eur. J.* **2010**, *16*, 13843-13849; f) L. Monnereau, D. Sémeril, D. Matt, *Green Chem.* **2010**, *12*, 1670-1673.

[9]   C. Jaime, J. de Mendoza, P. Prados, P. M. Nieto, C. Sánchez, *J. Org. Chem.* **1991**, *56*, 3372-3376.

[10] *Spartan 16 v. 1.1.2, Wavefunction Inc.,* Irvine, CA **2016**.

[11] a) A. van Rooy, P. C. J. Kamer, P. W. N. M. van Leeuwen, K. Goubitz, J. Fraanje, N. Veldman, A. L. Spek, *Organometallics* **1996**, *15*, 835-847; b) G. J. H. Buisman, L. A. van der Veen, P. C. J. Kamer, P. W. N. M. van Leeuwen, *Organometallics* **1997**, *16*, 5681-5687; c) L. A. van der Veen, M. D. K. Boele, F. R. Bregman, P. C. J. Kamer, P. W. N. M. van

Leeuwen, K. Goubitz, J. Fraanje, H. Schenk, C. Bo, *J. Am. Chem. Soc.* **1998**, *120*, 11616-11626; d) C. Bianchini, W. Oberhauser, A. Orlandini, C. Giannelli, P. Frediani, *Organometallics* **2005**, *24*, 3692-3702.

Cavitand chemistry: nickel half-sandwich complexes with imidazolylidene ligands bearing one or two resorcinarenyl substituents

Abstract

Imidazolium salts substituted with cavitand subunits have been synthesised and successfully employed for the synthesis of nickel cyclopentadienyl (Cp) complexes in which the NiCp moiety is embedded in the cavity. A complex in which both N atoms are substituted by a cavitand moiety was found significantly more active in ethylene dimerisation than an analogue containing the bulky IMes ligand.
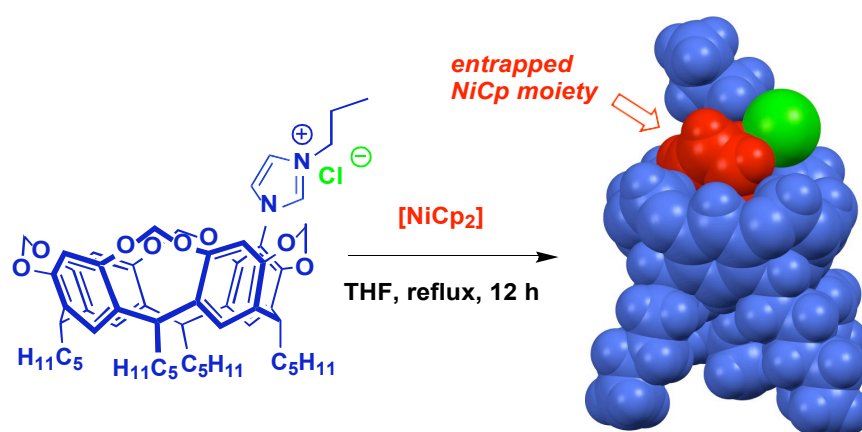
Introduction

The chemistry of nickel *N*-heterocyclic carbene complexes (Ni-NHCs) is a rapidly expanding field, complexes of this class subtly combining the intrinsic properties of nickel[1] (chemical versatility, high natural abundance, low cost) with those of the particular electronic and steric features of NHC ligands (electron richness, hemi-ovoidal encumbrance). Thus, valuable Ni(Cp)-NHC (Cp = cyclopentadienyl) catalysts have recently been developed for applications in a variety of catalytic reactions, including hydrosilylation,[2] Suzuki-Miyaura,[3] Kumada-Tamao-Corriu,[3c,d,4] Buchwald-Hartwig,[5] hydrothiolation,[6] ethylene dimerisation[7] or polymerisation of styrene,[3c, 8] phenylacetylene[9] and methacrylate.[10]

In several recent studies we have reported the synthesis of imidazolium salts having one of their nitrogen atoms substituted by a cavitand subunit, namely the (μ_4-tetramethylenedioxy)-2,8,14,20-tetrapentylresorcin[4]aren-5-yl group, and shown their high efficiency when used as proligands in palladium-[11] and nickel-catalysed[12] cross-couplings as well as in copper-catalysed allylic substitutions.[13] We further found that in the carbene complexes obtained from these salts, the metal ion (palladium, copper) is located outside the cavity of the resorcin[4]arene unit. To rationalise the remarkable performance of the corresponding catalysts, we proposed that during catalysis two flexible pentyl chains attached to the smaller rim of the resorcin[4]arene unit may sterically interact with substrates bound to the exo-oriented metal centre, thereby facilitating the reductive elimination steps. Thus, the cavity receptacle as such is not involved in the catalytic process in these cases.

As part of a programme aimed at the synthesis of cavitand-based Ni-NHC complexes, a hitherto unreported class of compounds, we have now found, for the first time, that resorcinarene-substituted imidazolium salts may give NHC-complexes having their metal centre positioned at the entrance of the cone delineated by the cavitand. The catalytic impact of the resulting confinement (Fig. 1) was assessed in ethylene dimerisation.
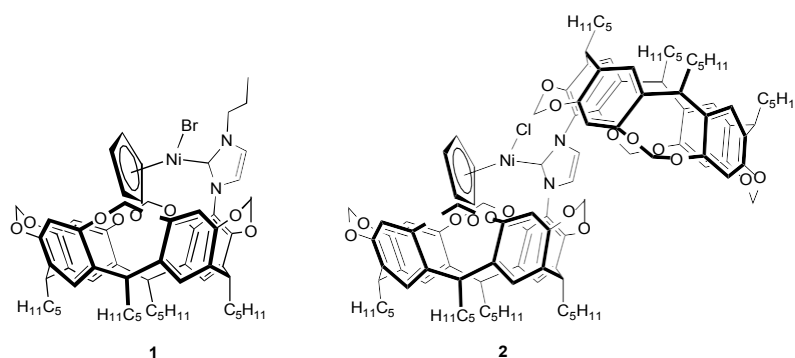
Figure 1: Half-sandwich nickel complexes investigated in the present study.

Results and Discussion

The synthesis of complexes **1** and **2** required that of the imidazolium salts **6** and **7**, respectively (Scheme 1). Precursor **6** was conveniently prepared according to a method reported earlier, *viz.* by Ullmann coupling between the mono-brominated cavitand **3** and imidazole, followed by alkylation of the resulting imidazolyl-substituted resorcinarene with *n*-propyl bromide. As a similar sequence cannot be applied to the synthesis of *bis-aryl*-substituted imidazoles, compound **7** was prepared via a conventional imidazole synthesis.[14]
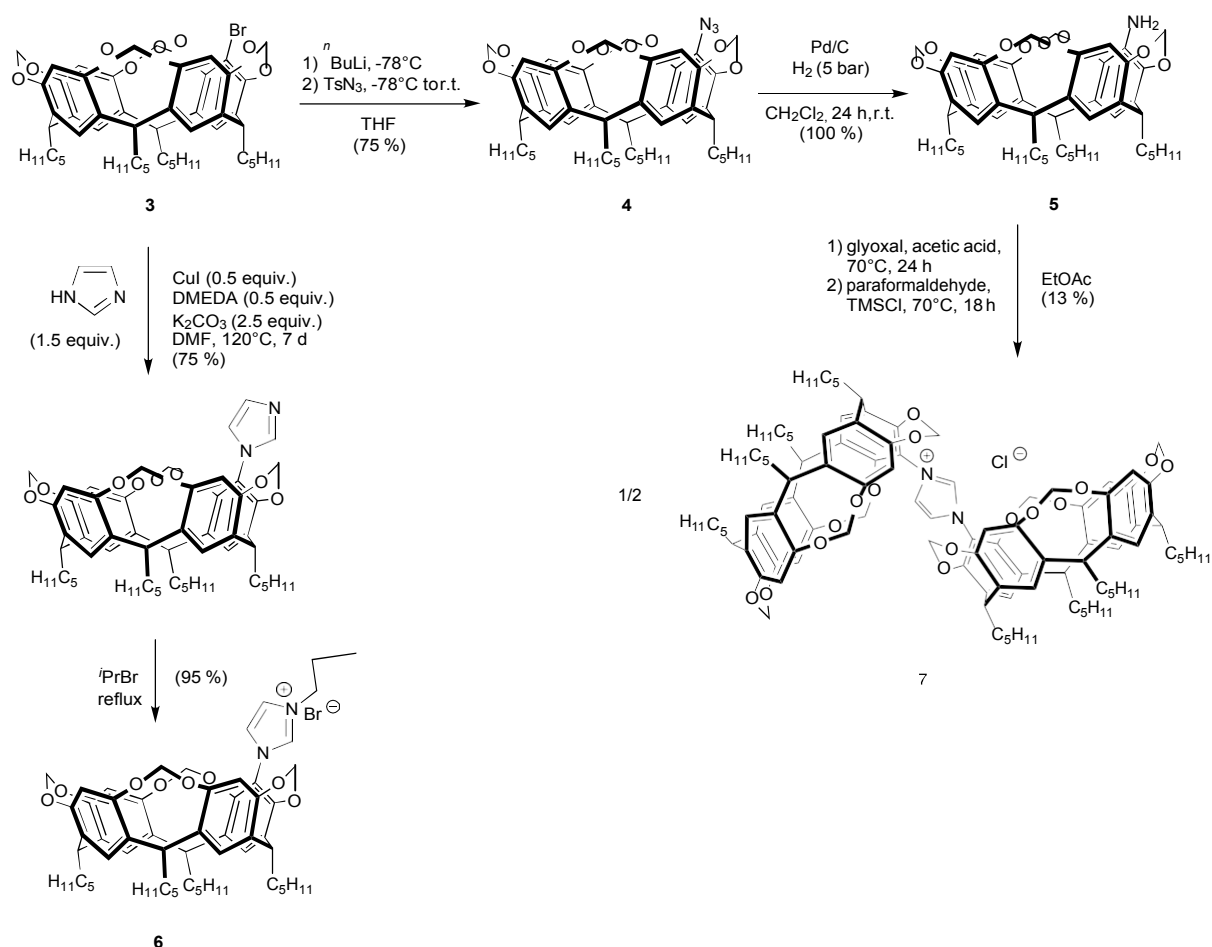
Scheme 1. Synthesis of the NHC precursors **6** and **7**

To this end, cavitand **3** was converted into azide **4** *via* a halogen/lithium exchange followed by reaction with tosyl azide (Scheme 1). Reduction of **4** with Pd/C under hydrogen (5 bar) led quantitatively to amine **5**. The latter was then reacted with glyoxal in the presence of acetic acid at 70 °C for 24 hours, and the resulting mixture treated with paraformaldehyde and

Me₃SiCl. Chromatographic separation afforded imidazolium salt **7** in 13 % yield. Despite several optimisation attempts, the yield of this reaction could not be improved due to rapid decomposition of the di-imine intermediate.

The new imidazolium salt **7** was characterised by elemental analysis, ESI-TOF MS and ^{1}H and ^{13}C NMR spectroscopy. Consistent with the presence of two equivalent *mono*-substituted resorcinarene units, the ^{1}H NMR spectrum of **7** displays two AB patterns (intensity 8:8) for the –OCH₂O– bridges and two triplets (intensity 4:4) for the methine protons. The signal of the NC*H*N proton appears in the expected range, at δ 8.88 ppm.

The two half-sandwich complexes **1** and **2** were obtained following a general method developed by Cowley,[15] which consisted of reacting the appropriate imidazolium salt with [NiCp₂] in refluxing THF for 12 hours (Scheme 2). The observed yields (20 % for **1** and 35 % for **2**) are relatively low, but such yields are not unusual for Ni(Cp)-NHC complexes obtained from [NiCp₂].[8a] In this study, for comparative purposes, the two cavity-free analogues **8** and **9**[15] (Fig. 2) were also prepared (yield: *ca*. 55% for both complexes). All complexes were characterized by ^{1}H and ^{13}C{^{1}H} NMR spectroscopy and by elemental analysis (see experimental part).
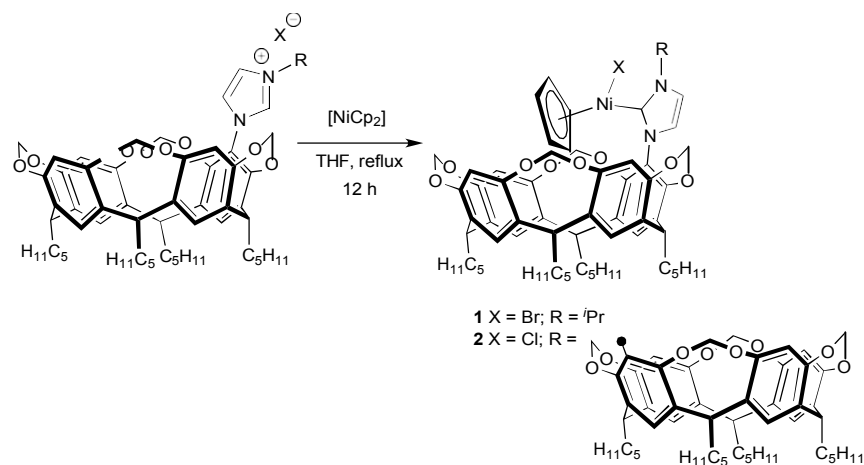
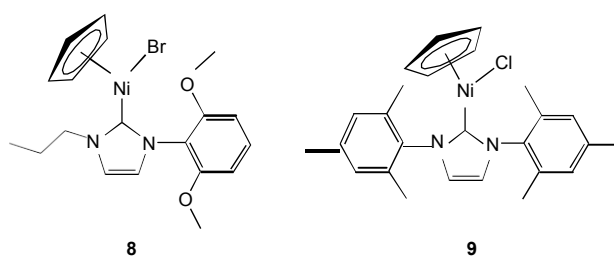Scheme 2: Synthesis of the half-sandwich complexes **1** and **2**.

Figure 2: Reference complexes **8** and **9**.

The cyclopentadienyl proton signals in the ^{1}H NMR spectra of complexes **1** and **2** show a significant upfield shift (δ 3.68 ppm (**1**); 3.71 ppm (**2**)) in comparison to those of the cavity-free complexes **8** and **9** (*cf.* 4.71 and 4.61 ppm for **8** and **9,** respectively) or other simple [NiCpXL] complexes.[15] These data are indicative of cavity-entrapped Cp rings, the observed shielding arising from the ring current created by aromatic units of the cavity wall. The proposed NiCp *endo*-orientation was confirmed in the case of complex **1** by a single-crystal X-ray diffraction study (*vide infra*). In line with a confined NiCp fragment, a ^{1}H-^{1}H ROESY spectrum for complex **2** (see the Supporting Information) revealed correlations between the Cp ligand and two aromatic protons of one of its resorcinarene units. Careful analysis also revealed evidence of the spatial proximity of an H atom of the imidazolyl ring and two close OCH$_2$O groups. Molecular models unambiguously show that these OCH$_2$O moieties must belong to the "empty" resorcinarene unit, this cavity having its wider entrance turned away from the nickel atom (Fig. 3).
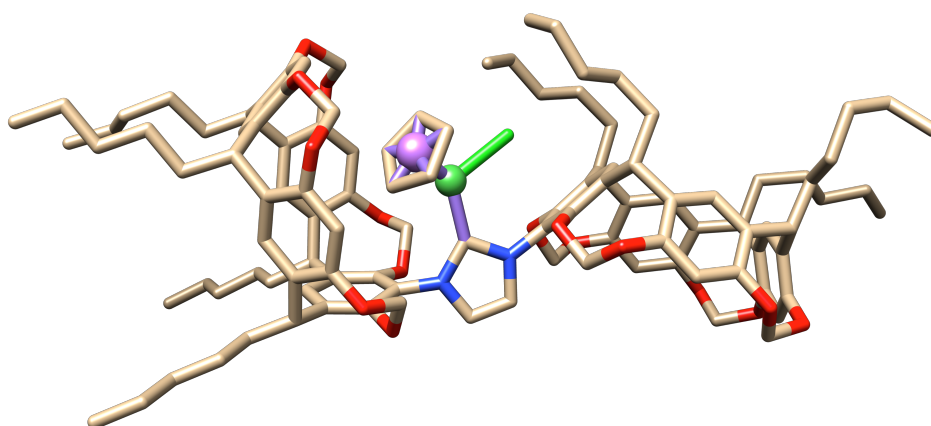
Figure 3. View of the proposed *anti* orientation of the two cavity subunits in **2**, as inferred from NMR experiments (minimisation with SPARTAN[16]).

It is further worth mentioning that while the room temperature ^{1}H NMR spectrum of **1** shows some broad signals indicative of relatively slow conformational changes, those of **2** are all sharp (see the Supporting Information). Possibly, the presence of the bulky Br atom in **1** slows down the rotation about the C–Ni bond of this complex, the corresponding rotation occurring much faster in the chloro complex **2** (blocked rotation should result in conformers with either an exo- or en endo-oriented Ni-X bond). However, attempts to freeze out this movement by lowering the temperature were unsuccessful.

Complex **1** (Fig. 4) crystallises in the triclinic space group *P*-1. The asymmetric unit

contains two inequivalent molecules (denoted A and B hereafter) and a molecule of benzene. Both complexes have three ligands bound to the Ni, with the Cp rings in the η^5-bonding mode, typical of [NiCpXL] complexes.[8a, 17] The Ni-C(carbene) bond lengths, 1.869(9) Å (A) and 1.898(9) Å (B), are close to those reported for the related complex **9** (1.917(9) Å).[15] The observed wider rim diameters (*i.e* the segments linking the C-2 aromatic carbon atoms of opposite resorcinol units), 7.53(1)/8.24(1) Å in molecule A and 7.42(1)/8.29(1) Å in molecule B, reveal that the resorcinol cavities possess an oval cross section, such an observation having been made for other mono-substituted resorcin[4]arene-cavitands with OCH_2O linkers.[18] As anticipated, both cavities of the unit cell host a NiCp moiety. Short separations can be seen between two H atoms of the entrapped Cp ring and the centroids of two opposite resorcinolic rings (2.90(1) Å /2.93(1) Å in A and 2.90(1)/2.89(1) Å in B), this being in line with the observation of an upfield shift in the Cp protons signal in the ^{1}H NMR spectrum.
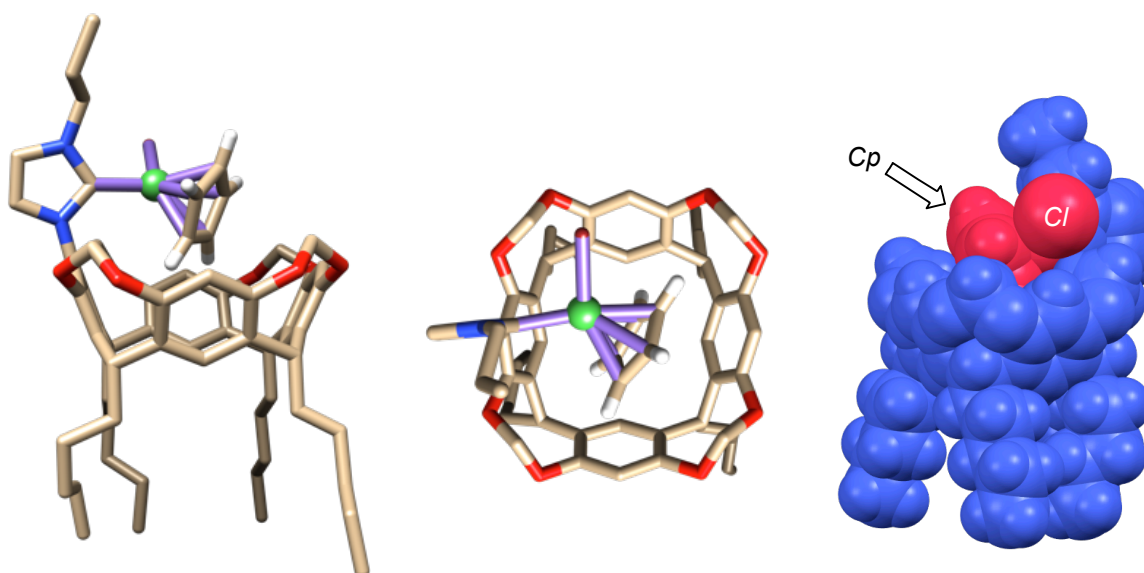
Figure 4: X-ray structure of complex **1** (left: side view with carbenic C at left; middle: view from top; right CPK-side view with carbenic C at right). Only one of the two molecules present in the unit cell is shown. The NiCpCl moiety is in red.

The X-ray structure determination carried out for **1** provided a means of estimating the buried volume (%V_{Bur}) of the corresponding carbene. This calculation was done using the SambVca tool,[19] which also provided a steric map allowing to visualise the encumbrance of the ligand. Application of the standard value of R = 3.5 Å to define the first coordination sphere around the metal led to a %V_{Bur} of 37.2 (H atoms included), a value similar to that reported for

IMes (36.5[20]). However, to obtain a realistic steric map taking into account the presence of a cavity surrounding the nickel atom, we found it better to apply an R value of 4.0 Å. The results of both calculations are shown in Fig. 5.

Figure 5 Topographic steric maps of **1** including H atoms. View along the z axis (left: calculation with a R value of 3.5 Å; right: calculation with R = 4.0 Å). The distances on the scales indicate the height along the z axis. The z axis points towards the reader and is located in the midde of the maps.

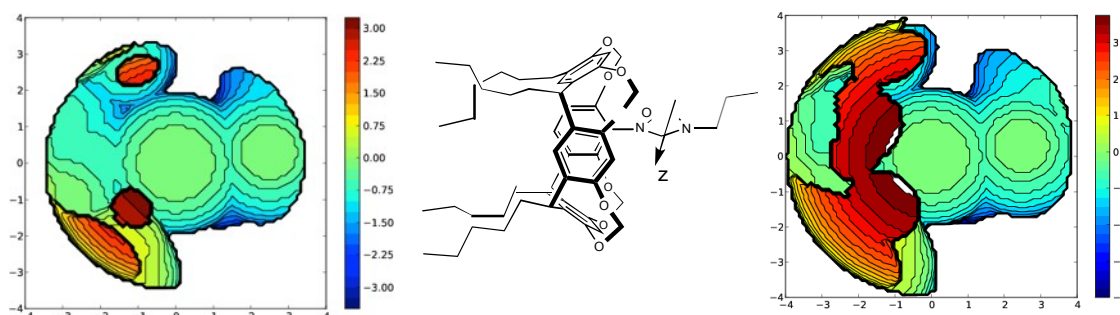Finally, it should be emphasised that there is no spectroscopic evidence for the NiCp moiety of **1** jumping out of the cavity in solution. This makes sense considering the high degree of confinement of the NiCp unit in **1** found in the solid state (illustrated in Fig. 4, CPK representation). However, the reason why this unit sits in the cavitand rather than being located outside the cavity is a matter of discussion. At this stage, it remains unclear whether the Ni—Cp bond formed inside (after formation of a NiCp$_2$ inclusion complex) or outside and notably whether its end-position (namely inside the bowl) arises from its thermodynamic stability.

The nickel complexes **1** and **2** were evaluated as catalysts for ethylene dimerization using NaBH$_4$ (one equiv. per Ni) as activator.[21] The corresponding tests were performed under 20 bar of ethylene in toluene at 90 °C for 1 hour (Scheme 3 and Table 1). At the end of each run, the autoclave was cooled down to 6 °C and depressurised over 8 minutes (to efficiently limit the loss of butene) (Table 1, entries 9 and 10).
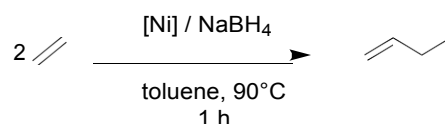
Scheme 3: Nickel-catalysed ethylene dimerization.

51

Under these conditions, complex **1** produced 1-butene with a turn-over frequency (TOF) of 85 mol(C$_2$H$_4$) mol(Ni)$^{-1}$ h^{-1} (Table 1, entry 1). The catalyst activity could be increased up to 350 mol(C$_2$H$_4$) mol(Ni)$^{-1}$ h^{-1} by adding one equivalent of PPh$_3$, phosphine coordination probably resulting in mixed electron-rich phosphine-NHC intermediates that facilitate the olefin insertion steps (Table 1, entry 2). A significantly higher TOF (555 mol(C$_2$H$_4$) mol(Ni)$^{-1}$ h^{-1}) was obtained with complex **2** (Table 1, entry 3). Interestingly, adding PPh$_3$ to the run performed with **2** drastically reduced the formation of 1-butene (Table 1, entry 5). It is likely that in this case, due to the high steric encumbrance of the carbene ligand (which bears two cavitand subunits), addition of phosphine mainly results in *trans*-(carbene,phosphine) intermediates (rather than *cis*-complexes as for **1**), a configuration which should prevent olefin insertion. Finally, we found that in none of the above runs did isomerisation of 1-butene occur.

Table 1. Nickel-catalysed ethylene dimerisation.[a]

Entry	Nickel complex	PPh$_3$	1-Butene (g)	TOF (mol(C$_2$H$_4$) mol(Ni)$^{-1}$ h^{-1}
1	**1**	no	0.012	85
2	**1**	yes	0.049	350
3	**2**	no	0.078	555
4[b]	**2**	no	0.108	385
5	**2**	yes	0.006	40
6	**8**	no	0.014	100
7	**8**	yes	0.013	90
8	**9**	no	0.050	355
9	**9**	yes	0.038	270
10[c]	**9**	yes	0.014	100

[a] Conditions: nickel complex (5 µmol), NaBH$_4$ (10 µmol), PPh$_3$ (5 µmol), toluene (15 mL) ethylene (20 bar), 90°C, 1 h, depressurisation over 6 min; [b] 2 h; [c] depressurisation over 2 min.

In order to better understand the possible influence of the resorcinarenyl substituent in **1** during catalysis, further runs were carried with the closely related, but cavity-devoid complex **8**.

In these experiments the butene production was nearly identical to that obtained with **1** (in the absence of PPh$_3$), thus suggesting that the carbene ligands of **1** and **8** have similar steric and electronic properties, and that in fact there is no effective participation of the cavity. Unlike with **1**, the activity of **8** remained nearly unchanged upon addition of PPh$_3$ (Table 1, entries 6 and 7). The latter observation is a clear indication that the presence of the phosphine, presumably leading to Ni(phosphine)(carbene) intermediates, augments the steric properties of the carbene ligand of **1** as a result of strong steric interactions between the phosphine and the resorcinarene moiety. Good activities, which however remained inferior to those of **2**, were also observed for the 1,3-dimesitylimidazol-2-ylidene complex **9** (Fig. 2; Table 1, entry 8). The activity of **9** dropped upon addition of PPh$_3$, this effect, being, as expected, weaker than that observed with the bulkier complex **2** (Table 1, entries 5 and 9).

Conclusions

We have shown that the reaction of resorcinarenyl-substituted imidazolium salts with [NiCp$_2$] results in half-sandwich [Ni(NHC)CpX] complexes in which the NiCpX moiety lies embedded in the cavitand part. In all previously reported complexes based on cavitand-derived NHCs the metal fragments were positioned outside the cavity. The ethylene dimerisation tests carried out with the reported complexes indicate that the presence of NHCs bearing resorcinarene N-substituents may positively impact on the catalytic activity, but this effect only operates if the metal centre is in a sufficiently bulky steric environment. Further work is aimed at exploiting cavitand *endo*-orientation of metal centres for performing shape selective reactions.

References

[1]   a) J. Yamaguchi, K. Muto and K. Itami, *Eur. J. Org. Chem.* **2013**, 19-30; b) S. Z. Tasker, E. A. Standley and T. F. Jamison, *Nature* **2014**, *509*, 299-309; c) V. P. Ananikov, *ACS Catal.* **2015**, 1964-1971.

[2]   a) L. P. Bheeter, M. Henrion, L. Brelot, C. Darcel, M. J. Chetcuti, J.-B. Sortais and V. Ritleng, *Adv. Synth. Catal.* **2012**, *354*, 2619-2624; b) L. Postigo and B. Royo, *Adv. Synth.*

Catal. **2012**, *354*, 2613-2618; c) M. Rocquin, V. Ritleng, S. Barroso, A. M. Martins and M. J. Chetcuti, *J. Organomet. Chem.* **2016**, *808*, 57-62.

[3]   a) V. Ritleng, A. M. Oertel and M. J. Chetcuti, *Dalton Trans.* **2010**, *39*, 8153-8160; b) J. Wu, A. Nova, D. Balcells, G. W. Brudvig, W. Dai, L. M. Guard, N. Hazari, P.-H. Lin, R. Pokhrel and M. K. Takase, *Chem. Eur. J.* **2014**, *20*, 5327-5337; c) Ł. Banach, P. A. Guńka, D. Górska, M. Podlewska, J. Zachara and W. Buchowicz, *Eur. J. Inorg. Chem.* **2015**, 5677-5686; d) P. Buchalski, R. Pacholski, K. Chodkiewicz, W. Buchowicz, K. Suwińskab and A. Shkurenko, *Dalton Trans.* **2015**, *44*, 7169-7176; e) S. Ando, H. Matsunaga and T. Ishizuka, *J. Org. Chem.* **2017**, *82*, 1266-1272; f) L. Benítez Junquera, F. E. Fernández, M. C. Puerta and P. Valerga, *Eur. J. Inorg. Chem.* **2017**, 2547-2556.

[4]   a) S. Tamba, K. Fuji, H. Meguro, S. Okamoto, T. Tendo, R. Komobuchi, A. Sugie, T. Nishino and A. Mori, *Chem. Lett.* **2013**, *42*, 281-283; b) Ł. Banach, P. A. Guńka and W. Buchowicz, *Dalton Trans.* **2016**, *45*, 8688-8692.

[5]   a) R. A. Kelly, N. M. Scott, S. Díez-González, E. D. Stevens and S. P. Nolan, *Organometallics* **2005**, *24*, 3442-3447; b) A. R. Martin, Y. Makida, S. Meiries, A. M. Z. Slawin and S. P. Nolan, *Organometallics* **2013**, *32*, 6265-6270.

[6]   a) D. A. Malyshev, N. M. Scott, N. Marion, E. D. Stevens, V. P. Ananikov, I. P. Beletskaya and S. P. Nolan, *Organometallics* **2006**, *25*, 4462-4470; b) Y.-H. Chen, K.-E. Peng, G.-H. Lee, S.-M. Peng and C.-W. Chiu, *RSC Adv.* **2014**, *4*, 62789-62792.

[7]   H. M. Sun, Q. Shao, D. M. Hu, W. F. Li, Q. Shen and Y. Zhang, *Organometallics* **2005**, *24*, 331-334.

[8]   a) W. Buchowicz, A. Kozioł, L. B. Jerzykiewicz, T. Lis, S. Pasynkiewicz, A. Pecherzewska and A. Pietrzykowski, *J. Mol. Catal. A: Chem.* **2006**, *257*, 118-123; b) W. Buchowicz, Ł. Banach, J. Conder, P. A. Guńka, D. Kubicki and P. Buchalski, *Dalton Trans.* **2014**, *43*, 5847-5857.

[9]   W. Buchowicz, W. Wojtczak, A. Pietrzykowski, A. Lupa, L. B. Jerzykiewicz, A. Makal and K. Wozniak, *Eur. J. Inorg. Chem.* **2010**, 648-656.

[10]   W. Buchowicz, J. Conder, D. Hryciuk and J. Zachara, *J. Mol. Catal A: Chem.* **2014**, *381*, 16-20.

[11]   a) N. Şahin, D. Sémeril, E. Brenner, D. Matt, İ. Özdemir, C. Kaya and L. Toupet, *ChemCatChem* **2013**, *5*, 1115-1125; b) N. Şahin, D. Sémeril, E. Brenner, D. Matt, C. Kaya and L. Toupet, *Turk. J. Chem.* **2015**, *39*, 1171-1179; c) M. Kaloğlu, D. Sémeril, E. Brenner, D. Matt, İ. Özdemir and L. Toupet, *Eur. J. Inorg. Chem.* **2016**, 1115-1120.

[12]   N. Şahin, D. Sémeril, E. Brenner, D. Matt, İ. Özdemir, C. Kaya and L. Toupet, *Eur. J. Org. Chem.* **2013**, 4443-4449.

[13] M. Kaloğlu, N. Şahin, D. Sémeril, E. Brenner, D. Matt, İ. Özdemir, C. Kaya and L. Toupet, *Eur. J. Org. Chem.* **2015**, 7310-7316.

[14] L. Hintermann, *Beilstein J. Org. Chem.* **2007**, *3*, No 22.

[15] C. D. Abernethy, A. H. Cowley and R. A. Jones, *J. Organomet. Chem.* **2000**, *596*, 3-5.

[16] Spartan v. 2.0.3, Wavefunction Inc., Irvine, CA.

[17] V. Ritleng, C. Barth, E. Brenner, S. Milosevic and M. J. Chetcuti, *Organometallics* **2008**, *27*, 4223-4228.

[18] a) H. El Moll, D. Sémeril, D. Matt and L. Toupet, *Eur. J. Org. Chem.* **2010**, 1158-1168; b) T. Chavagnan, D. Sémeril, D. Matt and L. Toupet, *Eur. J. Org. Chem.* **2017**, 313-323; c) F. Elaieb, D. Sémeril and D. Matt, *Eur. J. Inorg. Chem.* **2017**, 685-693.

[19] L. Falivene, R. Credendino, A. Poater, A. Petta, L. Serra, R. Oliva, V. Scarano and L. Cavallo, *Organometallics* **2016**, *35*, 2286-2293.

[20] Handbook of Reagents for Organic Synthesis: Reagents for Organocatalysis (Ed. T. Rovis), Wiley & Sons, Ltd., New York, 2016.

[21] a) D. Matt, M. Huhn, M. Bonnet, I. Tkatchenko, U. Englert and W. Kläui, *Inorg. Chem.* **1995**, *34*, 1288-1291; b) T. Chavagnan, D. Sémeril, D. Matt, J. Harrowfield and L. Toupet, *Chem. Eur. J.* **2015**, *21*, 6678-6681.

Chapter IV

Resorcin[4]arene-functionalised triazolium salts as a ligand source for Suzuki-Miyaura cross-coupling catalysts

Abstract:

Two bulky triazolium salts, namely 1-{4(24),6(10),12(16),18(22)-tetramethylenedioxy-2,8,14,20-tetrapentylresorcin[4]arene-5-yl}-4-phenyl-3-methyl-1H-1,2,3-triazolium tetrafluo roborate (**1**) and 1,4-bis{4(24),6(10),12(16),18(22)-tetramethylenedioxy-2,8,14,20-tetrapentyl resorcin[4]arene-5-yl}-3-methyl-1H-1,2,3-triazolium iodide (**2**), have been synthetised and assessed in the palladium-catalysed Suzuki-Miyaura cross-coupling of bulky aryl chlorides with sterically hindered aryl boronic acids. As a general trend, the activities observed with **1** were significantly higher (up to 5 times) than those obtained with **2**, this mainly reflecting a sterically more accessible metal centre in the catalytic intermediates formed with **1**. In addition, the presence in the latter of flexible pentyl chains able to interact in the exo-conformers with the metal centre may favour the reductive elimination step.

Introduction

In the last two decades *N*-heterocyclic carbenes (NHCs) have emerged as very efficient ligands for Pd-catalysed Suzuki-Miyaura (SM) cross coupling reactions.[1] Their success in these reactions mainly relies on their strong σ-donor properties, generally considered to be superior to that of phosphines, but also on the ease with which they can be made sterically bulky,[2] this being generally achieved by tethering appropriate substituents on their nitrogen atoms. These two features respectively promote the oxidative addition and the reductive elimination steps of the SM catalytic cycle.

More recently, cyclic carbenes in which the carbene centre is not flanked by two heteroatoms (N, S, O) have also attracted attention. Often referred to as abnormal (aNHCs) or mesoionic carbenes (MICs), such ligands typically display a stronger donation capacity when compared to that of the classical NHCs. In this context, following the pioneering work of Albrecht[3] (who synthesed the first aNHC-transition metal complexes) and Bertrand[4] (who isolated the first free, non-conventional carbenes), 1,2,3-triazol-5-ylidenes (tzNHCs) have been extensively studied. Their precursors, namely 1,2,3-triazoles, are readily accessible through copper-catalysed Huisgen [3 + 2] click-type cycloaddition of azides and alkynes (CuAAC)[5] followed by N3-quaternarization. The resulting 1,2,3-triazoliums salts can then be converted to transition metal complexes suitable, *i.a.*, for Suzuki-Miyaura,[6] Mizoroki-Heck[7] and Sonogashira coupling reactions[7a, 8] as well as for various reduction or oxidation reactions[9] and C-heteroatom bond forming reactions.[10]

As an extension to our studies on cavity-derived *N*-heterocyclic carbenes,[11] we now describe the synthesis of two sterically encumbered triazolium salts (Figure 1) and their use in the Pd-catalysed Suzuki-Miyaura cross-coupling of sterically hindered aryl chlorides with bulky arylboronic acids. Both salts have their triazole unit substituted by a resorcinarenyl group attached to the N1 atom and a methyl group attached to the N3 atom. The ring carbon atom bonded to N3 in **1** is susbtituted by a phenyl group, that of **2** by a resorcinarene moiety.
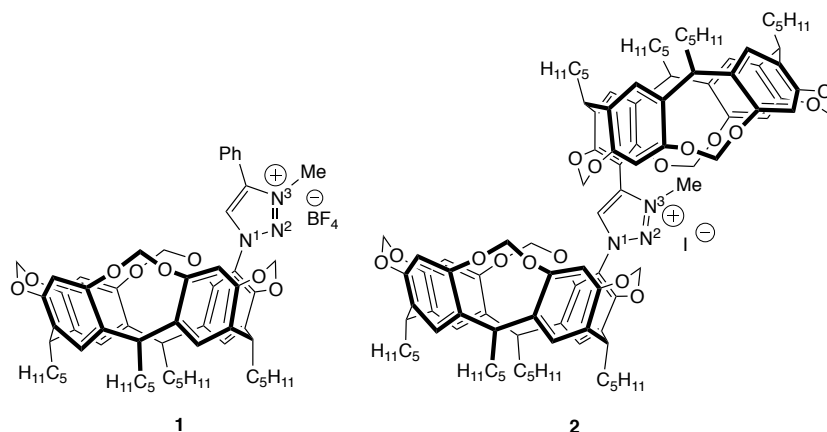

Figure 1: The resorcinarenyl-substituted triazolium salts used in this study.

Results and Discussion

58

The resorcin[4]arene-derived triazolium salts **1** and **2** were synthesised stepwise according to the sequences shown **Scheme** **1**. The two key steps, namely those leading to intermediates **7** and **8**, each involved a copper catalysed cycloaddition (CuAAC) between resorcinarene-azide **6** and an alkyne (with phenyacetylene for the synthesis of triazole **7**; with ethynyl-resorcinarene **5** for the synthesis of **8**) in the presence of $CuSO_4.5H_2O$ and sodium ascorbate in DMF. The precursors **5** and **6** were obtained through standard procedures from bromo-resorcinarene **3** (halogen/lithium exchange followed by reaction with tosyl azide for the synthesis of **5**; Pd-catalysed Sonogashira cross-coupling with trimethylsilylacetylene for the synthesis of **6**). The final methylation steps were carried out with Me_3OBF_4 for **1** (quantitative yield), and with MeI for **2** (yield 68 %).

The triazolium salts **1** and **2** were unambigously characterised by elemental analysis, ESI-TOF MS analysis, and ^{1}H and ^{13}C NMR spectroscopy (see experimental part). Consistent with a *Cs*-symmetrical compound, the ^{1}H NMR spectrum of salt **1** displays two AB patterns (intensity 4:4) for the four OCH_2O groups and two triplets (intensity 2:2) for the four methine atoms. That of **2** displays four AB patterns for the eight -OCH_2O- bridges. The signals of the triazolium NC*H* and NC*H₃* protons lie in the expected ranges (see experimental part).

Crystals of triazole **8** suitable for an X-ray diffraction study were obtained by slow diffusion of methanol into a dichloromethane solution of the product (Figure 2). Compound **8** crystallises in the monoclinic space group *C*2/*c*. In a first approximation, the asymmetric unit contains two practically identical molecules, A and B, but actually the B sites display a double occupancy (0.5:0.5) of molecules of **8** interchangeable through a plane perpendicular to the triazole ring and bissecting the N–$C_{carbene}$–C angle. The two aromatic rings of the resorcinarenes connected to the triazole moiety are roughly perpendicular to the triazole plane (dihedral angles in A: 85.1° and 79.8°). This is in line with observations made for conventional NHCs having their N atoms substituted by bulky aryl groups.[12] Both cavitands of **8** adopt the typical bowl-shaped structure of resorcin[4]arene-derived cavitands equipped with -OCH_2O- linkers, with wide rim diameters[13] (i.e., the segments linking the C-2 aromatic carbon atoms of opposite resorcinols) of 7.80/8.07 Å and 7.89/8.01 Å in the two macrocycles of molecule A and of 7.91/8.00 Å (averaged) in the cavitands of molecule B. Interestingly, the lower rims of the two resorcinarene units of each molecule are facing each other, thereby creating a pseudo capsular moiety.
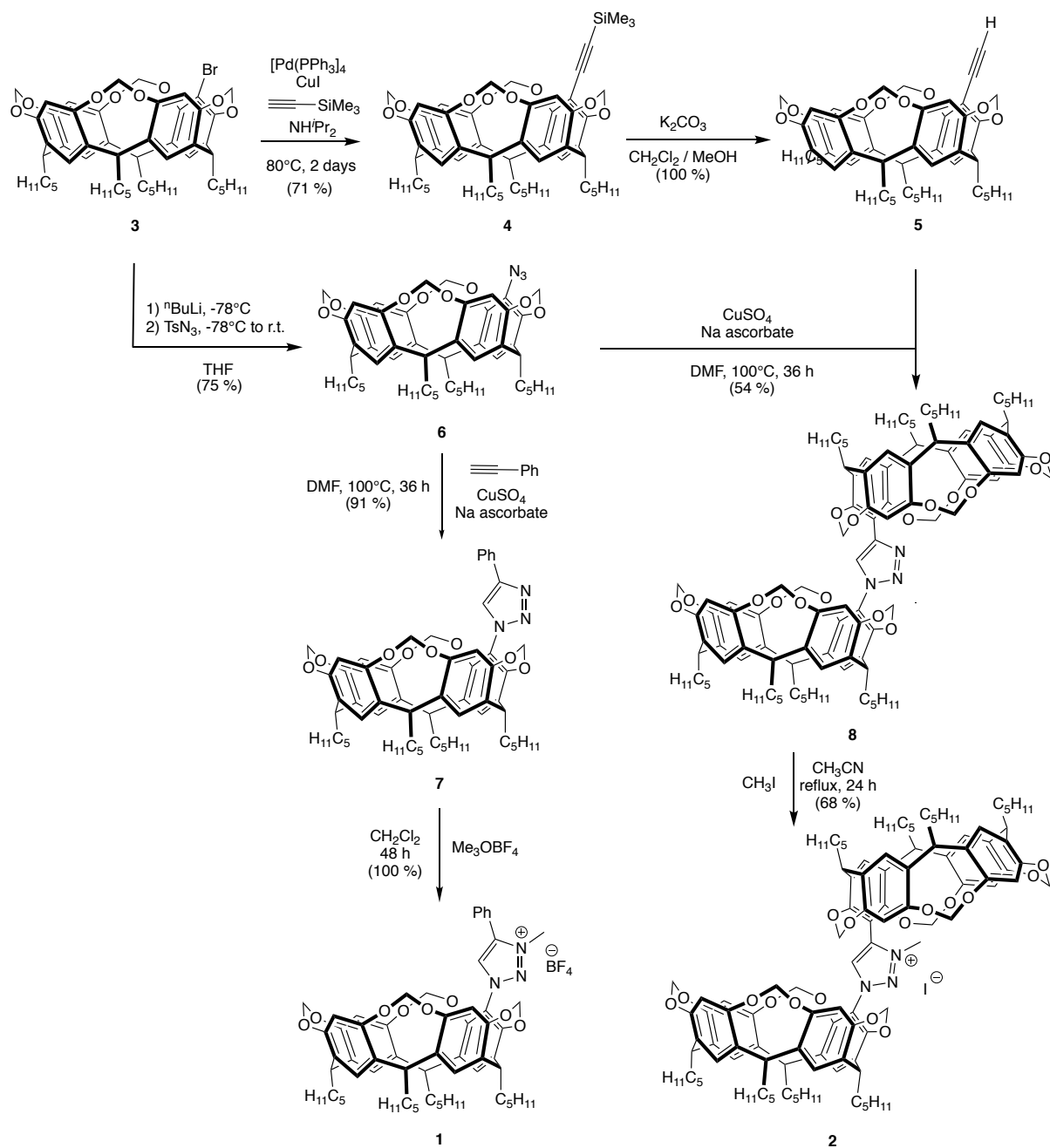
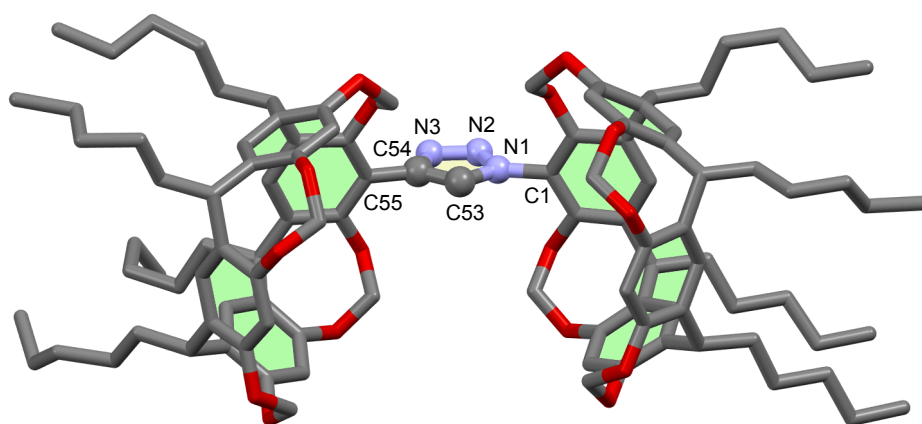Scheme 1: Synthesis of the resorcinarene-based triazolium salts **1** and **2**.

Figure 2: X-ray structure of triazole **8**. Only one of the two molecules present in the unit cell (molecule A) is shown. Selected bond lengths (Å): C1-N1 1.462(6); N1-N2 1.320(6); N2-N3 1.335(7); N3-C54 1.339(6); C54-C55 1.440(6); C53-C54 1.347(6); N1-C53 1.366(6).

The two triazolium salts were used as a ligand source for the synthesis of two PEPPSI-type complexes (**9** and **10**) (PEPPSI = pyridine-enhanced precatalyst preparation stabilisation and initiation).[14] These were obtained by reaction of **1** or **2** with [PdCl₂] in refluxing pyridine for 24 h in the presence of K_2CO_3 and a large excess of KBr in the case of salt **2** (Scheme 2). The observed yields (26 % for **9** and 28 % for **10**) were relatively low, but this is not unusual for reactions carried out with bulky NHC precursors.[11f, 15] Both complexes were characterised by elemental analysis and ¹H and ¹³C NMR spectroscopy. None of the mass spectra displayed the expected molecular peaks, but unambiguously revealed the formation of PdL species (L = carbene). Thus, the mass spectrum of complex **9** showed an intense peak at m/z = 1193.44 with the profile expected for the corresponding $[M - Cl]^+$ cation. Consistent with the proposed formula, the ¹H NMR of **9** shows two distinct AB systems for the methylenic OCH_2O atoms, two triplets for the four methine hydrogen atoms and a singlet at 4.05 ppm (3H) corresponding to the NCH₃ group. In the ¹³C NMR spectrum, the carbenic C atom appears as a singlet at 145.99 ppm. As could be inferred from a ¹H-¹H ROESY NMR spectrum, which revealed weak correlations between pyridinic and pentyl H atoms, the P-Pd bond of **9** must, at least temporarily, be turned away from the cavity. Molecular models suggest that such a conformation with an exo-oriented Pd atom is sterically favoured over those having the metal placed above the cavity entrance. However, there is no indication that endo-conformers exist in solution, unlike the observations recently made with related complexes based on classical NHCs.[11a]

The mass spectrum of **10** showed a strong peak at 1937.79 corresponding to [M - Br - pyridine + acetonitrile]$^+$ ions, which possibly formed in the spectrometer in the presence of adventitious acetonitrile. The ¹H NMR spectrum of **10** displays four NCH₃ singlets, at 3.85, 3.78, 3.73 and 3.66 ppm (relative intensities: 26/57/11/6), thus revealing the presence of four distinct conformers (Figure 3). This observation suggests the existence of high rotational barriers about the N-C$_{resorc}$ and C$_{triazole}$-C$_{resorc}$ bonds. The reason why several stable conformers can be seen here (and not in the case of 9), possibly arises from the difficulty of the "PdBr₂(pyridine)" moiety of **10** to adapt its orientation to the steric requirements imposed during the rotations about the N-C$_{resorc}$ and C$_{triazole}$-C$_{resorc}$ bonds.
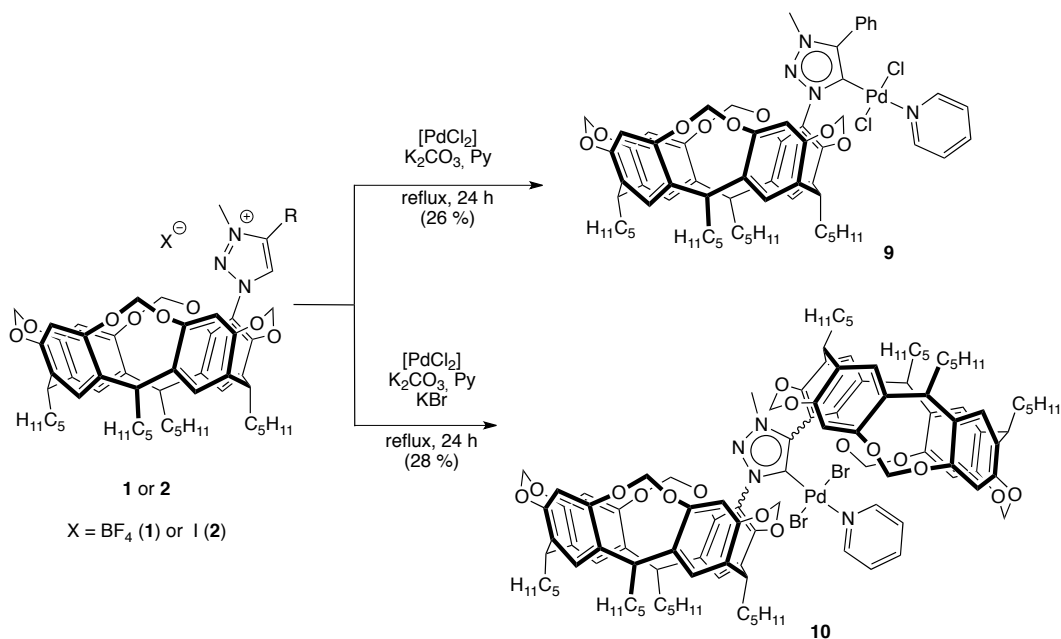
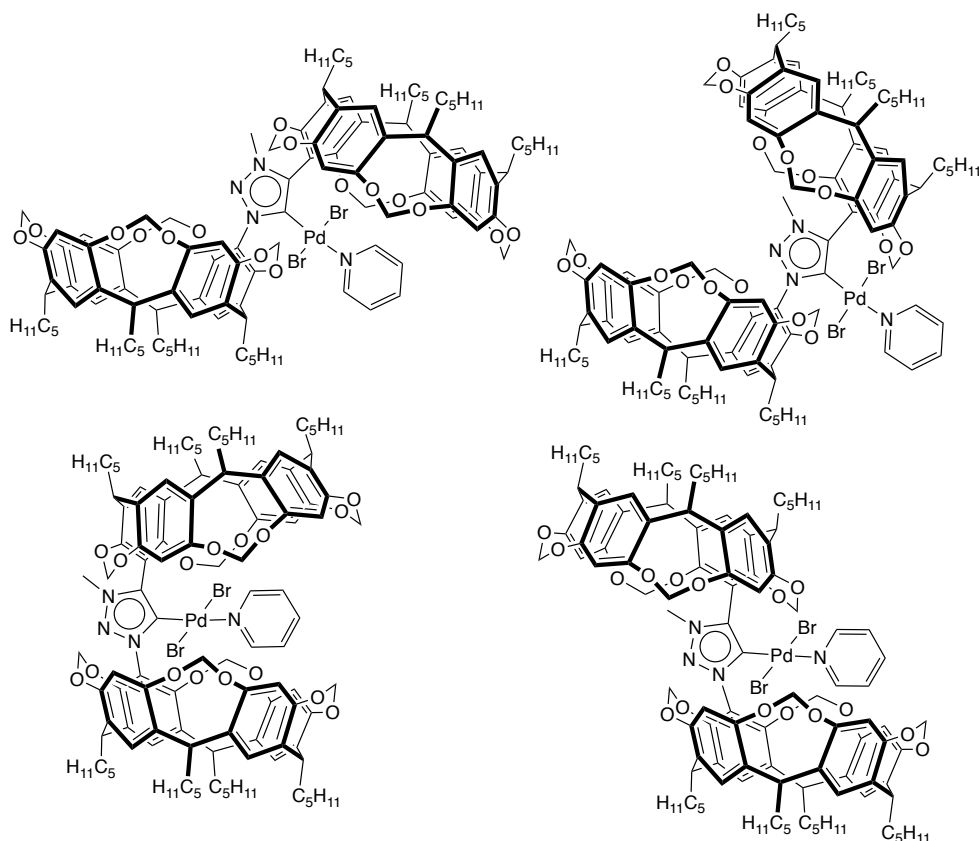Scheme 2: Synthesis of PEPPSI-type palladium complexes **9** and **10**.

Figure 3. Rotational conformers of complex **10**.

Catalytic Suzuki-Miyaura cross-coupling reactions with triazolium salts 1 and 2

Triazolium salts **1** and **2** were first assessed in cross coupling between phenyl boronic acid and 4-chloroanisole (Scheme 3). To determine the best catalyst, reactions were carried out by using a palladium loading of 0.5 mol %. The conversions were determined after 2 hour at 100°C. In a first series of runs in DMF and using [Pd(OAc)$_2$], we determined the optimal base from Cs$_2$CO$_3$, K$_2$CO$_3$, NaH, K$_3$PO$_4$ and ^{t}BuOK. As can be deduced from Table 1, the most efficient base was ^{t}BuOK, which led to conversions of 30.2 and 24.6 %, respectively with **1**

and **2** (Table 1, entries 9 and 11). In a second series of tests we investigated the influence on the reactivity of the palladium precursor. To this end, [Pd(OAc)$_2$], [PdCl(η^3-C$_3$H$_5$)]$_2$, [PdCl$_2$(PhCN)$_2$], [PdCl$_2$(cod)] and [Pd$_2$(dba)$_3$] were used. The highest conversions were obtained with [Pd(OAc)$_2$] and [PdCl$_2$(PhCN)$_2$] in combination with the salts **1** (30.2 %) and **2** (28.5 %), respectively (Table 1, entries 9 and 15). Repeating the runs in 1,4-dioxane instead of DMF increased the conversions up to 47.2 % and 42.9 %, respectively (Table 1, entries 10 and 16). Note that when the cross-coupling of 4-chloroanisole (under optimised conditions) was achieved with complex **9**, the conversions were nearly the same as those obtained with the corresponding *in-situ* generated catalysts (Table 1, entries 10 and 21).
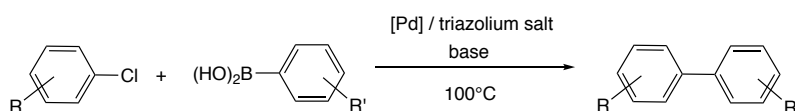
Scheme 3: Suzuki-Miyaura cross-coupling of aryl chlorides

Table 1. Suzuki-Miyaura cross-coupling reaction of 4-chloroanisole with phenylboronic acid: a search for optimal catalytic conditions.
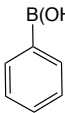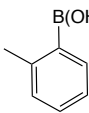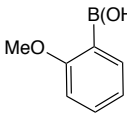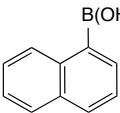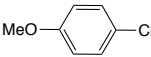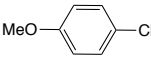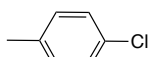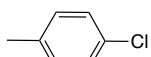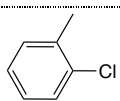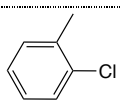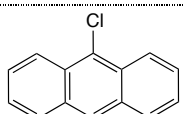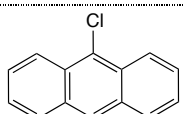
Entry	Triazolium salt	[Pd]	Base	Solvent	Conversion (%)
1	**1**	[Pd(OAc)$_2$]	Cs$_2$CO$_3$	DMF	2.6
2	**2**				8.1
3	**1**	[Pd(OAc)$_2$]	K$_2$CO$_3$	DMF	traces
4	**2**				traces
5	**1**	[Pd(OAc)$_2$]	NaH	DMF	1.0
6	**2**				18.0
7	**1**	[Pd(OAc)$_2$]	K$_3$PO$_4$	DMF	traces
8	**2**				traces
9	**1**			DMF	30.2
10	**1**	[Pd(OAc)$_2$]	^{t}BuOK	dioxane	47.2
11	**2**			DMF	24.6
12	**1**	[PdCl(η^3-C$_3$H$_5$)]$_2$	^{t}BuOK	DMF	traces
13	**2**				18.8
14	**1**			DMF	28.3
15	**2**	[PdCl$_2$(PhCN)$_2$]	^{t}BuOK	DMF	28.5
16	**2**			dioxane	42.9
17	**1**	[PdCl$_2$(cod)]	^{t}BuOK	DMF	30.5
18	**2**				23.4
19	**1**	[Pd$_2$(dba)$_3$]	^{t}BuOK	DMF	8.7
20	**2**				16.8
21	Palladium complex **9**		^{t}BuOK	dioxane	45.9

Reagents and conditions: [Pd] (0.5 mol %), triazolium salt (0.5 mol %), 4-MeOC$_6$H$_4$Cl (0.5 mmol), PhB(OH)$_2$ (0.75

mmol), base (0.75 mmol), decane (0.025 mL), solvent (2.00 mL), 100°C, 2 h. The conversions were determined by GC, the calibrations being based on decane.

The above optimised conditions (^{t}BuOK/[Pd(OAc)$_2$]/salt **1**; ^{t}BuOK/[PdCl$_2$(PhCN)$_2$]/salt **2**; dioxane at 100°C) were then applied to coupling reactions between four aryl chlorides, namely 4-chloroanisole, 4-chlorotoluene, 2-chlorotoluene and 9-chloroanthracene, and four boronic acids: phenylboronic acid, 2-methylphenylboronic acid, 2-methoxyphenylboronic acid and naphthalene-1-boronic acid (Table 2). High conversions (80-100%) were observed after 5 h with both triazolium salts in the reactions involving 4-chloroanisole or 4-chlorotoluene with any arylboronic acid. Unsurprisingly, the sterically more encumbered 2-chlorotoluene and 9-chloroanthracene substrates resulted in five times lower activities (Table 2, entries 5 and 6).

Table 2. Suzuki-Miyaura cross-coupling of aryl chlorides using triazolium salts **1** or **2**.

Entry	ArCl	Triazolium salt		B(OH)$_2$ (phenyl)	B(OH)$_2$ (2-methyl)	B(OH)$_2$ (MeO)	B(OH)$_2$ (naphthalene)
1	MeO—C$_6$H$_4$—Cl	**1** (5 h)	conv. (%)	99.8	97.7	99.6	98.3
2		**2** (5 h)	conv. (%)	95.6	80.6	79.8	77.7
3	CH$_3$—C$_6$H$_4$—Cl	**1** (5 h)	conv. (%)	94.8	77.4	80.0	99.2
4		**2** (5 h)	conv. (%)	99.8	84.7	83.0	99.6
5	2-chlorotoluene	**1** (24 h)	conv. (%)	100	100	62.7	97.3
6		**2** (24 h)	conv. (%)	83.2	64.5	52.3	76.0
7	9-chloroanthracene	**1** (24 h)	conv. (%)	99.8	98.9	95.1	99.7
8		**2** (24 h)	conv. (%)	97.7	99.0	83.4	99.4

Reagents and conditions: [Pd(OAc)$_2$] (0.5 mol %) in combination with salt **1** (0.5 mol %) or [PdCl$_2$(PhCN)$_2$] (0.5 mol %) in combination with salt **2** (0.5 mol %), ArCl (0.5 mmol), Ar'B(OH)$_2$ (0.75 mmol), ^{t}BuOK (0.75 mmol), decane (0.025 mL), dioxane (2.00 mL), 100°C, reaction time: 5h (for entries 1-4); 24h (for entries 5-8). The conversions were determined by GC, the calibrations being based on decane.

On the basis of a recent study on the use in Suzuki-Miyaura couplings of conventional NHCs substituted by a resorcinarenyl moiety,[11a-d] we assign the high efficiency of triazolium salt **1** in the above reactions to the presence of two flexible pentyl chains able to sterically interact with the metal centre in those complexes where the palladium displays an exo orientation with respect to the cavity (Figure 4), this facilitating then the reductive elimination step. The observation that salt **2** led to lower conversions than salt **1** is merely due to the high steric encumbrance created about the palladium in complexes formed from the bulky **2** which impedes the approach of the substrates.
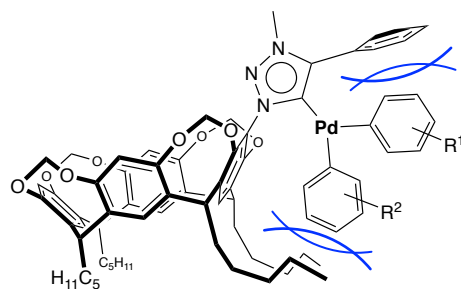
Figure 4. Catalysis with derivatives of **1**. Possible steric interactions during the catalytic cycle between pentyl groups and the metal centre.

Conclusion

In summary, we have described the first triazolium salts substituted by resorcinarene units (**1** and **2**) and assessed them in the palladium-catalysed Suzuki-Miyaura cross-coupling of bulky aryl chlorides with sterically hindered aryl boronic acids. Significantly better activities were observed with the sterically less hindered triazolium salt **1**, which bears a single resorcinarene substituent. Its higher efficiency compared to that of **2** likely reflects a higher substrate accessibility in the resulting catalytic intermediates as well as the presence of flexible pentyl groups that may interact with the metal centre so as to facilitate the reductive elimination step. Further studies are aimed at exploiting the steric as well as receptor properties of resorcinarene-derived triazolium salts in carbon-carbon bond forming reactions.

Experimental Section

General Remarks: All manipulations involving sensitive derivatives were carried out in Schlenk-type flasks under dry argon. Solvents were dried by conventional methods and were distilled immediately before use. CDCl$_3$ was passed down a 5 cm-thick alumina column and stored under nitrogen over molecular sieves (4 Å). Routine ^{1}H and ^{13}C{^{1}H} spectra were recorded with Bruker FT instruments (AC 400 and 500). ^{1}H NMR spectra were referenced to residual protiated solvents (δ = 7.26 ppm for CDCl$_3$). ^{13}C NMR chemical shifts are reported relative to deuterated solvents (δ = 77.16 ppm for CDCl$_3$). Chemical shifts and coupling constants are reported in ppm and Hz, respectively. Infrared spectra were recorded with a Bruker FTIR Alpha-P spectrometer. Elemental analyses were carried out by the Service de Microanalyse, Institut de Chimie, Université de Strasbourg. The catalytic solutions were analysed with a Varian 3900 gas chromatograph fitted with a WCOT fused silica column (25 m × 0.25 mm, 0.25 μm film thickness). 5-bromo-4(24),6(10),12(16),18(22)-tetramethylenedioxy-2,8,14,20-tetrapentylresorcin[4]arene (**3**),[16] and tosyl azide[17] were prepared by literature procedures.

5-(Trimethylsilyl)ethynyl-4(24),6(10),12(16),18(22)-tetramethylenedioxy-2,8,14,20-tetra pentylresorcin[4]arene (4): To a solution of bromo-cavitand **3** (2.000 g, 2.23 mmol), [Pd(PPh$_3$)$_4$] (0.265 g, 0.23 mmol) and CuI (0.023 g, 0.12 mmol) in NH^{i}Pr$_2$ (100 mL) was added trimethylsilylacetylene (3.1 mL, 22.30 mmol). The mixture turned rapidly from yellow to black. The resulting suspension was stirred for 48 h at 80°C, then cooled

to room temperature. The solution was evaporated to dryness and the resulting residue was dissolved in CH_2Cl_2 (200 mL). The organic solution was washed with brine (3 x 100 mL) and the aqueous layers were extracted with CH_2Cl_2 (2 x 100 mL). The combined organic layers were dried over $MgSO_4$, filtered and evaporated under reduced pressure, and the crude product was purified by column chromatography (Et_2O/petroleum ether, 10:90; Rf = 0.36) to give **4** (1.453 g, 71 %). ^{1}H NMR (500 MHz, $CDCl_3$): δ = 7.08 (s, 4H, arom. CH, resorcinarene), 6.50 (s, 3H, arom. CH, resorcinarene), 5.81 and 4.46 (AB spin system, 4H, OCH_2O, ^2J = 7.0 Hz), 5.74 and 4.44 (AB spin system, 4H, OCH_2O, ^2J = 7.0 Hz), 4.76 (t, 2H, CHCH$_2$, ^3J = 8.2 Hz), 4.72 (t, 2H, CHCH$_2$, ^3J = 8.2 Hz), 2.25-2.16 (m, 8H, CHCH_2), 1.45-1.31 (m, 24H $CH_2CH_2CH_2$CH$_3$), 0.91 (t, 12H, CH_2CH_3, ^3J = 7.0 Hz), 0.19 (s, 9H, Si(CH$_3$)$_3$) ppm. ^{13}C{^{1}H} NMR (126 MHz, $CDCl_3$): δ = 155.86-96.93 (arom. Cs), 112.74 (s, C≡CSiMe$_3$), 103.58 (s, C≡CSiMe$_3$), 99.63 (s, OCH$_2$O), 98.89 (s, OCH$_2$O), 36.51 (s, CHCH$_2$), 36.50 (s, CHCH$_2$), 32.17 (s, CH$_2$CH$_2$CH$_3$), 32.06 (s, CH$_2$CH$_2$CH$_3$), 29.98 (s, CHCH$_2$), 29.74 (s, CHCH$_2$), 27.70 (s, CHCH$_2$$CH_2$), 27.63 (s, CHCH$_2$$CH_2$), 22.84 (s, CH$_2CH_3$), 14.24 (s, CH$_2$$CH_3$), 0.05 (s, Si($CH_3$)$_3$) ppm. Elemental analysis calcd (%) for $C_{57}H_{72}O_8Si$ (913.26): C 74.96, H 7.95; found C 75.25, H 8.18.

5-Ethynyl-4(24),6(10),12(16),18(22)-tetramethylenedioxy-2,8,14,20-tetrapentylresorcin [4]arene (5): A solution of **4** (1.000 g, 2.90 mmol) and K_2CO_3 (1.508 g, 10.91 mmol) in CH_2Cl_2/MeOH (50 mL; 25:75 v/v) was stirred at room temperature for 16 h. The reaction mixture was evaporated to dryness and the residue was treated with a mixture of CH_2Cl_2/H_2O (500 mL; 1:1 v/ v). The aqueous layer was washed with CH_2Cl_2 (2 x 100 mL), then the combined organic layers were dried with $MgSO_4$. After filtration, the solvent was evaporated off under reduced pressure to afford **5** as a white solid (0.918 g, yield 100 %). ^{1}H NMR (500 MHz, $CDCl_3$): δ = 7.11 (s, 1H, arom. CH, resorcinarene), 7.09 (s, 3H, arom. CH, resorcinarene), 6.51 (s, 2H, arom. CH, resorcinarene), 6.50 (s, 1H, arom. CH, resorcinarene), 5.84 and 4.46 (AB spin system, 4H, OCH_2O, ^2J = 7.0 Hz), 5.75 and 4.44 (AB spin system, 4H, OCH_2O, ^2J = 7.0 Hz), 4.76 (t, 2H, CHCH$_2$, ^3J = 8.0 Hz), 4.72 (t, 4H, CHCH$_2$, ^3J = 8.0 Hz), 3.30 (s, 1H, C≡CH), 2.25-2.17 (m, 8H, CHCH_2), 1.45-1.31 (m, 24H, $CH_2CH_2CH_2$CH$_3$), 0.91 (t, 12 H, CH_2CH_3, ^3J = 7.0 Hz) ppm. ^{13}C{^{1}H} NMR (126 MHz, $CDCl_3$): δ = 156.18-111.71 (arom. Cs), 99.62 (s, OCH$_2$O), 99.11 (s, OCH$_2$O), 85.27 (s, C≡CH), 75.81 (s, C≡CH), 36.53 (s, CHCH$_2$), 36.48 (s, CHCH$_2$), 32.16 (s, CH$_2$CH$_2$CH$_3$), 32.10 (s, CH$_2$CH$_2$CH$_3$), 29.95 (s, CHCH$_2$), 29.78 (s, CHCH$_2$), 27.70 (s, CHCH$_2$$CH_2$), 27.64 (s, CHCH$_2$$CH_2$), 22.84 (s, CH$_2CH_3$), 14.26 (s, CH$_2$$CH_3$) ppm. Elemental analysis calcd (%) for $C_{54}H_{64}O_8$ (841.08): C 77.11, H 7.67; found C 77.26, H 7.89.

5-Azido-4(24),6(10),12(16),18(22)-tetramethylenedioxy-2,8,14,20-tetrapentylresorcin[4] arene (6): n-Butyllithium (1.6 M in hexane; 2.51 mL, 4.02 mmol) was slowly added to a solution of bromo-cavitand **3** (3.000 g, 3.35 mmol) in THF (150 mL) at -78 °C. After 1 h, the resulting anion was quenched with tosyl azide (0.792 g, 4.02 mmol), and the mixture was stirred at room temperature for 24 h. The reaction mixture was washed three times with brine (3 x 100 mL). The solvent was evaporated under reduced pressure, and the crude product was purified by column chromatography (Et_2O/petroleum ether, 5:95; Rf = 0.32) to give **6** (2.150 g, 75 %). ^{1}H NMR (500 MHz, $CDCl_3$): δ = 7.10 (s, 3H, arom. CH, resorcinarene), 6.88 (s, 1H, arom. CH, resorcinarene), 6.52 (s, 2H, arom. CH, resorcinarene), 6.48 (s, 1H, arom. CH, resorcinarene), 5.78 and 4.43 (AB spin system, 4H, OCH_2O, ^2J = 7.0 Hz), 5.75 and 4.42 (AB spin system, 4H, OCH_2O, ^2J = 7.0 Hz), 4.73 (t, 4H, CHCH$_2$, ^3J = 8.0 Hz), 2.24-2.17 (m, 8H, CHCH_2), 1.44-1.31 (m, 24H $CH_2CH_2CH_2$CH$_3$), 0.92 (t, 6H, CH$_2$CH_3, ^3J = 7.2 Hz), 0.91 (t, 6H, CH$_2$CH_3, ^3J = 7.2

Hz) ppm. ^{13}C{^{1}H} NMR (126 MHz, CDCl$_3$): δ = 155.13-115.50 (arom. Cs), 100.00 (s, OCH$_2$O), 99.70 (s, OCH$_2$O), 36.74 (s, CHCH$_2$), 36.50 (s, CHCH$_2$), 32.16 (s, CH$_2$CH$_2$CH$_3$), 32.12 (s, CH$_2$CH$_2$CH$_3$), 29.95 (s, CHCH$_2$), 29.91 (s, CHCH$_2$), 27.69 (s, CHCH$_2$$CH_2$), 27.67 (s, CHCH$_2$$CH_2$), 22.84 (s, CH$_2CH_3$), 14.25 (s, CH$_2$$CH_3$) ppm. IR: ν = 2103 and 1286 (N$_3$) cm^{-1}. Elemental analysis calcd (%) for C$_{52}$H$_{63}$N$_3$O$_8$ (858.07): C 72.79, H 7.40, N 4.90; found C 72.58, H 7.51, N 4.64.

1H-1,2,3-Triazole,1-{4(24),6(10),12(16),18(22)-tetramethylenedioxy-2,8,14,20-tetrapentyl resorcin[4]arene-5-yl}-4-phenyl (7): To a solution of azido-cavitand **6** (0.500 g, 0.58 mmol), CuSO$_4$·5H$_2$O (0.014 g, 0.06 mmol) and sodium ascorbate (0.012 g, 0.06 mmol) in DMF (50 mL) was added phenylacetylene (0.06 mL, 0.58 mmol). The mixture was stirred for 36 h at 100°C, then cooled to room temperature. The solution was evaporated to dryness and the resulting residue was dissolved in CH$_2$Cl$_2$ (200 mL). The organic solution was washed with brine (3 x 100 mL) and the aqueous layers were extracted with CH$_2$Cl$_2$ (2 x 100 mL). The combined organic layer were dried over MgSO$_4$, filtered and evaporated under reduced pressure, and the crude product was purified by column chromatography (Et$_2$O/petroleum ether, 20:80; Rf = 0.39) to give **7** (0.510 g, 91 %). ^{1}H NMR (500 MHz, CDCl$_3$): δ = 7.96 (s, 1H, CH, triazole), 7.87 (d, 2H, arom. CH, Ph, ^3J = 7.5 Hz) 7.46 (t, 2H, arom. CH, Ph, ^3J = 7.5 Hz), 7.37 (t, 1H, arom. CH, Ph, ^3J = 7.5 Hz), 7.34 (s, 1H, arom. CH, resorcinarene), 7.12 (s, 2H, arom. CH, resorcinarene), 7.12 (s, 1H, arom. CH, resorcinarene), 6.59 (s, 1H, arom. CH, resorcinarene), 6.47 (s, 2H, arom. CH, resorcinarene), 5.74 and 4.60 (AB spin system, 4H, OCH$_2$O, ^2J = 7.5 Hz), 5.42 and 4.36 (AB spin system, 4H, OCH$_2$O, ^2J = 7.5 Hz), 4.79 (t, 2H, CHCH$_2$, ^3J = 8.2 Hz), 4.74 (t, 2H, CHCH$_2$, ^3J = 8.0 Hz), 2.31-2.21 (m, 8H, CHCH_2), 1.48-1.33 (m, 24H $CH_2CH_2CH_2$CH$_3$), 0.94 (t, 6H, CH$_2$CH_3, ^3J = 7.5 Hz), 0.92 (t, 6H, CH$_2$CH_3, ^3J = 7.0 Hz) ppm. ^{13}C{^{1}H} NMR (101 MHz, CDCl$_3$): δ = 155.33-116.79 (arom. Cs), 122.90 (s, CH, triazole), 99.83 (s, OCH$_2$O), 99.52 (s, OCH$_2$O), 36.79 (s, CHCH$_2$), 36.51 (s, CHCH$_2$), 32.17 (s, CH$_2$CH$_2$CH$_3$), 32.11 (s, CH$_2$CH$_2$CH$_3$), 30.08 (s, CHCH$_2$), 29.80 (s, CHCH$_2$), 27.71 (s, CHCH$_2$$CH_2$), 22.83 (s, CH$_2CH_3$), 14.23 (s, CH$_2$$CH_3$) ppm. MS (ESI-TOF): m/z = 960.52 [M + H]$^+$, expected isotopic profile. Elemental analysis calcd (%) for C$_{60}$H$_{69}$N$_3$O$_8$ (960.21): C 75.05, H 7.24, N 4.38; found C 74.86, H 7.02, N 4.23.

1H-1,2,3-Triazole,1,4-bis{4(24),6(10),12(16),18(22)-tetramethylenedioxy-2,8,14,20-tetrapentylresorcin[4]arene-5-yl} (8): A solution of ethynyl-cavitand **5** (0.490 g, 0.58 mmol), azido-cavitand **6** (0.500 g, 0.58 mmol), CuSO$_4$·5H$_2$O (0.014 g, 0.06 mmol) and sodium ascorbate (0.012 g, 0.06 mmol) in DMF (50 mL) was stirred for 36 h at 100°C. Afterwards, the mixture was cooled to room temperature and evaporated to dryness. The resulting residue was dissolved in CH$_2$Cl$_2$ (200 mL). The organic solution was washed with brine (3 x 100 mL) and the aqueous layers were extracted with CH$_2$Cl$_2$ (2 x 100 mL). The combined organic layer were dried over MgSO$_4$, filtered and evaporated under reduced pressure, and the crude product was purified by column chromatography (Et$_2$O/petroleum ether, 20:80; Rf = 0.28) to give **8** (0.535 g, 54 %). ^{1}H NMR (500 MHz, CDCl$_3$): δ = 7.92 (s, 1H, CH, triazole), 7.34 (s, 1H, arom. CH, resorcinarene), 7.23 (s, 1H, arom. CH, resorcinarene), 7.12 (s, 2H, arom. CH, resorcinarene), 7.12 (s, 3H, arom. CH, resorcinarene), 7.11 (s, 1H, arom. CH, resorcinarene), 6.58 (s, 1H, arom. CH, resorcinarene), 6.54 (s, 1H, arom. CH, resorcinarene), 6.48 (s, 2H, arom. CH, resorcinarene), 6.46 (s, 2H, arom. CH, resorcinarene), 5.74 and 4.56 (AB spin system, 4H, OCH$_2$O, ^2J = 7.0 Hz), 5.73 and 4.51 (AB spin system, 4H, OCH$_2$O, ^2J = 7.0 Hz), 5.57 and 4.41 (AB spin system, 4H, OCH$_2$O, ^2J = 7.5 Hz), 5.32 and 4.29 (AB

spin system, 4H, OCH$_2$O, ^2J = 7.5 Hz), 4.83 (t, 2H, CH*CH$_2$*, ^3J = 8.0 Hz), 4.77 (t, 2H, CH*CH$_2$*, ^3J = 8.0 Hz), 4.74 (t, 2H, CH*CH$_2$*, ^3J = 7.5 Hz), 4.72 (t, 2H, CH*CH$_2$*, ^3J = 7.5 Hz), 2.30-2.21 (m, 16H, CHC*H$_2$*), 1.48-1.33 (m, 48H *CH$_2$CH$_2$CH$_2$*CH$_3$), 0.94 (t, 6H, CH$_2$C*H$_3$*, ^3J = 7.0 Hz), 0.93 (t, 6H, CH$_2$C*H$_3$*, ^3J = 7.0 Hz), 0.92 (t, 12H, CH$_2$C*H$_3$*, ^3J = 7.0 Hz) ppm. ^{13}C{^{1}H} NMR (126 MHz, CDCl$_3$): δ = 155.33-116.74 (arom. Cs), 127.33 (s, CH, triazole), 99.77 (s, OCH$_2$O), 99.65 (s, OCH$_2$O), 99.58 (s, OCH$_2$O), 99.52 (s, OCH$_2$O), 36.79 (s, *C*HCH$_2$), 36.51 (s, *C*HCH$_2$), 32.19 (s, *C*H$_2$CH$_2$CH$_3$), 32.14 (s, *C*H$_2$CH$_2$CH$_3$), 30.08 (s, CH*C*H$_2$), 29.96 (s, CH*C*H$_2$), 29.81 (s, CH*C*H$_2$), 27.78 (s, CHCH$_2$*C*H$_2$), 27.72 (s, CHCH$_2$*C*H$_2$), 22.85 (s, *C*H$_2$CH$_3$), 14.27 (s, CH$_2$*C*H$_3$) ppm. MS (ESI-TOF): m/z = 1698.93 [M + H]$^+$, expected isotopic profile. Elemental analysis calcd (%) for C$_{106}$H$_{127}$N$_3$O$_{16}$ (1697.16): C 74.93, H 7.53, N 2.47; found C 74.68, H 7.47, N 2.39.

1-{4(24),6(10),12(16),18(22)-Tetramethylenedioxy-2,8,14,20-tetrapentylresorcin[4]arene-5-yl}-4-phenyl-3-methyl-1*H*-1,2,3-triazolium tetrafluoroborate (1): Triazole-cavitand **7** (0.500 g, 0.52 mmol) and Me$_3$OBF$_4$ (0.115 g, 0.78 mmol) were dissolved in CH$_2$Cl$_2$ (20 mL) and the resulting solution was stirred for 2 days at room temperature. The organic solution was washed with brine (3 x 100 mL) and the aqueous layers were extracted with CH$_2$Cl$_2$ (2 x 100 mL). The combined organic layer were dried over MgSO$_4$, filtered and evaporated under reduced pressure. The crude product was dissolved in the minimum amount of CH$_2$Cl$_2$ and salt **1** was precipitated by addition of hexane (200 mL) , the solid was filtered and dried under vacuum (0.550 g, 100 %). ^{1}H NMR (500 MHz, CDCl$_3$): δ = 8.21 (s, 1H, CH, triazolium), 7.70 (d, 2H, arom. CH, phenyl, ^3J = 7.0 Hz) 7.66-7.59 (m, 3H, arom. CH, phenyl), 7.43 (s, 1H, arom. CH, resorcinarene), 7.12 (s, 1H, arom. CH, resorcinarene), 7.12 (s, 2H, arom. CH, resorcinarene), 6.59 (s, 2H, arom. CH, resorcinarene), 6.54 (s, 1H, arom. CH, resorcinarene), 5.73 and 4.59 (AB spin system, 4H, OCH$_2$O, ^2J = 7.5 Hz), 5.66 and 4.60 (AB spin system, 4H, OCH$_2$O, ^2J = 7.5 Hz), 4.79 (t, 2H, CH*CH$_2$*, ^3J = 8.2 Hz), 4.75 (t, 2H, CH*CH$_2$*, ^3J = 8.2 Hz), 4.35 (s, 3H, triazolium-CH$_3$), 2.30-2.18 (m, 8H, CHC*H$_2$*), 1.60-1.33 (m, 24H *CH$_2$CH$_2$CH$_2$*CH$_3$), 0.93 (t, 6H, CH$_2$C*H$_3$*, ^3J = 7.0 Hz), 0.92 (t, 6H, CH$_2$C*H$_3$*, ^3J = 7.0 Hz) ppm. ^{13}C{^{1}H} NMR (126 MHz, CDCl$_3$): δ = 155.77-117.32 (arom. Cs), 129.60 (s, CH, triazolium), 101.04 (s, OCH$_2$O), 99.60 (s, OCH$_2$O), 39.17 (s, triazolium-CH$_3$), 36.77 (s, *C*HCH$_2$), 36.49 (s, *C*HCH$_2$), 32.18 (s, *C*H$_2$CH$_2$CH$_3$), 32.07 (s, *C*H$_2$CH$_2$CH$_3$), 30.11 (s, CH*C*H$_2$), 29.77 (s, CH*C*H$_2$), 27.69 (s, CHCH$_2$*C*H$_2$), 22.84 (s, *C*H$_2$CH$_3$), 14.26 (s, CH$_2$*C*H$_3$), 14.25 (s, CH$_2$*C*H$_3$) ppm. MS (ESI-TOF): m/z = 974.53 [M - BF$_4$]$^+$, expected isotopic profile. Elemental analysis calcd (%) for C$_{61}$H$_{72}$N$_3$O$_8$BF$_4$ (1062.05): C 68.98, H 6.83, N 3.96; found C 69.16, H 6.72, N 3.82.

1,4-Bis{4(24),6(10),12(16),18(22)-tetramethylenedioxy-2,8,14,20-tetrapentylresorcin[4] arene-5-yl}-3-methyl-1*H*-1,2,3-triazolium iodide (2): To a solution of triazole-bis-cavitand **8** (0.100 g, 0.06 mmol) in CH$_2$Cl$_2$ (5 mL) was added MeI (0.12 mL, 0.29 mmol). The mixture was stirred for 2 days at room temperature. Then the salt **2** was precipitated by addition of hexane (50 mL), the solid was filtered and dried under vacuum (0.074 g, 68 %). ^{1}H NMR (500 MHz, CDCl$_3$): δ = 9.47 (s br, 1H, CH, triazolium), 7.64 (s, 2H, arom. CH, resorcinarene), 7.11 (s, 4H, arom. CH, resorcinarene), 7.09 (s, 1H, arom. CH, resorcinarene), 7.08 (s, 1H, arom. CH, resorcinarene), 6.58 (s, 2H, arom. CH, resorcinarene), 6.57 (s, 2H, arom. CH, resorcinarene), 6.54 (s, 1H, arom. CH, resorcinarene), 6.52 (s, 1H, arom. CH, resorcinarene), 5.66 and 4.65 (AB spin system, 4H, OCH$_2$O, ^2J = 7.5 Hz), 5.64 and 4.70 (AB spin system, 4H, OCH$_2$O, ^2J = 7.5 Hz), 5.47 and 4.72 (AB spin system, 4H, OCH$_2$O, ^2J = 7.0 Hz), 5.31 and 5.05 (AB spin system, 4H, OCH$_2$O, ^2J = 6.5 Hz), 4.75-4.70 (m, 8H, CH*CH$_2$*), 4.20 (s, 3H, triazolium-CH$_3$), 2.36-2.19 (m, 16H, CHC*H$_2$*),

1.47-1.32 (m, 48H $CH_2CH_2CH_2CH_3$), 0.93 (t, 12H, CH_2CH_3, ^3J = 7.0 Hz), 0.91 (t, 12H, CH_2CH_3, ^3J = 7.0 Hz) ppm. $^{13}C\{^1H\}$ NMR (126 MHz, CDCl$_3$): δ = 155.64-109.45 (arom. Cs), 117.36 (s, CH, triazolium), 99.56 (s, OCH$_2$O), 99.27 (s, OCH$_2$O), 99.15 (s, OCH$_2$O), 98.91 (s, OCH$_2$O), 39.23 (s, triazolium-CH$_3$), 36.68 (s, $CHCH_2$), 36.64 (s, $CHCH_2$), 36.45 (s, $CHCH_2$), 32.15 (s, $CH_2CH_2CH_3$), 32.02 (s, $CH_2CH_2CH_3$), 30.16 (s, CHCH_2), 30.11 (s, CHCH_2), 29.92 (s, CHCH_2), 29.80 (s, CHCH_2), 27.68 (s, CHCH$_2$CH$_2$), 27.63 (s, CHCH$_2$CH$_2$), 22.78 (s, CH_2CH_3), 22.76 (s, CH_2CH_3), 14.20 (s, CH$_2CH_3$) ppm. MS (ESI-TOF): m/z = 1712.95 [M - I]$^+$, expected isotopic profile. Elemental analysis calcd (%) for C$_{107}$H$_{130}$N$_3$O$_{16}$I (1839.10): C 69.80, H 7.12, N 2.28; found C 69.93, H 7.10, N 2.06.

trans-Dichloro-{1-[4(24),6(10),12(16),18(22)-tetramethylenedioxy-2,8,14,20-tetrapentylresorcin[4]arene-5-yl]-4-phenyl-3-methyl-1_H_-1,2,3-triazol-5-yliden}pyridine palladium(II) (9): A mixture of K$_2$CO$_3$ (0.155 g, 1.12 mmol), pyridine (5 mL), [PdCl$_2$] (0.040 g, 0.23 mmol) and triazolium salt **1** (0.200 g, 0.19 mmol) was heated at 80°C for 24 h. The reaction mixture was filtered through Celite, the filtrate was evaporated under vacuum, and the solid residue was purified by column chromatography (EtOAc/CH$_2$Cl$_2$, 10:90; Rf = 0.54) to afford complex **9** (0.060 g, 26 %). ^1H NMR (500 MHz, CDCl$_3$): δ = 8.74 (dd, 2H, arom. CH, pyridine, ^3J = 6.5 Hz, ^4J = 1.5 Hz), 8.11 (dd, 2H, arom. CH, phenyl, ^3J = 8.5 Hz, ^4J = 1.5 Hz), 7.65-7.54 (m, 4H, arom. CH, pyridine and phenyl), 7.43 (s, 1H, arom. CH, resorcinarene), 7.20-7.19 (m, 2H, arom. CH, pyridine), 7.17 (s, 2H, arom. CH, resorcinarene), 7.15 (s, 1H, arom. CH, resorcinarene), 6.55 (s, 1H, arom. CH, resorcinarene), 6.48 (s, 2H, arom. CH, resorcinarene), 5.76 and 4.52 (AB spin system, 4H, OCH$_2$O, ^2J = 7.0 Hz), 5.69 and 4.42 (AB spin system, 4H, OCH$_2$O, ^2J = 7.0 Hz), 4.94 (t, 2H, CHCH$_2$, ^3J = 8.0 Hz), 4.75 (t, 2H, CHCH$_2$, ^3J = 8.2 Hz), 4.05 (s, 3H, triazolyliden-CH$_3$), 2.38-2.21 (m, 8H, CHCH_2), 1.46-1.34 (m, 24H $CH_2CH_2CH_2CH_3$), 0.93 (t, 6H, CH$_2CH_3$, ^3J = 7.2 Hz), 0.92 (t, 6H, CH$_2CH_3$, ^3J = 7.2 Hz) ppm. $^{13}C\{^1H\}$ NMR (126 MHz, CDCl$_3$): δ = 155.13-116.61 (arom. Cs), 145.99 (s, C$_q$-Pd), 99.81 (s, OCH$_2$O), 99.55 (s, OCH$_2$O), 37.76 (s, triazolyliden-CH$_3$), 36.78 (s, $CHCH_2$), 36.54 (s, $CHCH_2$), 32.19 (s, $CH_2CH_2CH_3$), 32.09 (s, $CH_2CH_2CH_3$), 30.06 (s, CHCH_2), 29.81 (s, CHCH_2), 27.74 (s, CHCH$_2$CH$_2$), 27.58 (s, CHCH$_2$CH$_2$), 22.86 (s, CH_2CH_3), 14.26 (s, CH$_2CH_3$) ppm. MS (ESI-TOF): m/z = 1193.44 [M - Cl]$^+$, expected isotopic profile. Elemental analysis calcd (%) for C$_{66}$H$_{76}$N$_4$O$_8$PdCl$_2$ (1230.65): C 64.41, H 6.22, N 4.55; found C 64.18, H 6.03, N 4.42.

trans-Dibromo-{1,4-bis[4(24),6(10),12(16),18(22)-tetramethylenedioxy-2,8,14,20-tetrapentylresorcin[4]arene-5-yl]-3-methyl-1_H_-1,2,3-triazol-5-yliden}pyridine palladium(II) (10): A mixture of K$_2$CO$_3$ (0.081 g, 0.59 mmol), pyridine (5 mL), [PdCl$_2$] (0.021 g, 0.12 mmol), KBr (0.233 g, 1.96 mmol) and triazolium salt **2** (0.180 g, 0.10 mmol) was heated at 80°C for 24 h. The reaction mixture was filtered through Celite, the filtrate was evaporated under vacuum, and the solid residue was purified by column chromatography (pure CH$_2$Cl$_2$; Rf = 0.62) to afford complex **10** (0.056 g, 28 %). ^1H NMR (500 MHz, CDCl$_3$): δ = 8.93-8.87 (m, 0.6H, arom. CH, pyridine), 8.65-8.59 (m, 2H, arom. CH, pyridine), 7.79-7.65 (m, 1.4H, arom. CH, pyridine), 7.38-7.31 (m, 2H, arom. CH, pyridine and resorcinarene), 7.19-7.14 (m, 7H, arom. CH, resorcinarene), 4.54-6.33 (m, 6H, arom. CH, resorcinarene), 5.95 and 5.82 (AB spin system, 4H, OCH$_2$O, ^2J = 9.0 Hz), 5.77-5.62 and 4.50-4.24 (AB spin systems, 12H, OCH$_2$O), 4.92-4.68 (m, 8H, CHCH$_2$), 3.85-3.66 (m, 3H, triazolyliden-CH$_3$), 2.37-2.21 (m, 16H, CHCH_2), 1.50-1.31 (m, 48H $CH_2CH_2CH_2CH_3$), 0.96-0.86 (m, 24H, CH$_2CH_3$) ppm. $^{13}C\{^1H\}$ NMR (126 MHz, CDCl$_3$): δ = 155.32-115.41 (arom. Cs), 150.03 (s, C$_q$-Pd), 149.96 (s, C$_q$-Pd), 100.61 (s, OCH$_2$O), 100.12 (s, OCH$_2$O), 99.83 (s, OCH$_2$O), 99.68 (s,

OCH$_2$O), 99.56(s, OCH$_2$O), 99.36 (s, OCH$_2$O), 99.26 (s, OCH$_2$O), 38.13 (s, triazolyliden-CH$_3$), 37.82 (s, triazolyliden-CH$_3$), 37.62 (s, triazolyliden-CH$_3$), 36.74 (s, CHCH$_2$), 36.52 (s, CHCH$_2$), 32.22 (s, CH$_2$CH$_2$CH$_3$), 32.19 (s, CH$_2$CH$_2$CH$_3$), 32.14 (s, CH$_2$CH$_2$CH$_3$), (s, CH$_2$CH$_2$CH$_3$), 32.10 (s, CH$_2$CH$_2$CH$_3$), 31.99 (s, CH$_2$CH$_2$CH$_3$), 30.19 (s, CHCH$_2$), 30.10 (s, CHCH$_2$), 30.03 (s, CHCH$_2$), 29.97 (s, CHCH$_2$), 29.85 (s, CHCH$_2$), 29.82 (s, CHCH$_2$), 29.76 (s, CHCH$_2$), 27.83 (s, CHCH$_2$CH$_2$), 27.76 (s, CHCH$_2$CH$_2$), 27.72 (s, CHCH$_2$CH$_2$), 27.60 (s, CHCH$_2$CH$_2$), 22.86 (s, CH$_2$CH$_3$), 22.83 (s, CH$_2$CH$_3$), 22.72 (s, CH$_2$CH$_3$), 14.28 (s, CH$_2$CH$_3$), 14.24 (s, CH$_2$CH$_3$) ppm. MS (ESI-TOF): m/z = 1937.79 [M - Br - Py + NCCH$_3$]$^+$, expected isotopic profile. Elemental analysis calcd (%) for C$_{112}$H$_{134}$N$_4$O$_{16}$PdBr$_2$ (2058.51): C 65.35, H 6.56, N 2.72; found C 65.24, H 6.45, N 2.67.

Typical procedure for the palladium-catalysed Suzuki-Miyaura cross-coupling reactions: A 10 mL-Schlenk tube was filled with the palladium precursor (0.5 mol %), triazolium salt (0.5 mol %), aryl chloride (0.5 mmol), arylboronic acid (0.75 mmol), ^{t}BuOK (0.75 mmol) and decane (0.025 mL, internal reference). Dioxane (2 mL) was then added. The reaction mixture was stirred at 100°C during the desired time. An aliquot (0.3 mL) of the resulting solution was then passed through a Millipore filter and analysed by GC.

X-ray crystal structure analysis of triazole 8: Single crystals of **8** suitable for X-ray analysis were obtained by slow diffusion of methanol into a CH$_2$Cl$_2$ solution of the triazole. Crystal data: C$_{106}$H$_{127}$N$_3$O$_{16}$, Mr = 1699.10 g mol^{-1}, monoclinic, space group C 2/c, a = 52.4158(14) Å, b = 10.5297(3) Å, c = 56.6335(14) Å, β = 103.308(2)°, V = 30417.9(14) Å^3, Z = 12, D = 1.113 g cm^{-3}, μ = 0.592 mm^{-1}, F(000) = 10944, T = 173(2) K. The sample was studied on a Bruker APEX II CCD (graphite monochromated Cu-$K\alpha$ radiation, λ = 1.54178 Å). The data collection (2θmax = 66.9°, omega scan frames by using 0.7° omega rotation and 30 s per frame, range hkl: h -61,61 k -6,12 l -57,67) gave 128330 reflections. The structure was solved with SHELXS-2013,[18] which revealed the non-hydrogen atoms of the molecule. After anisotropic refinement, all of the hydrogen atoms were found with a Fourier difference map. The structure was refined with SHELXL-2013[18] by the full-matrix least-square techniques (use of F square magnitude; x, y, z, ij for C, N and O atoms; x, y, z in riding mode for H atoms); 1677 variables and 11315 observations with $I > 2.0 \sigma(I)$; calcd. $w = 1/[\sigma^2(Fo^2) + (0.1312P)^2]$ where $P = (Fo^2 + 2Fc^2)/3$, with the resulting R = 0.0921, R_W = 0.2703 and S_W = 0.964, $\Delta\rho$ < 0.599 eÅ^{-3}. CCDC entry 1848246 contains the supplementary crystallographic data. These data can be obtained free of charge from The Cambridge Crystallographic Data Centre via http://www.ccdc.cam.ac.uk/data_request/cif or by e-mailing data_request@ccdc.cam.ac.uk, or by contacting The Cambridge Crystallographic Data Centre, 12 Union Road, Cambridge CB2 1EZ, UK.

Keywords: Resorcinarene · Palladium complex · Triazolium salt · Catalysis · Suzuki-Miyaura cross-coupling

References

[1]   a) K. Öfele, *J. Organomet. Chem.* **1968**, P42-P43; b) H.-W. Wanzlick, H.-J. Schönherr, *Angew. Chem. Int. Ed.* **1968**, *7*, 141-142.

[2]   M. Teci, E. Brenner, D. Matt, L. Toupet, *Eur. J. Inorg. Chem.* **2013**, 2841-2848.

[3]   P. Mathew, A. Neels, M. Albrecht, *J. Am. Chem. Soc.* **2008**, *130*, 13534-13535.

[4]   G. Guisado-Barrios, J. Bouffard, B. Donnadieu, G. Bertrand, *Angew. Chem. Int. Ed.* **2010**, *49*, 4759-4762.

[5]   a) V. V. Rostovtsev, L. G. Green, V. V. Fokin, K. B. Sharpless, *Angew. Chem. Int. Ed.* **2002**, *41*, 2596-2599; b) C. W. Tornøe, C. Christensen, M. Meldal, *J. Org. Chem.* **2002**, *67*, 3057-3064.

[6]   a) T. Terashima, S. Inomata, K. Ogata, S.-I. Fukuzawa, *Eur. J. Inorg. Chem.* **2012**, 1387-1393; b) J. Huang, J.-T. Hong, S. H. Hong, *Eur. J. Org. Chem.* **2012**, 6630-6635; c) A. Bolje, J. Kosmrlj, *Org. Lett.* **2013**, *15*, 5084-5087; d) J. B. Shaik, V. Ramkumar, B. Varghese, S. Sankararaman, *Beilstein J. Org. Chem.* **2013**, *9*, 698-704; e) Y. Wei, A. Petronilho, H. Mueller-Bunz, M. Albrecht, *Organometallics* **2014**, *33*, 5834-5844; f) D. Mendoza-Espinosa, R. González-Olvera, G. E. Negrón-Silva, D. Angeles-Beltrán, O. R. Suárez-Castillo, A. Álvarez-Hernández, R. Santillan, *Organometallics* **2015**, *34*, 4529-4542; g) A. Mohan, V. Ramkumar, S. Sankararaman, *J. Organomet. Chem.* **2015**, *799-800*, 115-121; h) B. Sureshbabu, V. Ramkumar, S. Sankararaman, *J. Organomet. Chem.* **2015**, *799-800*, 232-238; i) T. Mitsui, M. Sugihara, Y. Tokoro, S.-I. Fukuzawa, *Tetrahedron* **2015**, *71*, 1509-1514; j) L. Hettmanczyk, B. Schmid, S. Hohloch, B. Sarkar, *Molecules* **2016**, *21*, 1561-1573; k) A. Kumar, A. P. Prakasham, M. Kumar Gangwar, P. Vishnoi, R. J. Butcher, P. Ghosh, *Eur. J. Inorg. Chem.* **2017**, 2144-2154.

[7]   a) S. Inomata, H. Hiroki, T. Terashima, K. Ogata, S.-I. Fukuzawa, *Tetrahedron* **2011**, *67*, 7263-7267; b) E. C. Keske, O. V. Zenkina, R. Wang, C. M. Crudden, *Organometallics* **2012**, *31*, 6215-6221.

[8]   M. Gazvoda, M. Virant, A. Pevec, D. Urankar, A. Bolje, M. Kocevar, J. Kosmrlj, *Chem. Commun.* **2016**, *52*, 1571-1574.

[9]   a) A. Ros, M. Alcarazo, J. Iglesias-Sigüenza, E. Díez, E. Álvarez, R. Fernández, J. M. Lassaletta, *Organometallics* **2008**, *27*, 4555-4564; b) S. Hohloch, F. L. Duecker, M. van der Meer, B. Sarkar, *Molecules* **2015**, *20*, 7379-7395; c) R. Maity, M. van der Meer, S. Hohloch, B. Sarkar, *Organometallics* **2015**, *34*, 3090-3096; d) S. Sabater, H. Mu ller-Bunz, M. Albrecht, *Organometallics* **2016**, *35*, 2256-2266; e) Y. Wei, S.-X. Liu, H. Mueller-Bunz, M. Albrecht, *ACS Catal.* **2016**, *6*, 8192-8200; f) A. Bolje, S. Hohloch, J. Košmrlj, B. Sarkar, *Dalton Trans.* **2016**, *45*, 15983-15993.

[10]   a) L. P. Bheeter, D. Wei, V. Dorcet, T. Roisnel, P. Ghosh, J.-B. Sortais, C. Darcel, *Eur. J. Inorg. Chem.* **2015**, 5226-5231; b) A. L. Schöffler, A. Makarem, F. Rominger, B. F. Straub, *Beilstein J. Org. Chem.* **2016**, *12*, 1566-1572; c) D. Mendoza-Espinosa , R. González-Olvera, C. Osornio, G. E. Negrón-Silva, A. Álvarez-Hernández, C. I. Bautista-Hernández, O. R. Suárez-Castillo, *J. Organomet. Chem.* **2016**, *803*, 142-149; d) F.-J. Guo, J. Sun, Z.-Q. Xu, F. E. Ku hn, S.-L. Zang, M.-D. Zhou, *Catal. Commun.* **2017**, *96*, 11-14; eI. Strydom, G. Guisado-Barrios, I. Fernández, D. C. Liles, E. Peris, D. I. Bezuidenhout, *Chem. Eur. J.* **2017**, *23*, 1393-1401.

[11]   a) N. Şahin, D. Sémeril, E. Brenner, D. Matt, İ. Özdemir, C. Kaya, L. Toupet, *ChemCatChem* **2013**, *5*, 1116-1125; b) N. Şahin, D. Sémeril, E. Brenner, D. Matt, İ. Özdemir, C. Kaya, L. Toupet, *Eur. J. Org. Chem.* **2013**, 4443-4449; c) N. Şahin, D. Sémeril, E. Brenner, D. Matt, C. Kaya, L. Toupet, *Turk. J. Chem.* **2015**, *39*, 1171-1179; d) M. Kaloğlu, D. Sémeril, E. Brenner, D. Matt, İ. Özdemir, L. Toupet, *Eur. J. Inorg. Chem.* **2016**, 1115-1120; e) M. Kaloğlu, N. Şahin, D. Sémeril, E. Brenner, D. Matt, İ. Özdemir, C. Kaya, L. Toupet, *Eur. J. Org. Chem.* **2015**, 7310-7316; f) N. Natarajan, T. Chavagnan, D. Sémeril, E. Brenner, D. Matt, R. Ramesh, L. Toupet, *Eur. J. Inorg. Chem.* **2018**.

[12]   J. M. Praetorius, C. M. Crudden, *Dalton Trans.* **2008**, 4079-4094

[13]   a) T. Chavagnan, D. Sémeril, D. Matt, L. Toupet, *Eur. J. Org. Chem.* **2017**, 70-76; b) T. Chavagnan, D. Sémeril, D. Matt, L. Toupet, *Eur. J. Org. Chem.* **2017**, 313-323; c) F. Elaieb, D. Sémeril, D. Matt, *Eur. J. Inorg. Chem.* **2017**, 685-693.

[14]   J. Nasielski, N. Hadei, G. Achonduh, E. A. B. Kantchev, C. J. O'Brien, A. Lough, M. G. Organ, *Chem. Eur. J.* **2010**, *16*, 10844-10853.

[15]   W. Buchowicz, A. Kozioł, L. B. Jerzykiewicz, T. Lis, S. Pasynkiewicz, A. Pecherzewska, A. Pietrzykowski, *J. Mol. Catal. A* **2006**, *257*, 118-123.

[16]   H. El Moll, D. Sémeril, D. Matt, L. Toupet, *Eur. J. Org. Chem.* **2010**, 1158-1168.

[17]   H. Hwang, J. Kim, J. Jeong, S. Chang, *J. Am. Chem. Soc.* **2014**, *136*, 10770-10776.

[18]   G. M. Sheldrick, *Acta. Cryst.* **2008**, *A64*, 112-122.

Conclusion générale

Cette thèse est consacrée à la synthèse et l'étude de leurs propriétés catalytiques d'un ensemble de coordinats construits sur des plateformes de la famille des calix[4]arènes et résorcin[4]arènes (Figure 1). Ces composés macrocycliques constitués de quatre unités aromatiques reliées entre elles par des ponts "CH$_2$" dans le cas des calixarènes ou "CHR" pour les résorcinarènes définissent des espaces cavitaires. Les synthons particuliers ayant servi à la construction des ligands étudiés sont les composés **1** et **2** (Figure 1) pour lesquels de nombreuses fonctionnalisations ont déjà été décrites dans la littérature. Alors que le macrocycle **1** présente une structure relativement flexible, la cavité **2,** dans laquelle les unités aromatiques adjacentes sont reliées par deux ponts distincts (–CHR– et –OCH$_2$O–), a une structure beaucoup plus *rigide*. Des composés de ce type sont fréquemment qualifiés de résorcinarènes-cavitands. A signaler que la plupart des résorcinarènes de la litérature sont dépourvus des doubles ponts (les seuls groupes pontants étant des untités –CHR–), conférant logiquement au macrocycle une structure relativement flexible.
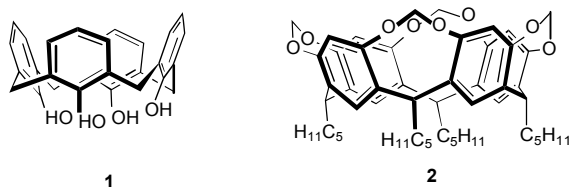
Figure 1 : Synthons calix[4]arène et résorcin[4]arène utilisés dans ce travail

Trois raisons essentielles nous ont motivé dans le choix ces deux plateformes :

- la possibilité d'ancrer sur ces plateformes circulaires un ensemble de ligands convergents, créant ainsi des ligands multitopiques sophistiqués susceptibles d'exercer un contrôle très fin sur les propriétés catalytiques d'un centre métallique complexé ;

- la possibilité de combiner au sein d'un complexe bâti sur un tel synthon à la fois une unité réceptrice *et* un centre catalytique, et ainsi d'accéder à des catalyseurs supramoléculaires ;

- la possibilité de synthétiser des coordinats cavitaires "introvertis" capables d'enserrer un centre catalytique dans la partie intérieure du macrocyle, et ainsi de disposer d'un centre catalytique ultra-confiné (ligands embrassants).

Les ligands considérés dans cette étude ont pour caractéristique commune d'avoir leurs centres coordinateurs greffés sur le bord supérieur d'une cavité conique. Les unités coordinatrices étudiées sont des phosphites, imidazoles et triazoles, les deux dernières entités étant des sources potentielles de ligands carbéniques.

Le premier chapitre du mémoire propose une mise au point succinte des applications catalytiques connues des ligands basés sur une plateforme résorcin[4]arène, que cette dernière soit rigide ou non. Il démontre tout l'intérêt de telles plateformes en chimie de coordination et catalyse.

Le premier objectif expérimental de cette thèse (chapitre 2) était de synthétiser les deux nouveaux bis-phosphites **3** et **4**, dont les centres phosphorés sont *directement* greffés sur la face supérieure de cavités coniques (Figure 2). Ils constituent les premiers phosphites de ce type. Ces deux ligands sont *chiraux* et potentiellement chélateurs et ont fait l'objet d'une évaluation en hydroformylation asymétrique d'arènes vinyliques (Schéma 1).
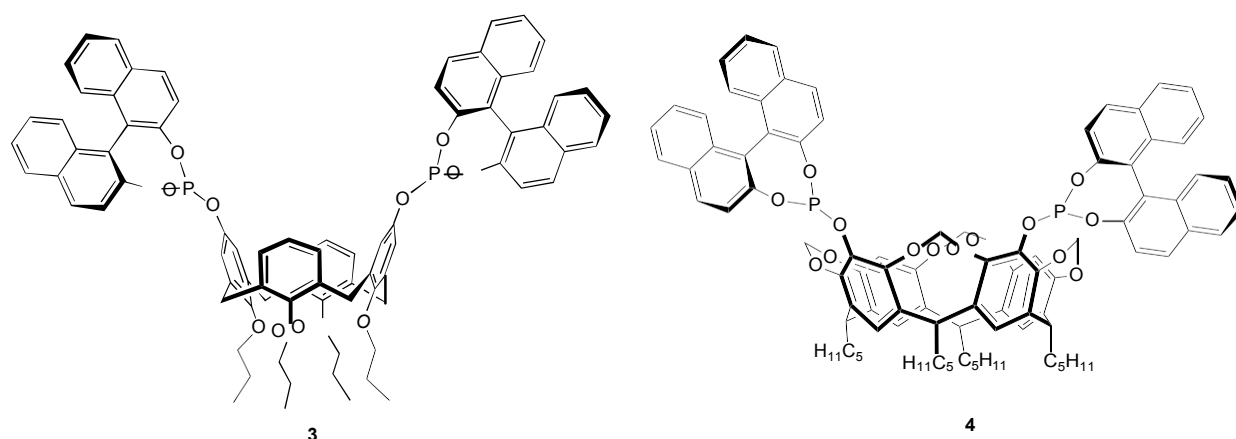
Figure 2 : Bis-phosphites bâtis sur des squelettes calix[4]arène (**3**) et résorcin[4]arène (**4**)
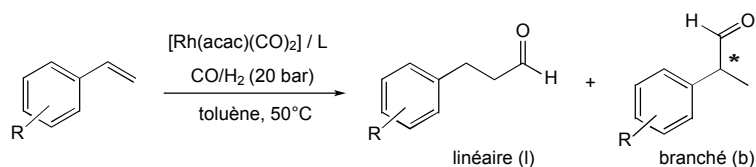
Schéma 1 : Hydroformylation asymétrique d'arènes vinyliques

Les essais catalytiques ont été effectués en mélangeant les ligands avec le précurseur [Rh(acac)(CO)$_2$] (0,1 mol %) et en opérant à 50°C sous 20 bars d'un mélange CO/H$_2$. Les substrats vinyliques employés étaient le styrène, le 4-fluoro-styrène, le 3-chloro-styrène, le 4-méthoxy-styrène, le 4-tert-butyl-styrène et le 2-vinylnaphtalène. L'utilisation du bis-phosphite **3** conduit principalement à la formation d'aldéhydes branchés, dont la proportion peut atteindre 91 % dans le cas du 4-tert-butyl-styrène. Les aldéhydes branchés sont par ailleurs obtenus avec de bons excès énantiomériques, ceux-ci s'élevant à 89 % dans le cas du styrène. Le bon transfert de chiralité observé avec ce ligand peut être attribué à la formation, au cours de la catalyse, d'espèces chélatées dans lesquelles les fragments binaphtyles "embrassent" efficacement le centre catalytique (Figure 3). Ces résultats se distinguent de ceux obtenus avec le disphosphite **4** qui conduit à des régiosélectivités et énantiosélectivités nettement inférieures. Ces dernières observations semblent refléter la formation préférentielle pendant le processus catalytique avec **4** de complexes oligomères, autrement dit d'espèces dans lesquelles le centre métallique est peu confiné.
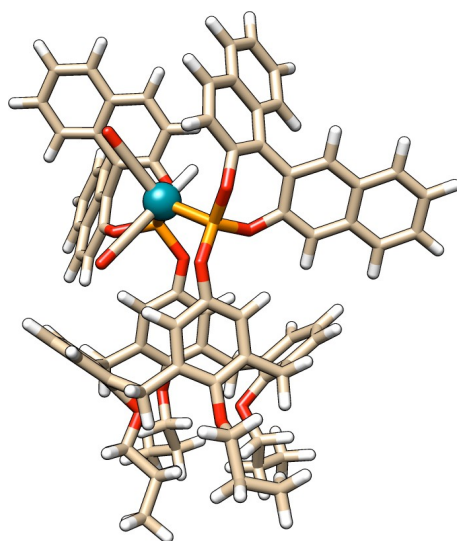
Figure 3: Structure calculée pour [RhH(CO)$_2$(**3**)]

Il est à noter que les résultats catalytiques obtenus avec le diphosphite-calixarène **3** tranchent avec ceux observés avec les ligands **5a-c**, précedemment synthétisés au laboratoire, où les entités phosphites sont greffées sur la face inférieure du calixarène (Figure 4). Ainsi, pour l'hydroformylation du styrène, les systèmes catalytiques Rh/**5a-c** conduisent majoritairement à l'aldéhyde *linéaire* (contrairement à **3** donnant des i-sélectivités classiques), la sélectivité la plus élevée ayant été obtenue avec le ligand portant deux substituants méthylnaphthalényles (ligand **5c** ; 77 % d'aldéhyde linéaire). L'origine de la *n*-sélectivité élevée observée avec **5a-c** résulte de la formation au cours de la catalyse de poches allongées autour du centre catalytique (le centre métallique est piégé dans un espace constitué des quatre substituants des O phénoliques) dont l'effet est d'orienter la réaction vers des produits linéaires, dont la forme est plus adaptée au déroulement de la réaction. L'espace catalytique est donc ici différent de celui créé avec **3**.
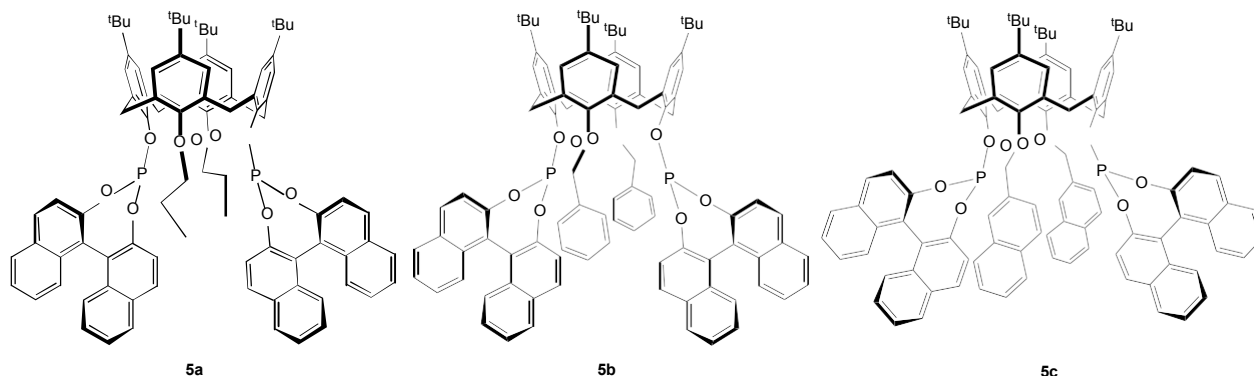
Figure 4 : Bis-phosphites **5a-c** précedemment synthétisés au laboratoire et favorisant la formation d'aldéhydes linéaires.

Le chapitre 3 est consacré à la synthèse de plusieurs complexes de nickel du type [NiCpXL] (Cp = η^5-cyclopentadiényle ; L = imidazolylidène ; X = Cl ou Br) dont l'entité N-hétérocyclique a été *N*-substituée soit par une (**6**), soit par deux (**7**) entités résorcinarène (Figure 5). Dans le complexe **6**, dont la structure à l'état solide a été déterminée par une étude de diffraction des rayons X, l'atome de nickel est positionné à l'embouchure du résorcinarène et l'entité cyclopentadiényle est supramoléculairement piégée dans la cavité par suite d'intéractions faibles avec les unités aromatiques du macrocycle (Figure 6). Un piégeage similaire se produit avec l'une des deux cavités de **6**, l'autre étant repoussée par le centre métallique.
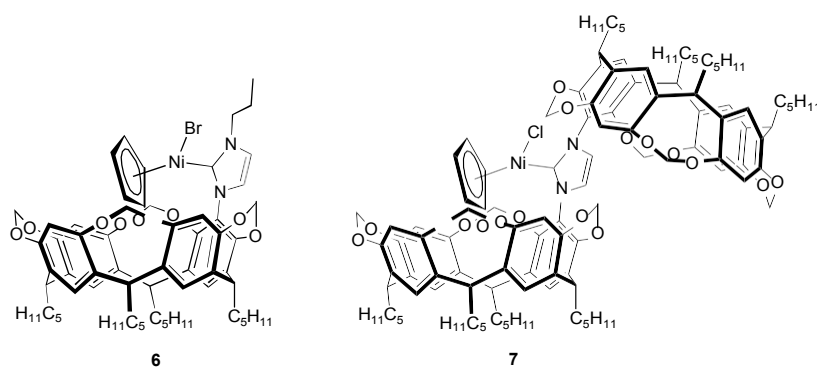
Figure 5 : Complexes [NiCpXL] **6** et **7**
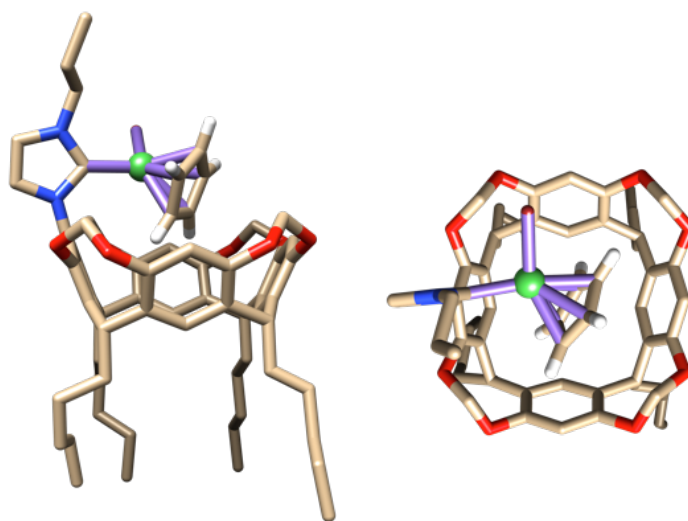
Figure 6 : Structure à l'état solide du complexe **6** (à gauche: vue latérale avec carbène C à gauche ; milieu: vue du haut)

Les deux complexes de nickel ont été testés en oligomérisation de l'éthylène en présence de NaBH$_4$ comme co-catalyseur (Schéma 2). Les tests ont été réalisés dans le toluène à 90°C sous une pression de 20 bar d'éthylène pendant une heure. Le complexe **7** s'est révélé le plus performant, son activité (TOF) atteignant 555 mol(C$_2$H$_4$).mol (Ni)$^{-1}$.h^{-1}. Cette observation montre clairement le rôle bénéfique joué par les deux substituants résorcinarèniques, qui, de part l'encombrement stérique qu'ils génèrent autour du centre métallique, permettent d'augmenter la stabilité de l'espèce active et *in fine* d'accroître la durée de vie du catalyseur.
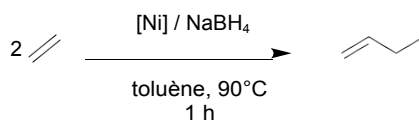
Schéma 2 : Dimérisation de l'éthylène

Dans le prolongement du programme ci-dessus, des carbènes anormaux dérivés des sels de triazolium **8** et **9** (Figure 7) ont également été étudiés. Ces sels ont respectivement été obtenus par cycloaddition Cu-catalysée entre un précurseur résorcinarène-azoture et soit du phénylacétylène (conduisant à **8**), soit un acétylène-résorcinarène (donnant **9**), chacune de ces réactions étant suivie d'une méthylation du triazole formé.
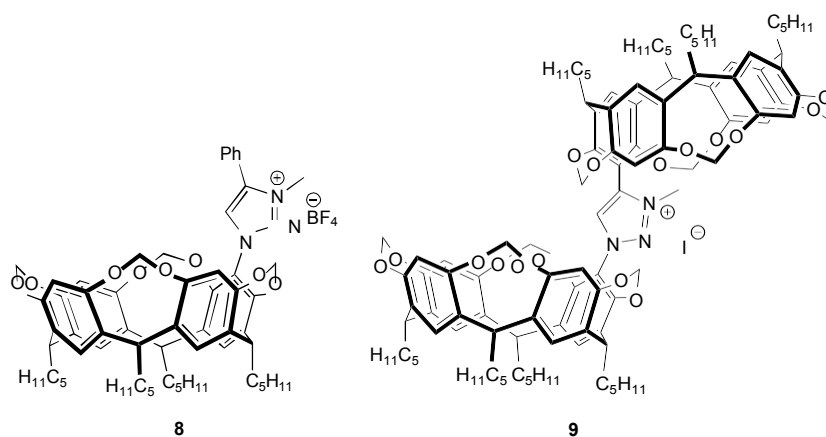
Figure 7 : Sels de triazolium **8** and **9** synthétisés

Les sels de triazolium **8** et **9** ont été évalués comme pro-ligands pour des couplages croisés de Suzuki-Miyaura (Schéma 3). Après optimisation, les catalyseurs ont été générés *in situ* à partir des systèmes [Pd(OAc)$_2$]/**8** ou [PdCl$_2$(PhCN)$_2$]/**9** dans le dioxane. Les catalyseurs formés se sont montrés efficaces en couplage croisé entre chlorures d'aryles et acides aryles boroniques
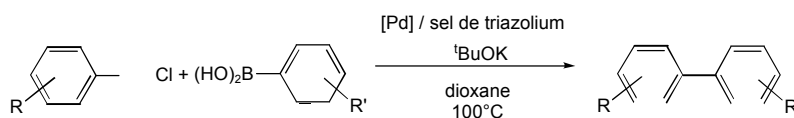
Schéma 3 : Couplage croisé de Suzuki-Miyaura

stériquement encombrés. Des activités significativement meilleures ont été obtenues avec le sel de triazolium **8** porteur d'un seul substituant résorcinarène et donc moins encombré. Sa plus grande efficacité reflète la formation d'espèces dans lesquelles les substrats peuvent plus facilement accéder au centre catalytique, mais probablement aussi la présence de groupes pentyles capables se replier vers le métal et de s'en approcher de manière à faciliter l'étape d'élimination réductrice (Figure 8).
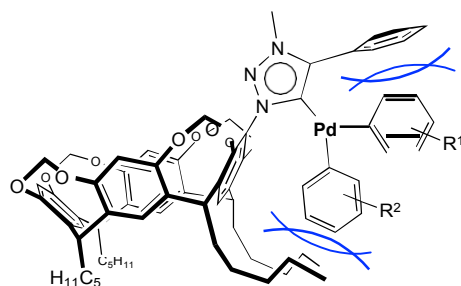
Figure 8 : Interactions stériques possibles pendant le cycle catalytique entre les groupes pentyles et le centre catalytique.

En résumé, dans cette thèse nous avons présenté de nouveaux ligands bâtis sur des plateformes cavitaires de type calix[4]arène et résorcin[4]arène et mis en relief leurs propriétés stériques dans réactions catalytiques de formation de liaisons carbone-carbone. L'ensemble des résultats présentés constitue une nouvelle illustration du potentiel des coordinats cavitaires en catalyse homogène.

Perspectives

Les résultats obtenus durant cette thèse permettent d'envisager les études ultérieures suivantes :

- l'exploitation de bis-phosphites macrocycliques en réduction asymétrique de cétones ou de doubles liaisons catalysée par du *nickel*, métal encore peu utilisé dans ces réactions (Schéma 1).
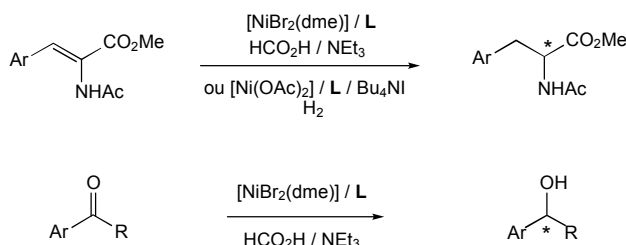
Schéma 1 : Réduction d'oléfines (haut) et de cétones (bas) catalysée par un complexe de nickel

- l'extension du travail sur les carbènes stériquement encombrés à des réactions catalytiques où plusieurs substrats sont en compétition. Avec ce type de ligands, nous pouvons anticiper que le substrat préférentiellement transformé sera celui qui pourra accéder le plus facilement au centre catalytique confiné, c'est-à-dire le substrat stériquement le moins encombré (Schéma 2).
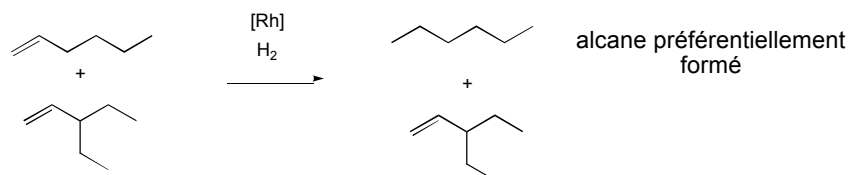
Schéma 2 : Hydrogénation compétitive d'oléfines

- Il serait également intéressant de rendre hydrosoluble ce type de ligand macrocyclique en greffant à leur périphérie des fonctions hydrosolubles, par exemple, des groupements *ammonium*. Les nanoréacteurs hydrosolubles ainsi générés fonctionneront alors comme des solvants monomoléculaires immergés dans l'eau (Figure 1).
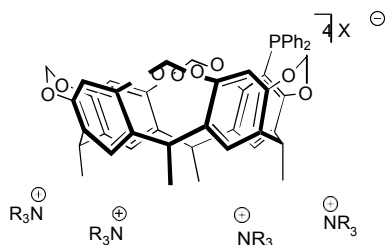
Figure 1 : Ligand bâti sur une plateforme résorcin[4]arène hydrosoluble

Annexe of chapter II

Experimental Section

General Remarks

All manipulations involving phosphorus derivatives were carried out in Schlenk-type flasks under dry argon. Solvents were dried by conventional methods and were distilled immediately before use. $CDCl_3$ was passed down a 5 cm-thick alumina column and stored under nitrogen over molecular sieves (4 Å). Routine ^1H, $^{13}C\{^1H\}$ and $^{31}P\{^1H\}$ spectra were recorded with Bruker FT instruments (AC 400 and 500). ^1H NMR spectra were referenced to residual protiated solvents (7.16 ppm for C_6D_6 and 7.26 ppm for $CDCl_3$). ^{13}C NMR chemical shifts are reported relative to deuterated solvents ($\delta = 128.00$ ppm for C_6D_6 and 77.16 ppm for $CDCl_3$). ^{31}P NMR spectroscopic data are given relative to external H_3PO_4. Chemical shifts and coupling constants are reported in ppm and Hz, respectively. Infrared spectra were recorded with a Bruker FT-IR Alpha-P spectrometer. Elemental analyses were carried out by the Service de Microanalyse, Institut de Chimie, Université de Strasbourg. The catalytic solutions were analysed with a Varian 3900 gas chromatograph fitted with a WCOT fused silica column (25 m x 0.25 mm) and a Chirasil-DEX CB column (25 m x 0.25 mm). 5,17-Dihydroxy-25,26,27,28-tetrapropyloxycalix[4]arene (**3**),[1] 5,11-dibromo-4(24),6(10),12(16),18(22)-tetramethylenedioxy-2,8,14,20-tetrapentylresorcin[4] arene (**4**),[2] 5-hydroxy-25,26,27,28-tetrapropyloxycalix[4]arene,[3] 5-hydroxy-4(24),6(10),12(16),18(22)-tetramethylenedioxy-2,8,14,20-tetrapentylresorcin[4]arene[4] and [(*S*)-(1,1'-binaphthalene-2,2'diyl)]chlorophosphite[5] were prepared by literature procedures.

References

[1]   O. G. Barton, B. Neumann, H.-G. Stammler, J. Mattay, *Org. Biomol. Chem.* **2008**, *6*, 104-111.

[2]   H. El Moll, D. Sémeril, D. Matt, L. Toupet, *Eur. J. Org. Chem.* **2010**, 1158-1168.

[3]   J. Budka, M. Dudič, P. L. Lhoták, I. Stibor, *Tetrahedron* **1999**, *55*, 12647-12654.

[4]   H. Staats, F. Eggers, O. Haß, F. Fahrenkrug, J. Matthey, U. Lüning, A. Lützen, *Eur. J. Org. Chem.* **2009**, 4777-4792.

[5]   N. Cramer, S. Laschat, A. Baro, *Organometallics* **2006**, *25*, 2284-2291.

5,11-Dihydroxy-4(24),6(10),12(16),18(22)-tetramethylenedioxy-2,8,14,20-tetrapentyl resorcin[4]arene (5)
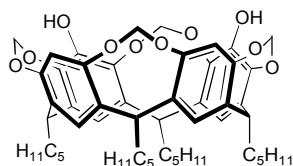
A solution of ^{n}BuLi (1.6 M, 4.0 mL, 6.46 mmol) was slowly added to a cold (-78 °C) solution of dibromo-resorcinarene **4** (3.000 g, 3.08 mmol) in THF (70 mL). After stirring for 0.5 h, B(OMe)$_3$ was added (10.3 mL, 92.3 mmol). The solution was then first allowed to warm to room temperature, then heated under stirring for a further 48 h at 65°C. The reaction mixture was cooled to 0°C before slow addition of a mixture 1:1 of NaOH (3 M)/H$_2$O$_2$ (30 %) (50 mL). After 18 h, the solution was washed with brine (100 mL) and the organic phase was separated. This operation was repeated twice. The aqueous layer was treated with ethyl acetate (2 x 100 mL). The combined organic layers were dried over Na$_2$SO$_4$. The solution was filtered and evaporated to dryness. The crude product was purified by column chromatography (Et$_2$O/CH$_2$Cl$_2$, 20:80, v/v) to afford 1.890 g of **5** (R_f = 0.18, Et$_2$O/CH$_2$Cl$_2$, 20:80, v/v) as a white solid (yield 63 %). ^{1}H NMR (CDCl$_3$, 500 MHz): δ = 7.09 (s, 2H, arom. CH), 6.64 (s, 2H, arom. CH), 6.50 (s, 2H, arom. CH), 5.95 and 4.44 (AB spin system, 2H, OCH$_2$O, ^2J = 7.0 Hz), 5.85 and 4.44 (AB spin system, 4H, OCH$_2$O, ^2J = 7.0 Hz), 5.75 and 4.44 (AB spin system, 2H, OCH$_2$O, ^2J = 7.0 Hz), 4.74-4,68 (m, 4H, CHCH$_2$), 2.23-2.15 (m, 8H, CHCH_2CH$_2$), 1.42-1.32 (m, 24H $CH_2CH_2CH_2$CH$_3$), 0.91 (t, 12H, CH$_2$CH_3, ^3J = 7.2 Hz) ppm. ^{13}C{^{1}H} NMR (126 MHz, CDCl$_3$): δ =154.99 (s, arom. C$_q$O), 154.87 (s, arom. C$_q$O), 142.09 (s, arom. C$_q$O), 142.00 (s, arom. C$_q$O), 140.91 (s, arom. C$_q$O), 138.67-109.97 (arom. Cs), 99.91 (s, OCH$_2$O), 99.80 (s, OCH$_2$O), 99.70 (s, OCH$_2$O), 36.95 (s, CHCH$_2$), 36.73 (s, CHCH$_2$), 36.50 (s, CHCH$_2$), 32.16 (s, CH_2CH$_2$CH$_3$), 29.95 (s, CHCH_2), 29.81 (s, CHCH_2), 29.58 (s, CHCH_2), 27.69 (s, CHCH$_2$CH_2), 22.85 (s, CH_2CH$_3$), 14.27 (s, CH$_2$CH_3) ppm. Anal. Calc. for C$_{52}$H$_{64}$O$_{10}$ (849.06): C 73.56, H 7.60; found: C 73.20, H 7.22
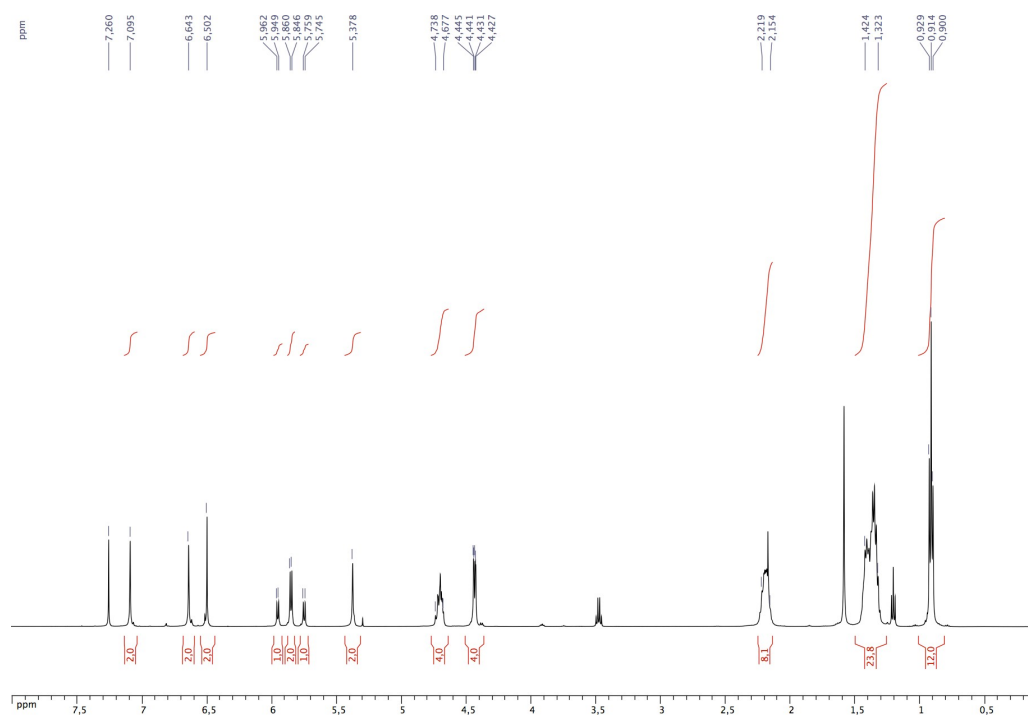
^{1}H NMR spectrum of **5** (CDCl$_3$)
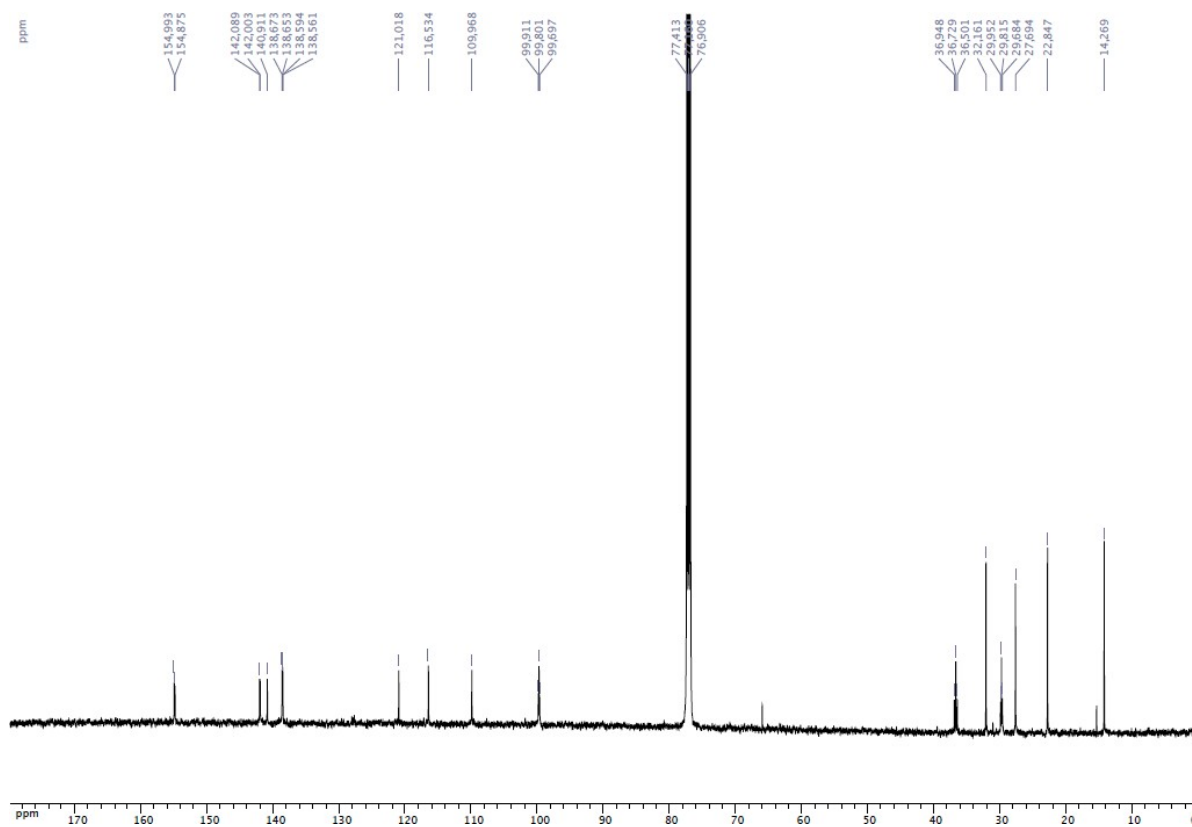
^{13}C{^{1}H} NMR spectrum of **5** (CDCl$_3$)

General procedure for the preparation of diphosphites 1 and 2 and monophosphites 7 and 8:

A suspension of the appropriate hydroxyl derivate (1.5 mmol) and NaH (60% dispersion in oil, 1.1 equiv/OH) in toluene was heated under reflux for 16 h. To this suspension was then added, at 0 °C, a toluene solution of [(S)-(1,1'-binaphthalene-2,2'diyl)]chlorophosphite (1.1 equiv/OH). The reaction mixture was stirred for an additional 2 h at room temperature, then filtered through a layer of aluminium oxide. The aluminium oxide was then washed with toluene (2 × 30 mL). The filtered solutions were evaporated to dryness, affording the phosphite as a pure white powder.

(*S,S*)-5,17-Bis(1,1'-binaphthyl-2,2'-dioxyphosphanyloxy)-25,26,27,28-tetrapropyloxycalix[4]arene (1)
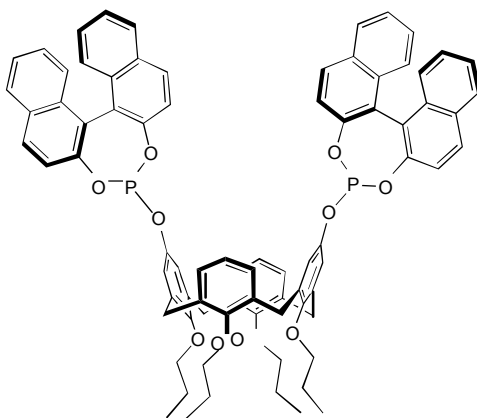
Yield 0.696 g (37 %). ^{1}H NMR (C$_6$D$_6$, 500 MHz): δ = 7.64-7.58 (m, 6H, arom. CH, binaphthyl), 7.51-7.46 (m, 8H, arom. CH, binaphthyl), 7.38 (d, 2H, arom. CH, binaphthyl, ^3J = 9.0 Hz), 7.13 (d, 4H, arom. CH, binaphthyl, ^3J = 7.5 Hz), 6.94-6.89 (m, 8H, arom. CH, binaphthyl and calixarene), 6.60 (d, 4H, arom. CH, calixarene, ^3J = 4.7 Hz), 6.55 (t, 2H, arom. CH, calixarene, ^3J = 4.7 Hz), 4.45 and 3.02 (AB spin system, 4H, ArCH_2Ar, ^2J = 13.2 Hz), 4.37 and 2.87 (AB spin system, 4H, ArCH_2Ar, ^2J = 13.2 Hz), 3.84 (t, 4H, OCH_2, ^3J = 7.7 Hz), 3.67 (t, 4H, OCH_2, ^3J = 7.0 Hz), 1.92 (sex, 4H, CH_2CH$_3$, ^3J = 7.5 Hz), 1.82 (sex, 4H, CH_2CH$_3$, ^3J = 7.5 Hz), 0.93 (t, 6H, CH$_2$CH_3, ^3J = 7.5 Hz), 0.92 (t, 6H, CH$_2$CH_3, ^3J = 7.5 Hz) ppm. ^{13}C{^{1}H} NMR (C$_6$D$_6$, 126 MHz): δ = 156.39-120.58 (arom. Cs), 77.05(s, OCH_2), 77.00 (s, OCH_2), 31.44 (s, ArCH_2Ar), 31.33 (s, ArCH_2Ar), 23.66 (s, CH_2CH$_3$), 23.49 (s, CH_2CH$_3$), 10.68 (s, CH$_2$CH_3), 10.41 (s, CH$_2$CH_3) ppm. ^{31}P{^{1}H} NMR (C$_6$D$_6$, 121 MHz): δ = 143.4 (s, OP(OAr)$_2$) ppm. MS (ESI TOF), *m/z*: 1275.43 [M + Na]$^+$ and 1291.41 [M + K]$^+$ expected isotopic profiles. Anal. Calc. for C$_{80}$H$_{70}$O$_{10}$P$_2$ (1253.36): C 76.66, H 5.63; found: 76.75, H 5.71.
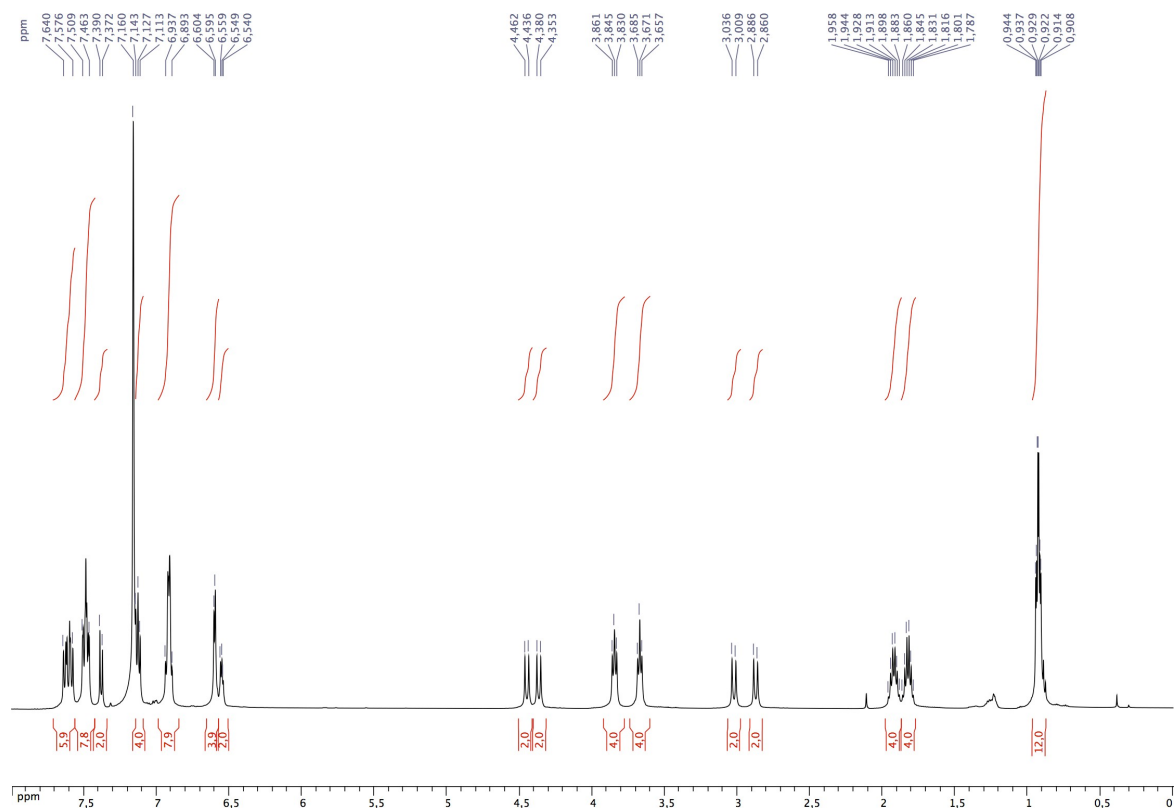
^{1}H NMR spectrum of **1** (C_6D_6)
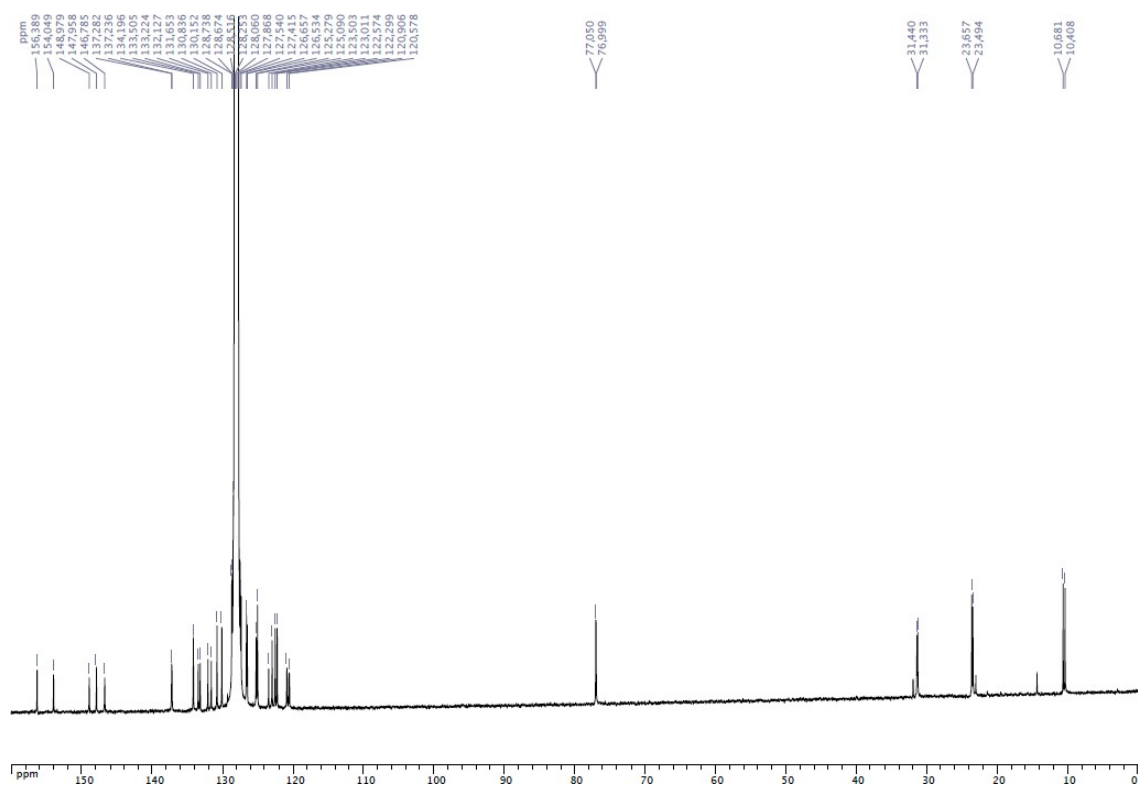
^{13}C{^{1}H} NMR spectrum of **1** (C_6D_6)
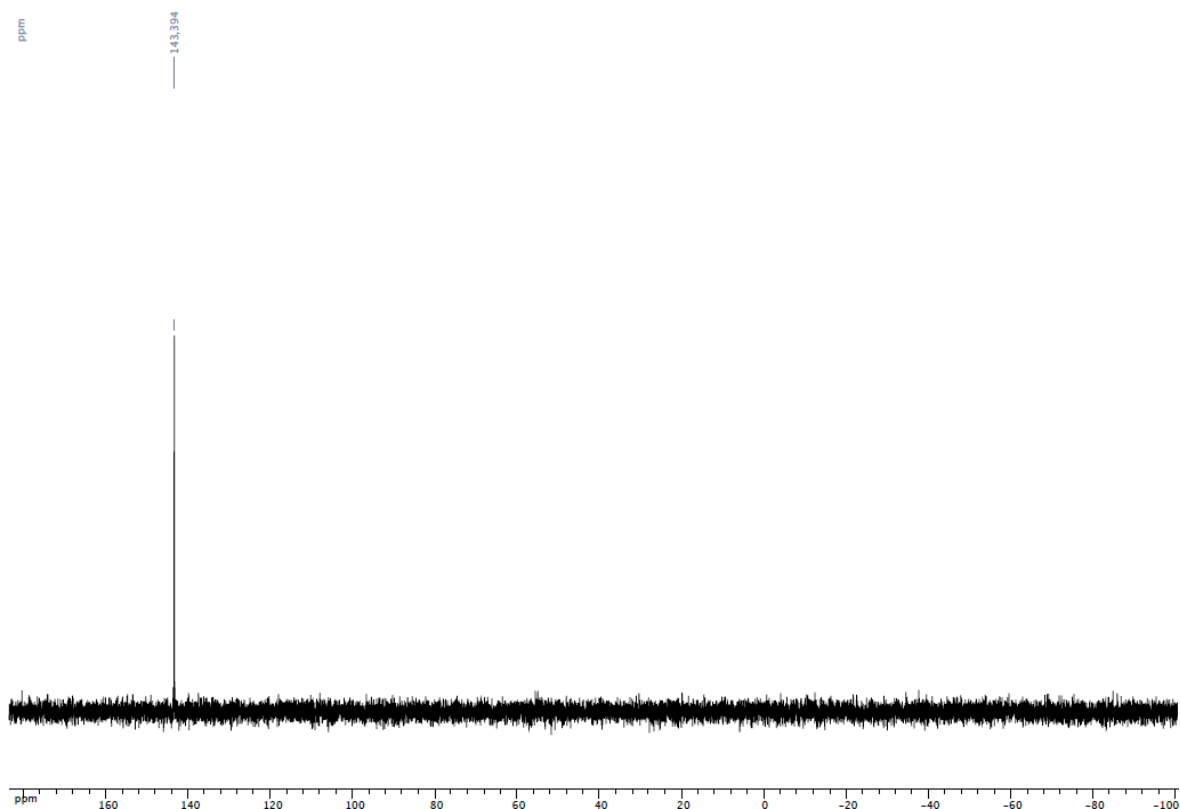
$^{31}\text{P}\{^1\text{H}\}$ NMR spectrum of **1** (C_6D_6)

(*S*,*S*)-5,11-Bis(1,1'-binaphthyl-2,2'-dioxyphosphanyloxy)-4(24),6(10),12(16),18(22)-etramethylenedioxy-2,8,14,20-tetrapentylresorcin[4]arene (2)
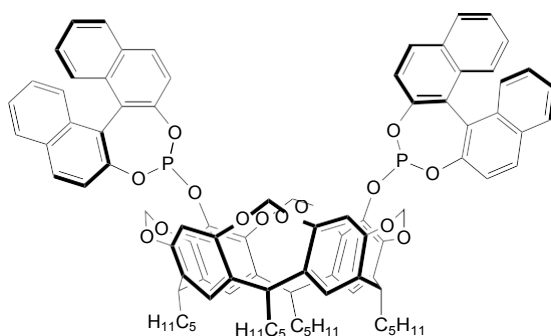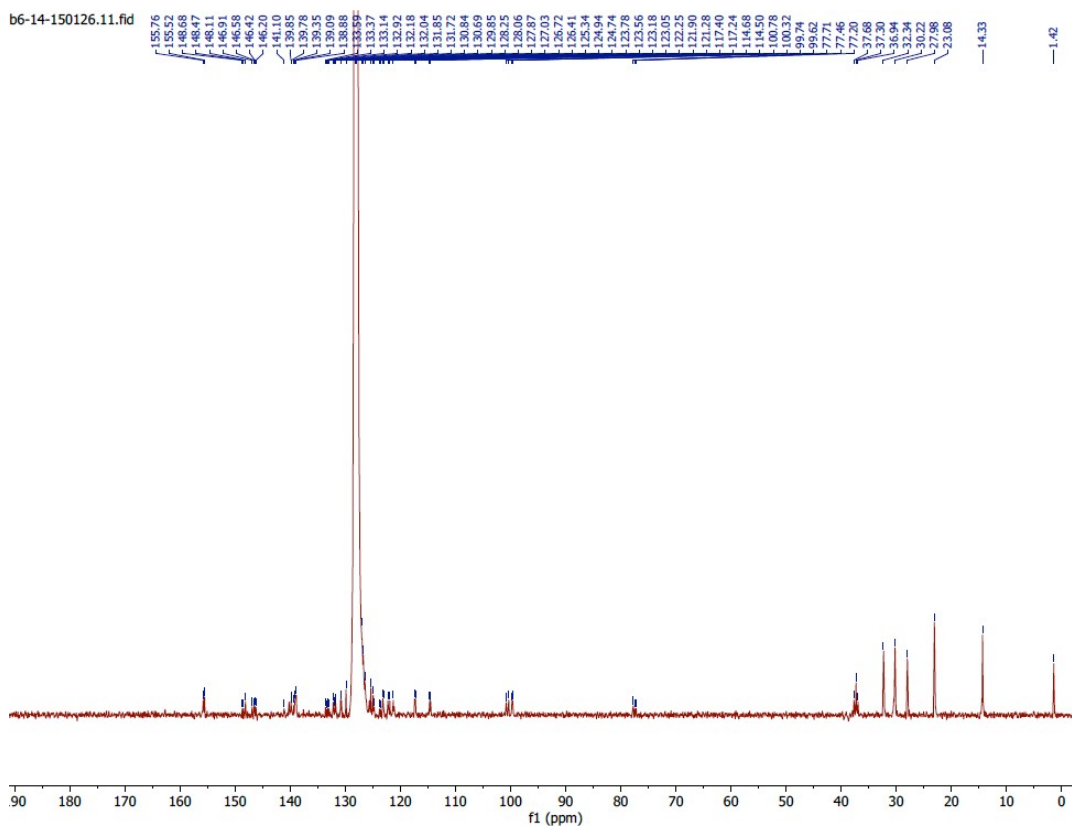

Yield 0.510 g (23 %). ^1H NMR (C_6D_6, 500 MHz): δ = 7.78 (d, 1H, arom. CH, binaphthyl, ^3J = 9.0 Hz), 7.72 (d, 2H, arom. CH, binaphthyl, ^3J = 8.50 Hz), 7.70-7.61 (m, 6H, arom. CH, binaphthyl), 7.58 (d, 1H, arom. CH, binaphthyl, ^3J = 8.0 Hz), 7.50 (d, 1H, arom. CH, binaphthyl, ^3J = 8.5 Hz), 7.49 (s, 1H, arom. CH, resorcinarene), 7.47 (s, 1H, arom. CH, resorcinarene), 7.42 (d, 1H, arom.

88

CH, binaphthyl, ^3J = 8.5 Hz), 7.40 (d, 1H, arom. CH, binaphthyl, ^3J = 8.5 Hz), 7.27 (d, 1H, arom. CH, binaphthyl, ^3J = 8.0 Hz), 7.26 (s, 1H, arom. CH, resorcinarene), 7.26 (s, 1H, arom. CH, resorcinarene), 7.21 (t, 2H, arom. CH, binaphthyl, ^3J = 8.0 Hz), 7.13-7.08 (m, 4H, arom. CH, binaphthyl), 7.04 (t, 1H, arom. CH, binaphthyl, ^3J = 8.0 Hz), 6.89 (t, 1H, arom. CH, binaphthyl, ^3J = 8.0 Hz), 6.80 (t, 1H, arom. CH, binaphthyl, ^3J = 8.0 Hz), 6.70 (t, 1H, arom. CH, binaphthyl, ^3J = 8.0 Hz), 6.51 (s, 1H, arom. CH, resorcinarene), 6.44 and 4.28 (AB spin system, 2H, OCH$_2$O, ^2J = 7.5 Hz), 6.41 (s, 1H, arom. CH, resorcinarene), 6.05 and 4.47 (AB spin system, 2H, OCH$_2$O, ^2J = 7.5 Hz), 6.03 and 4.47 (AB spin system, 2H, OCH$_2$O, ^2J = 7.5 Hz), 5.49 and 4.24 (AB spin system, 2H, OCH$_2$O, ^2J = 7.5 Hz), 5.27 (t, 1H, C*H*CH$_2$, ^3J = 8.0 Hz), 5.25 (t, 1H, C*H*CH$_2$, ^3J = 8.0 Hz), 5.20 (t, 1H, C*H*CH$_2$, ^3J = 8.2 Hz), 5.11 (t, 1H, C*H*CH$_2$, ^3J = 8.0 Hz), 2.38-2.25 (m, 8H, CHC*H$_2$*CH$_2$), 1.45-1.24 (m, 24H *CH$_2$CH$_2$CH$_2$*CH$_3$), 0.89 (t, 3H, CH$_2$*CH$_3$*, ^3J = 7.5 Hz), 0.86 (t, 3H, CH$_2$*CH$_3$*, ^3J = 7.0 Hz), 0.85 (t, 3H, CH$_2$*CH$_3$*, ^3J = 7.0 Hz), 0.83 (t, 3H, CH$_2$*CH$_3$*, ^3J = 7.0 Hz) ppm. ^{13}C{^{1}H} NMR (C$_6$D$_6$, 126 MHz): δ = 155.76-114.50 (arom. Cs), 100.78 (s, OCH$_2$O), 100.32 (s, OCH$_2$O), 99.74 (s, OCH$_2$O), 99.62 (s, OCH$_2$O), 37.68 (s, *C*HCH$_2$), 37.30 (s, *C*HCH$_2$), 36.94 (s, *C*HCH$_2$), 32.39 (s, *C*H$_2$CH$_2$CH$_3$), 32.34 (s, *C*H$_2$CH$_2$CH$_3$), 30.22 (s, CH*C*H$_2$), 28.04 (s, CHCH$_2$*C*H$_2$), 28.01 (s, CHCH$_2$*C*H$_2$), 27.98 (s, CHCH$_2$*C*H$_2$), 23.10 (s, *C*H$_2$CH$_3$), 23.08 (s, *C*H$_2$CH$_3$), 14.37 (s, CH$_2$*C*H$_3$), 14.33 (s, CH$_2$*C*H$_3$), 14.30 (s, CH$_2$*C*H$_3$) ppm. ^{31}P{^{1}H} NMR (C$_6$D$_6$, 162 MHz): δ = 149.7 (s, OP(OAr)$_2$), 149.2 (s, OP(OAr)$_2$) ppm. MS (ESI TOF), *m/z*: 1477.56 [M + H]$^+$ expected isotopic profile. Anal. Calc. for C$_{92}$H$_{86}$O$_{14}$P$_2$ (1476.61): C 74.78, H 5.87; found: C 74.97, H 6.02 %.
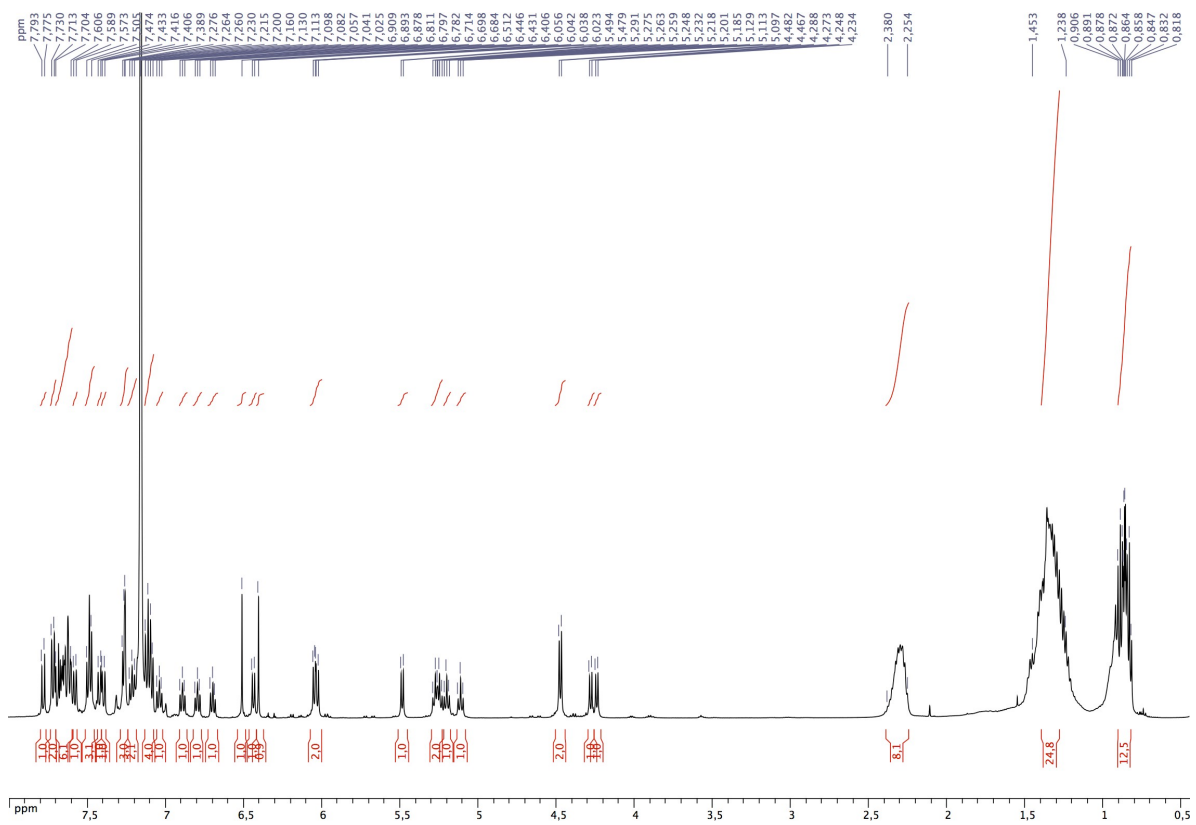
^{1}H NMR spectrum of **2** (CDCl$_3$)

^{13}C{^{1}H} NMR spectrum of **2** (CDCl$_3$)
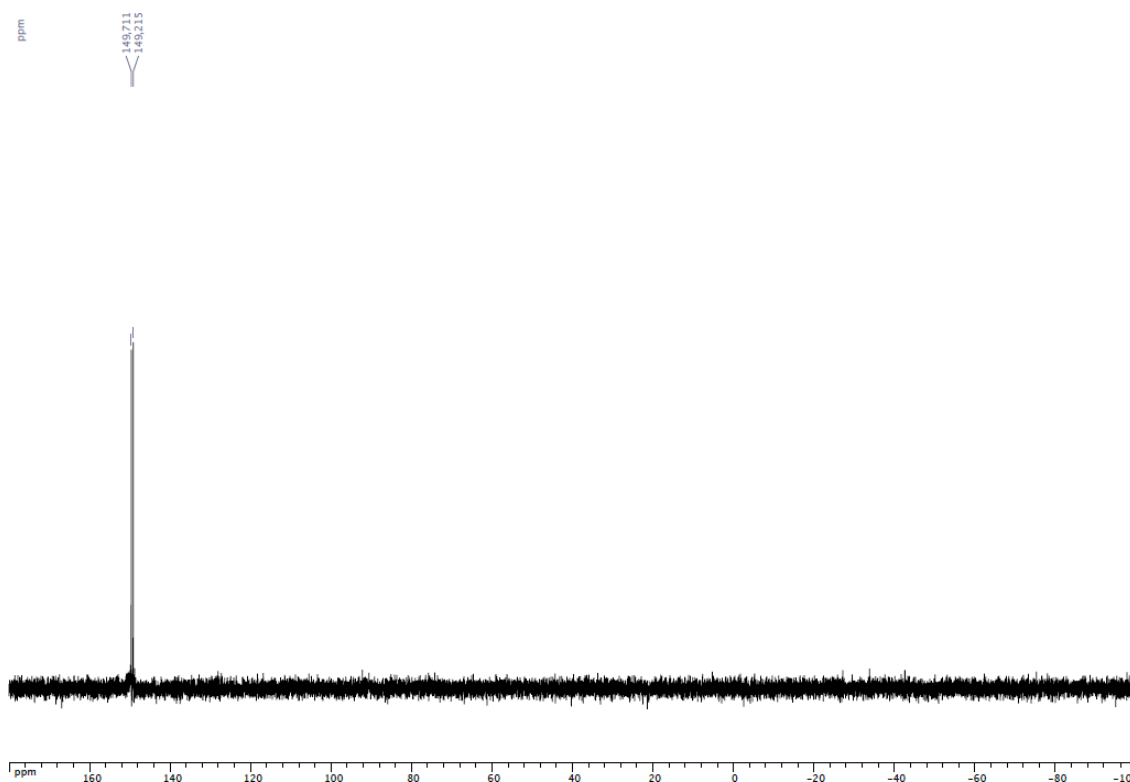
^{31}P{^{1}H} NMR spectrum of **2** (C$_6$D$_6$)

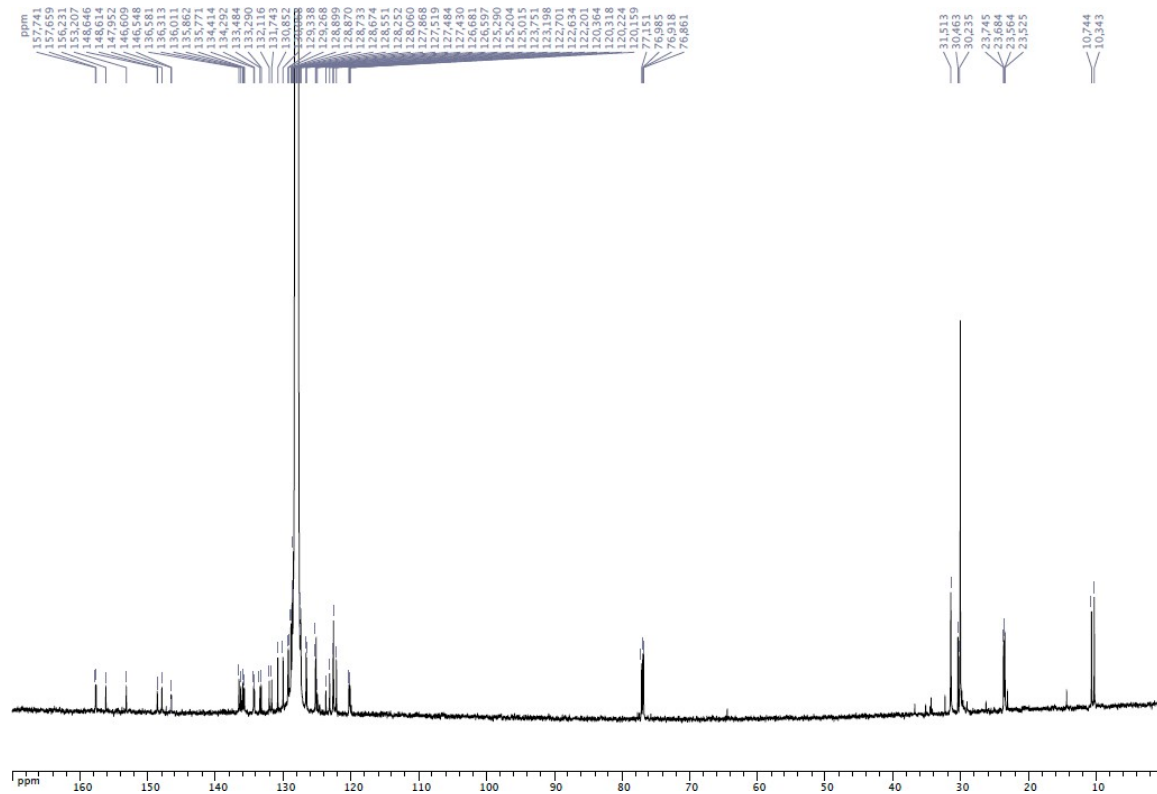**(*S*)-5-(1,1'-Binaphthyl-2,2'-dioxyphosphanyloxy)-25,26,27,28-tetrapropyloxycalix[4]arene (7)**
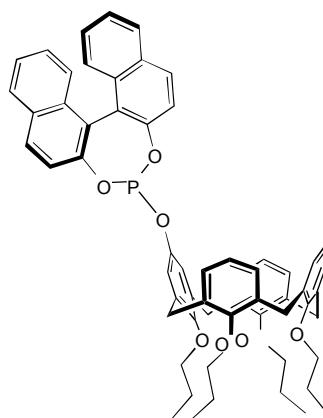
Yield 0.166 g (12 %). ^{1}H NMR (C$_6$D$_6$, 500 MHz): δ = 7.80 (d, 1H, arom. CH, binaphthyl, ^{3}J = 9.0 Hz), 7.68 (d, 1H, arom. CH, binaphthyl, ^{3}J = 8.0 Hz), 7.59 (d, 1H, arom. CH, binaphthyl, ^{3}J = 8.5 Hz), 7.53-7.48 (m, 3H, arom. CH, binaphthyl), 7.37-7.35 (m, 2H, arom. CH, binaphthyl), 7.13-7.11 (m, 2H, arom. CH, binaphthyl), 6.99 (t, 1H, arom. CH, calixarene, ^{3}J = 4.5 Hz), 6.95-6.85 (m,

7H, arom. CH, binaphthyl and calixarene), 6.66-6.60 (m, 3H, arom. CH, calixarene), 6.53 (s br, 1H, arom. CH, calixarene), 6.48 (d, 1H, arom. CH, calixarene, ^3J = 6.5 Hz), 4.56 and 3.19 (AB spin system, 2H, ArCH_2Ar, ^2J = 13.0 Hz), 4.52 and 3.12 (AB spin system, 2H, ArCH_2Ar, ^2J = 13.0 Hz), 4.49 and 3.07 (AB spin system, 2H, ArCH_2Ar, ^2J = 13.5 Hz), 4.45 and 2.99 (AB spin system, 2H, ArCH_2Ar, ^2J = 13.5 Hz), 3.97-3.88 (m, 4H, OCH_2), 3.70 (t, 2H, OCH_2, ^3J = 7.0 Hz), 3.67 (t, 2H, OCH_2, ^3J = 7.2 Hz), 1.98-1.91 (m, 4H, CH_2CH$_3$), 1.85-1.78 (m, 4H, CH_2CH$_3$), 0.96 (t, 3H, CH$_2$CH_3, ^3J = 7.5 Hz), 0.94 (t, 3H, CH$_2$CH_3, ^3J = 7.5 Hz), 0.89 (t, 6H, CH$_2$CH_3, ^3J = 7.5 Hz) ppm. ^{13}C{^{1}H} NMR (C$_6$D$_6$, 126 MHz): δ = 157.74-120.16 (arom. Cs), 77.15(s, OCH$_2$), 76.99 (s, OCH$_2$), 76.92(s, OCH$_2$), 76.86 (s, OCH$_2$), 31.56 (s, ArCH$_2$Ar), 31.53 (s, ArCH$_2$Ar), 31.51 (s, ArCH$_2$Ar), 31.57 (s, ArCH$_2$Ar), 23.75 (s, CH$_2$CH$_3$), 23.68 (s, CH$_2$CH$_3$), 23.56 (s, CH$_2$CH$_3$), 23.53 (s, CH$_2$CH$_3$), 10.76 (s, CH$_2$CH$_3$), 10.35 (s, CH$_2$CH$_3$) ppm. ^{31}P{^{1}H} NMR (C$_6$D$_6$, 121 MHz): δ = 145.7 (s, OP(OAr)$_2$) ppm. MS (ESI TOF), m/z: 945.39 [M + Na]$^+$ expected isotopic profile. Anal. Calc. for C$_{60}$H$_{59}$O$_7$P (923.08): C 78.07, H 6.44; found: 77.89, H 6.89.
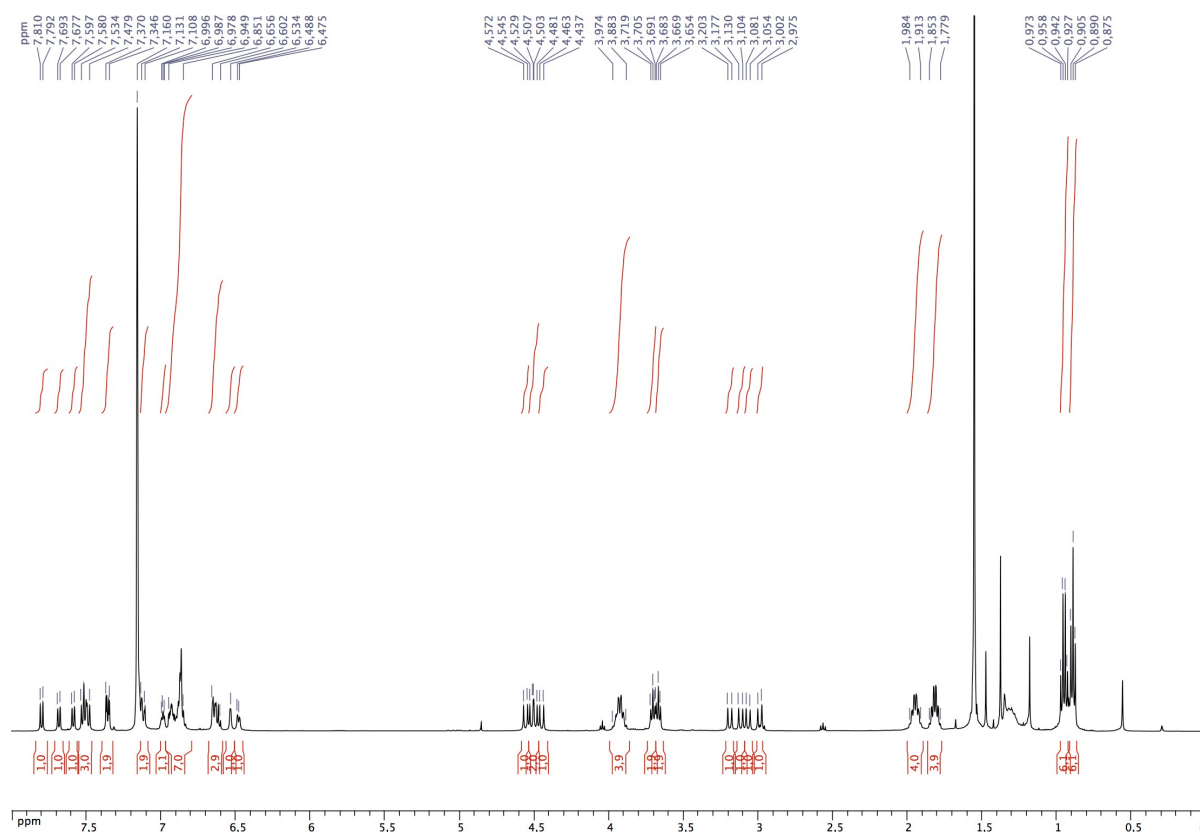
^{1}H NMR spectrum of **7** (C$_6$D$_6$)

$^{13}C\{^{1}H\}$ NMR spectrum of **7** (C_6D_6)
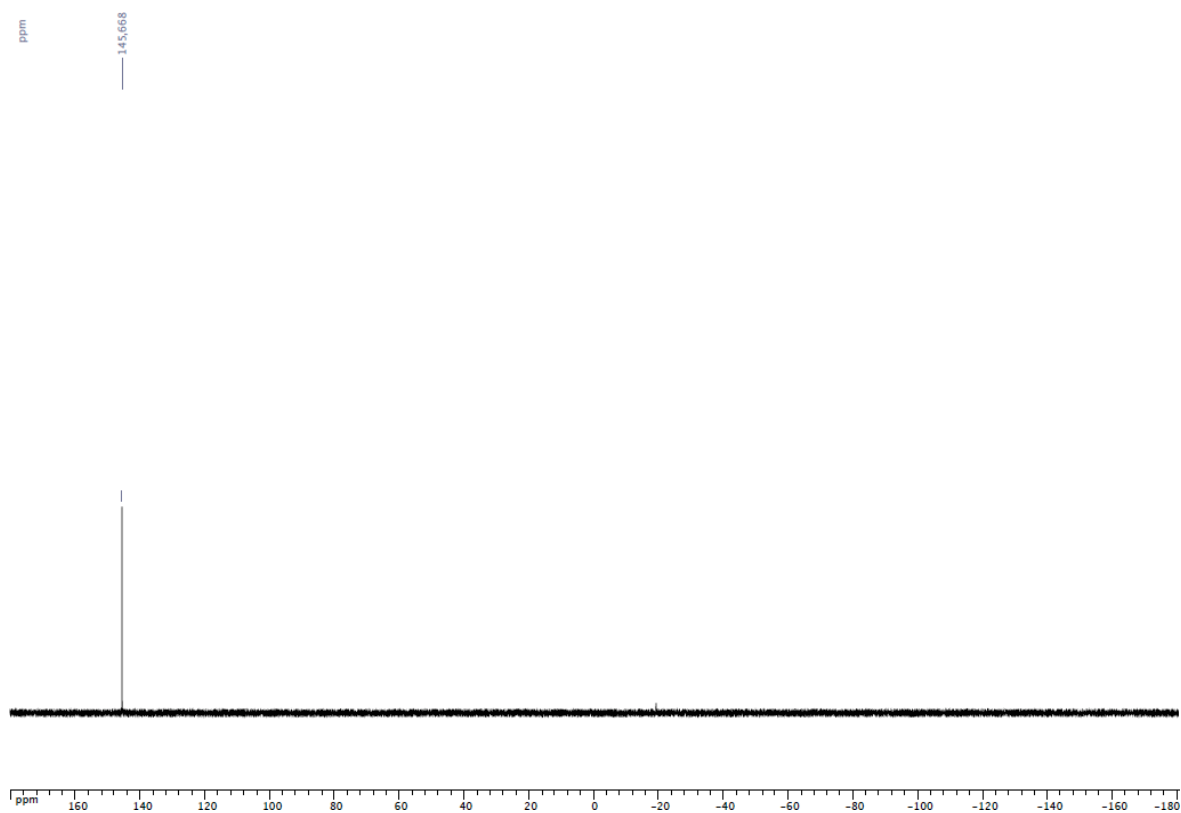
$^{31}P\{^{1}H\}$ NMR spectrum of **7** (C_6D_6)

(*S*)-5-(1,1'-Binaphthyl-2,2'-dioxyphosphanyloxy)-4(24),6(10),12(16),18(22)-tetramethyle nedioxy-2,8,14,20-tetrapentylresorcin[4]arene (8)
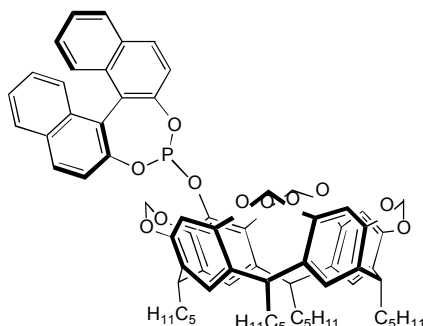
Yield 1.118 g (65 %). ^{1}H NMR (C$_6$D$_6$, 500 MHz): δ = 7.73 (d, 1H, arom. CH, binaphthyl, ^3J = 8.5 Hz), 7.66-7.63 (m, 2H, arom. CH, binaphthyl), 7.59-7.55 (m, 3H, arom. CH, binaphthyl), 7.51-7.49 (m, 2H, arom. CH, binaphthyl), 7.47 (s, 2H, arom. CH, resorcinarene), 7.29 (s, 1H, arom. CH, resorcinarene), 7.20 (s, 1H, arom. CH, resorcinarene), 7.18-7.16 (m, 2H, arom. CH, binaphthyl), 6.97-6.94 (m, 2H, arom. CH, binaphthyl), 6.68 (s, 1H, arom. CH, resorcinarene), 6.30 (s, 1H, arom. CH, resorcinarene), 6.19 (s, 1H, arom. CH, resorcinarene), 6.07 and 4.36 (AB spin system, 2H, OCH$_2$O, ^2J = 7.0 Hz), 6.03 and 4.37 (AB spin system, 2H, OCH$_2$O, ^2J = 7.5 Hz), 5.54 and 4.33 (AB spin system, 2H, OCH$_2$O, ^2J = 7.5 Hz), 5.54 and 4.28 (AB spin system, 2H, OCH$_2$O, ^2J = 7.0 Hz), 5.27 (t, 1H, C*H*CH$_2$, ^3J = 8.0 Hz), 5.19 (t, 1H, C*H*CH$_2$, ^3J = 8.0 Hz), 5.14 (t, 1H, C*H*CH$_2$, ^3J = 8.0 Hz), 5.13 (t, 1H, C*H*CH$_2$, ^3J = 8.0 Hz), 2.41-2.22 (m, 8H, CHC*H$_2$*CH$_2$), 1.46-1.20 (m, 24H *CH$_2$CH$_2$CH$_2$*CH$_3$), 0.86 (t, 3H, CH$_2$*CH$_3$*, ^3J = 7.5 Hz), 0.84 (t, 3H, CH$_2$*CH$_3$*, ^3J = 7.5 Hz), 0.83 (t, 3H, CH$_2$*CH$_3$*, ^3J = 7.5 Hz), 0.82 (t, 3H, CH$_2$*CH$_3$*, ^3J = 7.5 Hz) ppm. ^{13}C{^{1}H} NMR (C$_6$D$_6$, 126 MHz): δ = 155.66-114.51 (arom. Cs), 100.22 (s, OCH$_2$O), 99.71 (s, OCH$_2$O), 99.50 (s, OCH$_2$O), 37.34 (s, *C*HCH$_2$), 37.31 (s, *C*HCH$_2$), 36.93 (s, *C*HCH$_2$), 32.36 (s, *CH$_2$*CH$_2$CH$_3$), 32.31 (s, *CH$_2$*CH$_2$CH$_3$), 30.34 (s, CHC*H$_2$*), 30.28 (s, CHC*H$_2$*), 28.05 (s, CHCH$_2$*CH$_2$*), 27.98 (s, CHCH$_2$*CH$_2$*), 23.07 (s, *CH$_2$*CH$_3$), 14.35 (s, CH$_2$*CH$_3$*), 14.31 (s, CH$_2$*CH$_3$*) ppm. ^{31}P{^{1}H} NMR (C$_6$D$_6$, 121 MHz): δ = 149.1 (s, OP(OAr)$_2$) ppm. Anal. Calc. for C$_{72}$H$_{75}$O$_{11}$P (1147.34): C 75.37, H 6.59; found: C 75.44, H 7.42 %.
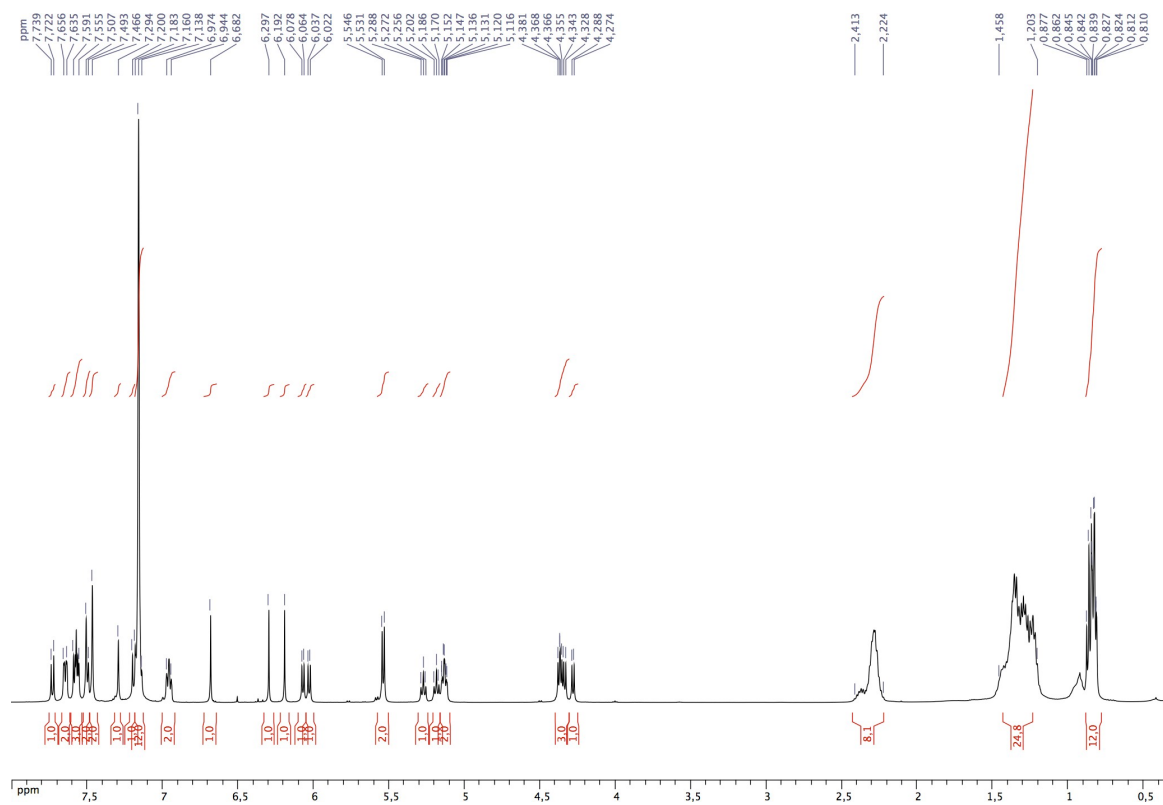
^{1}H NMR spectrum of **8** (C$_6$D$_6$)
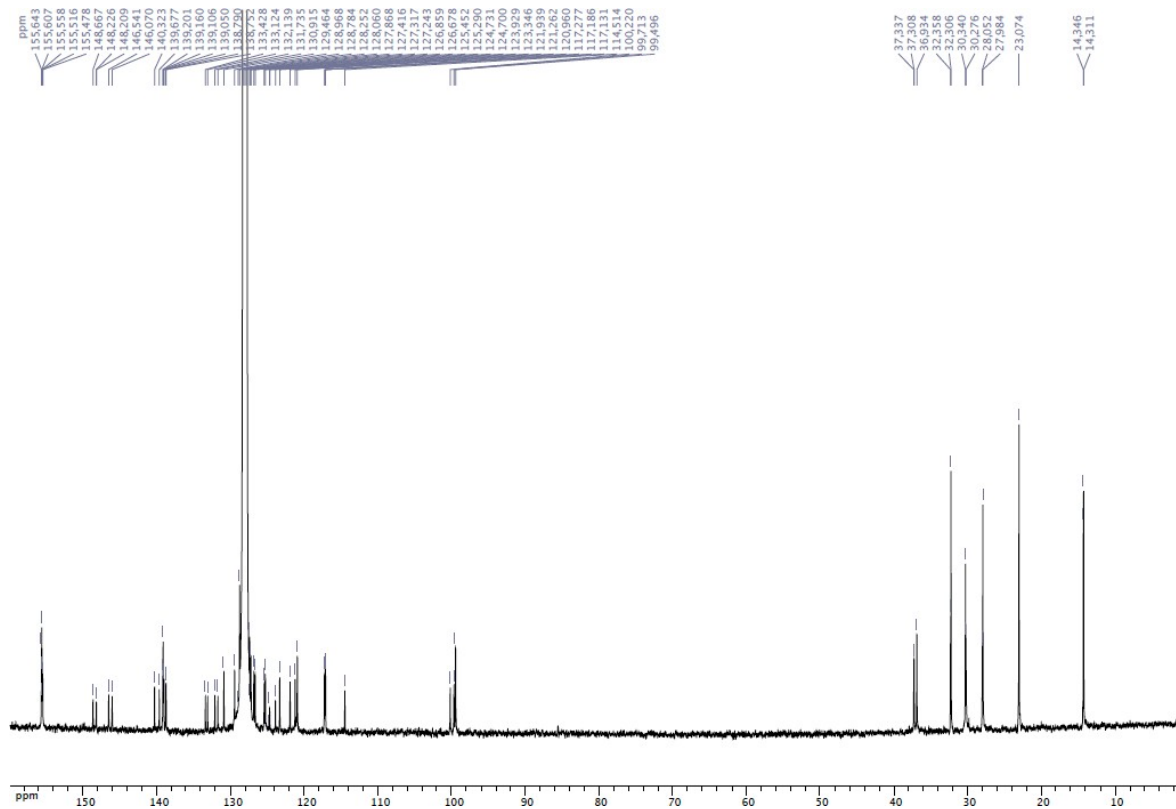
^{13}C{^{1}H} NMR spectrum of **8** (C$_6$D$_6$)
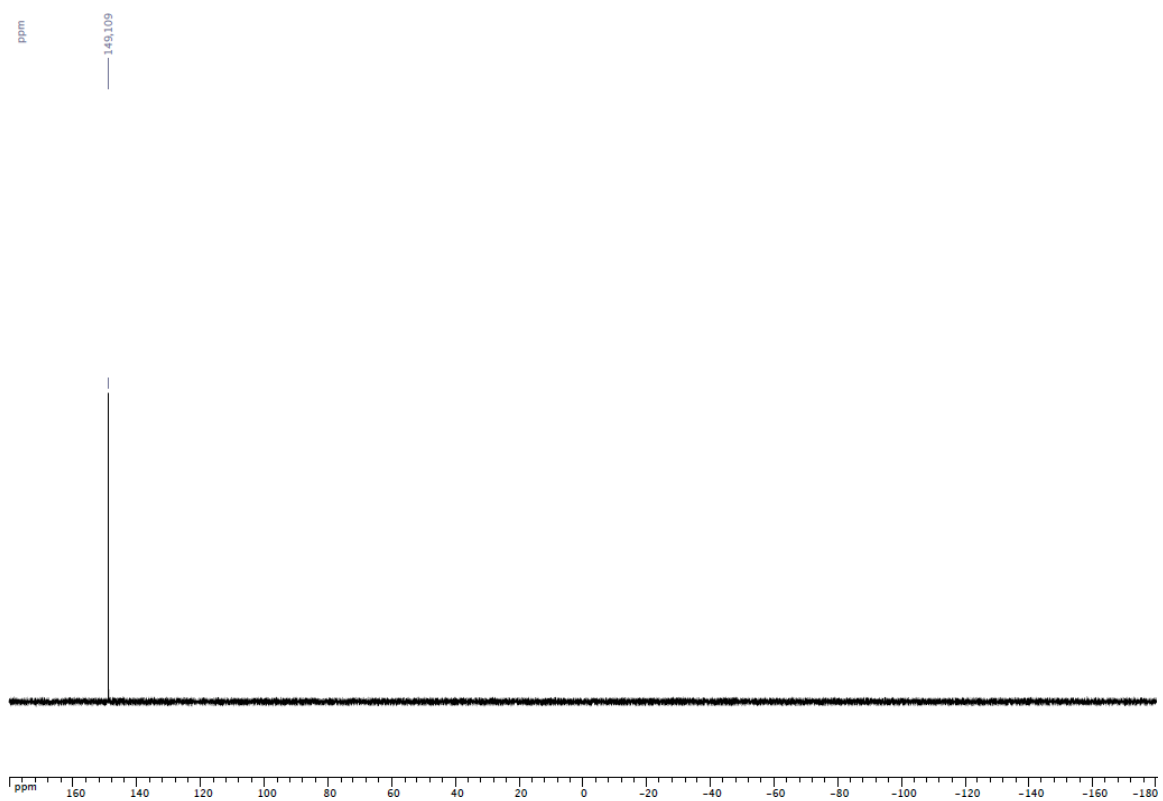
$^{31}P\{^{1}H\}$ NMR spectrum of **8** (C$_6$D$_6$)

Rhodium complex 6
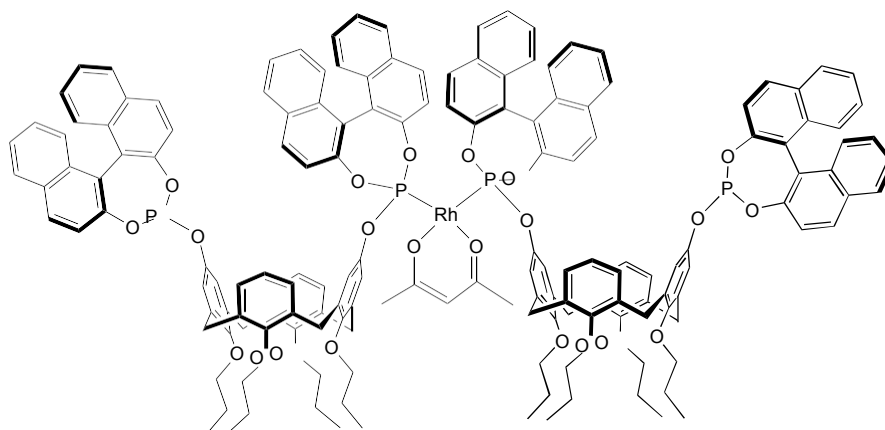


A solution of [Rh(acac)(CO)$_2$] (0.005 g, 0.02 mmol) in CH$_2$Cl$_2$ (300 mL) was slowly added to a solution of diphosphite **1** (0.050 g, 0.04 mmol) in CH$_2$Cl$_2$ (3000 mL). The reaction mixture was
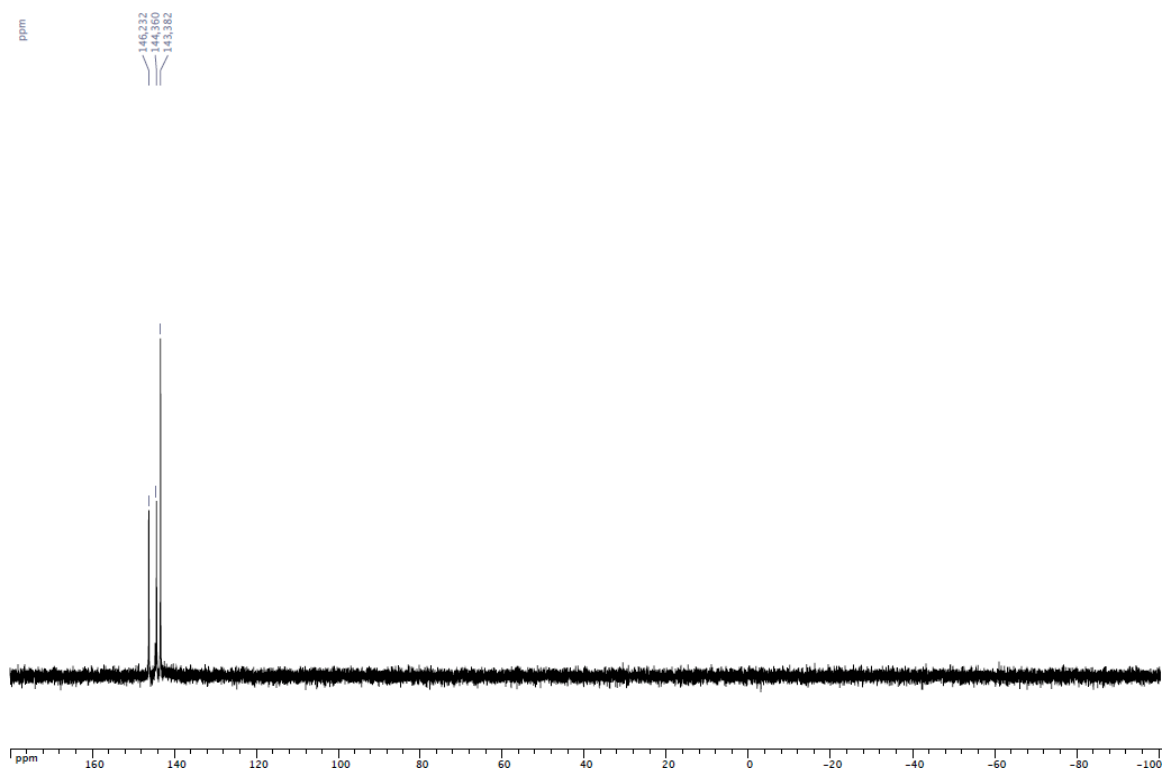
stirred at room temperature for 16 h. The solvent was evaporated to dryness, and the yellow residue washed with cold hexane (-78°C) before being dried under vacuum (yield: 0.052 g, 96 %). IR: ν 1585 (acac) cm^{-1}. ^{1}H NMR (C$_6$D$_6$, 400 MHz): δ = 7.70-7.56 (m, 14H, arom. CH, binaphthyl), 7.50-7.44 (m, 18H, arom. CH, binaphthyl), 7.25 (d, 4H, arom. CH, binaphthyl, ^3J = 7.6 Hz), 7.13-7.02 (m, 14H, arom. CH, binaphthyl and calixarene), 6.96-6.89 (m, 8H, arom. CH, binaphthyl and calixarene), 6.85 (t, 4H, arom. CH, calixarene, ^3J = 7.8 Hz), 6.60 (d, 4H, arom. CH, calixarene, ^3J = 4.7 Hz), 6.55 (t, 2H, arom. CH, calixarene, ^3J = 4.7 Hz), 5.41 (s, 1H, CH of acac), 4.62 and 3.22 (AB spin system, 4H, ArCH$_2$Ar, ^2J = 13.2 Hz), 4.51 and 3.03 (AB spin system, 4H, ArCH$_2$Ar, ^2J = 13.2 Hz), 4.45 and 3.03 (AB spin system, 4H, ArCH$_2$Ar, ^2J = 13.2 Hz), 4.36 and 2.87 (AB spin system, 4H, ArCH$_2$Ar, ^2J = 13.2 Hz), 4.18-4.13 (m, 4H, OCH$_2$), 3.85 (t, 4H, OCH$_2$, ^3J = 7.4 Hz), 3.68 (t, 4H, OCH$_2$, ^3J = 7.2 Hz), 3.60-3.56 (m, 4H, OCH$_2$), 2.11-2.04 (m, 4H, CH$_2$CH$_3$), 1.95-1.87 (m, 4H, CH$_2$CH$_3$), 1.92 (s, 6H, CH$_3$ of acac), 1.85-1.73 (m, 8H, CH$_2$CH$_3$), 1.01 (t, 6H, CH$_2$CH$_3$, ^3J = 7.4 Hz), 0.93 (t, 12H, CH$_2$CH$_3$, ^3J = 7.2 Hz), 0.88 (t, 6H, CH$_2$CH$_3$, ^3J = 7.4 Hz) ppm. ^{13}C\{^{1}H\} NMR (C$_6$D$_6$, 126 MHz): δ = 185.44 (s, CO of acac), 158.52-119.02 (arom. Cs), 101.87 (s, CH of acac), 77.29 (s, OCH$_2$), 77.03 (s, OCH$_2$), 77.01 (s, OCH$_2$), 76.90 (s, OCH$_2$), 31.84 (s, ArCH$_2$Ar), 31.42 (s, ArCH$_2$Ar), 31.31 (s, ArCH$_2$Ar), 27.87 (s, CH$_3$ of acac), 23.90 (s, CH$_2$CH$_3$), 23.64 (s, CH$_2$CH$_3$), 23.49 (s, CH$_2$CH$_3$), 23.38 (s, CH$_2$CH$_3$), 11.06 (s, CH$_2$CH$_3$), 10.34 (s, CH$_2$CH$_3$), 10.07 (s, CH$_2$CH$_3$) ppm. ^{31}P\{^{1}H\} NMR (C$_6$D$_6$, 162 MHz): δ = 145.3 (d, J_{PRh} = 303 Hz, OP(OAr)$_2$ coordinated to Rh), 143.4 (s, free OP(OAr)$_2$) ppm. MS (ESI TOF): m/z 2607.81 [M - acac]$^+$, expected isotopic profile. Anal. Calcd for C$_{165}$H$_{147}$O$_{22}$P$_4$Rh (2706.84): C 73.16, H 5.47; found: 73.24, H 5.58.
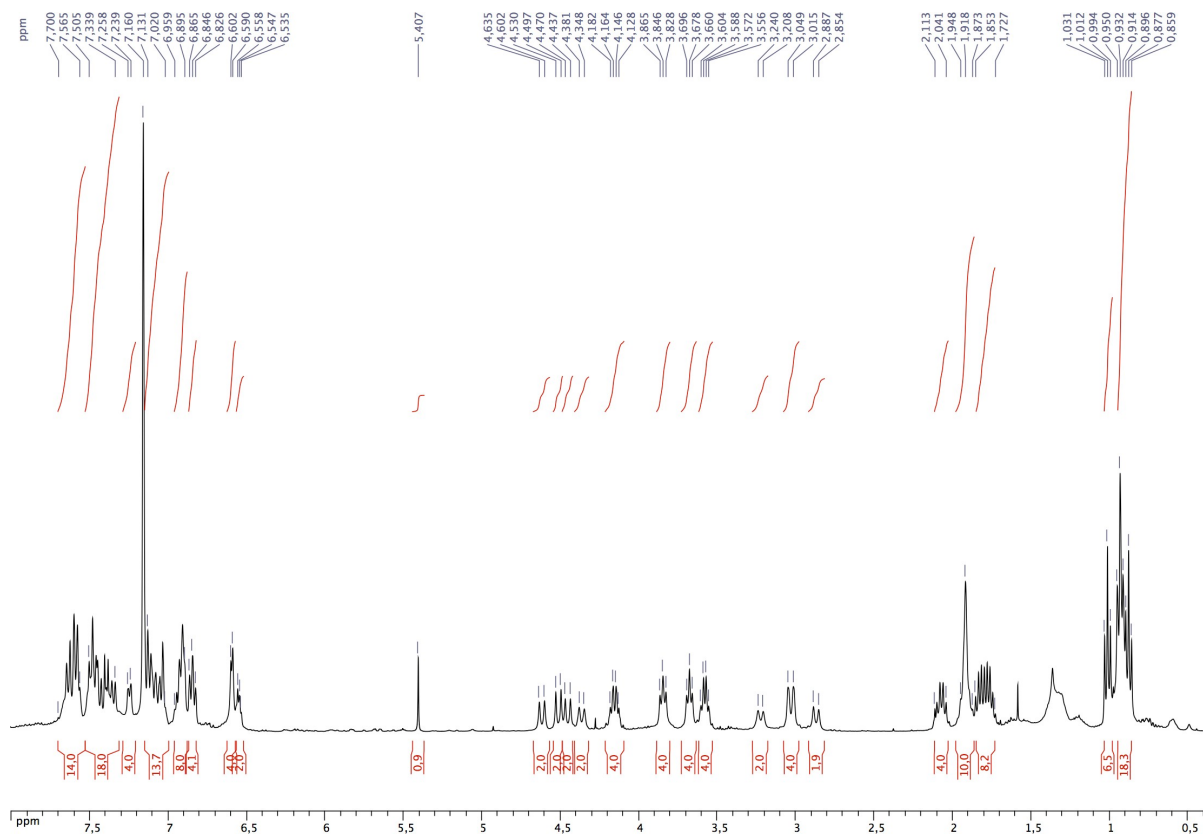
^{1}H NMR spectrum of **6** (C$_6$D$_6$)
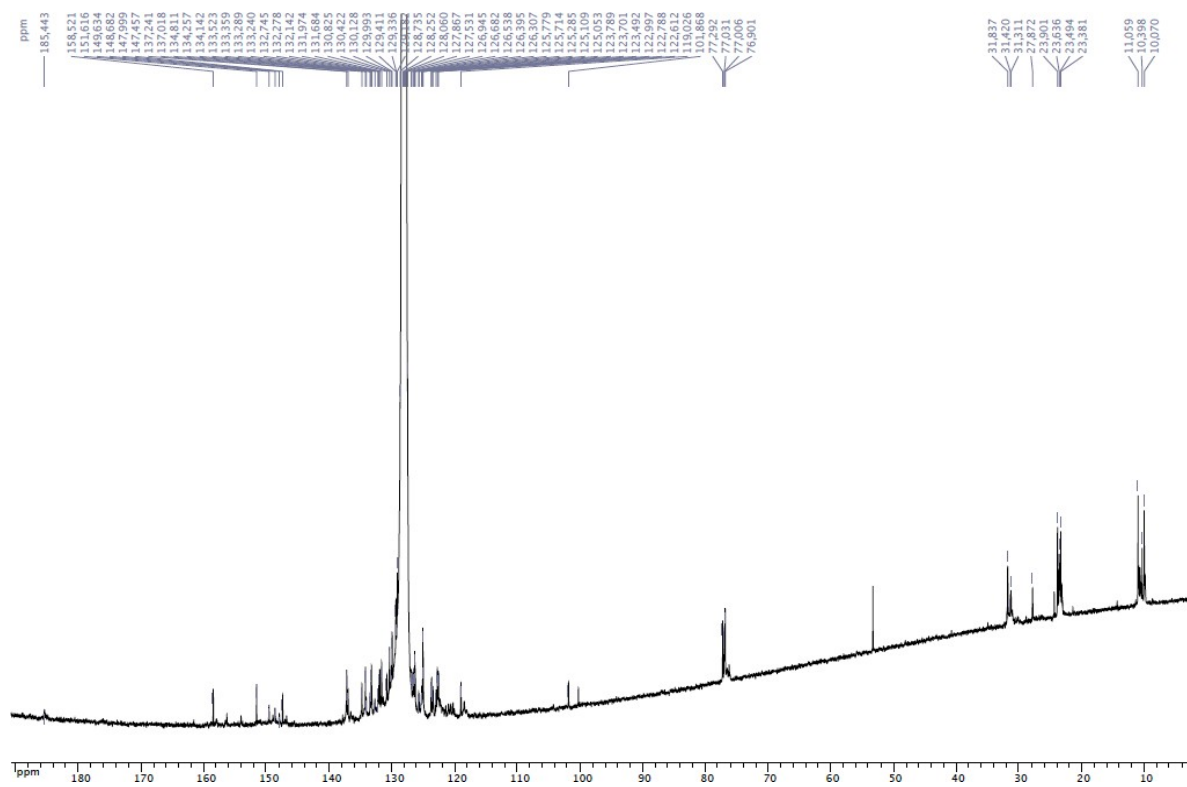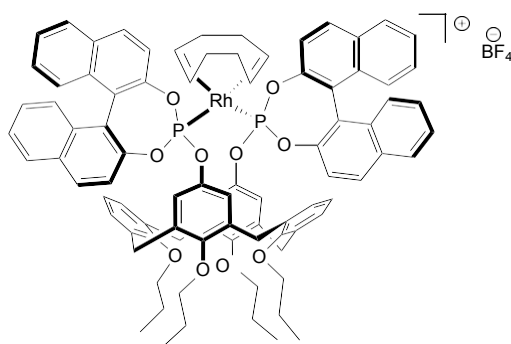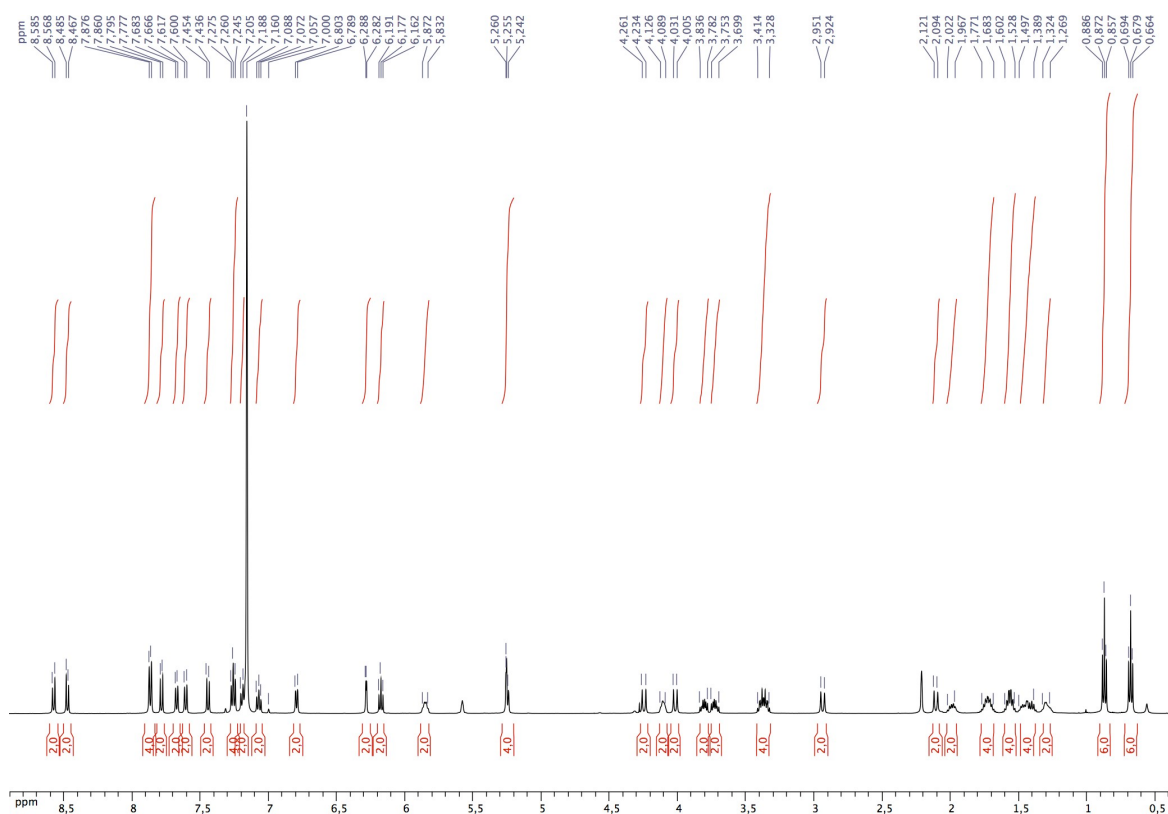

^{13}C{^{1}H} NMR spectrum of **6** (C$_6$D$_6$)

$^{31}\text{P}\{^1\text{H}\}$ NMR spectrum of **6** (C_6D_6)

[Rh(cod)(1)]BF₄ complex

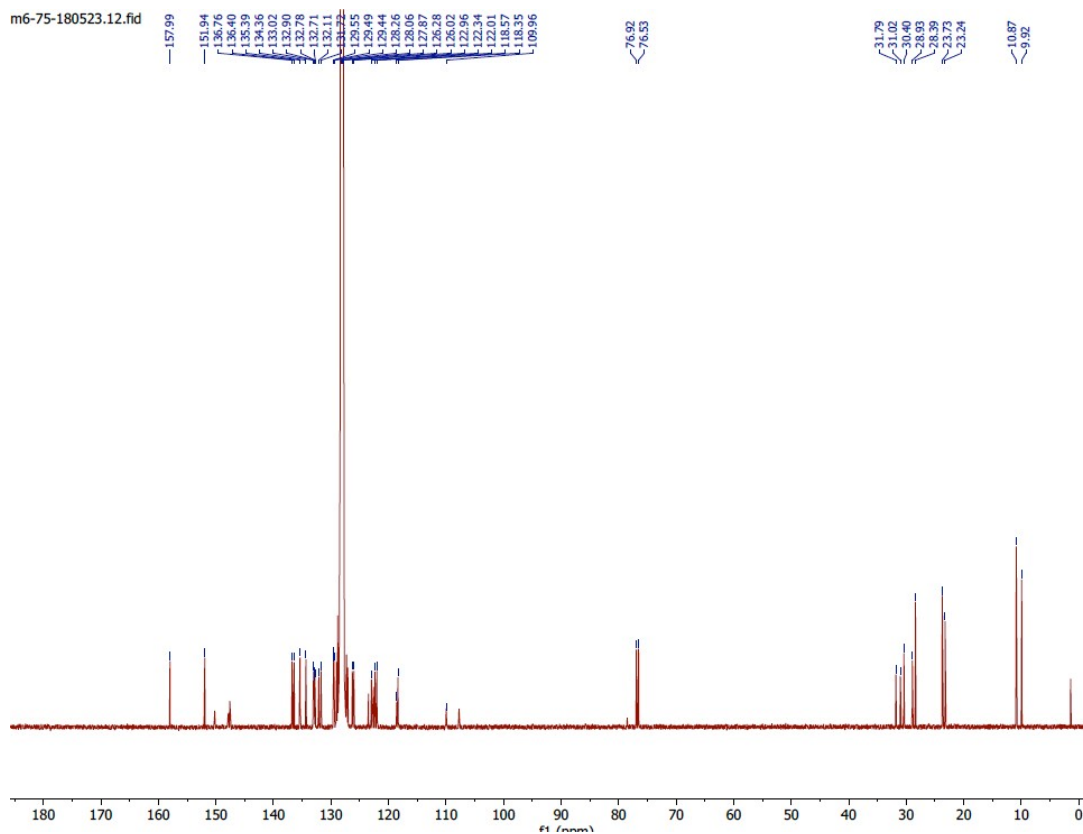A solution of [Rh(cod)₂]BF₄ (0.003 g, 0.008 mmol) in CH₂Cl₂ (50 mL) and a solution of diphosphite **1** (10 mg, 0.008 mmol) in CH₂Cl₂ (50 mL) were slowly and simultaneously added to a 500 mL Schlenk flask containing 200 mL of CH₂Cl₂. The reaction mixture was stirred at room temperature for 16 h. The solvent was evaporated to dryness, and the yellow solid was washed with cold hexane (-78°C) before being dried under vacuum (yield: 0.012 g, 95 %). ^1H NMR (C_6D_6, 500 MHz): δ = 8.58 (d, 2H, arom. CH, binaphthyl, ^3J = 8.5 Hz), 8.48 (d, 2H, arom. CH, binaphthyl, ^3J = 8.5 Hz), 7.87 (d, 4H, arom. CH, binaphthyl, ^3J = 8.0 Hz), 7.79 (d, 2H, arom. CH,

binaphthyl, $^3J = 9.0$ Hz), 7.67 (d, 2H, arom. CH, binaphthyl, $^3J = 8.5$ Hz), 7.61 (d, 2H, arom. CH, binaphthyl, $^3J = 8.5$ Hz), 7.44 (d, 2H, arom. CH, binaphthyl, $^3J = 9.0$ Hz), 7.26 (t, 4H, arom. CH, binaphthyl, $^3J = 8.5$ Hz), 7.19 (t, 2H, arom. CH, binaphthyl, $^3J = 8.5$ Hz), 7.07 (t, 2H, arom. CH, binaphthyl, $^3J = 8.5$ Hz), 6.80 (d, 2H, arom. CH, calixarene, $^3J = 7.0$ Hz), 6.28 (d, 2H, arom. CH, calixarene, $^4J_{PH} = 3.0$ Hz), 6.18 (t, 2H, arom. CH, calixarene, $^3J = 7.0$ Hz), 5.87-5.83 (m, 2H, CH, cod), 5.26 (d, 2H, arom. CH, calixarene, $^4J_{PH} = 3.0$ Hz), 5.24 (d, 2H, arom. CH, calixarene, $^3J = 7.0$ Hz), 4.25 and 2.94 (AB spin system, 4H, ArCH_2Ar, $^2J = 13.5$ Hz), 4.134.09 (m, 2H, CH, cod), 4.02 and 2.11 (AB spin system, 4H, ArCH_2Ar, $^2J = 13.5$ Hz), 3.84-3.78 (m, 2H, OCH_2), 3.75-3.70 (m, 2H, OCH_2), 3.41-3.33 (m, 4H, OCH_2), 2.02-1.97 (m, 2H, CH_2, cod), 1.77-1.68 (m, 4H, CH_2CH$_3$), 1.60-1.53 (m, 4H, CH_2CH$_3$), 1.50-1.39 (m, 4H, CH$_2$, cod), 1.32-1.27 (m, 2H, CH$_2$, cod), 0.87 (t, 6H, CH$_2$CH_3, $^3J = 7.2$ Hz), 0.68 (t, 6H, CH$_2$CH_3, $^3J = 7.5$ Hz) ppm. ^{13}C{^{1}H} NMR (C$_6$D$_6$, 126 MHz): $\delta = 157.98$-118.35 (arom. Cs), 109.96 (d, CH, cod, $^1J_{CRh} = 4.3$ Hz), 107.72 (d, CH, cod, $^1J_{CRh} = 3.8$ Hz), 76.92 (s, OCH$_2$), 76.53 (s, OCH$_2$), 31.80 (s, ArCH$_2$Ar), 31.02 (s, ArCH$_2$Ar), 30.40 (s, CH$_2$, cod), 28.94 (s, CH$_2$, cod), 28.40 (s, CH$_2$, cod), 23.74 (s, CH$_2$CH$_3$), 23.25 (s, CH$_2$CH$_3$), 10.87 (s, CH$_2$CH$_3$), 9.93 (s, CH$_2$CH$_3$) ppm. ^{31}P{^{1}H} NMR (C$_6$D$_6$, 202 MHz): $\delta = 114.3$ (d, $J_{PRh} = 269$ Hz, OP(OAr)$_2$) ppm. MS (ESI TOF): m/z 1463.45 [M - BF$_4$]$^+$ expected isotopic profile. Anal. Calcd for C$_{88}$H$_{82}$O$_{10}$P$_2$RhBF$_4$ (1551.25): C 68.13, H 5.33; found: 68.02, H 5.1

^{1}H NMR spectrum of [Rh(cod)(**1**)]BF$_4$ complex (C$_6$D$_6$)

$^{13}C\{^1H\}$ NMR spectrum of $[Rh(cod)(\mathbf{1})]BF_4$ complex (C_6D_6)
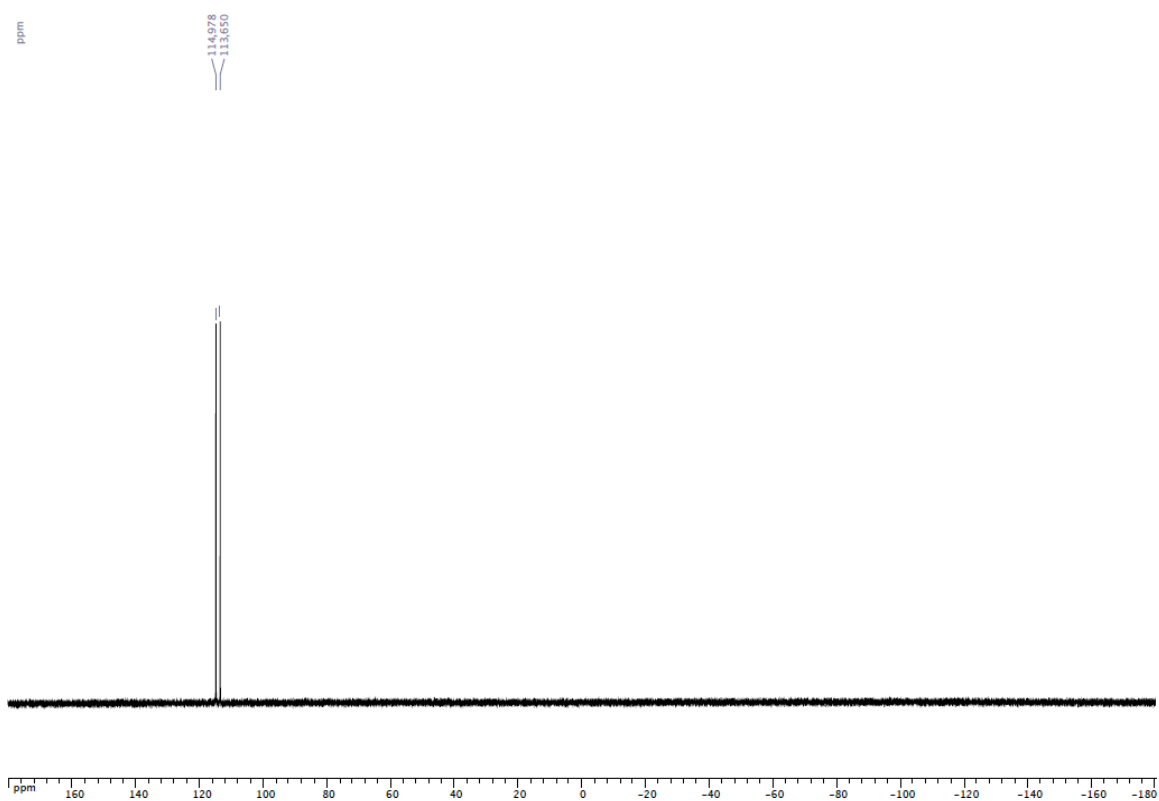
$^{31}P\{^1H\}$ NMR spectrum of $[Rh(cod)(\mathbf{1})]BF_4$ complex (C_6D_6)

[Rh$_2$(cod)$_2$(2)$_2$](BF$_4$)$_2$ complex
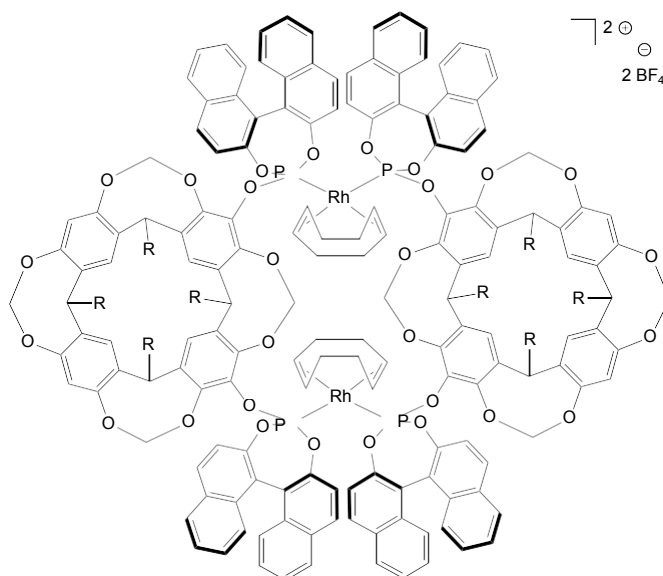
A solution of [Rh(cod)$_2$]BF$_4$ (0.003 g, 0.007 mmol) in CH$_2$Cl$_2$ (50 mL) and a solution of diphosphite **2** (10 mg, 0.007 mmol) in CH$_2$Cl$_2$ (50 mL) were dropwise and simultaneously added to a 500 mL Schlenk flask containing 200 mL of CH$_2$Cl$_2$. The reaction mixture was stirred at room temperature for 16 h. The solvent was evaporated to dryness, and the residue was washed with cold hexane (-78°C), then dried under vacuum. The resulting solid contained several unidentified compounds, which could not be separated. The ^{31}P NMR and the mass spectra of the crude reaction mixture revealed the formation of the dimer. ^{31}P{^{1}H} NMR (CDCl$_3$, 202 MHz): δ = 124.7 (ABX spin system, $^1J_{PRh}$ = 255 Hz, $^2J_{PP}$ = 50 Hz, O*P*(OAr)$_2$), 121.3 (ABX spin system, $^1J_{PRh}$ = 267 Hz, $^2J_{PP}$ = 50 Hz, O*P*(OAr)$_2$) ppm. MS (ESI TOF): *m/z* 1687.55 (*z* = 2) [M - 2 BF$_4$]$^{2+}$ expected isotopic profile.
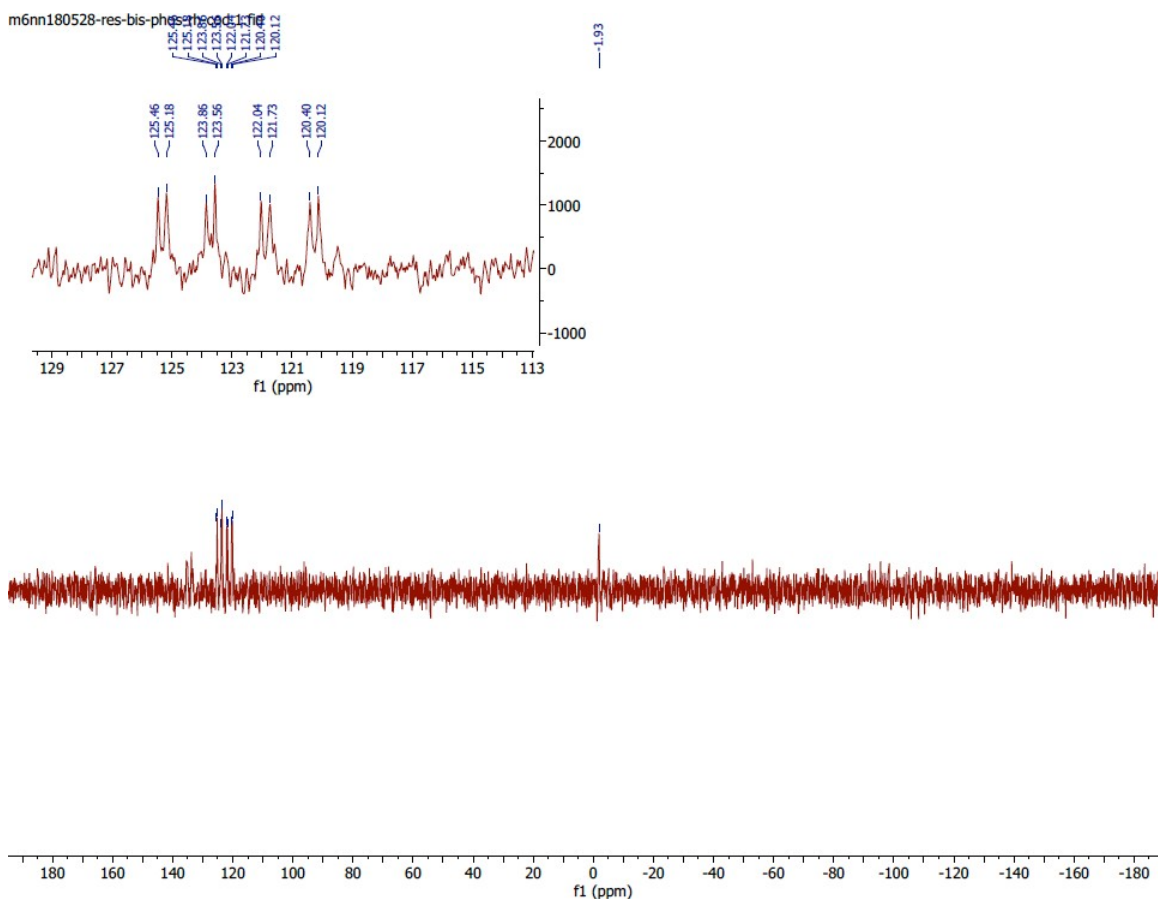
$^{31}P\{^{1}H\}$ NMR spectrum of the crude reaction mixture (CDCl$_3$)

General procedure for the hydroformylation experiments.

The hydroformylation experiments were carried out in a glass-lined, 100 mL stainless steel autoclave containing a magnetic stirring bar. In a typical run, the autoclave was charged with [Rh(acac)(CO)$_2$] and ligand then closed and flushed twice with vacuum/N$_2$. Toluene (15 mL) was added under N$_2$ and the autoclave was flushed twice with syngas (CO/H$_2$ 1:1 v/v), before being pressurised with 15 bar of a CO/H$_2$ mixture and heated under stirring at 80°C. After 16 h, the autoclave was cooled to r.t. and depressurised. Then vinyl arene and decane were added to the reaction mixture. The autoclave was pressurised and heated as mentioned in the Tables. At the end of each run, the autoclave was cooled to room temperature before being depressurised. A sample was taken and analysed by GC using a WCOT fused silica column (25m x 0.25mm). This also allowed to determine the conversion and the b:l ratio. In order to determine the enantiomeric excess, a sample of the reaction mixture (toluene) was treated with LiAlH$_4$ for 0.5 h. After filtration, the solution containing enantiomeric alcohols was analysed by GC with a Chirasil-DEX CB column (25 m x 0.25 mm).

Rhodium-catalysed hydroformylation of styrene using diphosphite **1** – search of the optimal catalytic conditions.[a]

Rh/**1**	T (°C)	P(CO)/P(H₂) (bar)	(v/v)	Time (h)	Conversion (%)[b]	l (%)[b]	b (%)[b]	ee (%)[c]
						Aldehydes distribution		
1/1	80	20	1:1	1	16	/	/	
				4	37	8	92	
				8	62	15	85	
				24	89	25	75	46
1/10	80	20	1:1	1	11	/	/	
				4	18	7	93	
				8	24	8	92	
				24	29	9	91	74
1/5	80	20	1:1	1	11	/	/	
				4	21	5	95	
				8	33	6	94	
				24	67	6	94	74
1/5	80	20	1:2	1	12	/	/	
				4	16	5	95	
				8	32	7	93	
				24	72	11	89	73
1/5	80	20	2:1	1	11	/	/	
				4	16	6	94	
				8	26	6	94	
				24	48	8	92	74
1/5	50	20	1:1	1	10	/	/	
				4	16	4	96	
				8	24	4	96	
				24	45	3	97	88

[a] Conditions: [Rh(acac)(CO)₂] (2 μmol), **1**, styrene (10 mmol), toluene/*n*-decane (15 mL/0.5 mL), 24 h, incubation over night at 80°C under P(CO/H₂) = 15 bar; [b] determined by GC using decane as internal standard; [c] determined by chiral-phase GC after reduction with LiAlH₄.

Annexe of chapter III

Experimental Section

General Remarks

All manipulations were carried out in Schlenk-type flasks under dry argon. Solvents were dried by conventional methods and were distilled immediately before use. $CDCl_3$ was passed down a 5 cm-thick alumina column, and stored under nitrogen over molecular sieves (4 Å). Routine ^{1}H and [13]C{[1]H} spectra were recorded with Bruker FT instruments (AC 300, 400 and 500). ^{1}H NMR spectra were referenced to residual protiated solvent peaks ($\delta = 2.05$ for acetone-d_6, 7.16 ppm for C_6D_6 and 7.26 ppm for $CDCl_3$). ^{13}C NMR chemical shifts are reported relative to deuterated solvent peaks ($\delta = 29.84$ and 206.26 for acetone-d_6, 128.00 ppm for C_6D_6 and 77.16 ppm for $CDCl_3$). Chemical shifts and coupling constants are reported in ppm and Hz, respectively. Infrared spectrum of **4** was recorded with a Bruker FT-IR Alpha-P spectrometer. Elemental analyses were carried out by the Service de Microanalyse, Institut de Chimie, Université de Strasbourg. The catalytic solutions were analysed with a Varian 3900 gas chromatograph fitted with a WCOT fused silica column (25 m×0.25 mm, 0.25 μm film thickness). 5-bromo-4(24),6(10),12(16),18(22)-tetramethylenedioxy-2,8,14,20-tetrapentylresorcin[4]arene (**3**),[1] tosyl azide,[2] 5-(3-propyl-1-imidazolylium)-4(24),6(10),12(16),18(22)-tetramethylenedioxy-2,8,14,20-tetrapentylresorcin[4]arene bromide (**6**),[3] chloro-(η^5-cyclopentadienyl)-[1,3-bis-(mesityl)-imidazol-2-yliden]nickel(II) (**9**)[4] and 1-(2,6-dimethoxyphenyl)-1H-imidazole[3] were prepared by literature procedures.

References

[1] H. El Moll, D. Sémeril, D. Matt and L. Toupet, *Eur. J. Org. Chem.* **2010**, 1158-1168.

[2] H. Hwang, J. Kim, J. Jeong and S. Chang, *J. Am. Chem. Soc.* **2014**, *136*, 10770-10776.

[3] N. Şahin, D. Sémeril, E. Brenner, D. Matt, İ. Özdemir, C. Kaya and L. Toupet, *ChemCatChem* **2013**, *5*, 1115-1125.

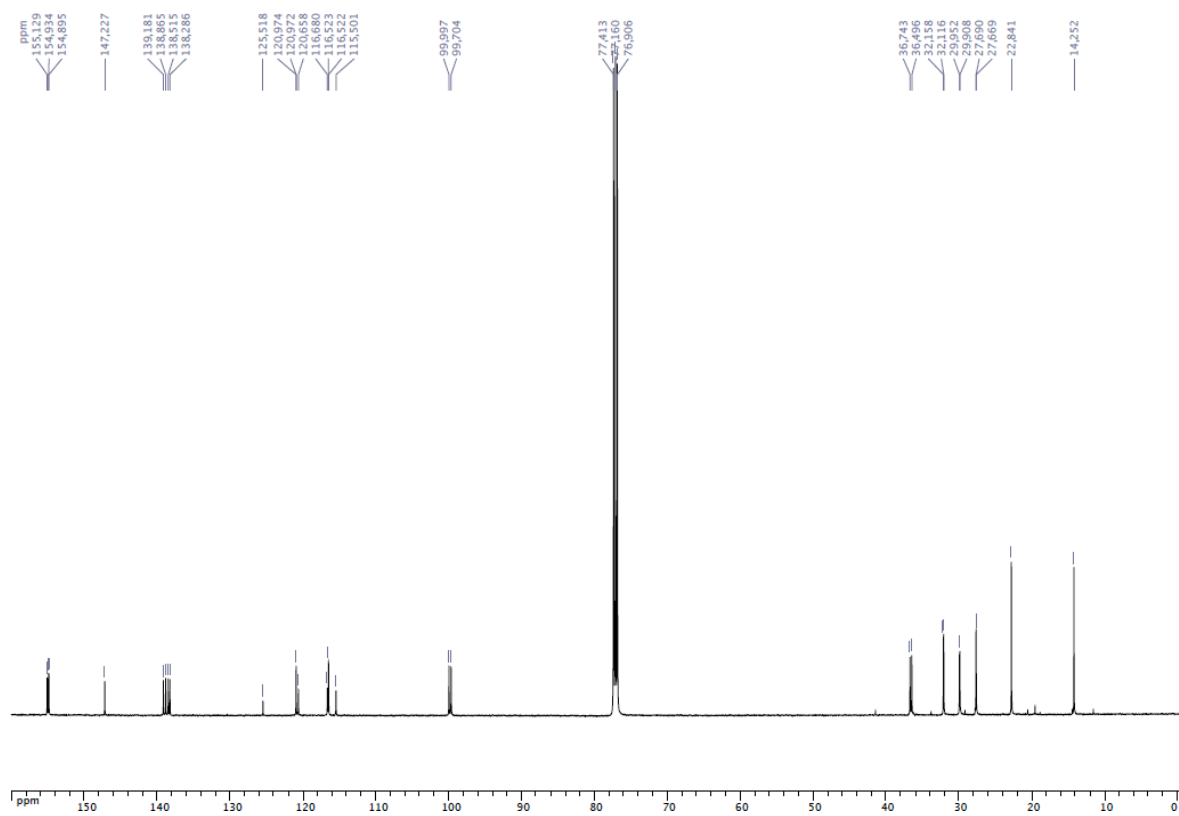[4] C. D. Abernethy, A. H. Cowley and R. A. Jones, *J. Organomet. Chem.* **2000**, *596*, 3-5.

5-Azido-4(24),6(10),12(16),18(22)-tetramethylenedioxy-2,8,14,20-tetrapentylresorcin[4]arene (4)
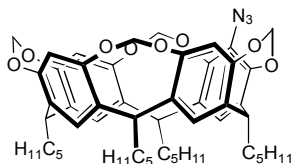
n-Butyllithium (1.6 M in hexane; 2.51 mL, 4.02 mmol) was slowly added to a solution of bromo-cavitand **3** (3.000 g, 3.35 mmol) in THF (150 mL) at -78 °C. After 1 h, the resulting anion was quenched with tosyl azide (0.792 g, 4.02 mmol), and the mixture was stirred at room temperature for 24 h. The reaction mixture was washed three times with brine (3 x 100 mL). The solvent was evaporated under reduced pressure, and the crude product was purified by column chromatography (Et$_2$O/petroleum ether, 5:95; Rf = 0.32) to give **4** (2.150 g, 75 %). ^{1}H NMR (500 MHz, CDCl$_3$): δ = 7.10 (s, 3H, arom. CH, resorcinarene), 6.88 (s, 1H, arom. CH, resorcinarene), 6.52 (s, 2H, arom. CH, resorcinarene), 6.48 (s, 1H, arom. CH, resorcinarene), 5.78 and 4.43 (AB spin system, 4H, OCH$_2$O, ^2J = 7.0 Hz), 5.75 and 4.42 (AB spin system, 4H, OCH$_2$O, ^2J = 7.0 Hz), 4.73 (t, 4H, C*H*CH$_2$, ^3J = 8.0 Hz), 2.24-2.17 (m, 8H, CHC*H$_2$*), 1.44-1.31 (m, 24H C*H$_2$CH$_2$CH$_2$*CH$_3$), 0.92 (t, 6H, CH$_2$C*H$_3$*, ^3J = 7.2 Hz), 0.91 (t, 6H, CH$_2$C*H$_3$*, ^3J = 7.2 Hz) ppm. ^{13}C{^{1}H} NMR (126 MHz, CDCl$_3$): δ = 155.13-115.50 (arom. C), 100.00 (s, OCH$_2$O), 99.70 (s, OCH$_2$O), 36.74 (s, *C*HCH$_2$), 36.50 (s, *C*HCH$_2$), 32.16 (s, *C*H$_2$CH$_2$CH$_3$), 32.12 (s, *C*H$_2$CH$_2$CH$_3$), 29.95 (s, CH*C*H$_2$), 29.91 (s, CH*C*H$_2$), 27.69 (s, CHCH$_2$*C*H$_2$), 27.67 (s, CHCH$_2$*C*H$_2$), 22.84 (s, *C*H$_2$CH$_3$), 14.25 (s, CH$_2$*C*H$_3$) ppm. IR: ν = 2103 and 1286 (N$_3$) cm^{-1}. Elemental analysis calcd (%) for C$_{52}$H$_{63}$N$_3$O$_8$ (858.07): C 72.79, H 7.40, N 4.90; found C 72.58, H 7.51 N 4.64.
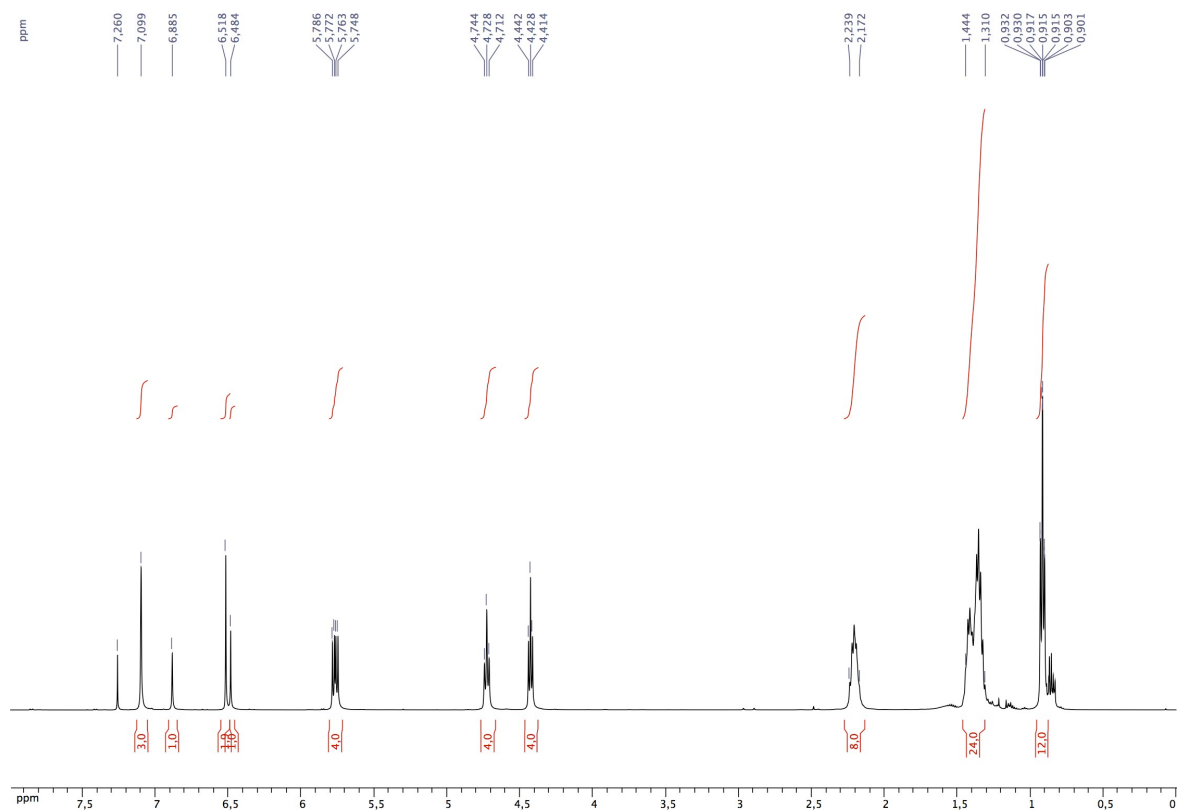
^{1}H NMR spectrum of **4** (CDCl$_3$)

^{13}C{^{1}H} NMR spectrum of **4** (CDCl$_3$)

5-Amino-4(24),6(10),12(16),18(22)-tetramethylenedioxy-2,8,14,20-tetrapentylresorcin[4]arene (5)
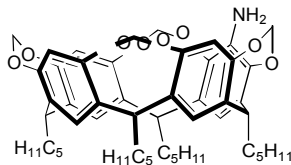

The hydrogenation experiment was carried out in a glass-lined stainless steel autoclave (100 mL) containing a magnetic stirrer bar. Palladium-on-carbon (10 % Pd w/w, 0.200 g) was added. The autoclave was closed, flushed twice with hydrogen, then a solution of azide-cavitand **4** (3.000 g, 3.50 mmol) in CH_2Cl_2 (15 mL) was added, the autoclave pressurised to 5 bar and the reaction mixture was stirred at room temperature for 24 h. The autoclave was depressurised, the solution was passed through a plug of Celite and the solvent was evaporated under reduced pressure to give **5** (2.897 g, 100 %). ^{1}H NMR (400 MHz, CDCl$_3$): δ = 7.10 (s, 3H, arom. CH, resorcinarene), 6.51 (s, 1H, arom. CH, resorcinarene), 6.50 (s, 1H, arom. CH, resorcinarene), 6.47 (s, 2H, arom. CH, resorcinarene), 5.79 and 4.38 (AB spin system, 4H, OCH$_2$O, ^2J = 7.0 Hz), 5.74 and 4.47 (AB spin system, 4H, OCH$_2$O, ^2J = 7.2 Hz), 4.72 (t, 2H, C*H*CH$_2$, ^3J = 8.4 Hz), 4.69 (t, 2H, C*H*CH$_2$, ^3J = 8.4 Hz), 3.76 (s, 2H NH$_2$), 2.25-2.17 (m, 8 H, CHC*H$_2$*CH$_2$), 1.45-1.32 (m, 24H *CH$_2$CH$_2$CH$_2$*CH$_3$) 0.92 (t, 12H, CH$_2$*CH$_3$*, ^3J = 7.0 Hz) ppm. ^{13}C{^{1}H} NMR (126 MHz, CDCl$_3$): δ = 154.98-107.39 (arom. C), 99.64 (s, OCH$_2$O), 99.26 (s, OCH$_2$O), 36.75 (s, *C*HCH$_2$), 36.49 (s, *C*HCH$_2$), 32.22 (s, *C*H$_2$CH$_2$CH$_3$), 32.18 (s, *C*H$_2$CH$_2$CH$_3$), 29.99 (s, CH*C*H$_2$), 29.87 (s, CH*C*H$_2$), 27.78 (s, CHCH$_2$*C*H$_2$), 27.72 (s, CHCH$_2$*C*H$_2$), 22.85 (s, *C*H$_2$CH$_3$), 14.27 (s, CH$_2$*C*H$_3$) ppm. MS (ESI-TOF): m/z = 832.48 [M + H]$^+$, expected isotopic profile. Elemental analysis calcd (%) for C$_{52}$H$_{65}$NO$_8$ (832.08): C 75.06, H 7.87, N 1.68; found C 75.22, H 7.80, N 1.79.
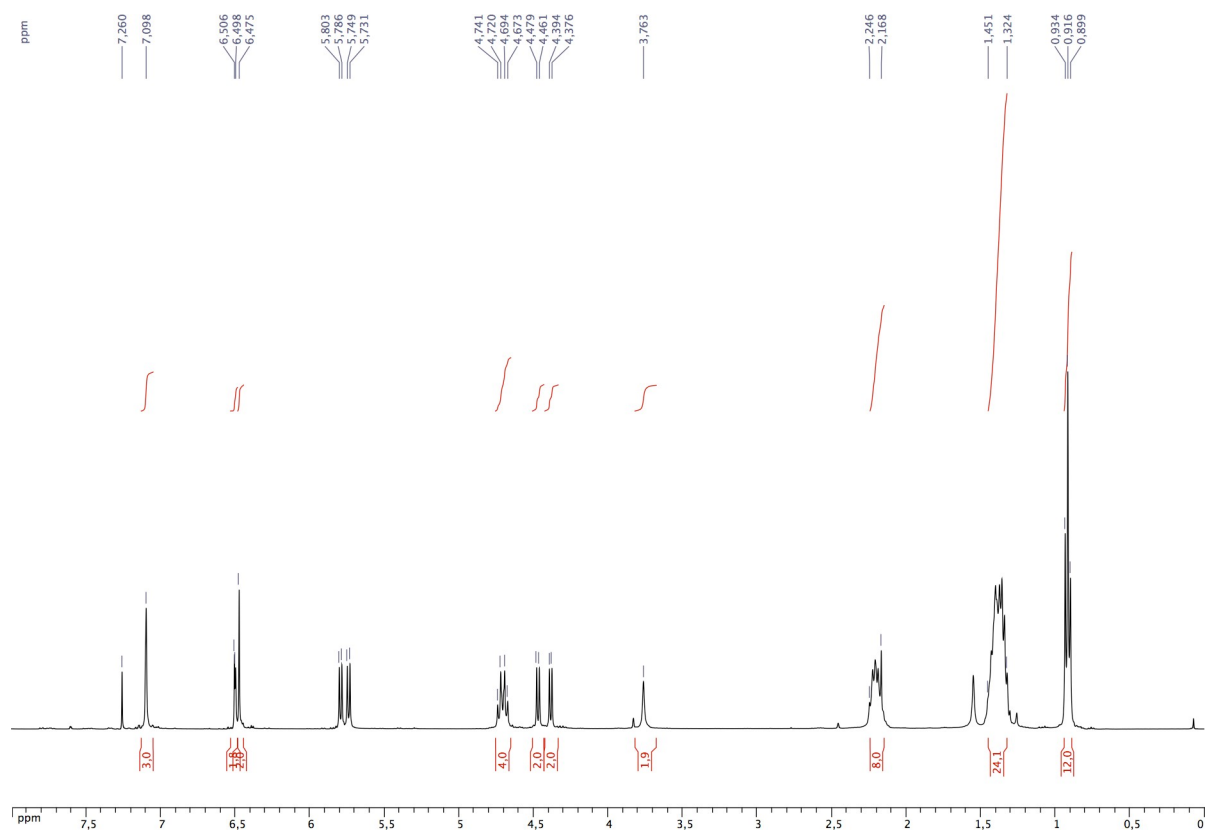
^{1}H NMR spectrum of **5** (CDCl$_3$)
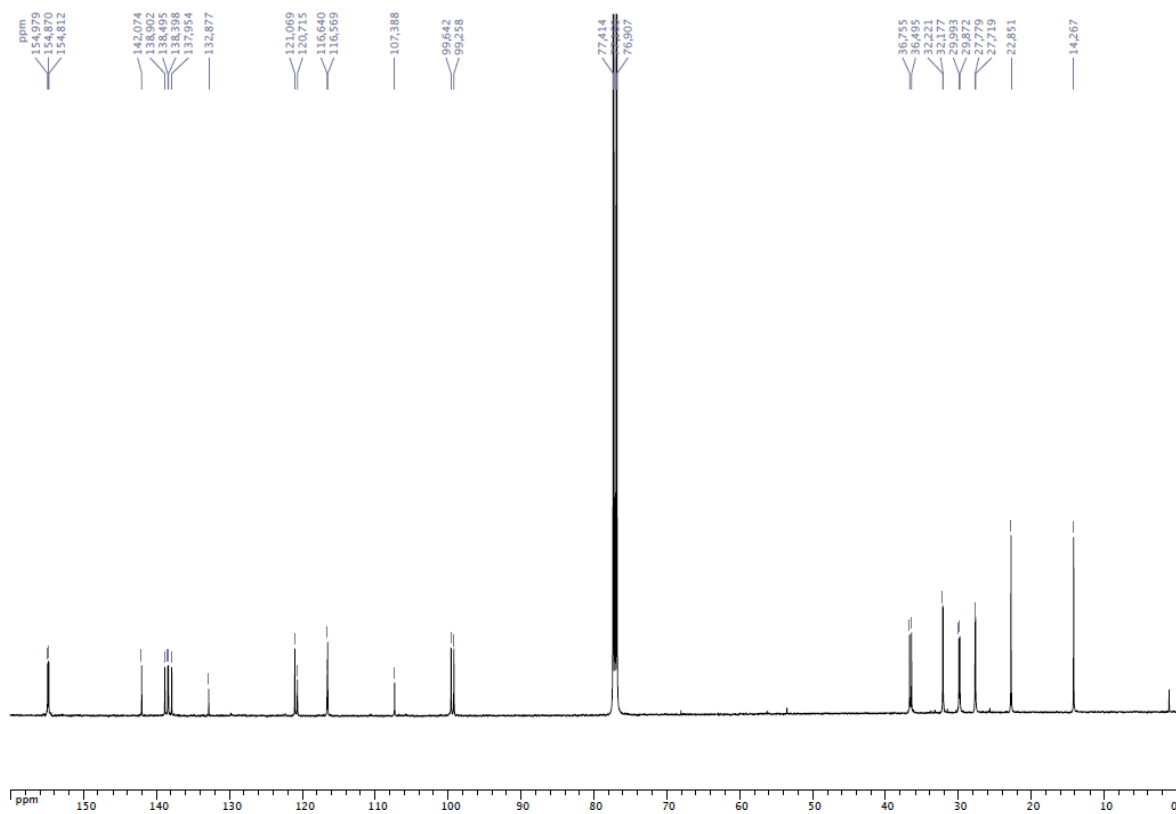
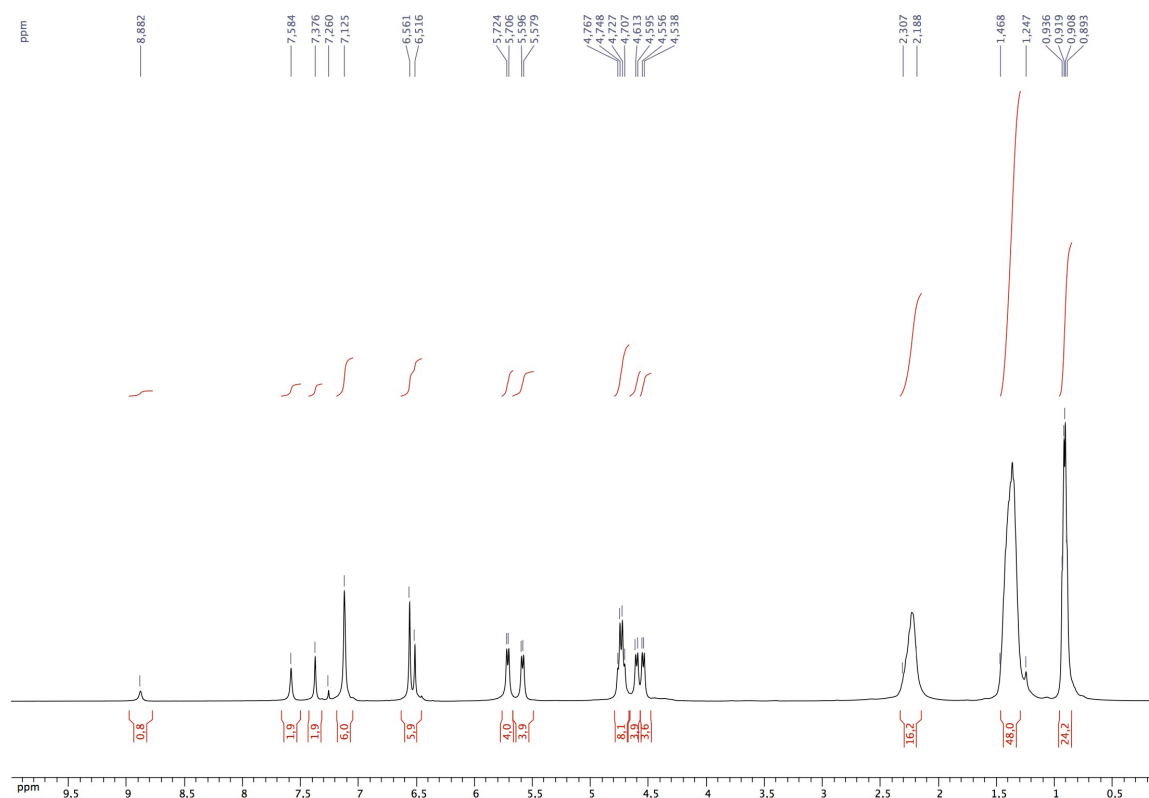^{13}C{^{1}H} NMR spectrum of **5** (CDCl$_3$)
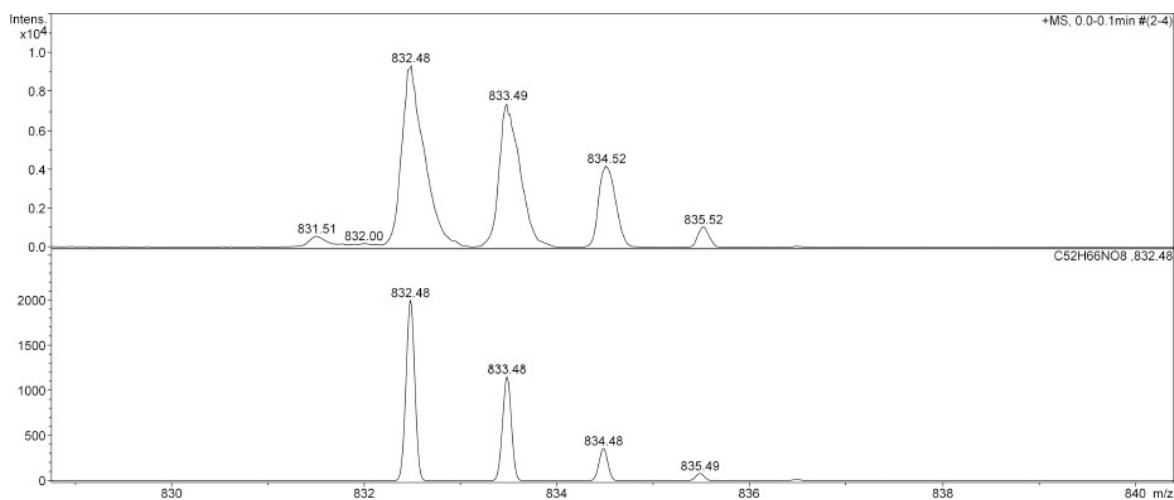
ESI-TOF spectrum of **5** (measured top and calculated for $C_{52}H_{66}NO_8$ bottom)

2-*N*-5-*N*-Bis-[4(24),6(10),12(16),18(22)-tetramethylenedioxy-2,8,14,20-tetrapentyl-resorcin[4]arene-5-yl]imidazolinium chloride (7)
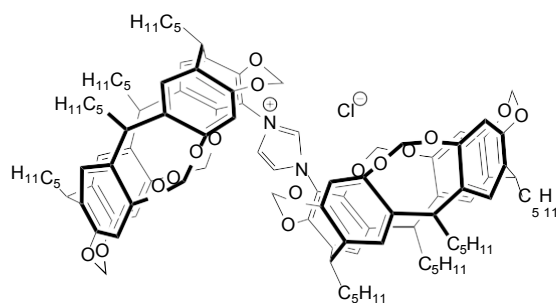

Amino-cavitand **5** (5.000 g, 6.01 mmol) was dissolved in 100 mL of EtOAc with acetic acid (0.5 mL) and the Schlenk tube was wrapped in aluminium foil. Glyoxal (40 % weight in water, 0.42 mL, 3.00 mmol) was then slowly added and the reaction mixture was stirred at 70 °C for 24 h. The yellow mixture was cooled to room temperature before addition of paraformaldehyde (0.090 g, 3.00 mmol) and TMSCl (0.38 mL, 3.00 mmol). The resulting solution was stirred at 70 °C for a further 18 h. After cooling to room temperature, the solvent was evaporated under reduced pressure and the crude product was purified by column chromatography (MeOH/CH$_2$Cl$_2$, 5:95; *R*f = 0.42) to give **7** (0.677 g, 13 %). ^{1}H NMR (400 MHz, CDCl$_3$): δ = 8.88 (s, 1H, NCHN), 7.59 (s, 2H, arom. CH, NCH=CHN), 7.38 (s, 2H, arom. CH, resorcinarene), 7.12 (s, 6H, arom. CH, resorcinarene), 6.56 (s, 4H, arom. CH, resorcinarene), 6.52 (s, 2H, arom. CH, resorcinarene), 5.72

110

and 4.55 (AB spin system, 8H, OCH$_2$O, ^2J = 7.2 Hz), 5.58 and 4.60 (AB spin system, 8H, OCH$_2$O, ^2J = 7.2 Hz), 4.75 (t, 4 H, CHCH$_2$, ^3J = 7.6 Hz), 4.73 (t, 4 H, CHCH$_2$, ^3J = 8.0 Hz), 2.31-2.19 (m, 16 H, CHCH$_2$CH$_2$), 1.47-1.25 (m, 48 H CH$_2$CH$_2$CH$_2$CH$_3$), 0.92 (t, 12H, CH$_2$CH$_3$, ^3J = 6.8 Hz), 0.91 (t, 12H, CH$_2$CH$_3$, ^3J = 6.8 Hz) ppm. ^{13}C{^{1}H} NMR (101 MHz, CDCl$_3$): δ = 155.75-117.28 (arom. C), 138.29 (s, arom. CH, NCHN), 125.44 (s, arom. CH, NCH=CHN), 100.52 (s, OCH$_2$O), 99.69 (s, OCH$_2$O), 36.80 (s, CHCH$_2$), 36.49 (s, CHCH$_2$), 32.13 (s, CH$_2$CH$_2$CH$_3$), 32.00 (s, CH$_2$CH$_2$CH$_3$), 30.08 (s, CHCH$_2$), 29.84 (s, CHCH$_2$), 27.66 (s, CHCH$_2$CH$_2$), 27.63 (s, CHCH$_2$CH$_2$), 22.78 (s, CH$_2$CH$_3$), 14.18 (s, CH$_2$CH$_3$) ppm. MS (ESI-TOF): m/z = 1697.93 [M - Cl]$^+$, expected isotopic profile. Elemental analysis calcd (%) for C$_{107}$H$_{129}$N$_2$O$_{16}$Cl (1734.63): C 74.09, H 7.50, N 1.61; found C 74.53, H 7.42, N 1.84.

^{1}H NMR spectrum of **7** (CDCl$_3$)
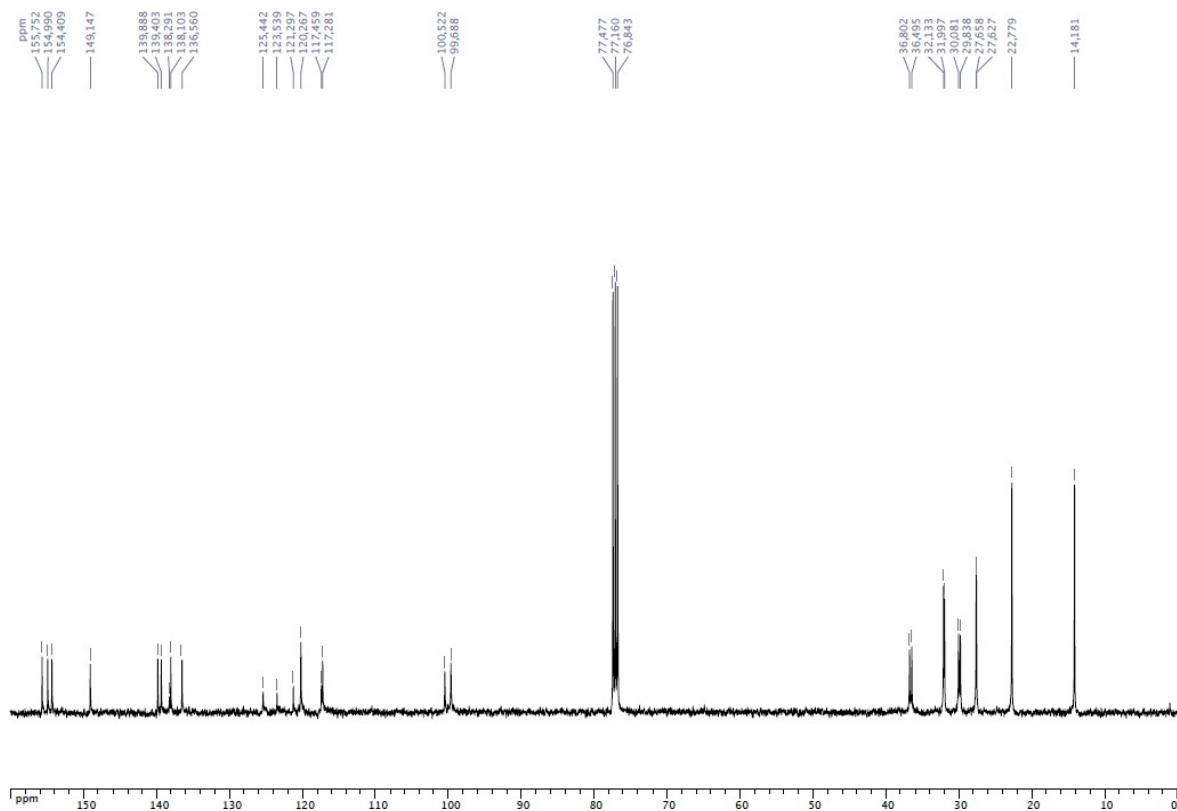
$^{13}C\{^1H\}$ NMR spectrum of **7** (CDCl$_3$)
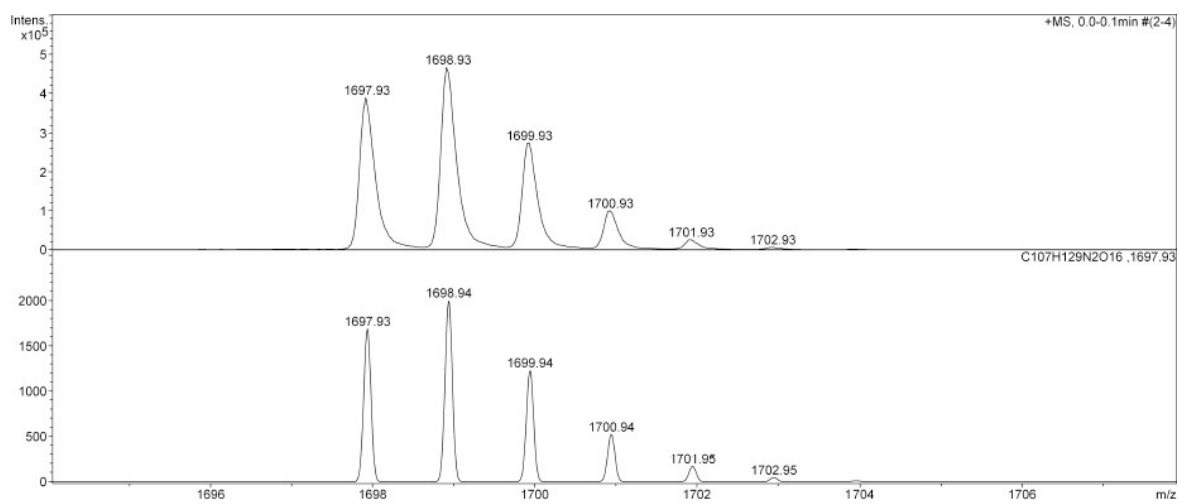
ESI-TOF spectrum of **7** (measured top and calculated for C$_{107}$H$_{129}$N$_2$O$_{16}$ bottom)

[2-*N*-(2,6-dimethoxyphenyl)-5-*N*-propyl]imidazolinium bromide
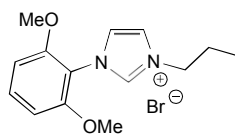
1-Aryl imidazole (0.306 g, 1.50 mmol) and propyl bromide (0.27 mL, 3.00 mmol) were heated at reflux for 2 days. After cooling to room temperature, the solution was evaporated to dryness. The residue was washed with petroleum ether and dried under vacuum to afford the imidazolium salt (0.455 g, 93 %). ^{1}H NMR (400 MHz, CDCl$_3$): δ = 10.28 (s, 1H, NCHN), 7.52 (br, 1H, NC*H*=CHN), 7.42 (t, 1H, arom. CH, *p*-H of C$_6$H$_3$(OMe)$_2$), ^3J = 8.6 Hz), 7.23 (br, 1H, NCH=C*H*N), 6.69 (d, 2H, arom. CH, *m*-H of C$_6$H$_3$(OMe)$_2$), ^3J = 8.6 Hz), 4.70 (t, 2H, NCH$_2$, ^3J = 7.2 Hz), 3.86 (s, 6H, OCH$_3$), 2.02 (quint, C*H$_2$*CH$_3$, ^3J = 7.2 Hz), 1.04 (t, 3H, CH$_2$C*H$_3$*, ^3J = 7.2 Hz) ppm. ^{13}C NMR (101 MHz, CDCl$_3$): δ = 154.58-104.74 (arom. C), 139.46 (s, NCHN), 124.23 (s, NC*H*=CHN), 120.84 (s, NCH=C*H*N), 56.72 (s, OCH$_3$), 51.69 (s, NCH$_2$), 24.03 (s, C*H$_2$*CH$_3$), 10.65 (s, CH$_2$C*H$_3$*) ppm. MS (ESI-TOF): *m/z*: 247.14 [M - Br]$^+$ expected isotopic profile. Elemental analysis calcd (%) for C$_{14}$H$_{19}$N$_2$O$_8$Br (M_r = 327.22): C 51.39, H 5.85, N 8.56; found: C 51.45, H 5.98, N 8.47.
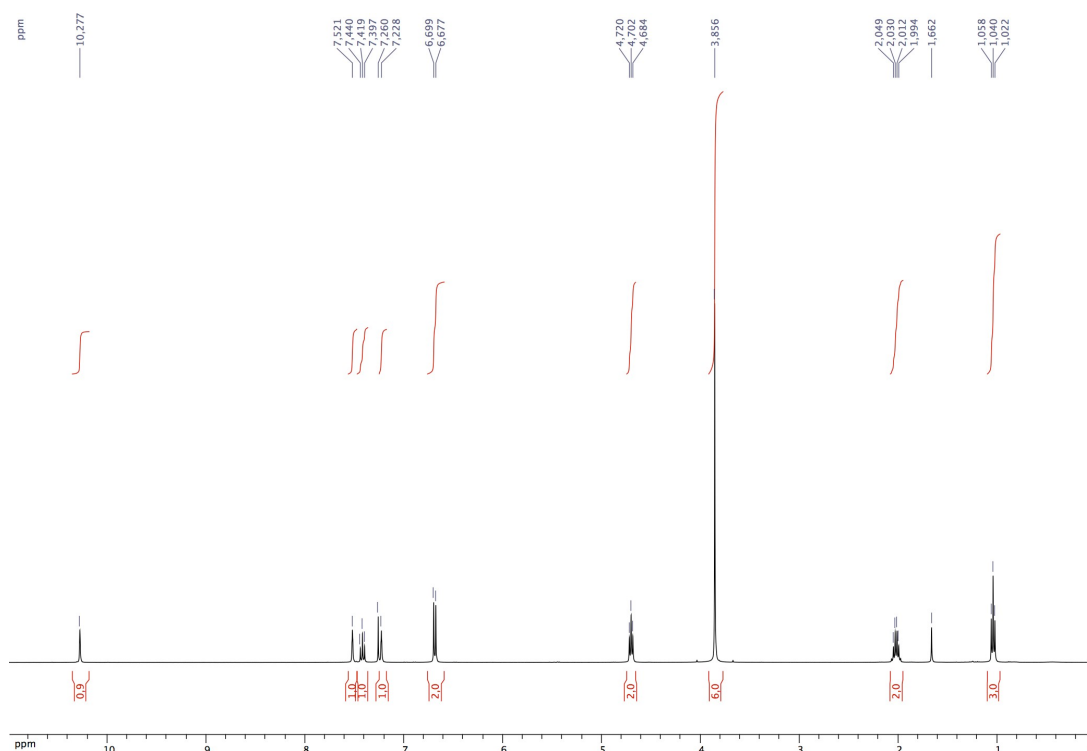
^{1}H NMR spectrum of the imidazolium salt (CDCl$_3$)
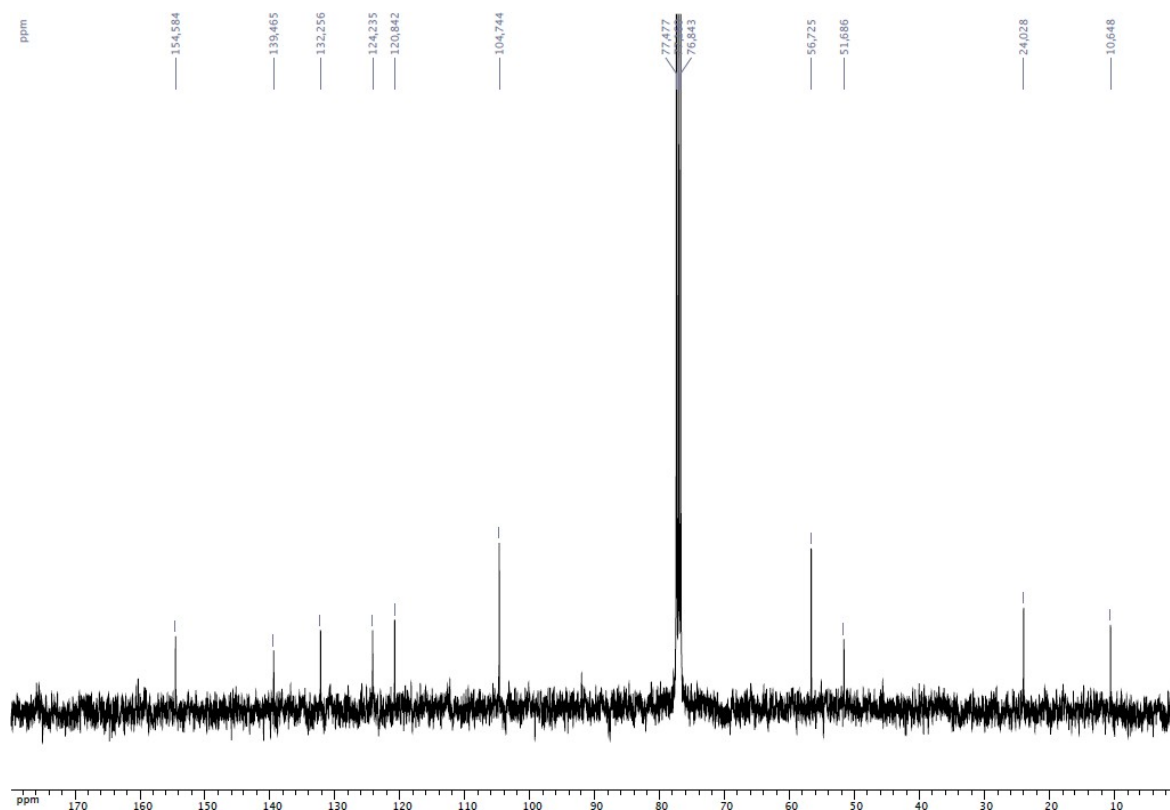
$^{13}C\{^{1}H\}$ NMR spectrum of the imidazolium salt (CDCl$_3$)
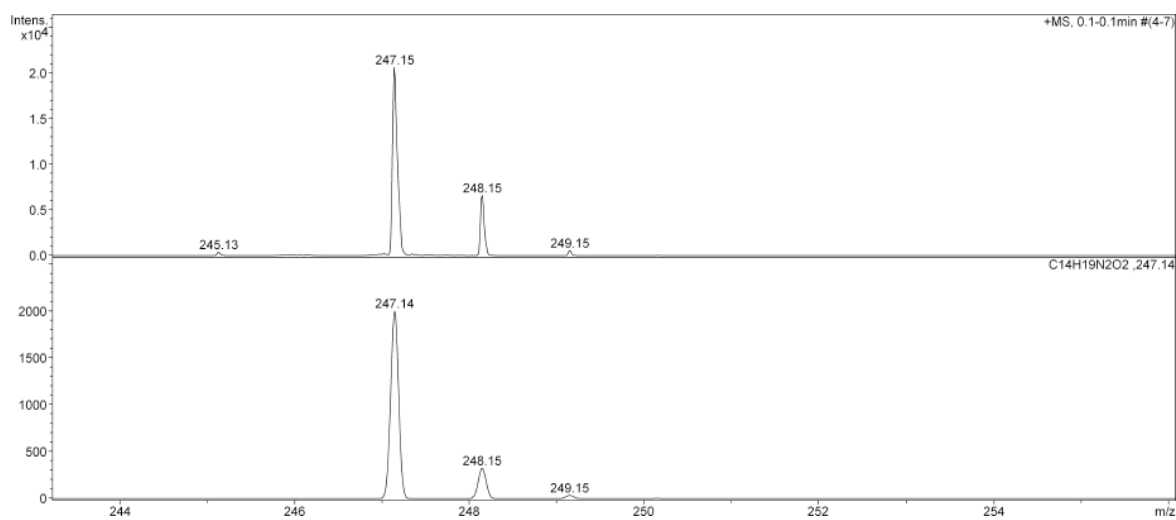
ESI-TOF spectrum of the imidazolium salt

(measured top and calculated for C$_{14}$H$_{19}$N$_2$O$_2$ bottom)

General procedure for the preparation of the nickel complexes 1, 2 and 8: A stoichiometric (1:1) mixture of [NiCp$_2$] and the appropriate imidazolium salt in THF was heated under reflux for 12 h. After cooling to room temperature, the solution was evaporated to dryness. The residue was purified by column chromatography to give the purple nickel complexes.

Bromo-(η^5-cyclopentadienyl)-[1-*N*-{4(24),6(10),12(16),18(22)-tetramethylenedioxy-2,8,14,20-tetrapentylresorcin[4]arene-5-yl}-3-*N*-propyl-imidazol-2-yliden]nickel(II) (1)
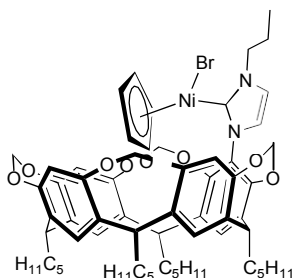
*R*f = 0.41 EtOAc/petroleum ether, 20:80. Yield 0.120 g (20 %). ^{1}H NMR (300 MHz, C$_6$D$_6$): δ = 7.60 (s, 1H, arom. CH, resorcinarene), 7.46 (s, 2H, arom. CH, resorcinarene), 7.40 (s, 1H, arom. CH, resorcinarene), 6.86-6.50 (br, 2H, arom. CH, resorcinarene), 6.36 (s, 1H, arom. CH, resorcinarene), 6.34 (d, 1H, NC*H*=CHN, ^3J = 2.5 Hz), 6.28 (d, 1H, NCH=C*H*N, ^3J = 2.5 Hz), 5.59 and 4.32 (AB spin system, only 2H are clearly visible, OCH$_2$O, ^2J = 7.2 Hz), 5.35 and 4.27 (AB spin system, weakly observed, OCH$_2$O, ^2J = 7.0 Hz), 5.31-5.21 (m, 2H, C*H*CH$_2$), 5.13-5.01 (m, 2H, C*H*CH$_2$), 4.97-4.90 (m, weakly observed, NCH$_2$), 3.68 (s, 5H, C$_5$H$_5$), 2.45-2.21 (m, 8H, CHC*H$_2$*), 1.83-1.69 (m, 2H, NCH$_2$C*H$_2$*), 1.47-1.19 (m, 24H, C*H$_2$*C*H$_2$*C*H$_2$*CH$_3$), 0.84 (t, 6H, CH$_2$C*H$_3$*, ^3J = 6.9 Hz), 0.81 (t, 6H, CH$_2$C*H$_3$*, ^3J = 7.2 Hz), 0.79 (t, 3H, N(CH$_2$)$_2$C*H$_3$*, ^3J = 7.2 Hz) ppm. ^{13}C NMR (75 MHz, C$_6$D$_6$): δ = 163.91-117.18 (arom. C), 125.14 (s, NC*H*=CHN), 122.80 (s, NCH=C*H*N), 99.96 (s, OCH$_2$O), 91.55 (s, C$_5$H$_5$), 54.75 (s, NCH$_2$), 37.25 (s, *C*HCH$_2$), 36.89 (s, *C*HCH$_2$), 32.30 (s, *C*H$_2$CH$_2$CH$_3$), 30.55 (s, CH*C*H$_2$), 28.09 (s, CHCH$_2$*C*H$_2$), 27.94 (s, CHCH$_2$*C*H$_2$), 24.43 (s, NCH$_2$*C*H$_2$), 23.12 (s, *C*H$_2$CH$_3$), 23.05 (s, *C*H$_2$CH$_3$), 14.30 (s, CH$_2$*C*H$_3$), 11.25 (s, N(CH$_2$)$_2$*C*H$_3$) ppm. MS (ESI-TOF): *m/z*: 1126.41 [M]$^+$ expected isotopic profile. Elemental analysis calcd (%) for C$_{63}$H$_{77}$N$_2$O$_8$NiBr (*M*$_r$ = 1128.89): C 67.03, H 6.87, N 2.48; found: C 66.89, H 6.82, N 2.41.
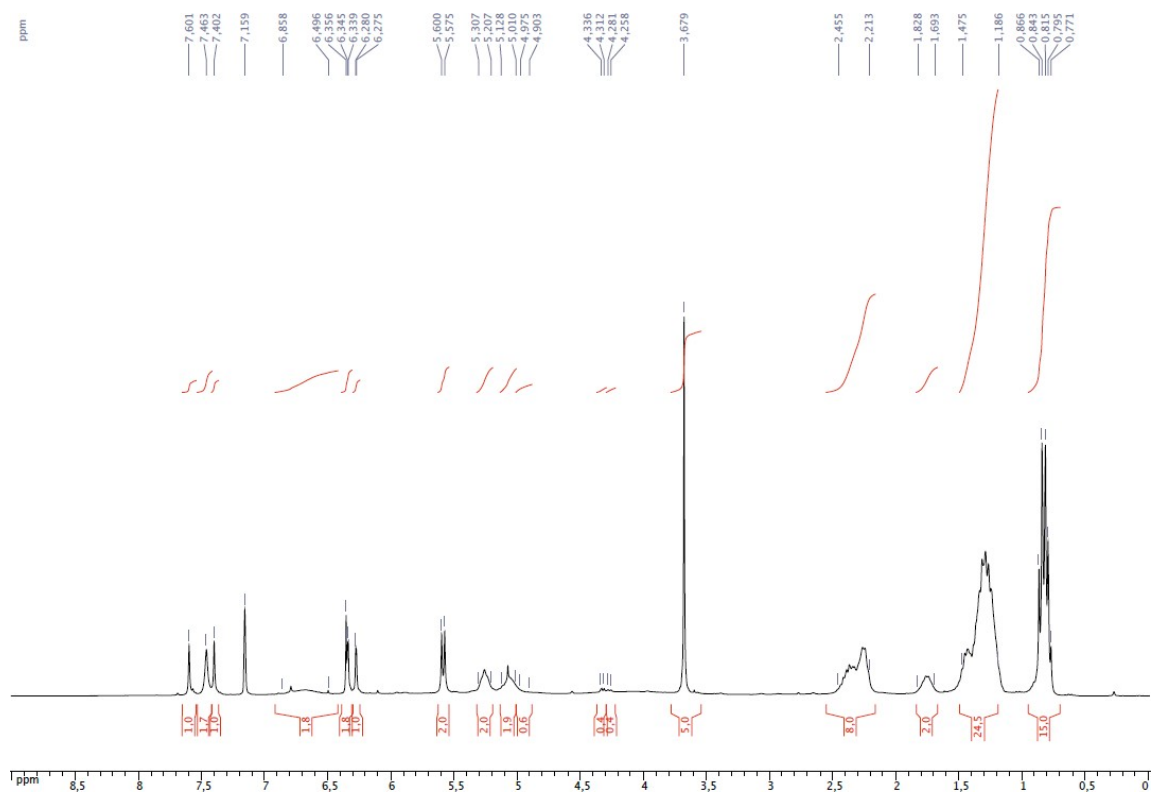
^{1}H NMR spectrum of **1** (C$_6$D$_6$)
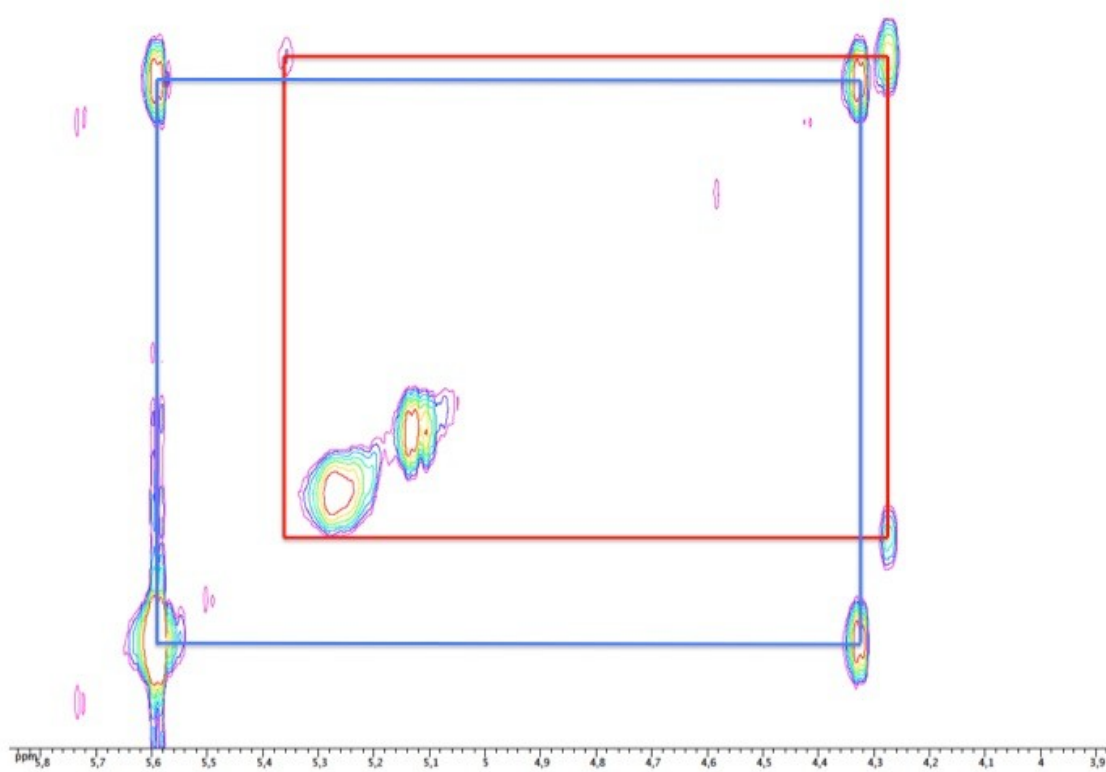
Part of the ^{1}H/^{1}H COSY (ArCH$_2$Ar region) spectrum of **1** (C$_6$D$_6$)
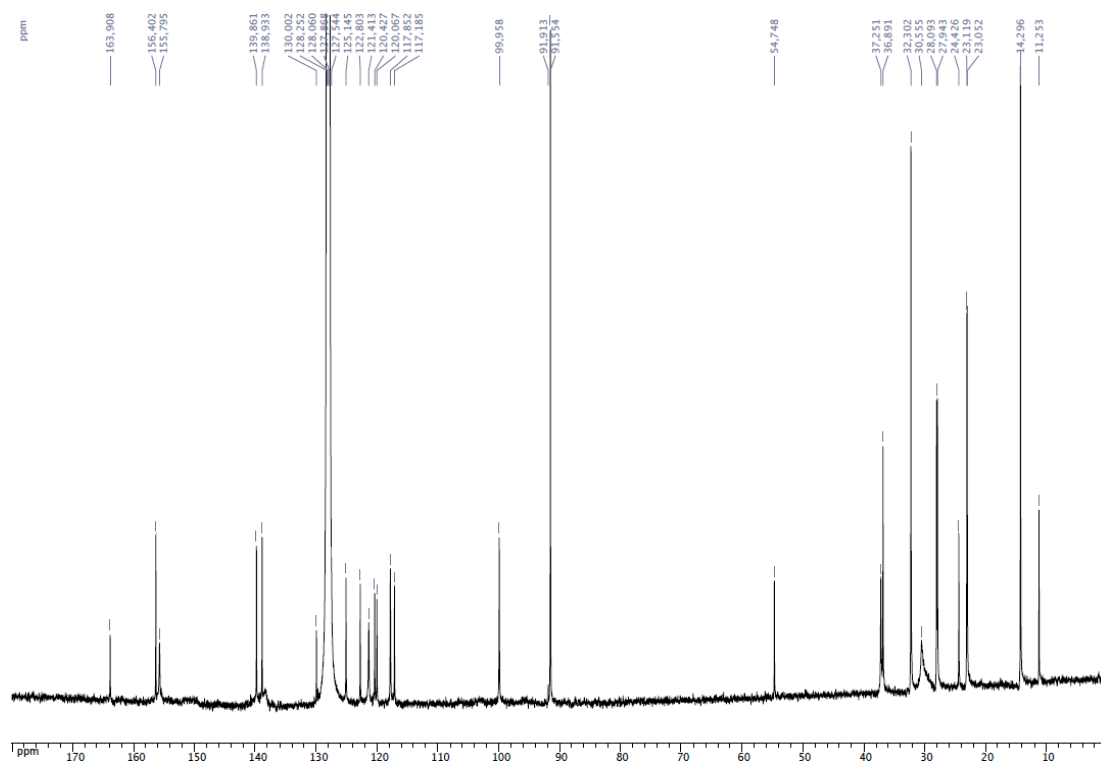
$^{13}C\{^1H\}$ NMR spectrum of **1** (C_6D_6)
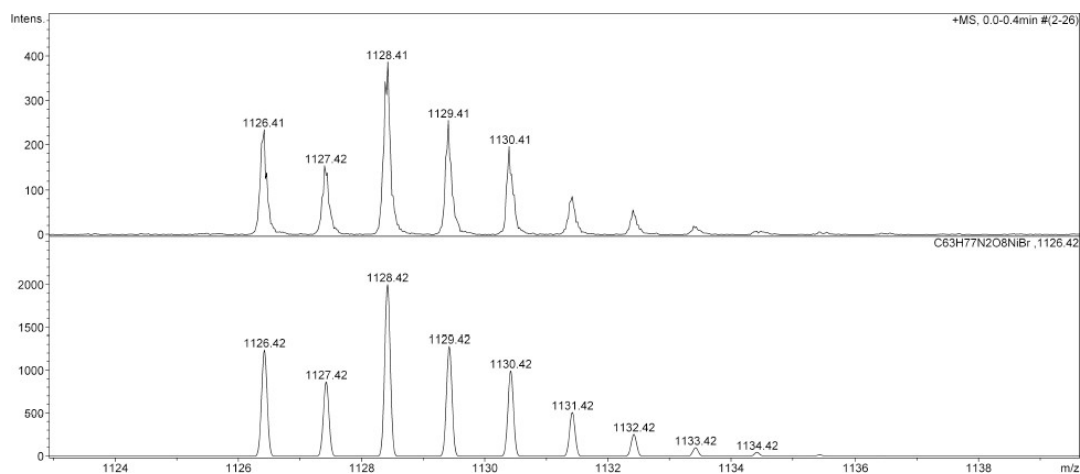
ESI-TOF spectrum of **1** (measured top and calculated for $C_{63}H_{77}N_2O_8NiBr$ bottom)

X-ray crystal structure analysis of nickel complex 1: Single crystals of **1** suitable for X-ray diffraction were obtained by slow diffusion of hexane into a benzene solution of the complex. Crystal data: $C_{126}H_{154}Br_2N_4Ni_2O_{16} \cdot C_6H_6$, $Mr = 2335.88$ g mol^{-1}, triclinic, space group P -1, $a = 14.1582(8)$ Å, $b = 15.919(1)$ Å, $c = 27.059(1)$ Å, $\alpha = 106.797(5)°$, $\beta = 91.670(4)°$, $\gamma = 91.253(5)°$, $V = 5833.1(5)$ Å^3, $Z = 2$, $D = 1.330$ g cm^{-3}, $\mu = 1.075$ mm^{-1}, $F(000) = 2468.0$, $T = 120(2)$ K. The sample was studied on a Oxford Diffraction Xcalibur Sapphire 3 diffractometer (graphite

monochromated Mo-K_α radiation, $\lambda = 0.71073$ Å). The data collection ($2\theta_{max} = 27.0°$, omega scan frames by using 0.7 ° omega rotation and 30 s per frame, range *hkl*: *h* -17,18 *k* -20,20 *l* -33,34) gave 47133 reflections. The structure was solved with SIR- 97,[1] which revealed the non-hydrogen atoms of the molecule. After anisotropic refinement, all of the hydrogen atoms were found with a Fourier difference map. The structure was refined with SHELXL97[2] by the full-matrix least-square techniques (use of *F* square magnitude; *x*, *y*, *z*, ij for C, Br, N, Ni and O atoms; *x*, *y*, *z* in riding mode for H atoms); 1406 variables and 4978 observations with $I > 2.0\ \sigma(I)$; calcd. $w = 1/[\sigma^2(F_o^2) + (0.0P)^2 + 0.0P]$ where $P = (F_o^2 + 2F_c^2)/3$, with the resulting $R = 0.0595$, $R_W = 0.1109$ and $S_W = 0.822$, $\Delta\rho < 0.469$ e Å^{-3}. CCDC entry 876002 contains the supplementary crystallographic data. These data can be obtained free of charge from The Cambridge Crystallographic Data Centre via http://www.ccdc.cam.ac.uk/data_request/cif or by e-mailing data_request@ccdc.cam.ac.uk, or by contacting The Cambridge Crystallographic Data Centre, 12 Union Road, Cambridge CB2 1EZ, UK.

References

[1]   A. Altomare, M. C. Burla, M. Camalli, G. Cascarano, C. Giacovazzo, A. Guagliardi, A. G. G. Moliterni, G. Polidori and R. Spagna, *SIR97,* an integrated package of computer programs for the solution and refinement of crystal structures using single crystal data.

[2]   G. M. Sheldrick, SHELX-97. Program for the refinement of crystal structures. University of Göttingen, Germany. **1997**.

Chloro-(η^5-cyclopentadienyl)-[1-*N*-3-*N*-bis-{4(24),6(10),12(16),18(22)-tetramethylene dioxy-2,8,14,20-tetrapentylresorcin[4]arene-5-yl}-imidazol-2-yliden] nickel(II) (2)
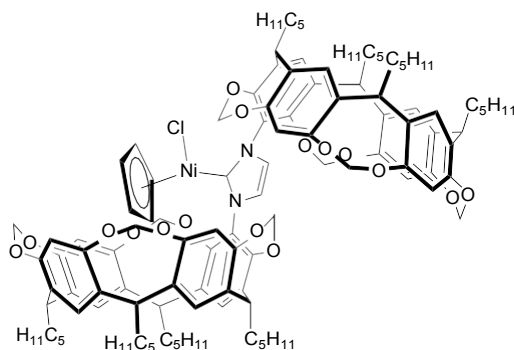

*R*f = 0.34 EtOAc/petroleum ether, 20:80. Yield 0.144 g (35 %).^{1}H NMR (300 MHz, C$_6$D$_6$): δ = 7.69 (s, 1H, arom. CH, resorcinarene), 7.65 (s, 1H, arom. CH, resorcinarene), 7.61 (s, 2H, arom.

CH, resorcinarene), 7.52 (s, 1H, arom. CH, resorcinarene), 7.47 (s, 2H, arom. CH, resorcinarene), 7.41 (s, 1H, arom. CH, resorcinarene), 6.82 (s, 2H, arom. CH, resorcinarene), 6.68 (s, 2H, arom. CH, resorcinarene), 6.49 (s, 1H, NC*H*=CHN), 6.33 (s, 1H, arom. CH, resorcinarene), 6.21 (s, 1H, arom. CH, resorcinarene), 6.13 and 5.71 (AB spin system, 4H, OCH$_2$O, ^2J = 7.5 Hz), 5.60 and 4.33 (AB spin system, 4H, OCH$_2$O, ^2J = 7.5 Hz), 5.53 and 4.07 (AB spin system, 4H, OCH$_2$O, ^2J = 7.0 Hz), 5.37 and 4.33 (AB spin system, 4H, OCH$_2$O, ^2J = 7.0 Hz), 5.31-5.27 (m, 5H, NCH=C*H*N and C*H*CH$_2$), 5.17 (t, 2H, C*H*CH$_2$, ^3J = 8.0 Hz), 5.06 (t, 2H, C*H*CH$_2$, ^3J = 8.0 Hz), 3.71 (s, 5H, C$_5$H$_5$), 2.55-2.46 (m, 2H, CHC*H*$_2$), 2.43-2.30 (m, 10H, CHC*H*$_2$), 2.27-2.23 (m, 4H, CHC*H*$_2$), 1.54-1.48 (m, 4H, C*H*$_2$CH$_2$CH$_2$CH$_3$), 1.46-1.19 (m, 44H, C*H*$_2$CH$_2$CH$_2$CH$_3$), 0.87-0.80 (m, 24H, CH$_2$C*H*$_3$) ppm. ^{13}C NMR (126 MHz, C$_6$D$_6$): δ = 171.57-117.03 (arom. C), 124.17 (s, NC*H*=CHN), 123.66 (s, NCH=C*H*N), 99.93 (s, OCH$_2$O), 99.47 (s, OCH$_2$O), 99.36 (s, OCH$_2$O), 98.95 (s, OCH$_2$O), 92.03 (s, C$_5$H$_5$), 37.47 (s, *C*HCH$_2$), 37.31 (s, *C*HCH$_2$), 37.04 (s, *C*HCH$_2$), 36.88 (s, *C*HCH$_2$), 32.35 (s, *C*H$_2$CH$_2$CH$_3$), 32.32 (s, *C*H$_2$CH$_2$CH$_3$), 32.30 (s, *C*H$_2$CH$_2$CH$_3$), 32.28 (s, *C*H$_2$CH$_2$CH$_3$), 30.56 (s, CH*C*H$_2$), 30.38 (s, CH*C*H$_2$), 29.94 (s, CH*C*H$_2$), 28.10 (s, CHCH$_2$*C*H$_2$), 27.99 (s, CHCH$_2$*C*H$_2$), 27.94 (s, CHCH$_2$*C*H$_2$), 23.14 (s, *C*H$_2$CH$_3$), 23.10 (s, *C*H$_2$CH$_3$), 23.06 (s, *C*H$_2$CH$_3$), 23.04 (s, *C*H$_2$CH$_3$), 14.30 (s, CH$_2$*C*H$_3$) ppm. MS (ESI-TOF): *m/z*: 1819.90 [M - Cl]$^+$ expected isotopic profile. Elemental analysis calcd (%) for C$_{112}$H$_{133}$N$_2$O$_{16}$NiCl (M_r = 1857.41): C 72.42, H 7.22, N 1.91; found: C 72.11, H 7.15, N 1.53.
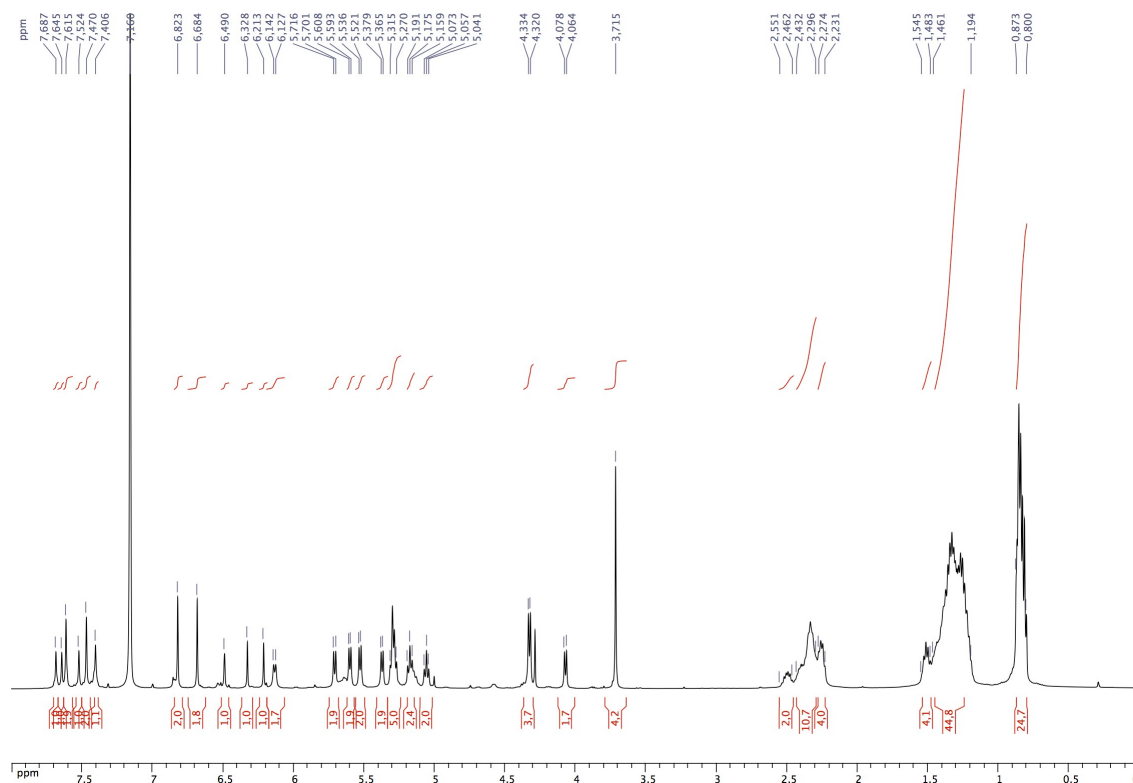
^{1}H NMR spectrum of **2** (C$_6$D$_6$)
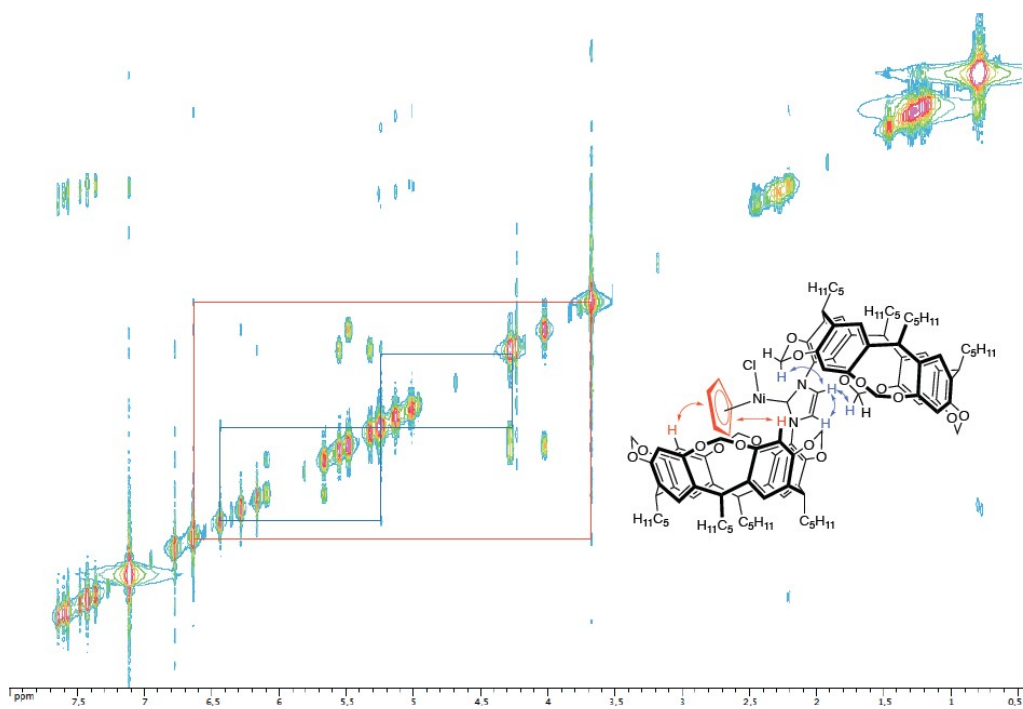
^{1}H/^{1}H ROESY spectrum of **2** (C$_6$D$_6$)
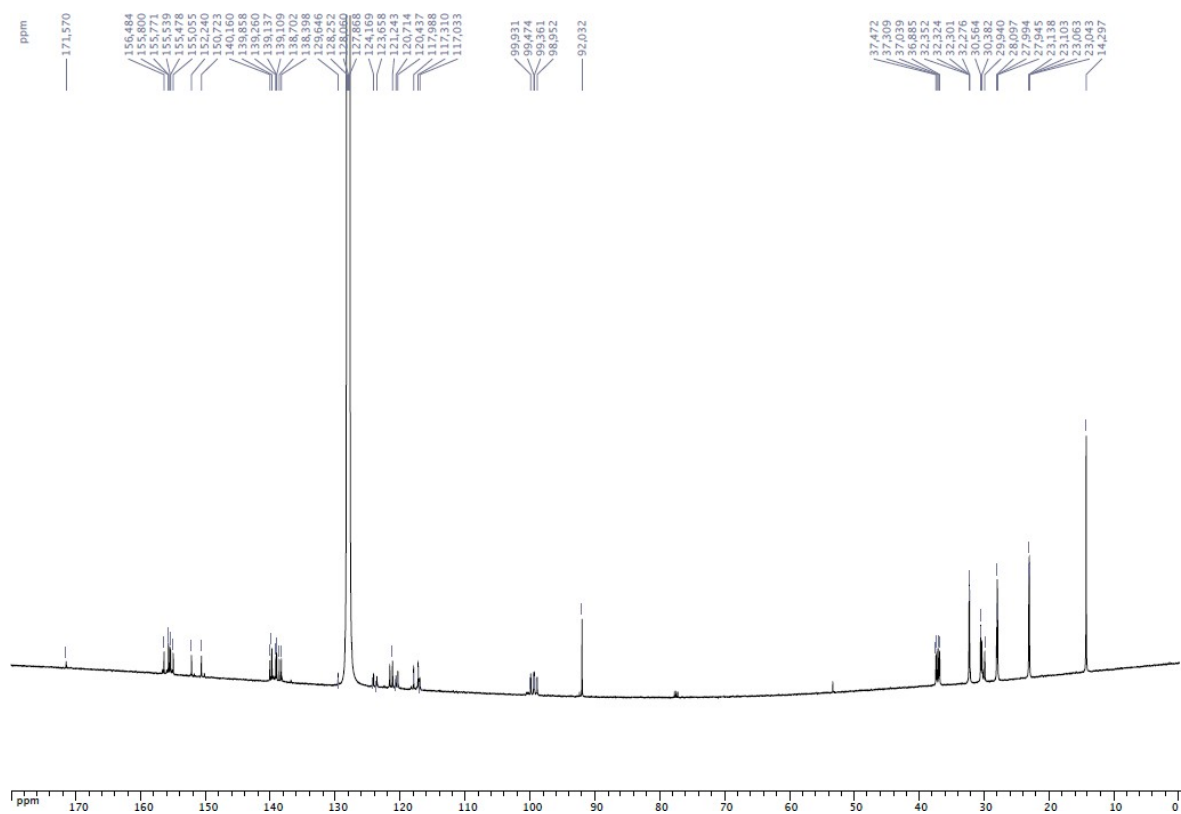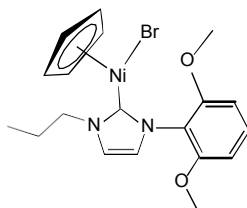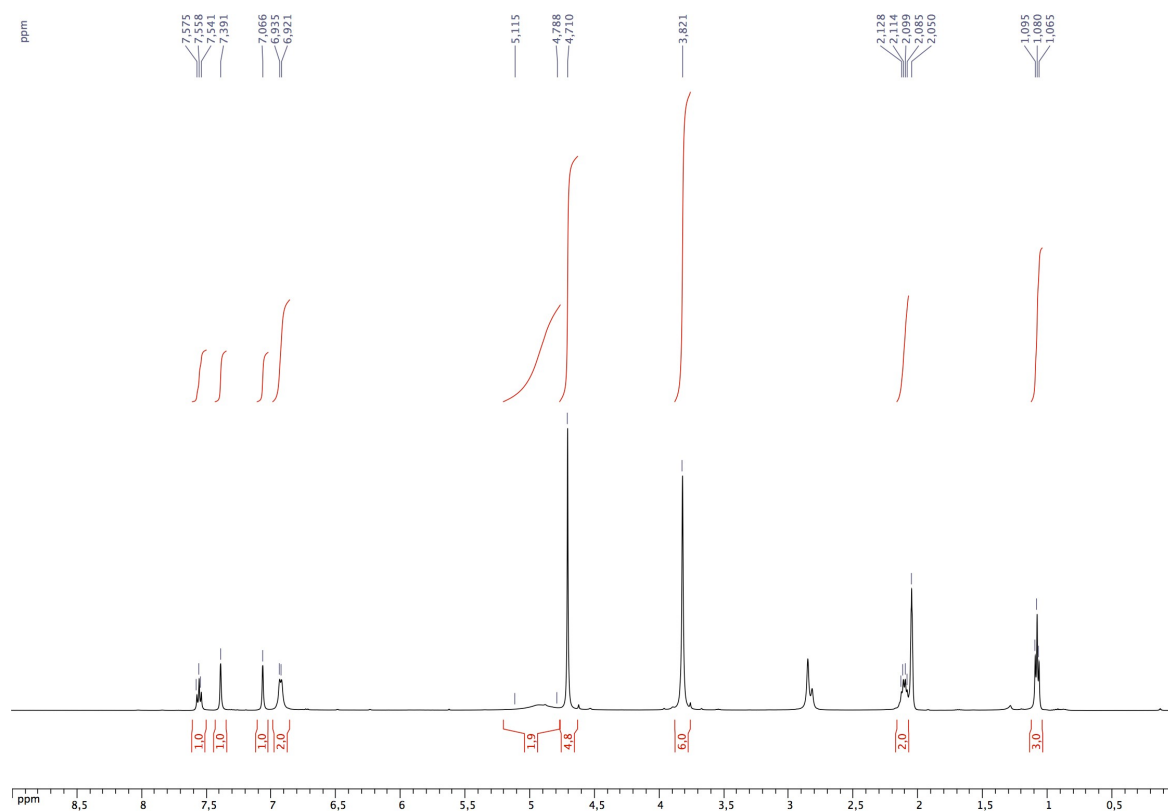

^{13}C{^{1}H} NMR spectrum of **2** (C$_6$D$_6$)
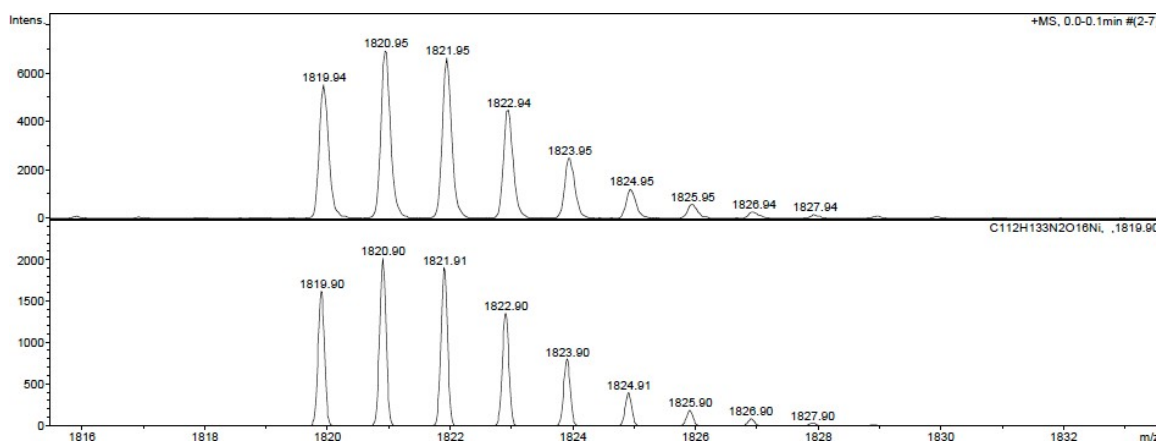
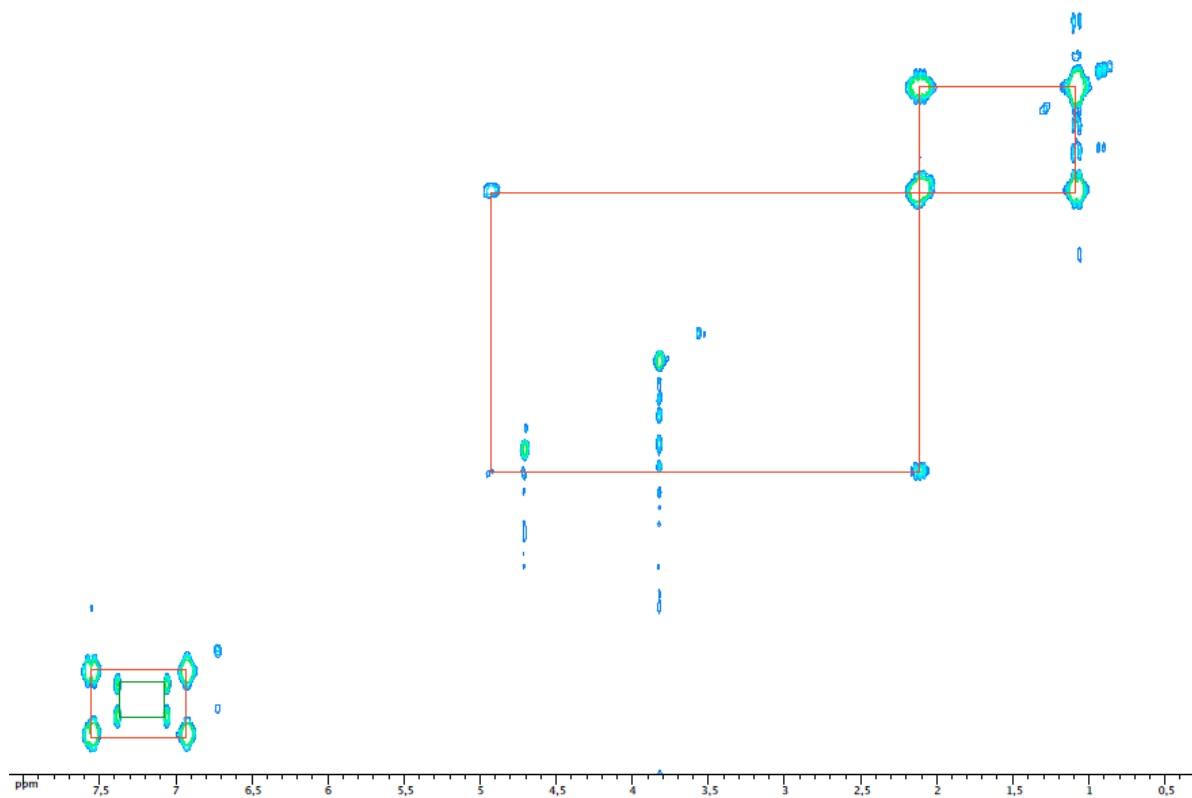ESI-TOF spectrum of **2** (measured top and calculated for $C_{112}H_{133}N_2O_{16}Ni$ bottom)

## Bromo-(η^5-cyclopentadienyl)-[1-*N*-(2,6-dimethoxyphenyl)-3-*N*-pentyl)-imidazol-2-yliden] nickel(II) (**8**)

*R*f = 0.45 EtOAc/petroleum ether, 20:80. Yield 0.259 g (55 %). ^{1}H NMR (500 MHz, acetone-d_6): δ = 7.56 (t, 1H, arom. CH, *p*-H of C_6H_3(OMe)$_2$), ^3J = 7.7 Hz), 7.39 (s, 1H, NC*H*=CHN), 7.07 (s, 1H, NCH=C*H*N), 6.92 (d, 2H, arom. CH, *m*-H of C_6H_3(OMe)$_2$), ^3J = 7.7 Hz), 5.11-4.79 (m, 2H, NCH$_2$), 4.71 (s, 5H, C_5H_5), 3.82 (s, 6H, OCH$_3$), 2.10 (quint, C*H*$_2$CH$_3$, ^3J = 7.5 Hz), 1.08 (t, 3H, CH$_2$C*H*$_3$, ^3J = 7.5 Hz) ppm. ^{13}C NMR (101 MHz, acetone-d_6): δ = 164.45-105.41 (arom. C), 157.96 (s, C-Ni), 126.07 (s, N*C*H=CHN), 122.82 (s, NCH=*C*HN), 91.71 (s, C_5H_5), 56.63 (s, OCH$_3$), 54.30 (s, NCH$_2$), 24.91 (s, *C*H$_2$CH$_3$), 11.55 (s, CH$_2$*C*H$_3$) ppm. MS (ESI-TOF): *m/z*: 369.11 [M - Br]$^+$ expected isotopic profile. Elemental analysis calcd (%) for $C_{19}H_{23}N_2O_2NiBr$ (M_r = 450.00): C 50.71, H 5.15, N 6.22; found: C 50.55, H 5.06, N 6.14.
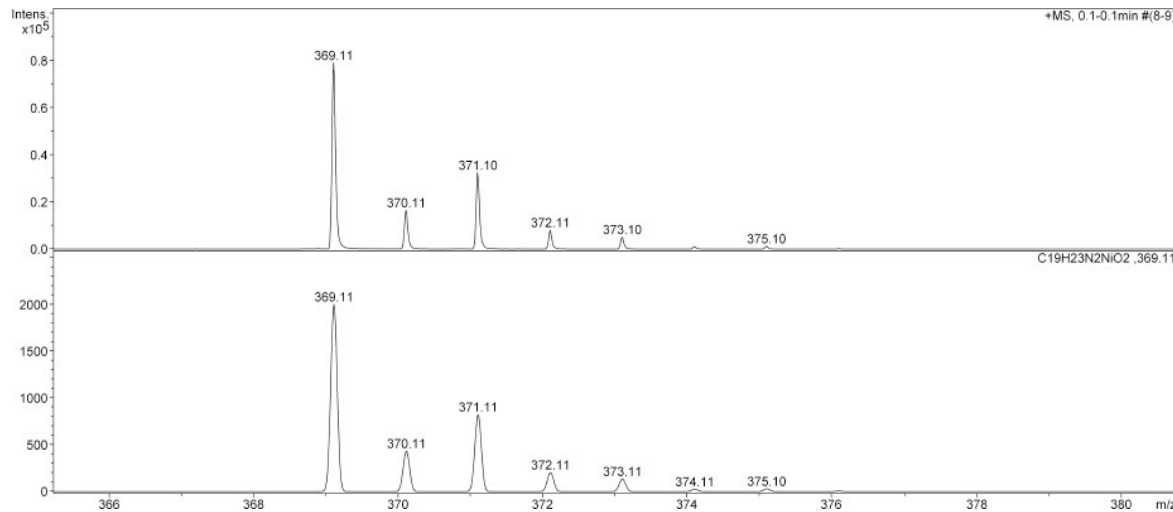
^{1}H NMR spectrum of **8** (acetone-d_6)

^{1}H/^{1}H COSY spectrum of **8** (acetone-d_6)
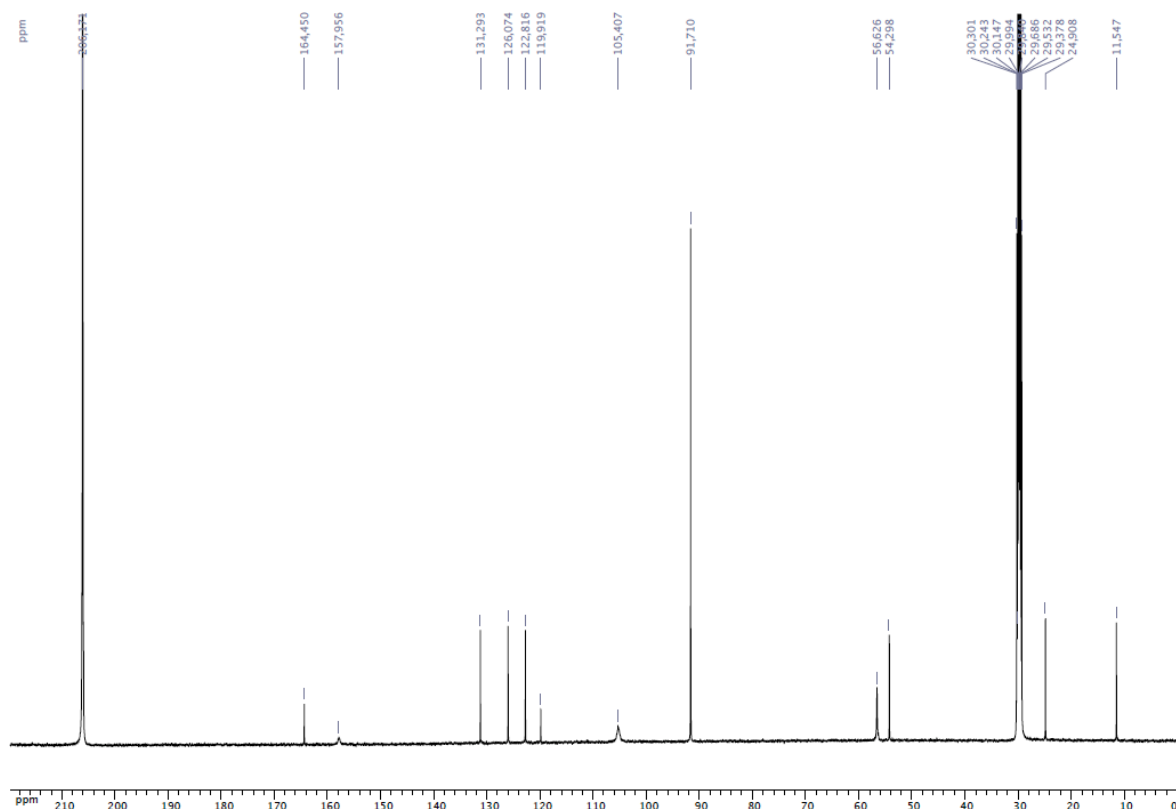
$^{13}C\{^1H\}$ NMR spectrum of **8** (acetone-d_6)

ESI-TOF spectrum of **8** (measured top and calculated for $C_{19}H_{23}N_2O_2Ni$ bottom)

General catalytic testing procedure for ethylene dimerisation: The catalytic runs were carried out in a glass-lined stainless steel autoclave (100 mL) containing a magnetic stirrer bar. The autoclave was closed, flushed twice with ethylene, then a solution of nickel complex (5 µmol) in toluene (5 mL) and a solution of NaBH$_4$ (10 µmol) in toluene (10 mL) were added, the autoclave

pressurised to 20 bar and the reaction mixture stirred at 90 °C for 1 h. At the end of the run, the autoclave was cooled down to 6 °C and depressurised over 8 minutes. The flask containing the reaction mixture was weighed. This procedure was performed as quickly as possible to minimise the potential evolution of the butene products. The solution was analysed by GC. The reaction yield was determined from the final mass of reaction mixture versus the mass of the control reaction solution. To determine the mass of the control reaction solution (reaction mixture with no catalyst or co-catalyst), toluene (15 mL) was added to the autoclave and stirred under 20 bar of ethylene at 90 °C for 1 h. The reactor was cooled down to 6 °C, vented to ambient pressure over 8 minutes and the flask containing the reaction mixture was weighed. Each catalytic test was repeated three times.

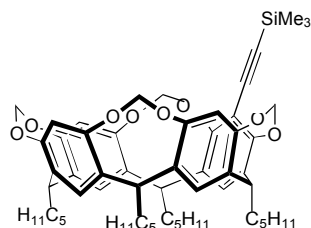# Annexe of chapter IV

Experimental Section

General Remarks

All manipulations involving sensitive derivatives were carried out in Schlenk-type flasks under dry argon. Solvents were dried by conventional methods and were distilled immediately before use. CDCl$_3$ was passed down a 5 cm-thick alumina column and stored under nitrogen over molecular sieves (4 Å). Routine ^{1}H and ^{13}C{^{1}H} spectra were recorded with Bruker FT instruments (AC 400 and 500). ^{1}H NMR spectra were referenced to residual protiated solvents (δ = 7.26 ppm for CDCl$_3$). ^{13}C NMR chemical shifts are reported relative to deuterated solvents (δ = 77.16 ppm for CDCl$_3$). Chemical shifts and coupling constants are reported in ppm and Hz, respectively. Infrared spectra were recorded with a Bruker FTIR Alpha-P spectrometer. Infrared spectrum of **6** was recorded with a Bruker FT-IR Alpha-P spectrometer. Elemental analyses were carried out by the Service de Microanalyse, Institut de Chimie, Université de Strasbourg. The catalytic solutions were analysed with a Varian 3900 gas chromatograph fitted with a WCOT fused silica column (25 m × 0.25 mm, 0.25 µm film thickness). 5-bromo-4(24),6(10),12(16),18(22)-tetramethylenedioxy-2,8,14,20-tetrapentylresorcin[4]arene (**3**)[1] and tosylazide[2] were prepared by literature procedures.
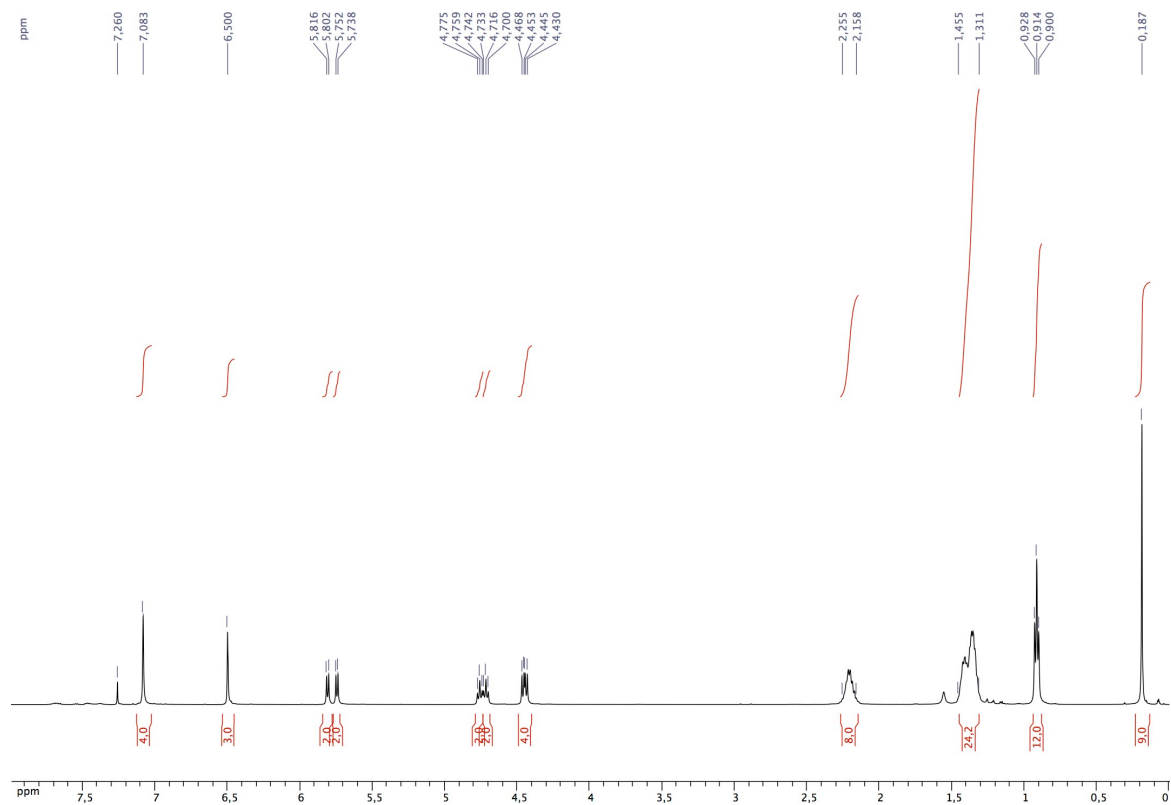
References

[1] H. El Moll, D. Sémeril, D. Matt, L. Toupet, *Eur. J. Org. Chem.* **2010**, 1158-1168.
[2] H. Hwang, J. Kim, J. Jeong, S. Chang, *J. Am. Chem. Soc.* **2014**, *136*, 10770-10776.
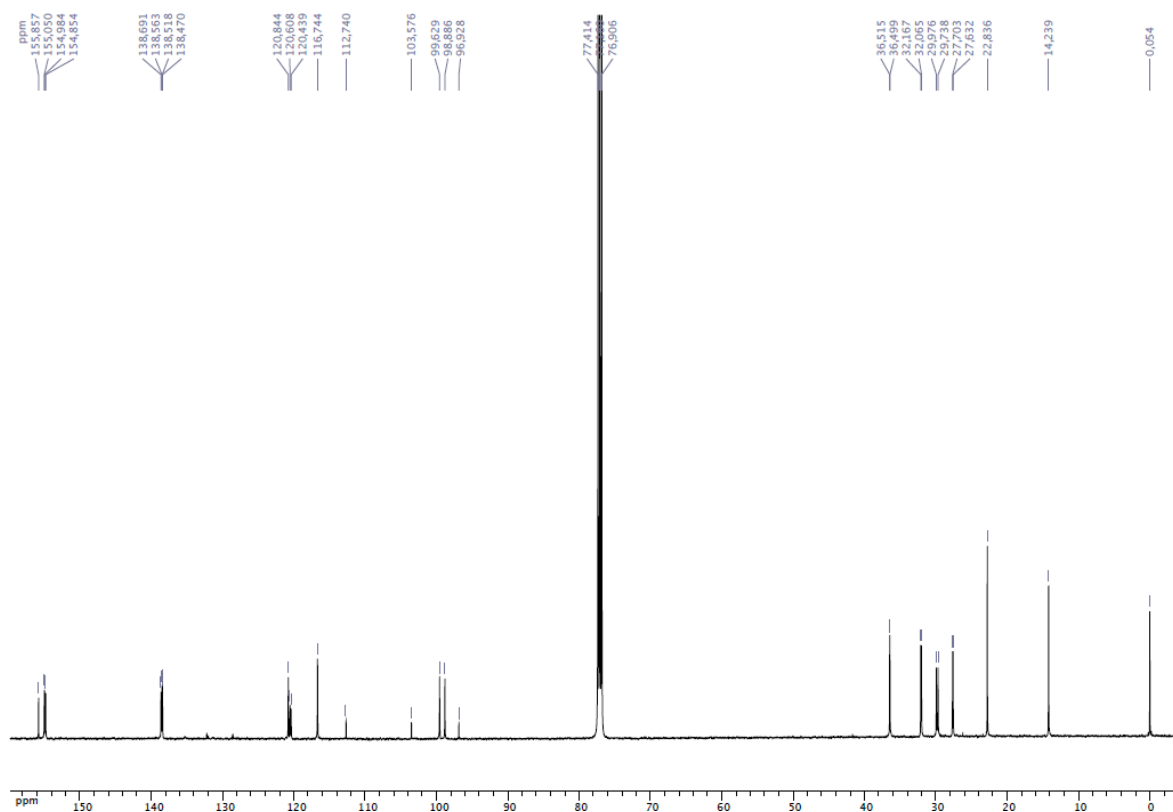
5-(Trimethylsilyl)ethynyl-4(24),6(10),12(16),18(22)-tetramethylenedioxy-2,8,14,20-tetrapentylresorcin[4]arene (4)

To a solution of bromo-cavitand **3** (2.000 g, 2.23 mmol), [Pd(PPh$_3$)$_4$] (0.265 g, 0.23mmol) and CuI (0.023 g, 0.12mmol) in NH^{i}Pr$_2$ (100 mL) was added trimethylsilylacetylene (3.1 mL, 22.30mmol). The mixture turned rapidly from yellow to black. The resulting suspension was stirred for 48 h at 80°C, then cooled to room temperature. The solution was evaporated to dryness and the resulting residue was dissolved in CH$_2$Cl$_2$ (200 mL). The organic solution was washed with brine (3 x 100 mL) and the aqueous layers were extracted with CH$_2$Cl$_2$ (2 x 100 mL). The combined organic layers were dried over MgSO$_4$, filtered and evaporated under reduced pressure, and the crude product was purifiedby column chromatography (Et$_2$O/petroleum ether, 10:90; Rf = 0.36) to give **4** (1.453 g, 71 %). ^{1}H NMR (500 MHz, CDCl$_3$): δ = 7.08 (s, 4H, arom. CH, resorcinarene), 6.50 (s, 3H, arom. CH, resorcinarene), 5.81 and 4.46 (AB spin system, 4H, OCH$_2$O, ^2J = 7.0 Hz), 5.74 and 4.44 (AB spin system, 4H, OCH$_2$O, ^2J = 7.0 Hz), 4.76 (t, 2H, C*H*CH$_2$, ^3J = 8.2 Hz), 4.72 (t, 2H, C*H*CH$_2$, ^3J = 8.2 Hz), 2.25-2.16 (m, 8H, CHC*H$_2$*), 1.45-1.31 (m, 24H *CH$_2$CH$_2$CH$_2$CH$_3$*), 0.91 (t, 12H, CH$_2$C*H$_3$*, ^3J = 7.0 Hz), 0.19 (s, 9H, Si(CH$_3$)$_3$) ppm. ^{13}C{^{1}H} NMR (126 MHz, CDCl$_3$): δ = 155.86-96.93 (arom. Cs), 112.74 (s, C≡*C*SiMe$_3$), 103.58 (s, *C*≡CSiMe$_3$), 99.63 (s, OCH$_2$O), 98.89 (s, OCH$_2$O), 36.51 (s, *C*HCH$_2$), 36.50 (s, *C*HCH$_2$), 32.17 (s, *C*H$_2$CH$_2$CH$_3$), 32.06 (s, *C*H$_2$CH$_2$CH$_3$), 29.98 (s, CHC*H$_2$*), 29.74 (s, CHC*H$_2$*), 27.70 (s, CHCH$_2$*C*H$_2$), 27.63 (s, CHCH$_2$*C*H$_2$), 22.84 (s, *C*H$_2$CH$_3$), 14.24 (s, CH$_2$*C*H$_3$), 0.05 (s, Si(CH$_3$)$_3$) ppm. Elemental analysis calcd (%) for C$_{57}$H$_{72}$O$_8$Si (913.26): C 74.96, H 7.95; found C 75.25, H 8.18.
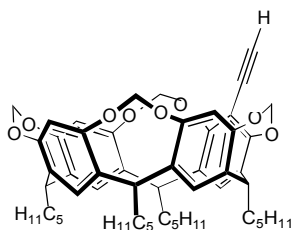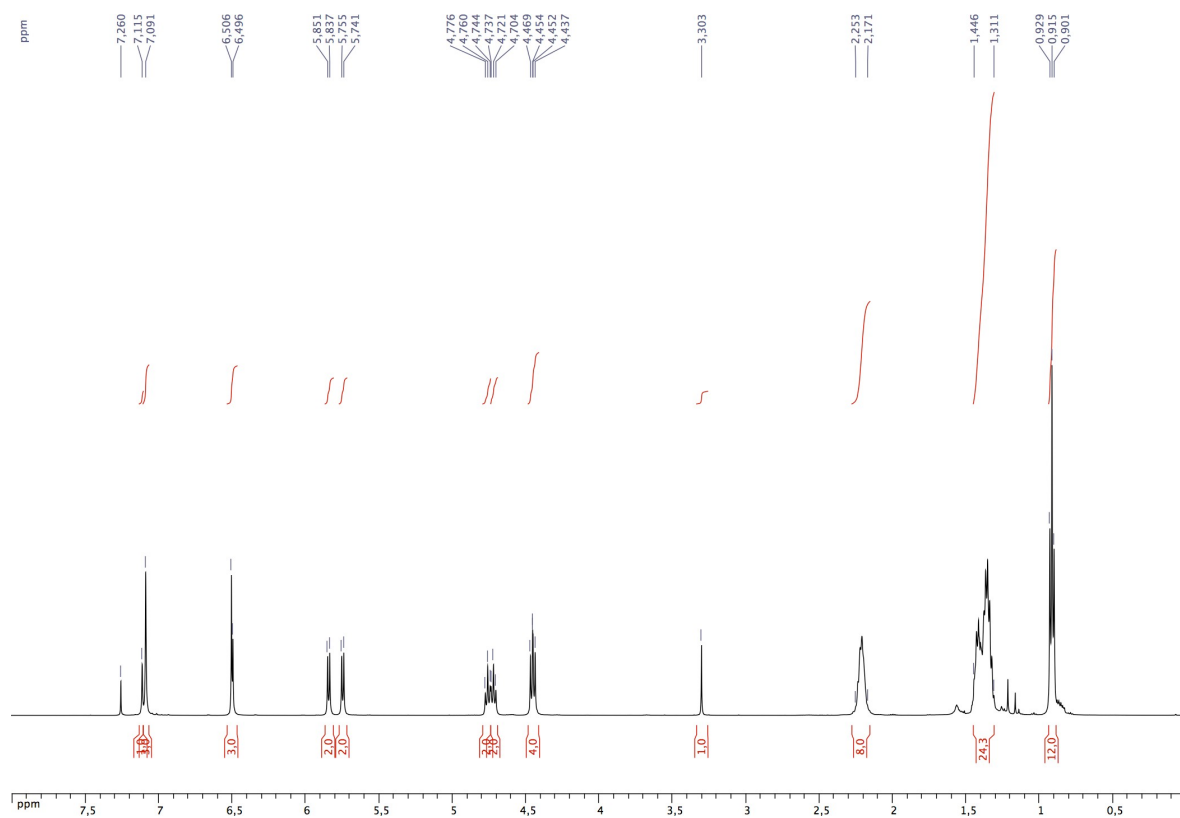
^{1}H NMR spectrum of **4** (CDCl$_3$)
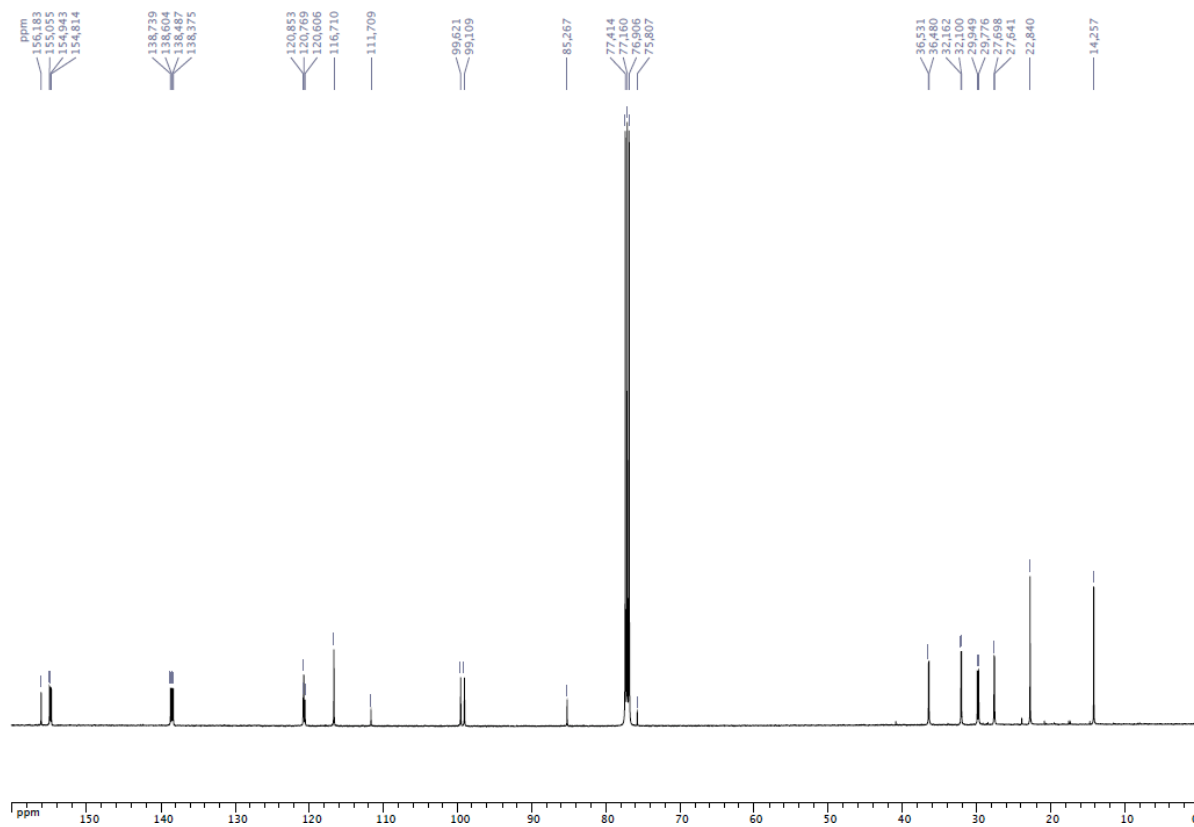

^{13}C{^{1}H} NMR spectrum of **4** (CDCl$_3$)

5-Ethynyl-4(24),6(10),12(16),18(22)-tetramethylenedioxy-2,8,14,20-tetrapentylresorcin[4]arene (5)

A solution of **4** (1.000 g, 2.90 mmol) and K_2CO_3 (1.508 g, 10.91 mmol) in CH_2Cl_2/MeOH (50 mL; 25:75 v/v) was stirred at room temperature for 16 h. The reaction mixture was evaporated to dryness and the residue was treated with a mixture of CH_2Cl_2/H_2O (500 mL; 1:1 v/ v). The aqueous layer was washed with CH_2Cl_2 (2 x 100 mL), then the combined organic layers were dried with $MgSO_4$. After filtration, the solvent was evaporated off under reduced pressure to afford **5** as a white solid (0.918 g, yield 100 %). ^1H NMR (500 MHz, $CDCl_3$): δ = 7.11 (s, 1H, arom. CH, resorcinarene), 7.09 (s, 3H, arom. CH, resorcinarene), 6.51 (s, 2H, arom. CH, resorcinarene), 6.50 (s, 1H, arom. CH, resorcinarene), 5.84 and 4.46 (AB spin system, 4H, OCH_2O, ^2J = 7.0 Hz), 5.75 and 4.44 (AB spin system, 4H, OCH_2O, ^2J = 7.0 Hz), 4.76 (t, 2H, $CHCH_2$, ^3J = 8.0 Hz), 4.72 (t, 4H, $CHCH_2$, ^3J = 8.0 Hz), 3.30 (s, 1H, $C{\equiv}CH$), 2.25-2.17 (m, 8H, $CHCH_2$), 1.45-1.31 (m, 24H, $CH_2CH_2CH_2CH_3$), 0.91 (t, 12 H, CH_2CH_3, ^3J = 7.0 Hz) ppm. $^{13}C\{^1H\}$ NMR (126 MHz, $CDCl_3$): δ = 156.18-111.71 (arom. Cs), 99.62 (s, OCH_2O), 99.11 (s, OCH_2O), 85.27 (s, $C{\equiv}CH$), 75.81 (s, $C{\equiv}CH$), 36.53 (s, $CHCH_2$), 36.48 (s, $CHCH_2$), 32.16 (s, $CH_2CH_2CH_3$), 32.10 (s, $CH_2CH_2CH_3$), 29.95 (s, $CHCH_2$), 29.78 (s, $CHCH_2$), 27.70 (s, $CHCH_2CH_2$), 27.64 (s, $CHCH_2CH_2$), 22.84 (s, CH_2CH_3), 14.26 (s, CH_2CH_3) ppm. Elemental analysis calcd (%) for $C_{54}H_{64}O_8$ (841.08): C 77.11, H 7.67; found C 77.26, H 7.89.

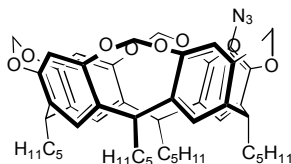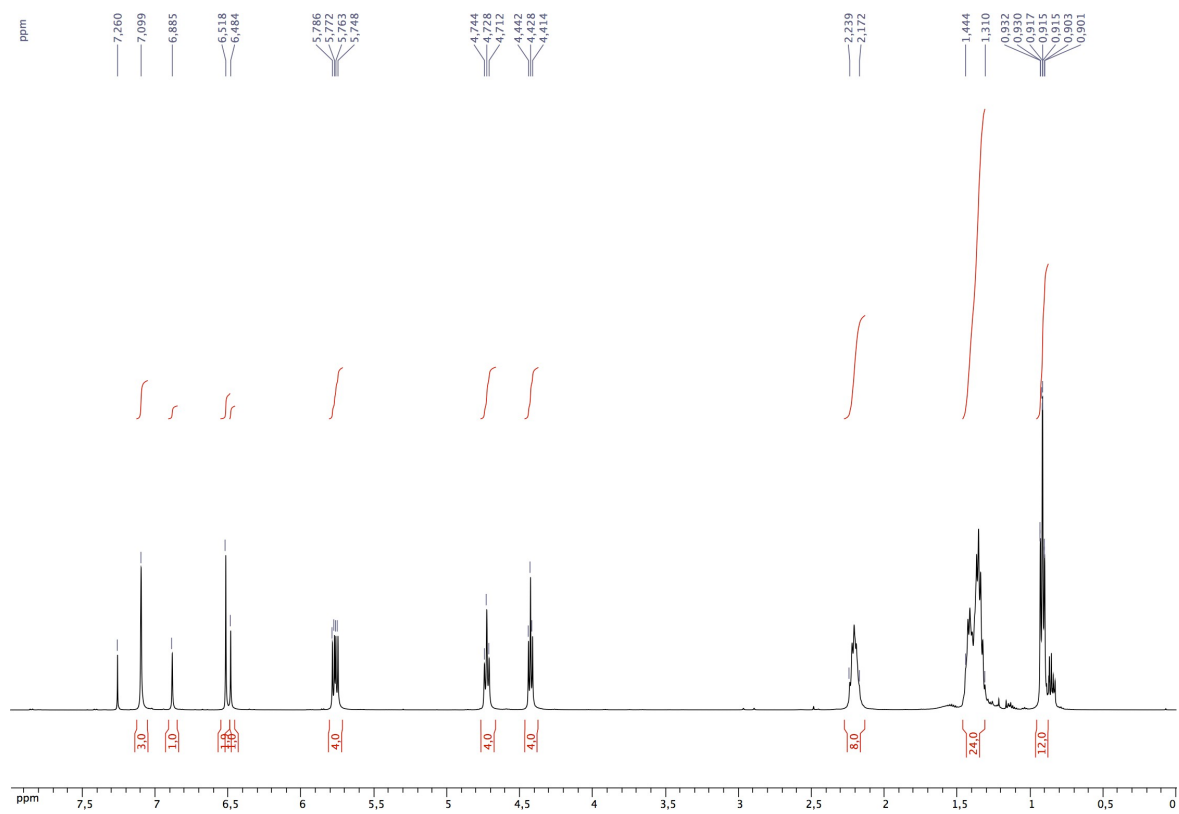^{1}H NMR spectrum of **5** (CDCl$_3$)

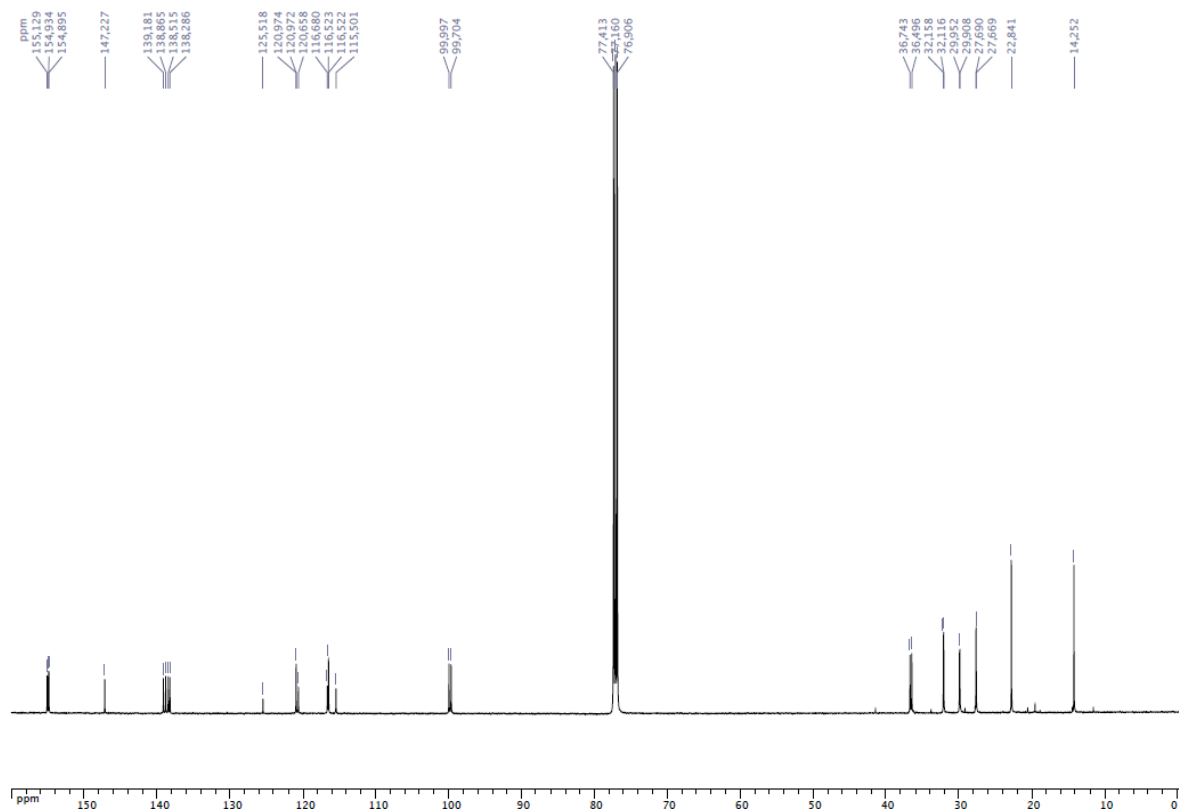^{13}C{^{1}H} NMR spectrum of **5** (CDCl$_3$)

5-Azido-4(24),6(10),12(16),18(22)-tetramethylenedioxy-2,8,14,20-tetrapentylresorcin[4] arene (6)

n-Butyllithium (1.6 M in hexane; 2.51 mL, 4.02 mmol) was slowly added to a solution of bromo-cavitand **3** (3.000 g, 3.35 mmol) in THF (150 mL) at -78 °C. After 1 h, the resulting anion was quenched with tosylazide (0.792 g, 4.02 mmol), and the mixture was stirred at room temperature for 24 h. The reaction mixture was washed three times with brine (3 x 100 mL). The solvent was evaporated under reduced pressure, and the crude product was purified by column chromatography (Et$_2$O/petroleum ether, 5:95; Rf = 0.32) to give **6** (2.150 g, 75 %). ^{1}H NMR (500 MHz, CDCl$_3$): δ = 7.10 (s, 3H, arom. CH, resorcinarene), 6.88 (s, 1H, arom. CH, resorcinarene), 6.52 (s, 2H, arom. CH, resorcinarene), 6.48 (s, 1H, arom. CH, resorcinarene), 5.78 and 4.43 (AB spin system, 4H, OCH$_2$O, ^2J = 7.0 Hz), 5.75 and 4.42 (AB spin system, 4H, OCH$_2$O, ^2J = 7.0 Hz), 4.73 (t, 4H, C*H*CH$_2$, ^3J = 8.0 Hz), 2.24-2.17 (m, 8H, CHC*H$_2$*), 1.44-1.31 (m, 24H C*H$_2$CH$_2$CH$_2$*CH$_3$), 0.92 (t, 6H, CH$_2$C*H$_3$*, ^3J = 7.2 Hz), 0.91 (t, 6H, CH$_2$C*H$_3$*, ^3J = 7.2 Hz) ppm. ^{13}C{^{1}H} NMR (126 MHz, CDCl$_3$): δ = 155.13-115.50 (arom. Cs), 100.00 (s, OCH$_2$O), 99.70 (s, OCH$_2$O), 36.74 (s, *C*HCH$_2$), 36.50 (s, *C*HCH$_2$), 32.16 (s, *C*H$_2$CH$_2$CH$_3$), 32.12 (s, *C*H$_2$CH$_2$CH$_3$), 29.95 (s, CH*C*H$_2$), 29.91 (s, CH*C*H$_2$), 27.69 (s, CHCH$_2$*C*H$_2$), 27.67 (s, CHCH$_2$*C*H$_2$), 22.84 (s, *C*H$_2$CH$_3$), 14.25 (s, CH$_2$*C*H$_3$) ppm. IR: ν = 2103 and 1286 (N$_3$) cm^{-1}. Elemental analysis calcd (%) for C$_{52}$H$_{63}$N$_3$O$_8$ (858.07): C 72.79, H 7.40, N 4.90; found C 72.58, H 7.51, N 4.64.

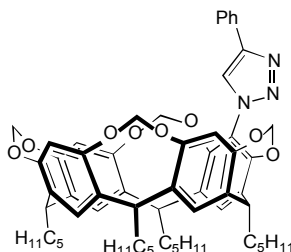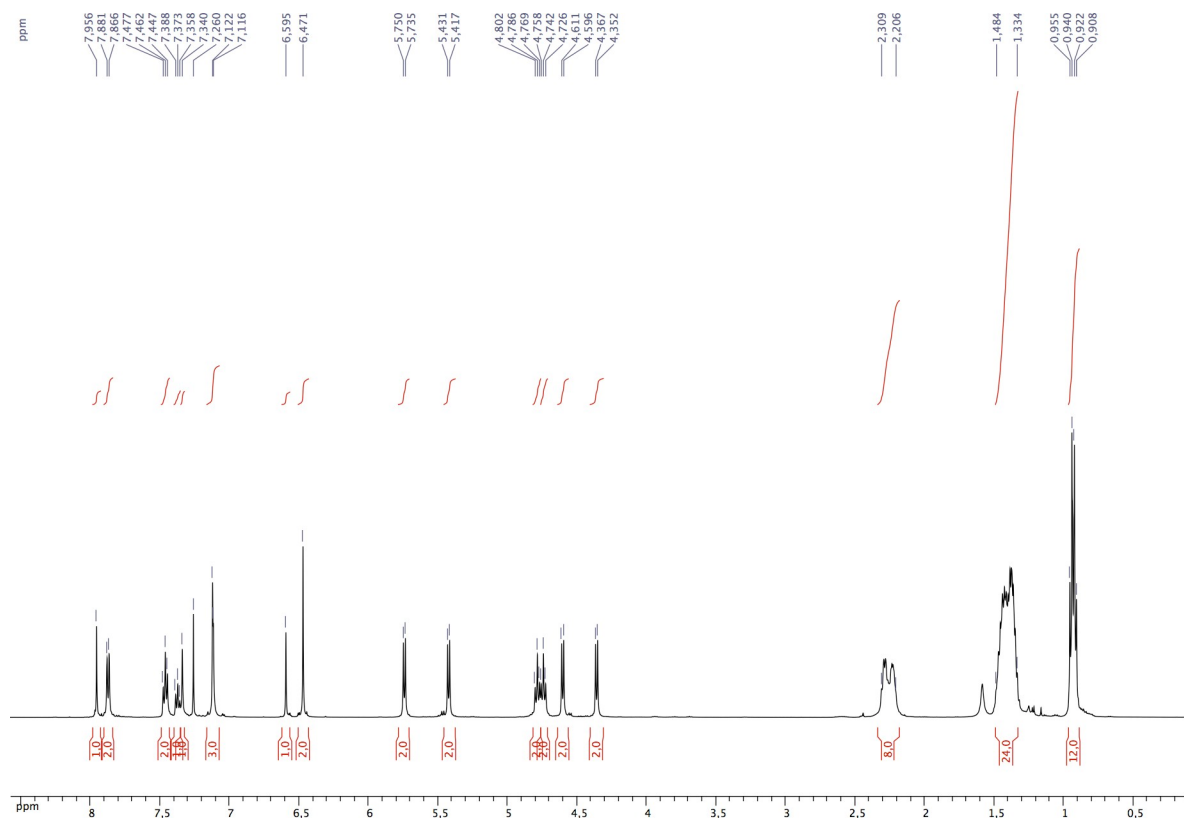^{1}H NMR spectrum of **6** (CDCl$_3$)

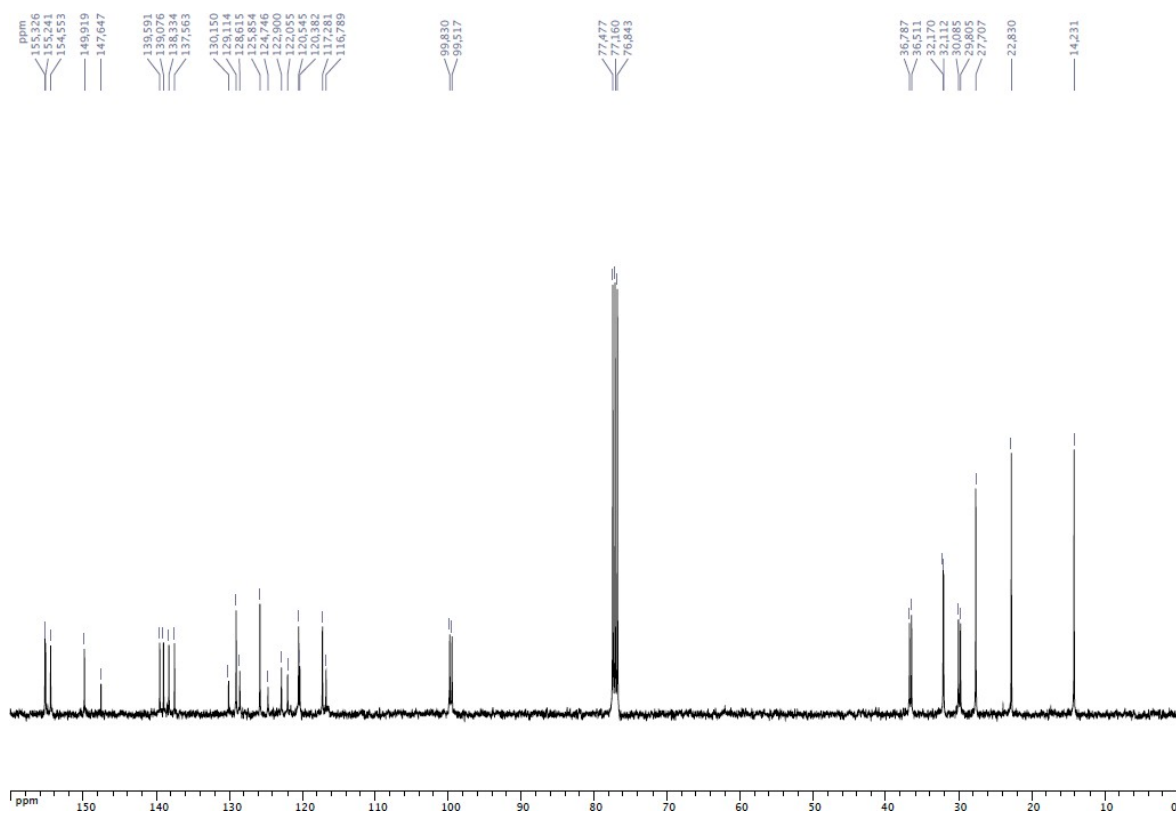^{13}C{^{1}H} NMR spectrum of **6**(CDCl$_3$)

1*H*-1,2,3-Triazole,1-{4(24),6(10),12(16),18(22)-tetramethylenedioxy-2,8,14,20-tetrapentyl resorcin[4]arene-5-yl}-4-phenyl (7)
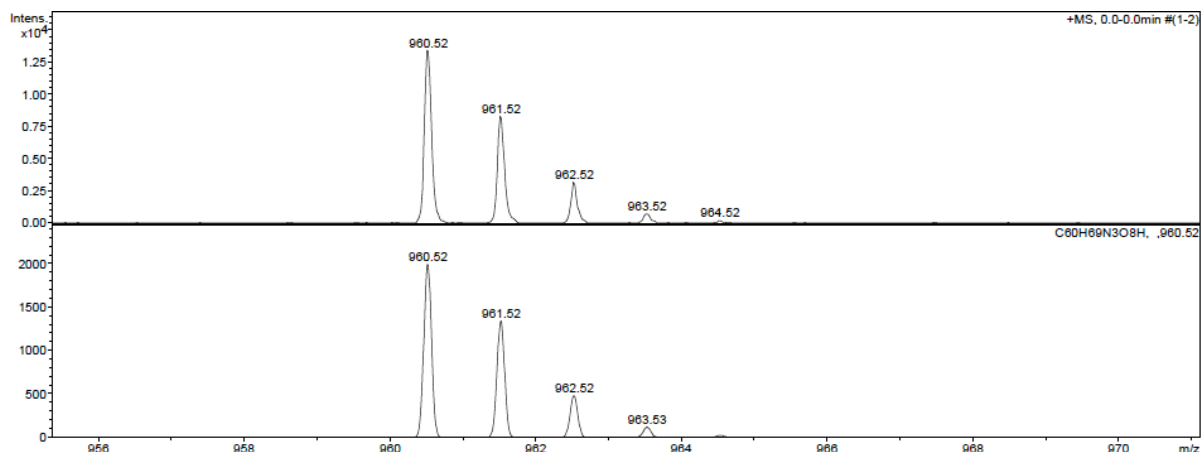

To a solution of azido-cavitand **6** (0.500 g, 0.58 mmol), CuSO$_4$·5H$_2$O (0.014 g, 0.06 mmol) and sodium ascorbate (0.012 g, 0.06 mmol) in DMF (50 mL) was added phenylacetylene (0.06 mL, 0.58 mmol). The mixture was stirred for 36 h at 100°C, then cooled to room temperature. The solution was evaporated to dryness and the resulting residue was dissolved in CH$_2$Cl$_2$ (200 mL). The organic solution was washed with brine (3 x 100 mL) and the aqueous layers were extracted with CH$_2$Cl$_2$ (2 x 100 mL). The combined organic layer were dried over MgSO$_4$, filtered and evaporated under reduced pressure, and the crude product was purified by column chromatography (Et$_2$O/petroleum ether, 20:80; Rf = 0.39) to give **7** (0.510 g, 91 %). ^{1}H NMR (500 MHz, CDCl$_3$): δ =7.96 (s, 1H, CH, triazole), 7.87 (d, 2H, arom. CH, Ph, ^3J = 7.5 Hz) 7.46 (t, 2H, arom. CH, Ph, ^3J = 7.5 Hz), 7.37 (t, 1H, arom. CH, Ph, ^3J = 7.5 Hz), 7.34 (s, 1H, arom. CH, resorcinarene), 7.12 (s, 2H, arom. CH, resorcinarene), 7.12 (s, 1H, arom. CH,resorcinarene), 6.59 (s, 1H, arom. CH,resorcinarene), 6.47 (s, 2H, arom. CH,resorcinarene), 5.74 and 4.60 (AB spin system, 4H, OCH$_2$O, ^2J = 7.5 Hz), 5.42 and 4.36 (AB spin system, 4H, OCH$_2$O, ^2J = 7.5 Hz), 4.79 (t, 2H, C*H*CH$_2$, ^3J = 8.2 Hz), 4.74 (t, 2H, C*H*CH$_2$, ^3J = 8.0 Hz), 2.31-2.21 (m, 8H, CHC*H*$_2$), 1.48-1.33 (m, 24H *CH$_2$CH$_2$CH$_2$*CH$_3$), 0.94 (t, 6H, CH$_2$C*H$_3$*,^3J = 7.5 Hz), 0.92 (t, 6H, CH$_2$C*H$_3$*, ^3J = 7.0 Hz) ppm. ^{13}C{^{1}H} NMR (101 MHz, CDCl$_3$): δ = 155.33-116.79 (arom. Cs), 122.90 (s, CH, triazole), 99.83 (s, OCH$_2$O), 99.52 (s, OCH$_2$O), 36.79 (s, *C*HCH$_2$), 36.51 (s, *C*HCH$_2$), 32.17 (s, *C*H$_2$CH$_2$CH$_3$), 32.11 (s, *C*H$_2$CH$_2$CH$_3$), 30.08 (s, CHC*H$_2$*), 29.80 (s, CHC*H$_2$*), 27.71 (s, CHCH$_2$*C*H$_2$), 22.83 (s, *C*H$_2$CH$_3$), 14.23 (s, CH$_2$*C*H$_3$) ppm. MS (ESI-TOF): *m/z* = 960.52 [M + H]$^+$, expected isotopic profile. Elemental analysis calcd (%) for C$_{60}$H$_{69}$N$_3$O$_8$ (960.21): C 75.05, H 7.24, N 4.38; found C 74.86, H 7.02, N 4.23.
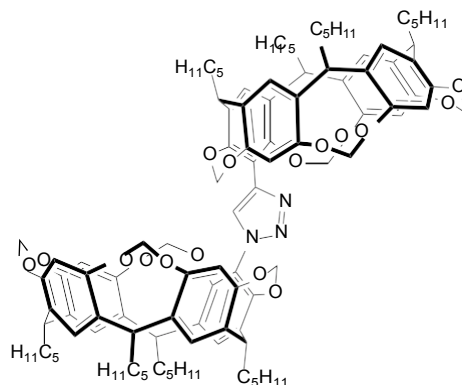
^{1}H NMR spectrum of **7** (CDCl$_3$)

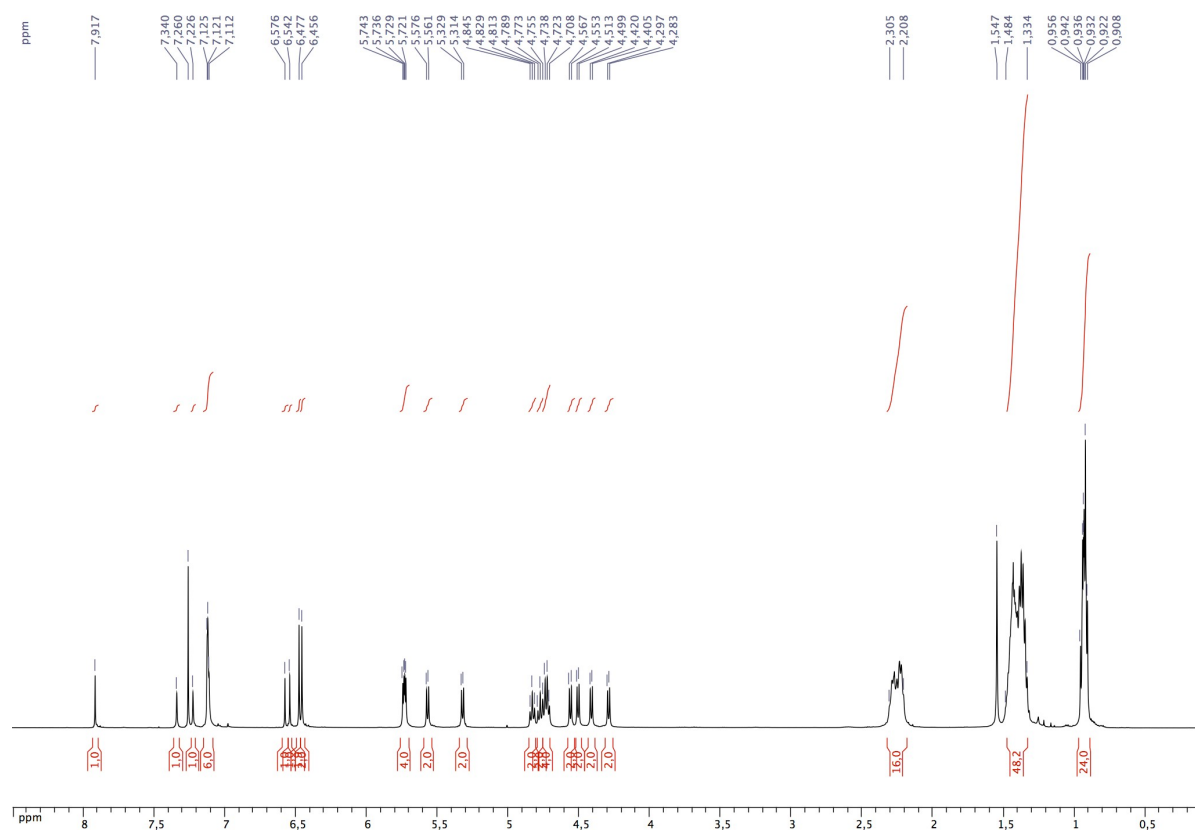^{13}C{^{1}H} NMR spectrum of **7** (CDCl$_3$)

133

ESI-TOF spectrum of **7** (measured top and calculated for $C_{60}H_{70}N_3O_8$ bottom)

1*H*-1,2,3-Triazole,1,4-bis{4(24),6(10),12(16),18(22)-tetramethylenedioxy-2,8,14,20-tetrapentylresorcin[4]arene-5-yl} (8)


A solution of ethynyl-cavitand **5** (0.490 g, 0.58 mmol), azido-cavitand **6** (0.500 g, 0.58 mmol), CuSO$_4$·5H$_2$O (0.014 g, 0.06 mmol) and sodium ascorbate (0.012 g, 0.06 mmol) in DMF (50 mL) was stirred for 36 h at 100°C. Afterwards, the mixture was cooled to room temperature and evaporated to dryness. The resulting residue was dissolved in CH$_2$Cl$_2$ (200 mL). The organic solution was washed with brine (3 x 100 mL) and the aqueous layers were extracted with CH$_2$Cl$_2$ (2 x 100 mL). The combined organic layer were dried over MgSO$_4$, filtered and evaporated under reduced pressure, and the crude product was purified by column chromatography (Et$_2$O/petroleum ether, 20:80; *R*f = 0.28) to give **8** (0.535 g, 54 %). ^{1}H NMR (500 MHz, CDCl$_3$): δ = 7.92 (s, 1H, CH, triazole), 7.34 (s, 1H, arom. CH, resorcinarene), 7.23 (s, 1H, arom. CH, resorcinarene), 7.12

(s, 2H, arom. CH, resorcinarene), 7.12 (s, 3H, arom. CH, resorcinarene), 7.11 (s, 1H, arom. CH, resorcinarene), 6.58 (s, 1H, arom. CH, resorcinarene), 6.54 (s, 1H, arom. CH, resorcinarene), 6.48 (s, 2H, arom. CH, resorcinarene), 6.46 (s, 2H, arom. CH, resorcinarene), 5.74 and 4.56 (AB spin system, 4H, OCH$_2$O, ^2J = 7.0 Hz), 5.73 and 4.51 (AB spin system, 4H, OCH$_2$O, ^2J = 7.0 Hz), 5.57 and 4.41 (AB spin system, 4H, OCH$_2$O, ^2J = 7.5 Hz), 5.32 and 4.29 (AB spin system, 4H, OCH$_2$O, ^2J = 7.5 Hz), 4.83 (t, 2H, C*H*CH$_2$, ^3J = 8.0 Hz), 4.77 (t, 2H, C*H*CH$_2$, ^3J = 8.0 Hz), 4.74 (t, 2H, C*H*CH$_2$, ^3J = 7.5 Hz), 4.72 (t, 2H, C*H*CH$_2$, ^3J = 7.5 Hz), 2.30-2.21 (m, 16H, CHC*H$_2$*), 1.48-1.33 (m, 48H *CH$_2$CH$_2$CH$_2$*CH$_3$), 0.94 (t, 6H, CH$_2$C*H$_3$*, ^3J = 7.0 Hz), 0.93 (t, 6H, CH$_2$C*H$_3$*, ^3J = 7.0 Hz), 0.92 (t, 12H, CH$_2$C*H$_3$*, ^3J = 7.0 Hz) ppm. ^{13}C{^{1}H} NMR (126 MHz, CDCl$_3$): δ = 155.33-116.74 (arom. Cs), 127.33 (s, CH, triazole), 99.77 (s, OCH$_2$O), 99.65 (s, OCH$_2$O), 99.58 (s, OCH$_2$O), 99.52 (s, OCH$_2$O), 36.79 (s, *C*HCH$_2$), 36.51 (s, *C*HCH$_2$), 32.19 (s, *C*H$_2$CH$_2$CH$_3$), 32.14 (s, *C*H$_2$CH$_2$CH$_3$), 30.08 (s, CH*C*H$_2$), 29.96 (s, CH*C*H$_2$), 29.81 (s, CH*C*H$_2$), 27.78 (s, CHCH$_2$*C*H$_2$), 27.72 (s, CHCH$_2$*C*H$_2$), 22.85 (s, *C*H$_2$CH$_3$), 14.27 (s, CH$_2$*C*H$_3$) ppm. MS (ESI-TOF): *m/z* = 1698.93 [M + H]$^+$, expected isotopic profile. Elemental analysis calcd (%) for C$_{106}$H$_{127}$N$_3$O$_{16}$ (1697.16): C 74.93, H 7.53, N 2.47; found C 74.68, H 7.47, N 2.39.

^{1}H NMR spectrum of **8** (CDCl$_3$)
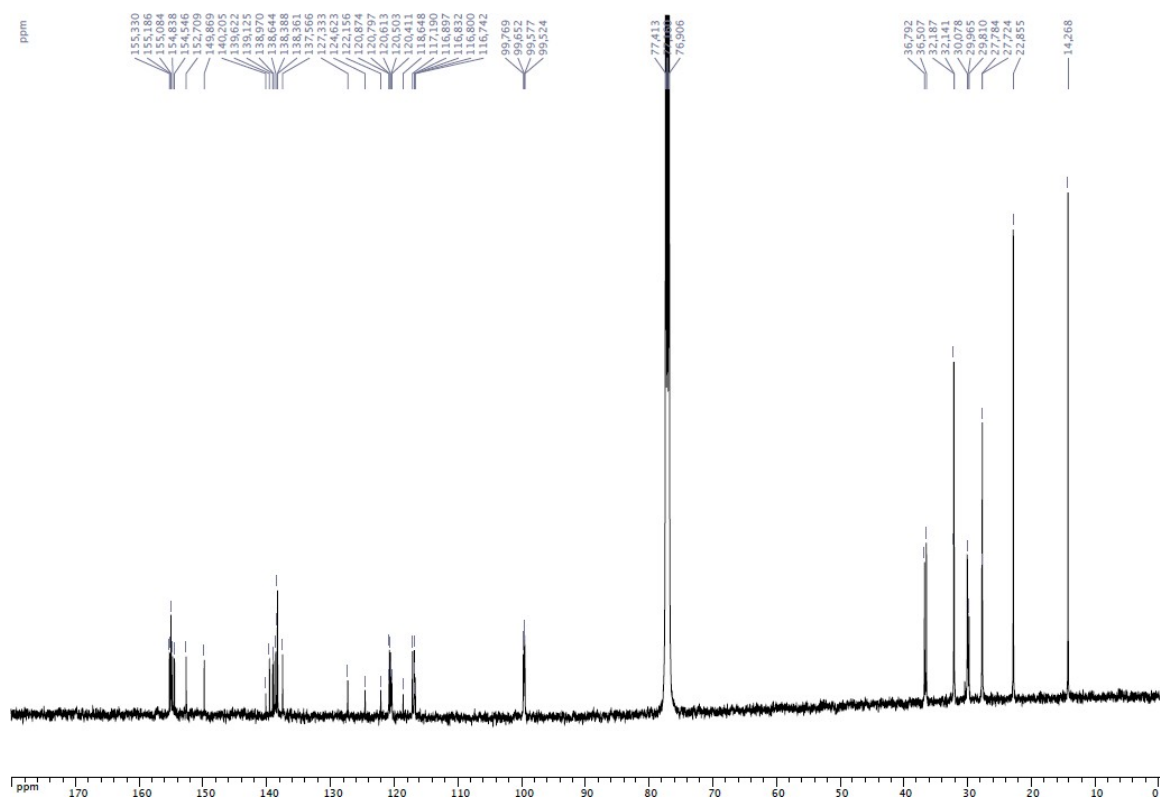
$^{13}C\{^1H\}$ NMR spectrum of **8** (CDCl$_3$)
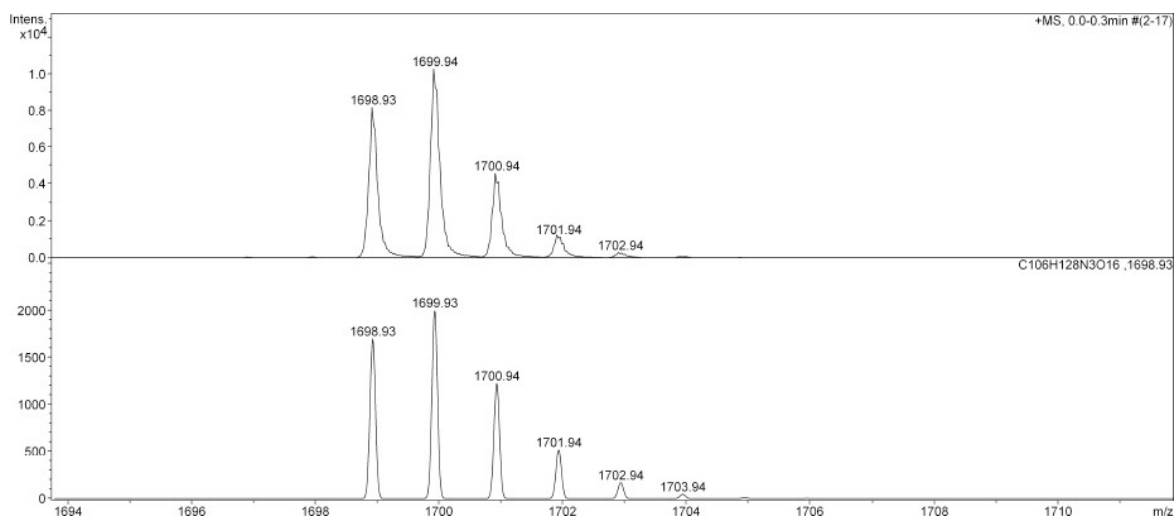
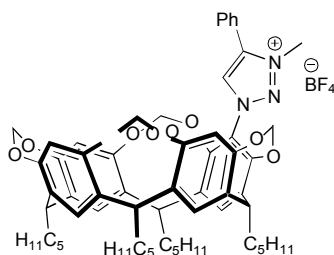ESI-TOF spectrum of **8** (measured top and calculated for C$_{106}$H$_{128}$N$_3$O$_{16}$ bottom)

X-ray crystal structure analysis of triazole 8: Single crystals of **8** suitable for X-ray analysis were obtained by slow diffusion of methanol into a CH$_2$Cl$_2$ solution of the triazole. Crystal data: C$_{106}$H$_{127}$N$_3$O$_{16}$, Mr = 1699.10 g mol^{-1}, monoclinic, space group C2/c, a = 52.4158(14) Å, b = 10.5297(3) Å, c = 56.6335(14) Å, β= 103.308(2)°, V = 30417.9(14) Å^3, Z = 12, D = 1.113 g cm^{-3},

136

μ = 0.592 mm^{-1}, $F(000)$ = 10944, T = 173(2) K. The sample was studied on a Bruker APEXII CCD (graphite monochromatedCu-$K\alpha$ radiation, λ = 1.54178 Å). The data collection (2θmax = 66.9°, omega scan frames by using 0.7° omega rotation and 30 s per frame, range hkl: h -61,61 k -6,12l -57,67) gave 128330 reflections. The structure was solved with SHELXS-2013,[1] which revealed the non-hydrogen atoms of the molecule. After anisotropic refinement, all of the hydrogen atoms were found with a Fourier difference map. The structure was refined with SHELXL-2013[1] by the full-matrix least-square techniques (use of F square magnitude; x, y, z, ij for C, N and O atoms; x, y, z in riding mode for H atoms); 1677 variables and 11315 observations with I > 2.0 $\sigma(I)$; calcd. w= 1/[$\sigma^2(Fo^2)$ + (0.1312P)^2] where P = (Fo^2 + 2Fc^2)/3, with the resulting R = 0.0921, R_W = 0.2703 and S_W = 0.964, $\Delta\rho$< 0.599 eÅ^{-3}. CCDC entry 1848246 contains the supplementary crystallographic data. These data can be obtained free of charge from The Cambridge Crystallographic Data Centre via http://www.ccdc.cam.ac.uk/data_request/cif or by e-mailing data_request@ccdc.cam.ac.uk, or by contacting The Cambridge Crystallographic Data Centre, 12 Union Road, Cambridge CB2 1EZ, UK.

Reference

[1]   G. M. Sheldrick, *Acta. Cryst.* **2008**, *A64*, 112-122.
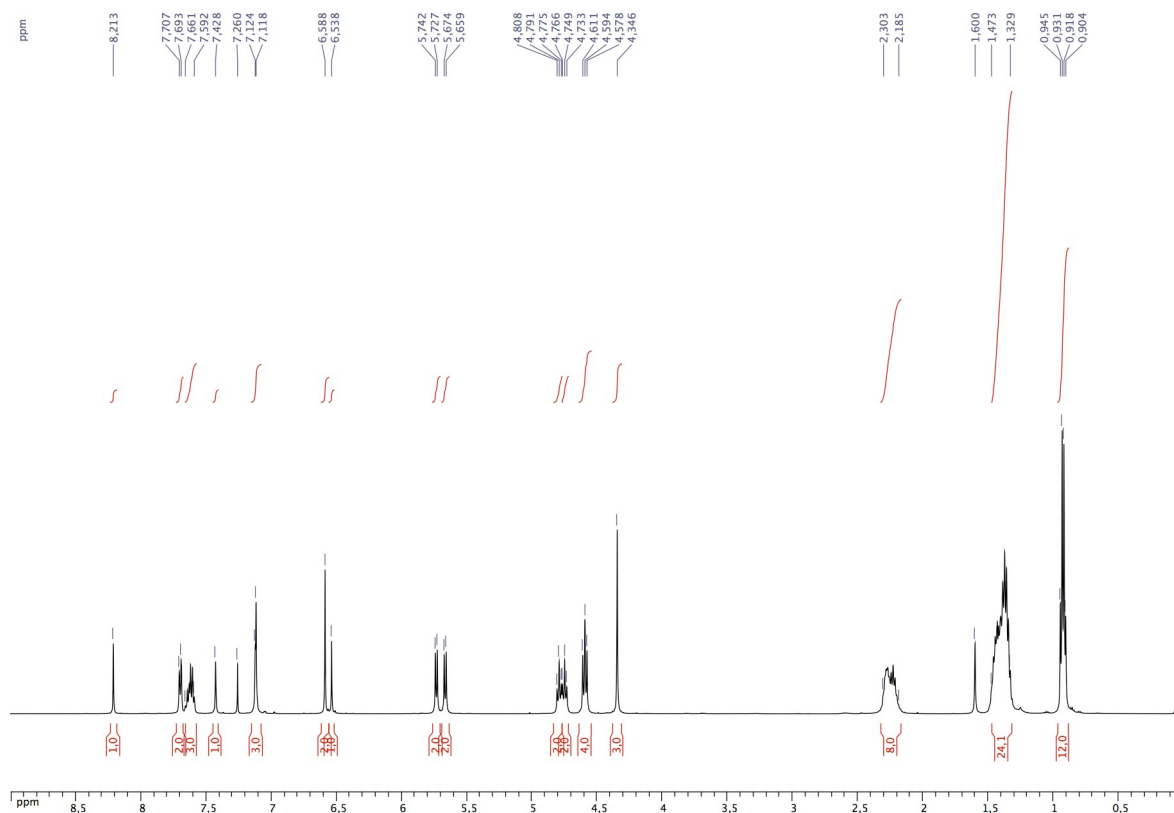
1-{4(24),6(10),12(16),18(22)-Tetramethylenedioxy-2,8,14,20-tetrapentylresorcin[4]arene-5-yl}-4-phenyl-3-methyl-1*H*-1,2,3-triazolium tetrafluoroborate (1)


Triazole-cavitand **7** (0.500 g, 0.52 mmol) and Me$_3$OBF$_4$ (0.115 g, 0.78 mmol) were dissolved in CH$_2$Cl$_2$ (20 mL) and the resulting solution was stirred for 2 days at room temperature. The organic solution was washed with brine (3 x 100 mL) and the aqueous layers were extracted with CH$_2$Cl$_2$ (2 x 100 mL). The combined organic layer were dried over MgSO$_4$, filtered and evaporated under reduced pressure. The crude product was dissolved in the minimum amount of CH$_2$Cl$_2$ and salt **1**

was precipitated by addition of hexane (200 mL), the solid was filtered and dried under vacuum (0.550 g, 100 %). ^{1}H NMR (500 MHz, CDCl$_3$): δ = 8.21 (s, 1H, CH, triazolium), 7.70 (d, 2H, arom. CH, phenyl, ^3J = 7.0 Hz), 7.66-7.59 (m, 3H, arom. CH, phenyl), 7.43 (s, 1H, arom. CH, resorcinarene), 7.12 (s, 1H, arom. CH, resorcinarene), 7.12 (s, 2H, arom. CH, resorcinarene), 6.59 (s, 2H, arom. CH, resorcinarene), 6.54 (s, 1H, arom. CH, resorcinarene), 5.73 and 4.59 (AB spin system, 4H, OCH$_2$O, ^2J = 7.5 Hz), 5.66 and 4.60 (AB spin system, 4H, OCH$_2$O, ^2J = 7.5 Hz), 4.79 (t, 2H, CHCH$_2$, ^3J = 8.2 Hz), 4.75 (t, 2H, CHCH$_2$, ^3J = 8.2 Hz), 4.35 (s, 3H, triazolium-CH$_3$), 2.30- 2.18 (m, 8H, CHCH$_2$), 1.60-1.33 (m, 24H, CH$_2$CH$_2$CH$_2$CH$_3$), 0.93 (t, 6H, CH$_2$CH$_3$, ^3J = 7.0 Hz),

0.92 (t, 6H, CH$_2$CH$_3$, ^3J = 7.0 Hz) ppm. ^{13}C{^{1}H} NMR (126 MHz, CDCl$_3$): δ = 155.77-117.32 (arom. Cs), 129.60 (s, CH, triazolium), 101.04 (s, OCH$_2$O), 99.60 (s, OCH$_2$O), 39.17 (s, triazolium-CH$_3$), 36.77 (s, CHCH$_2$), 36.49 (s, CHCH$_2$), 32.18 (s, CH$_2$CH$_2$CH$_3$), 32.07 (s, CH$_2$CH$_2$CH$_3$), 30.11 (s, CHCH$_2$), 29.77 (s, CHCH$_2$), 27.69 (s, CHCH$_2$CH$_2$), 22.84 (s, CH$_2$CH$_3$), 14.26 (s, CH$_2$CH$_3$), 14.25 (s, CH$_2$CH$_3$) ppm. MS (ESI-TOF): m/z = 974.53 [M - BF$_4$]$^+$, expected isotopic profile. Elemental analysis calcd (%) for C$_{61}$H$_{72}$N$_3$O$_8$BF$_4$ (1062.05): C 68.98, H 6.83, N 3.96; found C 69.16, H 6.72, N 3.82.

^{1}H NMR spectrum of **1** (CDCl$_3$)
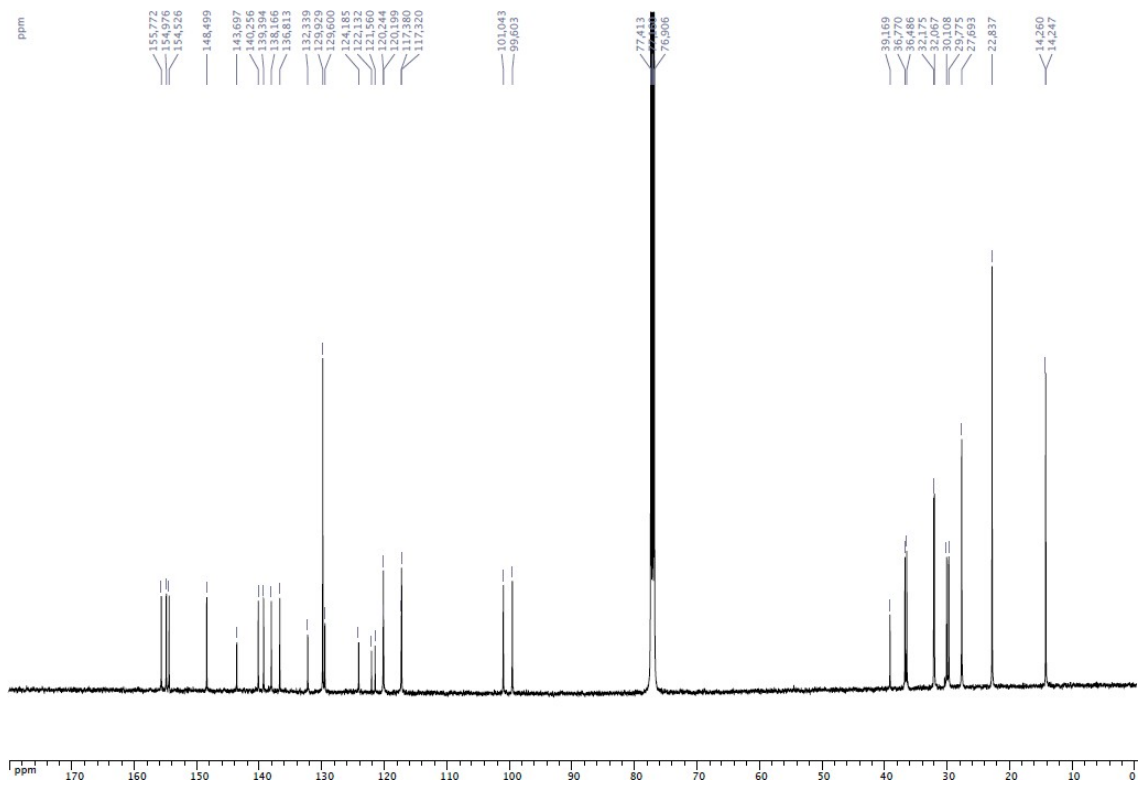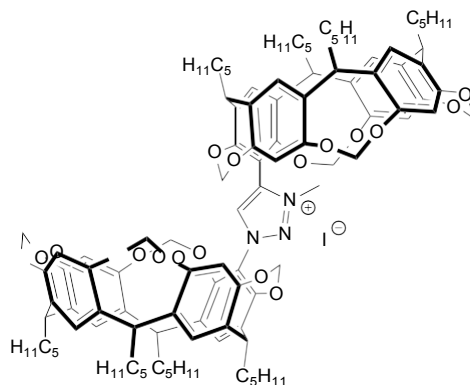
$^{13}C\{^1H\}$ NMR spectrum of **1** (CDCl$_3$)
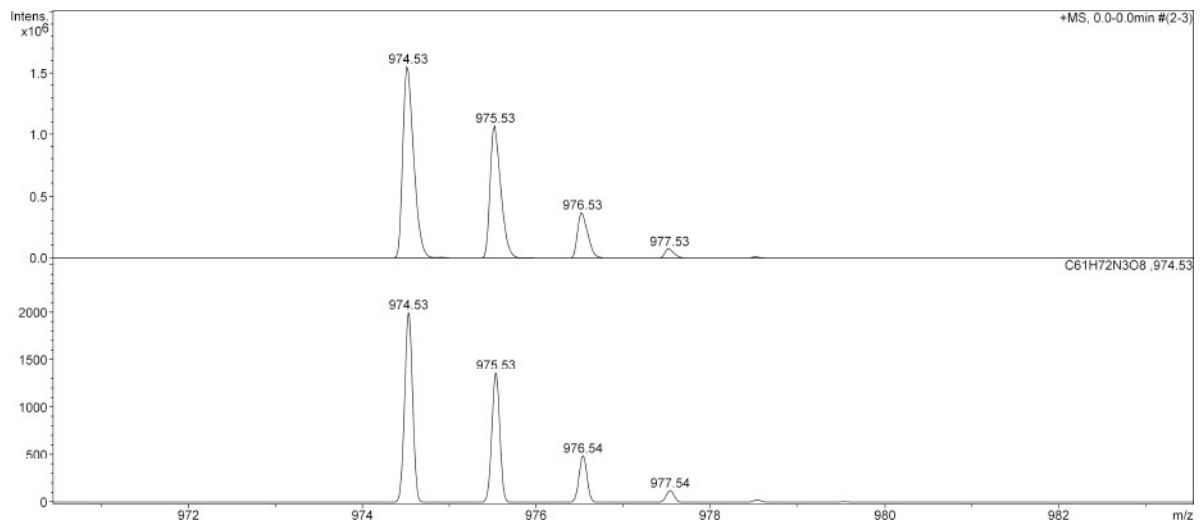
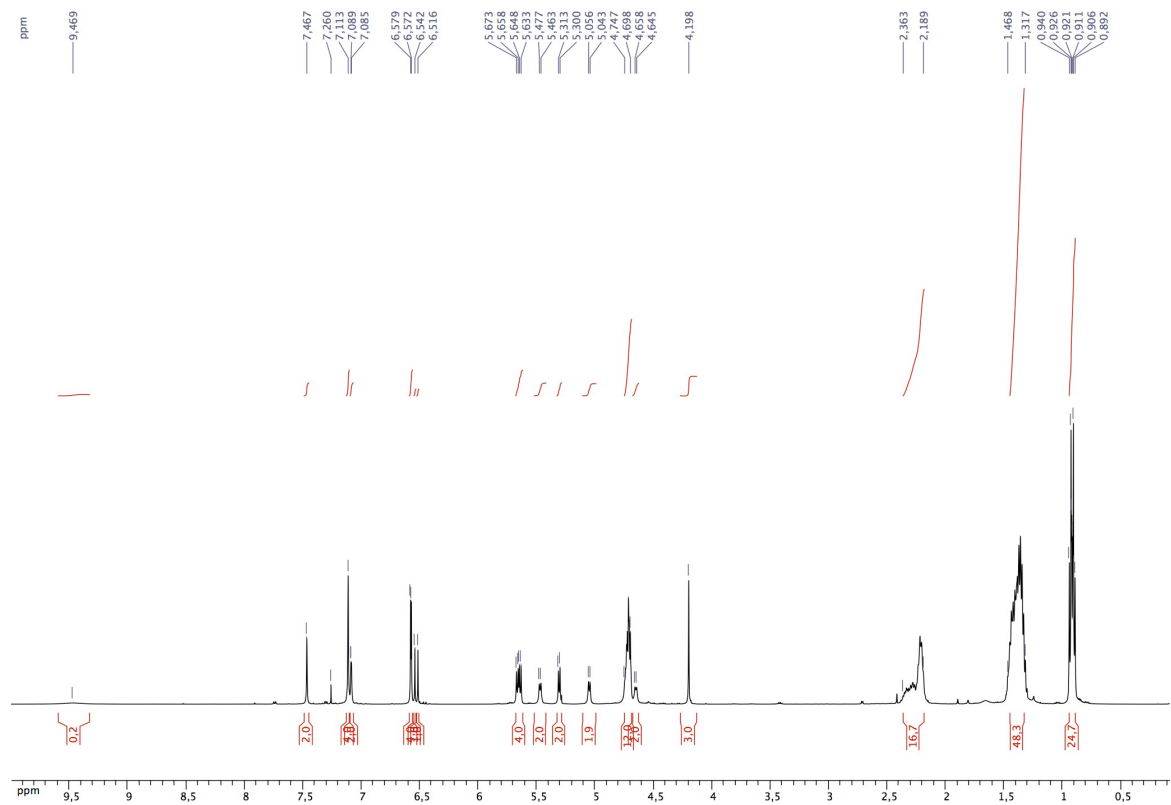ESI-TOF spectrum of **1** (measured top and calculated for C$_{61}$H$_{72}$N$_3$O$_8$ bottom)
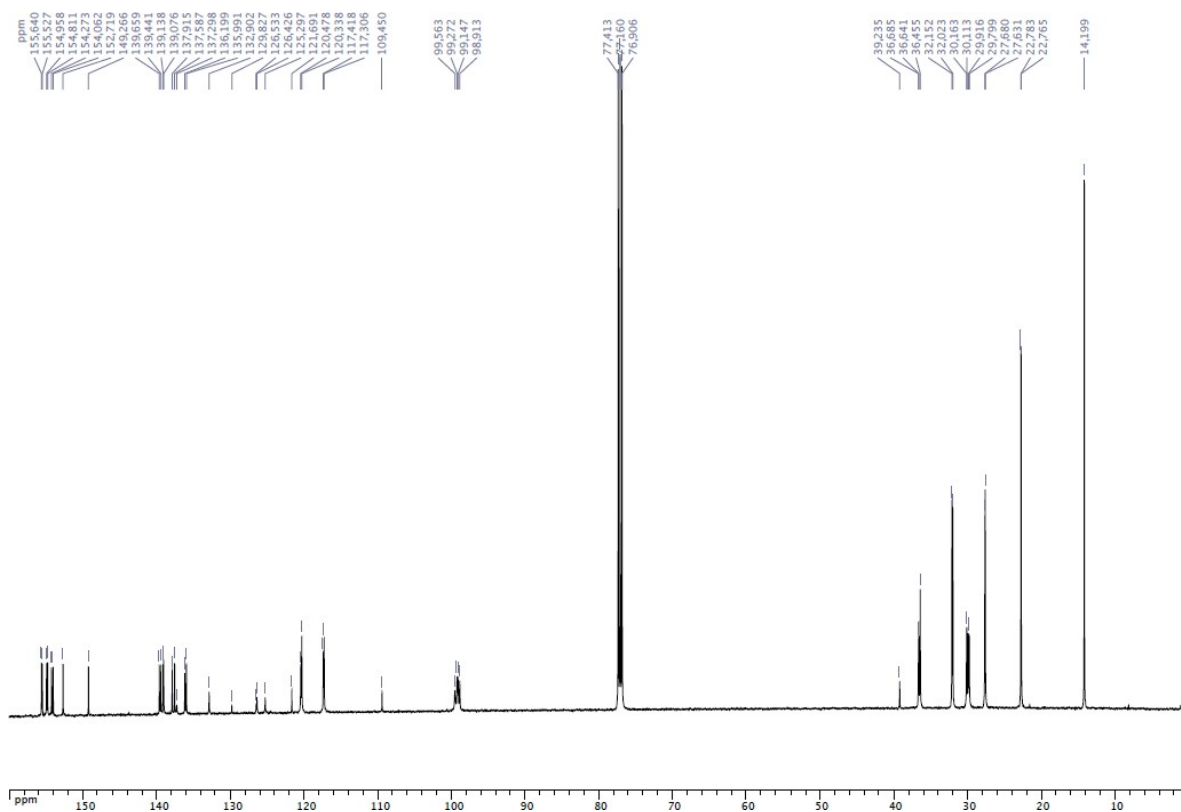
1,4-Bis{4(24),6(10),12(16),18(22)-tetramethylenedioxy-2,8,14,20-tetrapentylresorcin[4]arene-5-yl}-3-methyl-1*H*-1,2,3-triazolium iodide (2)


To a solution of triazole-bis-cavitand **8** (0.100 g, 0.06 mmol) in CH_2Cl_2 (5 mL) was added MeI (0.12 mL, 0.29 mmol). The mixture was stirred for 2 days at room temperature. Then the salt **2** was precipitated by addition of hexane (50 mL), the solid was filtered and dried under vacuum (0.074 g, 68 %). ^{1}H NMR (500 MHz, CDCl$_3$): δ = 9.47 (s br, 1H, CH, triazolium), 7.64 (s, 2H, arom. CH, resorcinarene), 7.11 (s, 4H, arom. CH, resorcinarene), 7.09 (s, 1H, arom. CH, resorcinarene), 7.08 (s, 1H, arom. CH, resorcinarene), 6.58 (s, 2H, arom. CH, resorcinarene), 6.57 (s, 2H, arom. CH, resorcinarene), 6.54 (s, 1H, arom. CH, resorcinarene), 6.52 (s, 1H, arom. CH, resorcinarene), 5.66 and 4.65 (AB spin system, 4H, OCH$_2$O, ^2J = 7.5 Hz), 5.64 and 4.70 (AB spin system, 4H, OCH$_2$O, ^2J = 7.5 Hz), 5.47 and 4.72 (AB spin system, 4H, OCH$_2$O, ^2J = 7.0 Hz), 5.31 and 5.05 (AB spin system, 4H, OCH$_2$O, ^2J = 6.5 Hz), 4.75-4.70 (m, 8H, C*H*CH$_2$), 4.20 (s, 3H, triazolium-CH$_3$), 2.36-2.19 (m, 16H, CHC*H$_2$*), 1.47-1.32 (m, 48H *CH$_2$CH$_2$CH$_2$*CH$_3$), 0.93 (t, 12H, CH$_2$C*H$_3$*, ^3J = 7.0 Hz), 0.91 (t, 12H, CH$_2$C*H$_3$*, ^3J = 7.0 Hz) ppm. ^{13}C{^{1}H} NMR (126 MHz, CDCl$_3$): δ = 155.64-109.45 (arom. Cs), 117.36 (s, CH, triazolium), 99.56 (s, OCH$_2$O), 99.27 (s, OCH$_2$O), 99.15 (s, OCH$_2$O), 98.91 (s, OCH$_2$O), 39.23 (s, triazolium-CH$_3$), 36.68 (s, *C*HCH$_2$), 36.64 (s, *C*HCH$_2$), 36.45 (s, *C*HCH$_2$), 32.15 (s, *C*H$_2$CH$_2$CH$_3$), 32.02 (s, *C*H$_2$CH$_2$CH$_3$), 30.16 (s, CH*C*H$_2$), 30.11 (s, CH*C*H$_2$), 29.92 (s, CH*C*H$_2$), 29.80 (s, CH*C*H$_2$), 27.68 (s, CHCH$_2$*C*H$_2$), 27.63 (s, CHCH$_2$*C*H$_2$), 22.78 (s, *C*H$_2$CH$_3$), 22.76 (s, *C*H$_2$CH$_3$), 14.20 (s, CH$_2$*C*H$_3$) ppm. MS (ESI-TOF): m/z = 1712.95 [M - I]$^+$, expected isotopic profile. Elemental analysis calcd (%) for C$_{107}$H$_{130}$N$_3$O$_{16}$I (1839.10): C 69.80, H 7.12, N 2.28; found C 69.93, H 7.10, N 2.06.
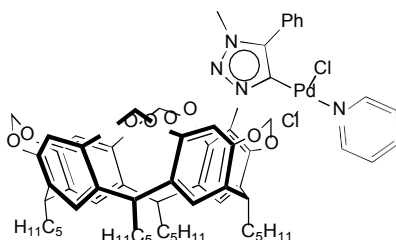
^{1}H NMR spectrum of **2** (CDCl$_3$)

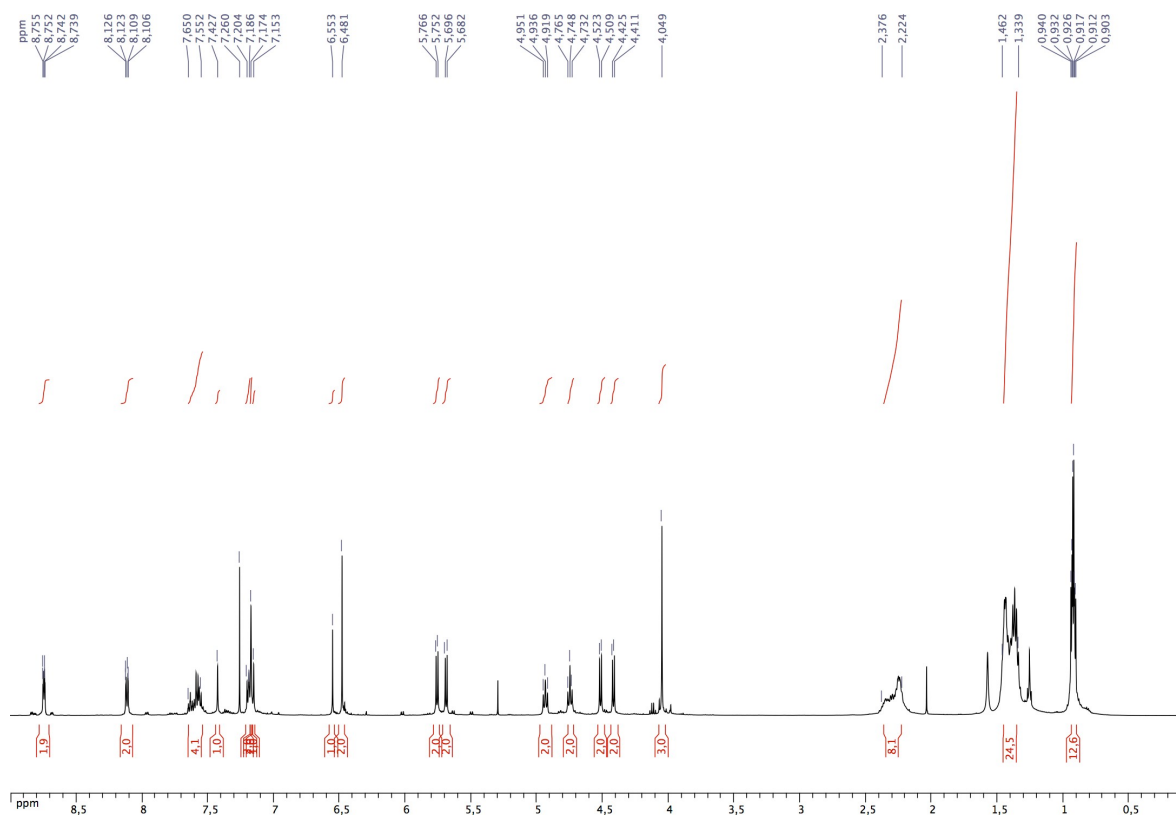^{13}C{^{1}H} NMR spectrum of **2** (CDCl$_3$)

141
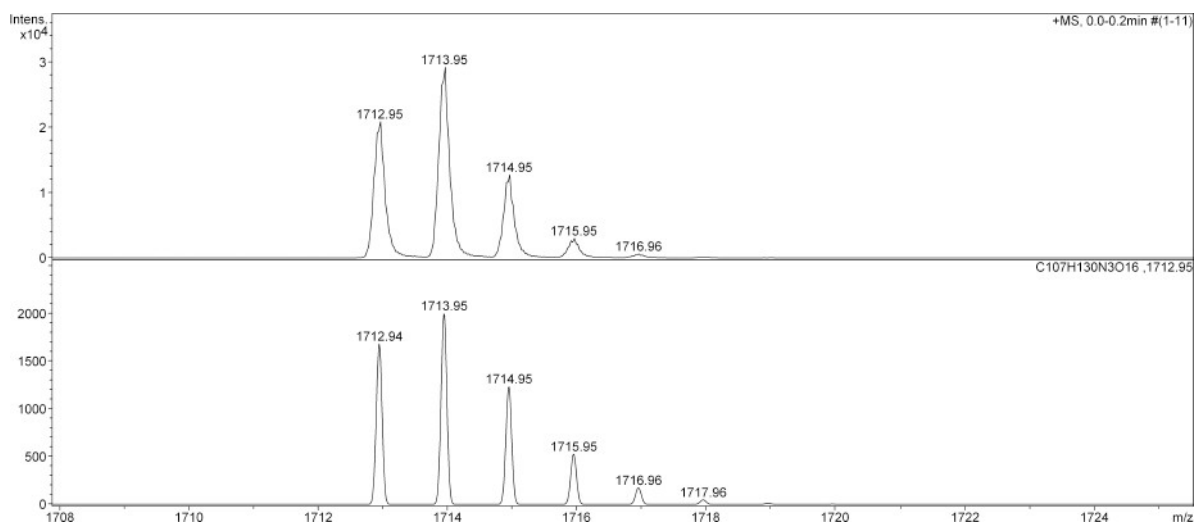
ESI-TOF spectrum of **2** (measured top and calculated for $C_{107}H_{130}N_3O_{16}$ bottom)

trans-Dichloro-{1-[4(24),6(10),12(16),18(22)-tetramethylenedioxy-2,8,14,20-tetrapentylresorcin[4]arene-5-yl]-4-phenyl-3-methyl-1_H_-1,2,3-triazol-5-yliden}pyridine palladium(II) (9)
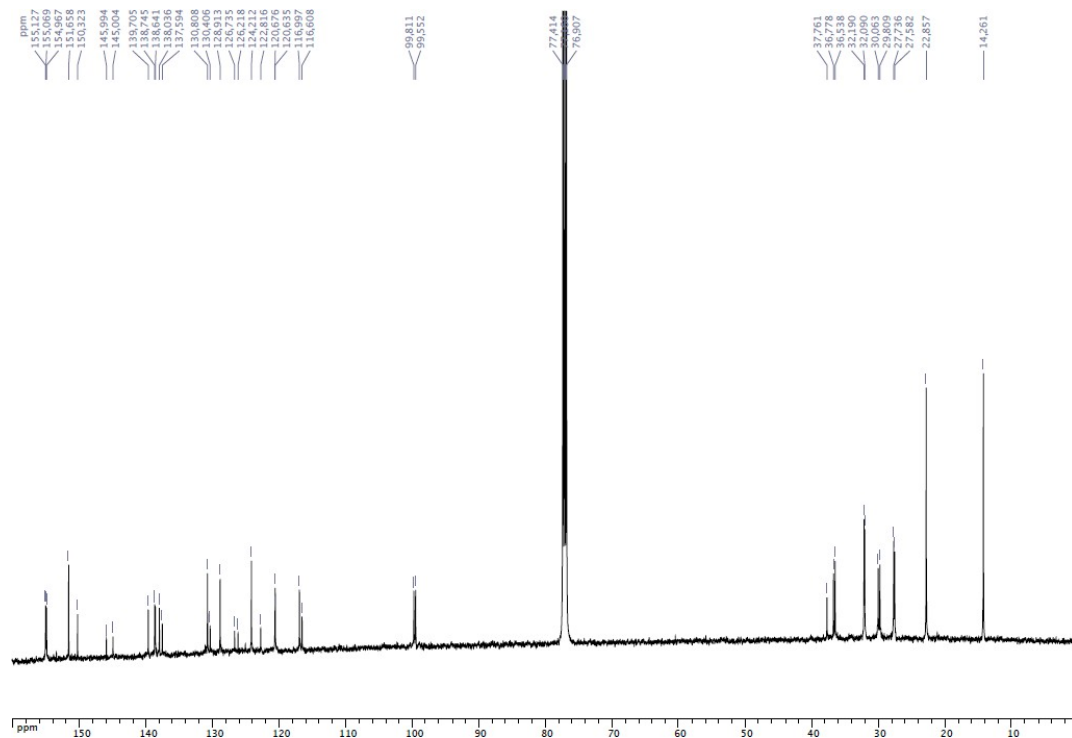

A mixture of K_2CO_3 (0.155 g, 1.12 mmol), pyridine (5 mL), $[PdCl_2]$ (0.040 g, 0.23 mmol) and triazolium salt **1** (0.200 g, 0.19 mmol) was heated at 80°C for 24 h. The reaction mixture was filtered through Celite, the filtrate was evaporated under vacuum, and the solid residue was purified by column chromatography (EtOAc/CH_2Cl_2, 10:90; Rf = 0.54) to afford complex **9** (0.060 g, 26 %). ^{1}H NMR (500 MHz, CDCl$_3$): δ =8.74 (dd, 2H, arom. CH, pyridine, ^3J = 6.5 Hz, ^4J = 1.5 Hz), 8.11 (dd, 2H, arom. CH, phenyl, ^3J = 8.5 Hz, ^4J = 1.5 Hz), 7.65-7.54 (m, 4H, arom. CH, pyridine and phenyl), 7.43 (s, 1H, arom. CH, resorcinarene), 7.20-7.19 (m, 2H, arom. CH, pyridine), 7.17 (s, 2H, arom. CH, resorcinarene), 7.15 (s, 1H, arom. CH, resorcinarene), 6.55 (s, 1H, arom. CH, resorcinarene), 6.48 (s, 2H, arom. CH, resorcinarene), 5.76 and 4.52 (AB spin system, 4H, OCH$_2$O, ^2J = 7.0 Hz), 5.69 and 4.42 (AB spin system, 4H, OCH$_2$O, ^2J = 7.0 Hz), 4.94

142

(t, 2H, CHCH$_2$, ^3J = 8.0 Hz), 4.75 (t, 2H, CHCH$_2$, ^3J = 8.2 Hz), 4.05 (s, 3H, triazolyliden-CH$_3$), 2.38-2.21 (m, 8H, CHCH_2), 1.46-1.34 (m, 24H $CH_2CH_2CH_2$CH$_3$), 0.93 (t, 6H, CH$_2$CH_3, ^3J = 7.2 Hz), 0.92 (t, 6H, CH$_2$CH_3, ^3J = 7.2 Hz) ppm. ^{13}C{^{1}H} NMR (126 MHz, CDCl$_3$): δ = 155.13-116.61 (arom. Cs), 145.99 (s, C$_q$-Pd), 99.81 (s, OCH$_2$O), 99.55 (s, OCH$_2$O), 37.76 (s, triazolyliden-CH$_3$), 36.78 (s, CHCH$_2$), 36.54 (s, CHCH$_2$), 32.19 (s, CH$_2$CH$_2$CH$_3$), 32.09 (s, CH$_2$CH$_2$CH$_3$), 30.06 (s, CHCH$_2$), 29.81 (s, CHCH$_2$), 27.74 (s, CHCH$_2$$CH_2$), 27.58 (s, CHCH$_2$$CH_2$), 22.86 (s, CH$_2CH_3$), 14.26 (s, CH$_2$$CH_3$) ppm. MS (ESI-TOF): m/z = 1193.44 [M - Cl]$^+$, expected isotopic profile. Elemental analysis calcd (%) for C$_{66}$H$_{76}$N$_4$O$_8$PdCl$_2$ (1230.65): C 64.41, H 6.22, N 4.55; found C 64.18, H 6.03, N 4.42.
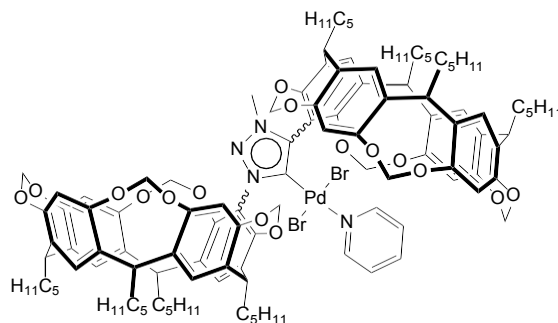

^{1}H NMR spectrum of **9** (CDCl$_3$)

$^{13}C\{^1H\}$ NMR spectrum of **9** (CDCl$_3$)
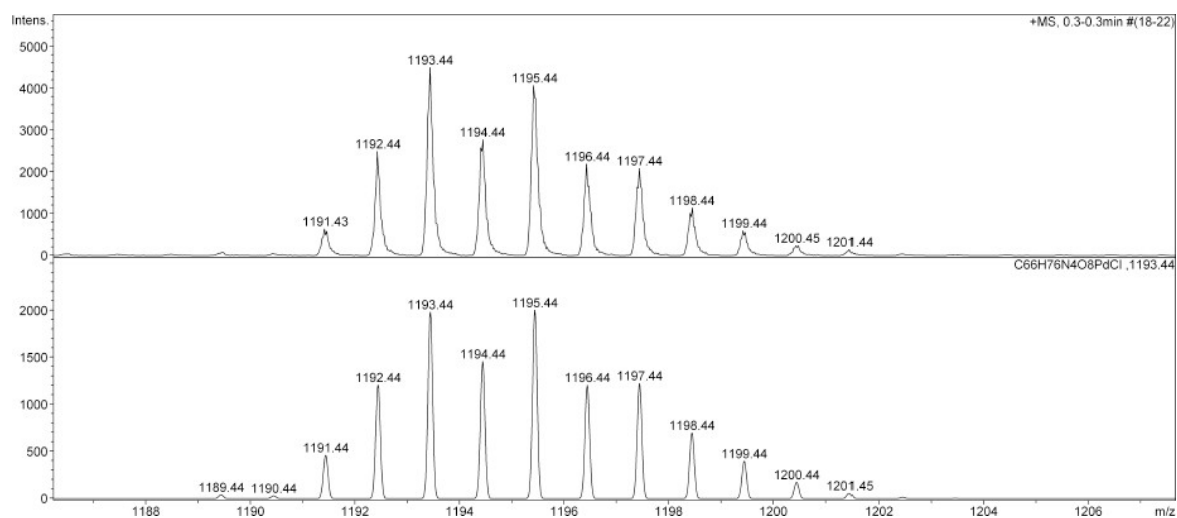
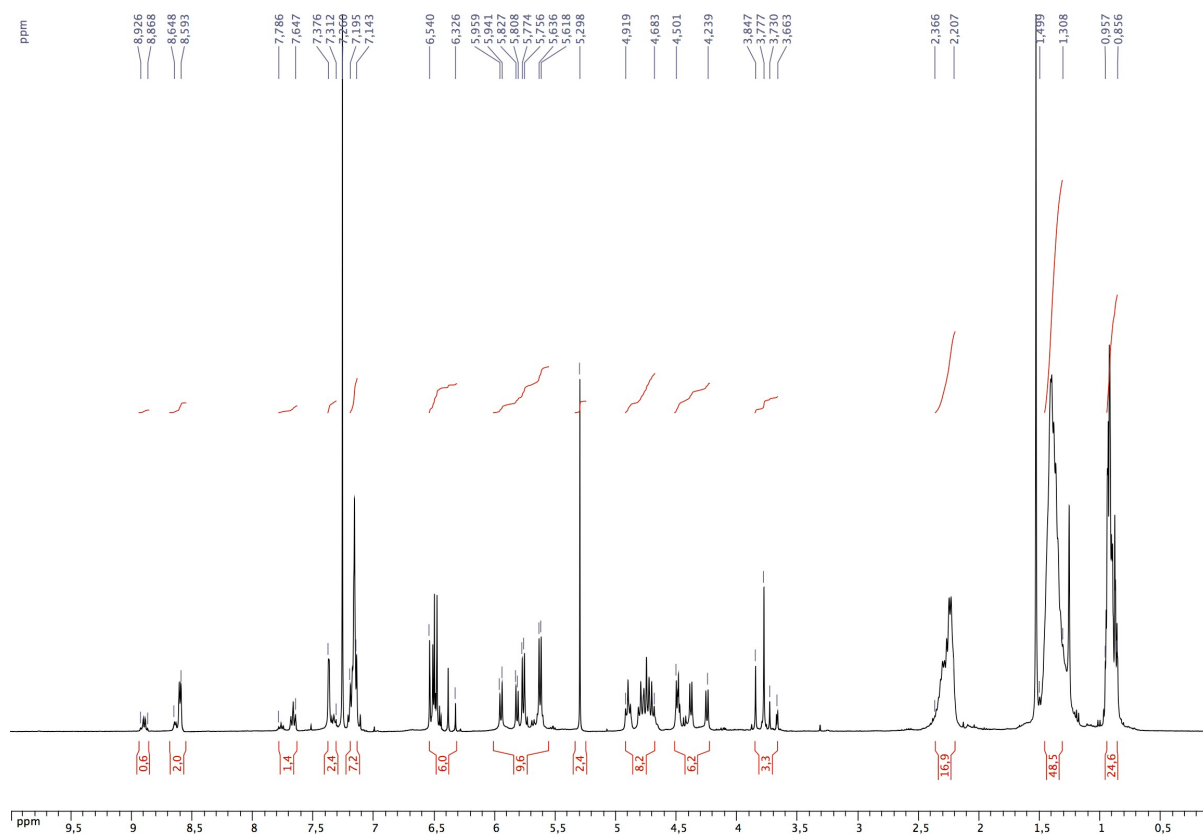ESI-TOF spectrum of the **9** (measured top and calculated for C$_{66}$H$_{76}$N$_4$O$_8$PdCl bottom)

trans-Dibromo-{1,4-bis[4(24),6(10),12(16),18(22)-tetramethylenedioxy-2,8,14,20-tetrapentylresorcin[4]arene-5-yl]-3-methyl-1_H_-1,2,3-triazol-5-yliden}pyridine palladium(II)

(10)

A mixture of K_2CO_3 (0.081 g, 0.59 mmol), pyridine (5 mL), [$PdCl_2$] (0.021 g, 0.12 mmol), KBr (0.233 g, 1.96 mmol) and triazolium salt **2** (0.180 g, 0.10 mmol) was heated at 80°C for 24 h. The reaction mixture was filtered through Celite, the filtrate was evaporated under vacuum, and the solid residue was purified by column chromatography (pure CH_2Cl_2; Rf = 0.62) to afford complex **10** (0.056 g, 28 %). ^{1}H NMR (500 MHz, $CDCl_3$): δ = 8.93-8.87 (m, 0.6H, arom. CH, pyridine), 8.65-8.59 (m, 2H, arom. CH, pyridine), 7.79-7.65 (m, 1.4H, arom. CH, pyridine), 7.38-7.31 (m, 2H, arom. CH, pyridine and resorcinarene), 7.19-7.14 (m, 7H, arom. CH, resorcinarene), 4.54-6.33 (m, 6H, arom. CH, resorcinarene), 5.95 and 5.82 (AB spin system, 4H, OCH_2O, ^2J = 9.0 Hz), 5.77-5.62 and 4.50-4.24 (AB spin systems, 12H, OCH_2O), 4.92-4.68 (m, 8H, CHCH_2), 3.85-3.66 (m, 3H, triazolyliden-CH_3), 2.37-2.21 (m, 16H, CHCH_2), 1.50-1.31 (m, 48H $CH_2CH_2CH_2CH_3$), 0.96-0.86 (m, 24H, CH_2CH_3) ppm. ^{13}C{^{1}H} NMR (126 MHz, $CDCl_3$): δ = 155.32-115.41 (arom. Cs), 150.03 (s, C_q-Pd), 149.96 (s, C_q-Pd), 100.61 (s, OCH_2O), 100.12 (s, OCH_2O), 99.83 (s, OCH_2O), 99.68 (s, OCH_2O), 99.56(s, OCH_2O), 99.36 (s, OCH_2O), 99.26 (s, OCH_2O), 38.13 (s, triazolyliden-CH_3), 37.82 (s, triazolyliden-CH_3), 37.62 (s, triazolyliden-CH_3), 36.74 (s, CHCH_2), 36.52 (s, CHCH_2), 32.22 (s, $CH_2CH_2CH_3$), 32.19 (s, $CH_2CH_2CH_3$), 32.14 (s, $CH_2CH_2CH_3$), (s, $CH_2CH_2CH_3$), 32.10 (s, $CH_2CH_2CH_3$), 31.99 (s, $CH_2CH_2CH_3$), 30.19 (s, CHCH_2), 30.10 (s, CHCH_2), 30.03 (s, CHCH_2), 29.97 (s, CHCH_2), 29.85 (s, CHCH_2), 29.82 (s, CHCH_2), 29.76 (s, CHCH_2), 27.83 (s, CHCH_2CH_2), 27.76 (s, CHCH_2CH_2), 27.72 (s, CHCH_2CH_2), 27.60 (s, CHCH_2CH_2), 22.86 (s, CH_2CH_3), 22.83 (s, CH_2CH_3), 22.72 (s, CH_2CH_3), 14.28 (s, CH_2CH_3), 14.24 (s, CH_2CH_3) ppm. MS (ESI-TOF): m/z = 1937.79 [M - Br - Py + $NCCH_3$]$^+$, expected isotopic profile. Elemental analysis calcd (%) for $C_{112}H_{134}N_4O_{16}PdBr_2$ (2058.51): C 65.35, H 6.56, N 2.72; found C 65.24, H 6.45, N 2.67.

^{1}H NMR spectrum of **10** (CDCl$_3$)

^{13}C{^{1}H} NMR spectrum of **10** (CDCl$_3$)

146
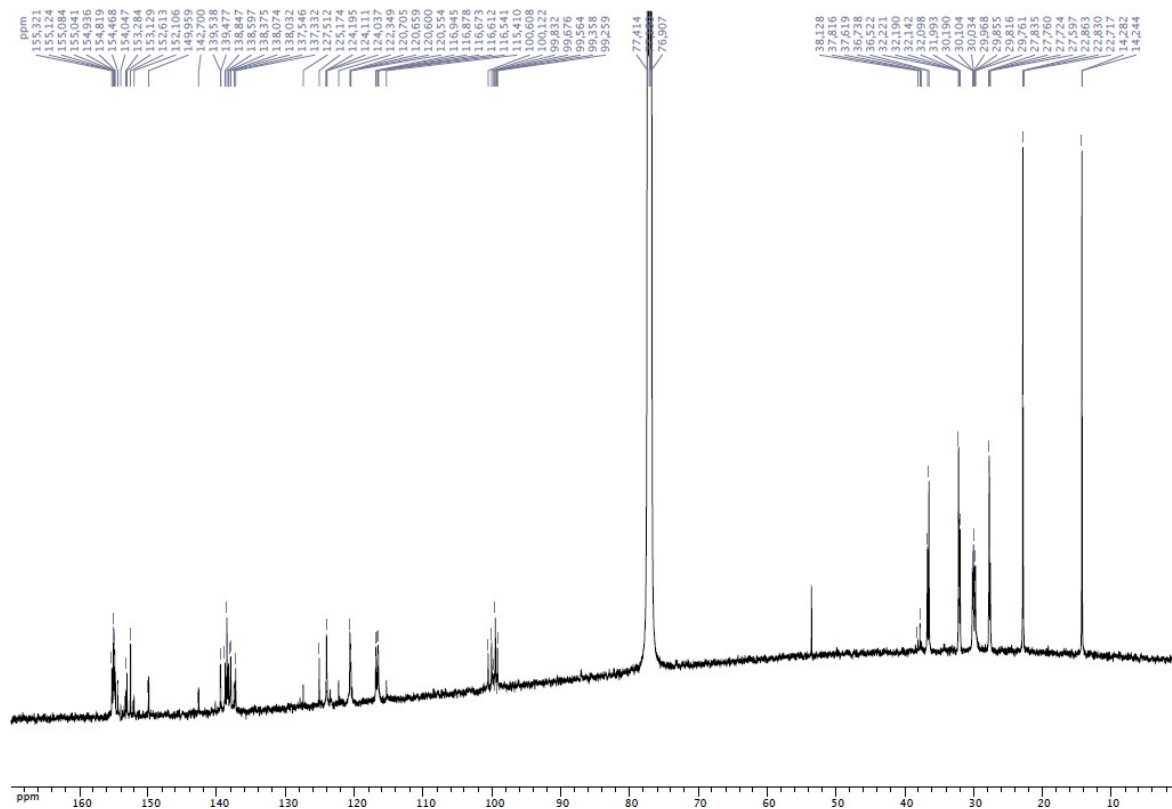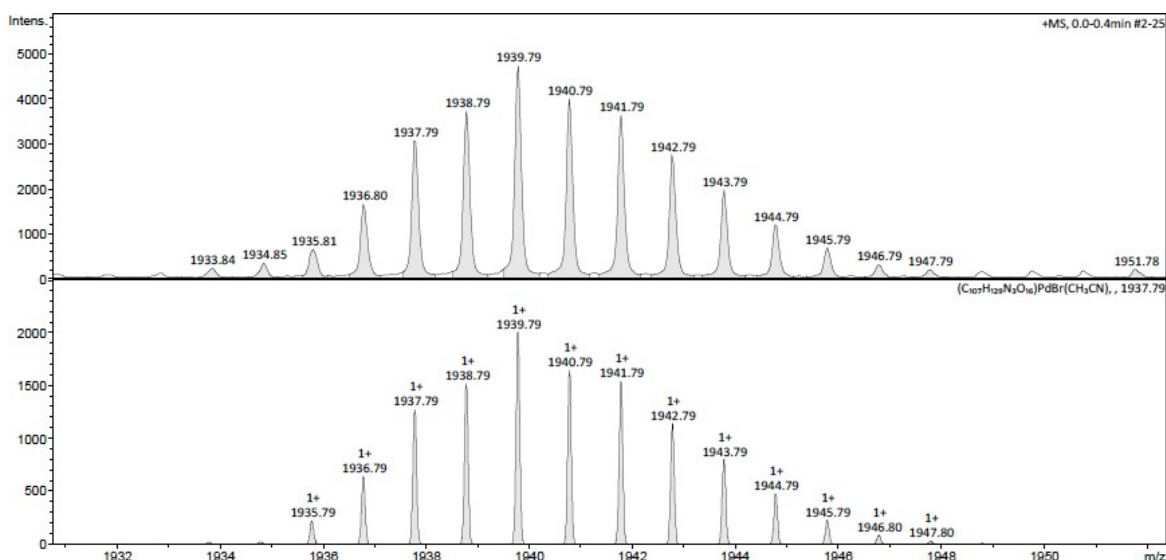
ESI-TOF spectrum of **10** (measured top and calculated for $C_{111}H_{132}N_4O_{16}PdBr$ bottom)

Typical procedure for the palladium-catalysed Suzuki-Miyaura cross-coupling reactions: A 10 mL-Schlenk tube was filled with the palladium precursor (0.5 mol %), triazolium salt (0.5 mol %), aryl chloride (0.5 mmol), arylboronic acid (0.75 mmol), ^tBuOK (0.75 mmol) and decane (0.025 mL, internal reference). Dioxane (2 mL) was then added. The reaction mixture was stirred at 100°C during the desired time. An aliquot (0.3 mL) of the resulting solution was then passed through a Millipore filter and analysed by GC.

Some homocoupling product (Ar'-Ar' coming from Ar'B(OH)$_2$) was detected in each run, but the Ar'-Ar':Ar-Ar' ratio did never exceed 2 %. NMR unambiguously identified the products after their isolation. Their NMR spectra were compared to those reported in the literature.

In this study the following products were prepared: 4-methoxybiphenyl,[1] 4-methoxy-2'-methylbiphenyl,[2] 2,4'-dimethoxybiphenyl,[3] 1-*p*-anisylnaphthalene,[4] 2,4'-dimethylbiphenyl,[5] 4-methylbiphenyl,[1] 2-methylbiphenyl,[6] 2,2'-dimethylbiphenyl,[7] 2-methoxy-2′-methylbiphenyl,[8] 2-methoxy-4'-methylbiphenyl,[9] 1-*p*-tolylnaphthalene,[10] 9-*o*-anisolanthracene,[11] 9-(1-naphthalenyl)-anthracene,[11] 9-*o*-tolyl anthracene,[11] 9-phenylanthracene[7] and 1-*o*-tolylnaphthalene.[10]

References

[1]   C. Röhlich, K. Köhler, *Adv. Synth. Catal.,* **2010**, *352*, 2263-2274.

[2]   B. Tao, D. W. Boykin, *J. Org. Chem.*, **2004**, *69*, 4330-4335.

[3]   J.Yang, *Appl.Organometal.Chem.*, **2017**,*31*, e3734.

[4]   F.He, Z.-X. Wang, *Tetrahedron*, **2017**,*73*, 4450-4457.

[5]   Y. Lai, Z. Zong, Y. Tang, W. Mo, N. Sun, B. Hu, Z. Shen, L. Jin,W.H. Sun, X. Hu, *Beilstein J. Org. Chem.,* **2017**, *13,213*-221.

[6]   X.-H. Fan, L.-M. Yang, *Eur. J. Org. Chem.,* **2010**, 2457-2460.

[7]   E. Schmid, D. C. Jones, O. Songis, O. Diebolt, M. R. L. Furst, A. M. Z. Slawin, C. S. J. Cazin, *Dalton Trans.,* **2013**, *42*, 7345-7353

[8]   L. Ackermann, A. R. Kapdi, S. Fenner, C. Kornhaaß, C. Schulzke, *Chem. Eur. J.,* **2011**, *17*, 2965-2971.

[9]   S. M. Wong, C. M. So, K. H. Chung, C. P. Lau, F. Y. Kwong, *Eur. J. Org. Chem.* **2012**, 4172-4177.

[10]   G.-J. Chen and F.-S. Han, *Eur. J. Org. Chem.,* **2012**, 3575-3579.

[11]   C. Wolf, H. Xu, *J. Org. Chem.*, **2008**, *73*, 162-167.

Résumé

Cette thèse présente la synthèse de ligands originaux construits sur des plateformes coniques de type résorcin[4]arène ou calix[4]arène étant susceptibles de positionner un métal à proximité d'une unité réceptrice: a) des bis-binaphtylphosphites optiquement actifs dont les centres phosphorés ont été greffés sur le bord supérieur de cavités génériques. Ces coordinats ont été testés en hydroformylation asymétrique d'arènes vinyliques et ont conduit à une sélectivité iso très élevée avec de bons, voire très bons excès énantiomériques; b) des carbènes *N*-hétérocycliques ayant soit un, soit les deux atomes d'azote substitués par des unités résorcinarényle (variante cavitand) et leur utilisation pour la formation d'espèces comportant un centre métallique supramoléculairement piégé dans la partie cavitaire (complexes du type [NiXCpL] (X = Br ou Cl, Cp = cyclopentadiényle, LH = NHC). Ces complexes se sont avérés efficaces en dimérisation de l'éthylène; c) des carbènes *N*-hétérocyliques anormaux obtenus à partir de sels de triazolium comportant un ou deux substituants résorcinarène. Ces composés à fort encombrement ont été efficacement employés en couplage croisé de Suzuki-Miyaura entre des chlorures d'aryles volumineux et des acides arylboroniques stériquement encombrés. Les activités les plus importantes ont été obtenues avec le sel de triazolium stériquement le moins encombré, celui portant un seul substituant résorcinarène. Sa plus grande efficacité est due à une approche plus facile des substrats dans les intermédiaires catalytiques correspondants ainsi que de la présence de groupes pentyles flexibles pouvant interagir stériquement avec le centre métallique de manière à faciliter l'étape d'élimination réductrice.

Mots clés: résorcin[4]arène, calix[4]arène, phosphite, carbène *N*-hétérocyclique, sel de triazolium, catalyse homogène, catalyse asymétrique.

Abstract

This thesis describes the synthesis of a series of compounds built on conical resorcin[4]arene and calix[4]arene platforms: a) diphosphites derived from optically active binol, in which the phosphite moieties have been grafted to the wider rim of the generic cones. These ligands were assessed in asymmetric hydroformylation of vinyl arenes and led to high iso selectivity with good to excellent enantiomeric excess; b) N-heterocyclic carbenes bearing either one or two cavitand moieties and their use for the synthesis of [NiXCpL] complexes (X = Br or Cl, Cp = cyclopentadienyl, LH = NHC) in which the NiCp moiety has been supramolecularly trapped in a resorcinarene bowl. These complexes were found active in ethylene dimerization; c) bulky triazolium salts with one or two resorcinarene substituents that were found suitable for the synthesis of complexes with abnormal NHCs. The latter were tested in palladium-catalysed Suzuki-Miyaura cross-coupling of bulky aryl chlorides with sterically hindered aryl boronic acids. Better activities were observed with the sterically less hindered triazolium salt, which bears a single resorcinarene substituent. Its higher efficiency arises from a higher substrate accessibility in the resulting catalytic intermediates as well as the presence of flexible pentyl groups that may interact with the metal centre so as to facilitate the reductive elimination step.

Key words: resorcin[4]arene, calix[4]arene, phosphite, *N*-heterocyclic carbene, triazolium salt, homogeneous catalysis, asymmetric catalysis.